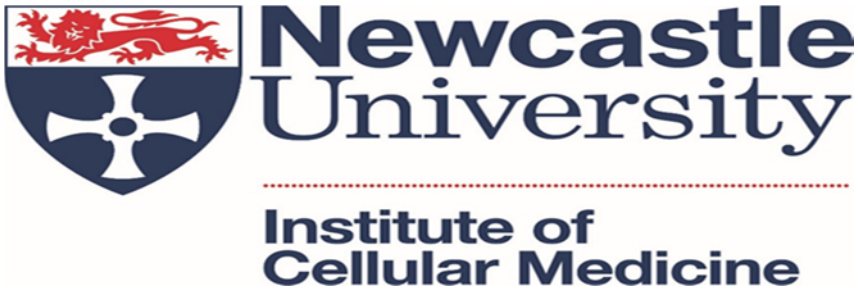

The molecular mechanisms by which metformin inhibits gluconeogenesis

Ahmed F. Alshawi

Thesis submitted for the Degree of Doctor of Philosophy

Newcastle University

Faculty of Medical Sciences

Institute of Cellular Medicine

April 2019

Declaration

I declare that this thesis is my own work and that I have correctly acknowledged the work of others. This thesis has not been previously submitted for assessment at Newcastle University or elsewhere and is in accordance with University and School guidance on good academic conduct.

Abstract

The mechanisms by which metformin (dimethylbiguanide) inhibits hepatic gluconeogenesis at concentrations relevant for type 2 diabetes therapy remain debated. Two proposed mechanisms are: inhibition of mitochondrial Complex 1 with consequent compromised ATP and AMP homeostasis; or inhibition of mitochondrial glycerophosphate dehydrogenase (mGPDH) and thereby attenuated transfer of reducing equivalents from the cytoplasm to mitochondria resulting in a raised lactate/pyruvate ratio and redox-dependent inhibition of gluconeogenesis from reduced but not oxidised substrates.

This thesis used primary hepatocytes to investigate the mechanism(s) by which low metformin concentrations relevant to the therapeutic dose inhibit gluconeogenesis. It tested the hypotheses of involvement of inhibition of Complex 1 and / or inhibition of mGPDH.

The results from this study show that metformin has a biphasic effect on the mitochondrial NADH/NAD redox state in hepatocytes. A low cell dose of metformin (therapeutic equivalent: < 2nmol/mg) caused a more oxidised mitochondrial NADH/NAD state and an increase in the lactate/pyruvate ratio, whereas a higher metformin dose (≥5nmol/mg) caused a more reduced mitochondrial NADH/NAD state similar to Complex 1 inhibition by rotenone. The low metformin dose inhibited gluconeogenesis from both oxidised (dihydroxyacetone) and reduced (xylitol) substrates by preferential partitioning of substrate towards glycolysis by a redox-independent mechanism that is best explained by allosteric regulation at phosphor-fructokinase-1 (PFK1) and/or fructose bisphosphatase-1 (FBP-1) in association with a decrease in cell glycerol 3-P, an inhibitor of PFK1 rather than by inhibition of transfer of reducing equivalents.

This study supports the conclusion that at a low pharmacological load, the metformin effects on the lactate/pyruvate ratio are explained by attenuation of transmitochondrial electrogenic transport mechanisms with consequent compromised malate-aspartate shuttle and the inhibition of gluconeogenesis is best explained by changes in allosteric effectors of PFK1 and FBP1 independently of inhibition of both Complex 1 and mGPDH.

Acknowledgements

Firstly, I would like to thank my supervisor, Professor Loranne Agius, I am extremely grateful for her support, encourage, and guidance throughout my PhD. I think I am very luck to work with Loranne's research group. I do not have enough words to convey my appreciation for her hard work, friendship, and help to achieve this thesis.

I would also like to thank every current and previous members of the lab for their help, support, and friendship. In particular I would like to thank Dr. Catherine Arden and Dr. Francesco Zummo who have been a great help to me with western blotting technique and solve many problems. I would also like to thank my previous colleague Tabassum Moonira and my current colleagues Dr. Brian Ford and Dr. Shruti Chachra for their friendly help and support.

I would like to say a huge thank my family, especially my father, to soul of my mother, brothers, sister, my children and also my lovely wife for their patience, encourage, and support during my study.

Finally, I am indebted to my sponsor the Higher Committee for Education Development in Iraq (HCED) to their supporting and funding my PhD.

Table of Contents

List of tables

List of figures

Abbreviations

Acac	Acetoacetate
ACC	Acetyl CoA carboxylase
ADP	Adenosine 5'di-phosphate
AICAR	5-Aminoimidazole-4-carboxamide ribonucleotide
AMP	Adenosine 5' monophosphate
AMPK	Adenosine 5' monophosphate-activated protein kinase
AOA	Aminooxyacetate
ATA	Aurintricarboxylic acid
ATP	Adenosine 5'-triphosphate
cAMP	Adenosine 3', 5'-cyclic monophosphate
CaMKK-β	Calcium/Calmodulin-activated protein kinase kinase-β
CBS	Cystathionine β-synthase domain
ChREBP	Carbohydrate response element binding protein
cGPDH	Cytoplasmic glycerophosphate dehydrogenase
CVD	Cardiovascular disease
DCMU	(3,4-dichlorophenyl)-1,1-dimethylurea
db-cAMP	Dibutyryl Adenosine 3', 5'-cyclic monophosphate
DCIP	2,6-dichlorophenol-indophenol
DHA	Dihydroxyacetone
DHAP	Dihydroxyacetone phosphate
DNP	2,4-Dinitrophenol
ECL	enzyme chemiluminescence
F1,6-P_2	Fructose 1, 6-bisphosphate
F2,6-P_2	Fructose 2, 6-bisphosphate
F6P	Fructose 6-phosphate
FAD	Flavin adenine dinucleotide
FADH	Flavin adenine dinucleotide, reduced
FBP-1	Fructose 1,6-bisphosphatase-1

FBPi	Fructose 1,6-bisphosphate-1 inhibitor
FGF21 A	Fibroblast growth factor 21A
G3P	Glycerol 3-phosphate
G3PDH	Glycerophosphate dehydrogenase
G6P	Glucose 6-phosphate
G6PDH	Glucose 6-phosphate dehydrogenase
G6Pc	Glucose 6-phosphatase
GAPDH	Glyceraldehyde 3-phosphate dehydrogenase
Gpi	STK017597; glycerophosphate dehydrogenase inhibitor
Gpd2	Mitochondrial glycerophosphate dehydrogenase gene
HbA1c	Glycated hemoglobin
HOB	3-hydroxybutyrate
IDDM	Insulin dependent diabetes mellitus
LKB-1	Liver kinase B-1
MATE1	Multidrug and toxin extrusion-1 transporter
MAS	Malate-aspartate shuttle
mGPDH	Mitochondrial glycerophosphate dehydrogenase
NAD	β-Nicotinamide adenine dinucleotide
NADH	β-Nicotinamide adenine dinucleotide, reduced
NIDDM	Non-insulin depending diabetes mellitus
NNT	Nicotinamide nucleotide transhydrogenase
OCT	Organic cation transporter
PCR	Polymerase chain reaction
PEPCK	Phosphoenolpyruvate carboxykinase
PFK-1	6-phosphofructo-1-kinase
PFK-KD	Kinase deficient variant of phosphofructokinase 2/ fructose bisphosphatase 2
PKA	Protein kinase A
PMSF	Phenylmethylsulfonyl fluoride
PPAR-γ	Peroxisome proliferator activated receptor-γ

S4048	Chlorogenic acid derivative (1-[2-(4-chloro-phenyl)-cyclopropylmethoxy]-3,4-dihydroxy-5-(3-imidazo[4,5-b]pyrudin-1-y1-3-phenyl-acryloyloxy)-cyclohexanecarboxlic acid
SGLT2	Sodium glucose co-transporter 2 inhibitors
T2D	Type 2 diabetes
Txnip	Thioredoxin interacting protein
WT	Wild-type

CHAPTER 1

INTRODUCTION

Chapter. 1 Introduction

1.1 Diabetes Mellitus

Diabetes mellitus has been defined by the World Health Organization as a metabolic dis-function of multiple causes featured by chronic hyperglycaemia with changes in glucose, protein and fat metabolism due to a defect in insulin secretion, insulin action, or both (Bolen et al., 2007). The number people with diabetes is expected to reach 366 million in 2030 (World Health, 2006).

1.2 Types of diabetes mellitus

The two commonest forms of diabetes (Type 1 and Type 2) are linked to several genetic associations and environmental predisposing factors. In addition diabetes can also be linked to single gene disorders, for example as a result of gene defects in glucokinase or various transcription factors involved in insulin production (Thorsby et al., 1998) (Krupanidhi et al., 2009) (Froguel, 2000)

1.2.1 Type 1 diabetes mellitus

Type-1 diabetes was previously called Insulin-dependent diabetes mellitus (IDDM) or Juvenile-onset diabetes. It accounts for about 5% of diabetes. It is due to insufficient insulin secretion from pancreatic β-cells because of autoimmune destruction of the β-cells (Novotna et al., 2015)

1.2.2 Type 2 diabetes mellitus: -

Type-2 diabetes previously known as Non-Insulin Dependent Diabetes Mellitus (NIDDM), is the most common type of diabetes accounting for ~ 90% of diabetes. This disease is caused by insufficient insulin secretion or resistance to insulin action resulting in increased blood glucose (World Health, 2006, Crook, 2006). Type 2 diabetes results from both genetic and environmental factors. The large increase in prevalence of type 2 around the world is attributed to the increase in obesity, and changes in diet and decrease in physical activity T2D (Olokoba et al., 2012)

Insulin produced by the pancreatic β-cells plays a vital role in maintaining blood glucose homeostasis by increasing the cellular uptake of glucose from blood to insulin sensitive tissues (muscle, fat tissues) and inhibiting hepatic glucose production by glycogenolysis and gluconeogenesis. Insufficient insulin secretion from the β-cells leads to elevated blood glucose and increased hepatic glucose production. Current evidence shows that lack of treatment or failure to restore blood glucose within the normal range in T2D increases the risk of

development and progression of microvascular complications (retinopathy, nephropathy, and neuropathy) and macrovascular disease (Myocardial infarction) (Gardner et al., 2007, Group, 1998) .

Diagnosis of diabetes was previously based on the level of either fasting blood glucose (FBG) or the glucose excursion during an oral glucose tolerance test (OGTT). In 2009 the criteria for diagnosis of diabetes were changed by an International Expert Committee that included representatives of the American Diabetes Association (ADA), the International Diabetes Federation (IDF), and the European Association for the Study of Diabetes (EASD) to the measurement of glycated haemoglobin (HbA1c ≥6.5%) (2013). HbA1c is a form of haemoglobin that is bound to glucose as a result of a raised blood glucose. The lifespan of red blood cells which carry haemoglobin is around 120 days and accordingly the level of HbA1c is an approximate measure of the average blood glucose level during the previous 120 days. (Kahn and Fonseca, 2008, Kojic Damjanov et al., 2014)

1.3 Treatments for Type 2 Diabetes

1.3.1 Sulphonylureas

Sulphonylureas are one of the oldest class of anti-diabetic drugs. These drugs were previously used as antibiotics, in patients with typhoid fever, and were found to cause hypoglycaemia. These drugs were developed in 1956 as first-generation sulphonylureas for treatment of T2D in the United State (Selizer, 1980). The second generation of sulphonylureas included glibenclamide and glipizide (Thulé and Umpierrez, 2014). The main mechanism of action of sulphonylureas is to stimulate insulin secretion from pancreatic β-cells. The molecular mechanism involves binding to the sulphonylureas receptor (SUR1), and this binding inhibits the potassium flux via closure of the K_{ATP} channels depolarizing the pancreatic β-cells membrane. An extrapancreatic effect, of sulphonylureas was also reported in the rat perfused liver by reducing insulin clearance in liver and this was also confirmed in man (Barzilai et al., 1995, Thulé and Umpierrez, 2014). Hypoglycaemia and weight gain are the most common side effect associated with sulphonylureas (Kunte et al., 2007). In comparison with metformin, treatment with sulphonylureas was associated with incidence of cardiovascular events (Jorgensen et al., 2010)

1.3.2 Thiazolidinediones

Elevation of blood glucose leads to many complications such as increased the risk of cardiovascular disease (CVD) which accounts for about 80% of deaths in T2D patients (Abdul-Ghani et al., 2017). Thiazolidinediones are one of the anti-diabetic drugs which are associated with improved the risk of CVD through lowering insulin resistance (Della-Morte et al., 2014). Thiazolidinediones exert their effect through activation of peroxisome proliferator activated receptors-γ (PPAR-γ), a nuclear receptor, resulting in heterodimeric complex formation with retinoid X receptor (RXR). Binding of this transcription factor complex with target gene promoters, results in increased or decreased transcription of many genes involved in fat storage in adipose tissue. This facilities fat storage in adipose tissue resulting in lower accumulation of lipids in other tissues and in the circulation (Della-Morte et al., 2014, Inzucchi et al., 2015, Ferrannini and DeFronzo, 2015)

1.3.3 Sodium glucose co-transporter 2 inhibitors (SGLT2)

Inhibition of glucose reabsorption in the proximal renal tubules through inhibition of sodium-glucose co-transport type 2 has a beneficial role in glucose homeostasis. SGLT2 inhibitors (canagliflozin, dapagliflozin, and empagliflozin) are anti-hyperglycaemic agents by targeting the kidney to increase the excretion of glucose in urine and decrease the level of glucose in circulation by lowering the renal threshold (Nauck, 2014). SGLT2 inhibitors did not associate with hypoglycaemia, but they have many side effects such as increased uric acid, weight loss, lowering blood pressure, dehydration and urinary tract infections (Inzucchi et al., 2015, Vasilakou et al., 2013)

1.3.4 Metformin

Metformin (dimethylbiguanide) is a member of the biguanide family, which include (phenformin, metformin, and bufromin) (Figure 1-1). Biguanides have been used as anti-hyperglycaemic agents in the last century, phenformin and bufromin were withdrawn due to their toxicity and metformin was used because it is least toxic (Bailey, 1992). Metformin derived from *Galega officinalis*, a traditional herbal medicine, is the first line treatment prescribed for T2D because it is the safest effective anti-hyperglycaemic agent with lowest risk for CVD and other side effects including weight gain. Studies showed that the incidence of side effects resulting from metformin treatment is very rare (Viollet and Foretz, 2013, Inzucchi et al., 2014). The main effects of metformin are inhibition of hepatic glucose production (gluconeogenesis) (Hundal et al., 2000), increase uptake of glucose by muscle, and lower glucose absorption from the gut (Natali and Ferrannini, 2006). An exciting point of metformin is that studies have shown that besides its role in the lowering of blood glucose in T2D, metformin can be used to treat many other diseases. Recent studies reported that metformin can be used to treat a common endocrine disorder, polycystic ovary syndrome (PCOS) which is associated with obesity and insulin resistance (Naderpoor et al., 2015, Grigoryan et al., 2014, Glintborg et al., 2014). Metformin also lowered the risk of CVD in T2D patients (Hong et al., 2013, Malin et al., 2013, Skov et al., 2014, Holman et al., 2008) .

Furthermore, several studies reported that metformin has a beneficial effect in decreasing the incidence of malignancy such as inhibition of endometrial cancer *in vivo* (Mitsuhashi et al., 2014), breast cancer (Niraula et al., 2012), prostatic cancer (Preston et al., 2014), and pancreatic cancer in T2D patients (Zhou et al., 2017) and in animal models (Chen et al., 2017). However, other studies suggested that more investigations are necessary to allow the final conclusion about the effect of metformin on improving cancer treatment (Wei et al., 2019). Several studies reported that there was no effect of metformin on cancer progression (Feng et al., 2015, Kowall et al., 2015).

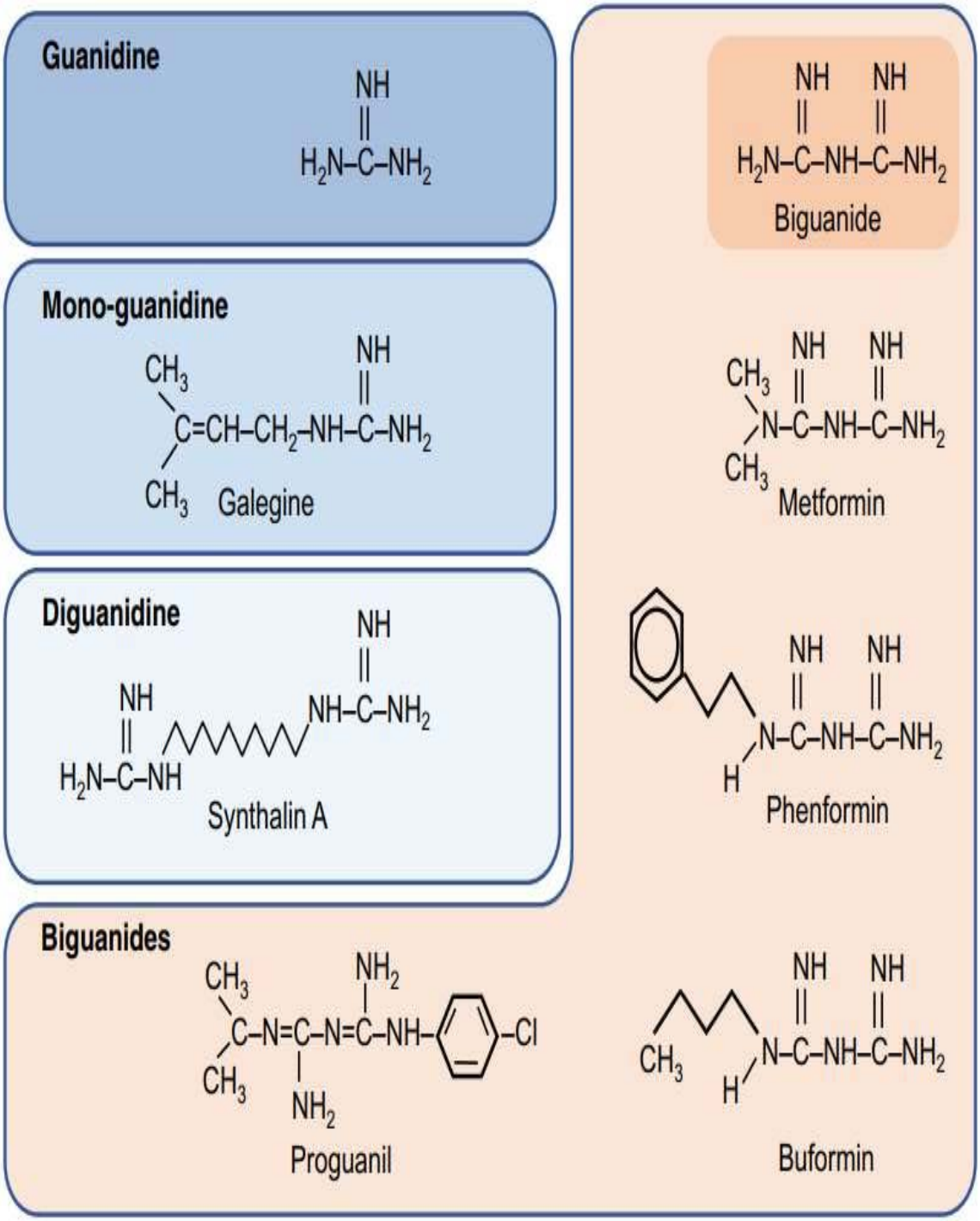

Figure 1-1: Chemical structure of Biguanides and related compounds

(Bailey, 2017)

1.4 Pharmaceutical dose and cellular uptake of Metformin

Metformin is taken orally by patients either once or twice a day to a maximum daily dose of 3g. The plasma peak of metformin concentrations reached three hours after an oral dose of 500 mg is 1.0-1.6mg/L, while 1.5g/day increases the level to 3mg/L. The plasma level rapidly declines after a single dose and the level of metformin in urine rises. Studies in man reported that fecal concentration was about 30% of oral metformin dose, while nothing presented after intravenous injection of metformin (Tucker et al., 1981, Graham et al., 2011). It has been shown that metformin absorption takes place in the small intestinal by solute carrier organic transporters. Transport of metformin from the lumen into the enterocytes is by the plasma membrane monoamine transporter (PMAT) expressed on the luminal membrane (Zhou et al., 2007) and the organic cation transporter-3 (OCT-3) expressed on the brush border (He and Wondisford, 2015) . Transport of metformin from the enterocytes into the interstitial fluid is by organic cation transporter-1 (OCT-1) which is expressed on the basolateral membrane of the enterocyte (Muller et al., 2005). Metformin is transported to the liver, via the portal vein. The metformin concentration in the portal vein after a therapeutic load reaches 40-70µM. Hepatocytes take up about 25-50% of the metformin in the portal vein through OCT1 and OCT3 transporters which are located on the basolateral membrane of hepatocytes. Metformin is also a substrate for the multidrug and toxin extrusion 1 transporter (MATE1), which is expressed at high levels in the liver. However, the role of MATE1 in hepatic secretion of metformin is controversial because in man there is negligible biliary excretion. Metformin is chemically stable and not-metabolized and about 90% of the absorbed dose is excreted by the kidneys (Gong et al., 2012). Metformin is transported into the renal epithelial cells by OCT2 which is expressed on the basolateral membrane of renal tubules and it is then transported from the epithelial cell into the lumen by MATE1/2K located on the apical membrane (He and Wondisford, 2015) .

The tissue metformin content has been determined in mice after an oral load of metformin (50mg/kg) using ^{14}C-metformin, this concentration is equivalent to the therapeutic dose in man (3 g per 60 kg). The highest accumulation of metformin was found in jejunum and ileum (gastrointestinal), kidney and liver, and the lowest metformin concentration was found in brain and white adipose tissue (Wilcock and Bailey, 1994)

1.5 Molecular mechanisms of metformin

Metformin has been approved for treatment of T2D in Europe from 1950s and in the United State since 1995, however, its molecular mechanism is still a controversial issue (Viollet et al., 2012, Rena et al., 2017, Rena et al., 2013).

1.5.1 Inhibition of Mitochondrial respiratory chain-complex-I by metformin

The electron transport chain is a series of chemical reactions catalyzed by multi-enzyme complexes that couple the oxidation of NADH to NAD^+ and FADH to FAD^+ to the reduction of molecular oxygen to water by transferring electrons from NADH and FADH through a series of intermediates. The first enzyme complex designated complex 1 is NADH-ubiquinone oxidoreductase. This multiprotein complex has three functions: to oxidise NADH to NAD^+; to transfer the electron to ubiquinone and to pump protons from the matrix to outside the mitochondria. This process serves to harness the energy from the oxidation of NADH to the generation of the mitochondrial proton gradient. This proton gradient serves to drive ATP-synthase, nicotinamide nucleotide transhydrogenase and other energy-dependent processes in mitochondria. Compounds that inhibit any component of the respiratory chain including complex 1 are expected to affect the generation of the proton gradient, the function of ATP-synthase and other energy-dependent reactions in mitochondria as well as gluconeogenesis (Hirst, 2013). Complex 1comprises 45 proteins of which 14 are conserved subunits and the other 31 are designated supernumerary. The conserved proteins comprise 7 hydrophilic proteins, that catalyze the redox reactions and extend into the mitochondrial matrix and 7 hydrophobic proteins (ND units) that are embedded in the membrane. The hydrophobic proteins are encoded by the mitochondrial genome and the hydrophilic and supernumerary proteins by the nuclear genome. The hydrophilic domain composed on 7 proteins has a Y-shape with the lower part linked to the hydrophobic ND domains and the upper part composed of 2 subdomains which form the NADH active site and flavin mononucleotide cofactor site and a chain of iron-sulfur (Fe-S) clusters that link the flavin molecule with the ubiquinone site. Transfer of electrons from the flavin through the Fe-S clusters is thought to transfer the energy through conformational changes in the hydrophobic ND subunits which are involved in the proton transport mechanism (Hirst, 2013, Zickermann et al., 2015, Ohnishi, 1998)

Halestrap and colleagues proposed that stimulation of NADH oxidation in hepatocytes by glucagon or phenylephrine has an important role in increasing hepatic glucose production. They also reported that inhibition of the respiratory chain using mild respiratory chain inhibitors 3-(3,4-dichlorophenyl)-1,1-dimethylurea (DCMU) or amytal in hepatocytes from starved rats

reversed the effect of gluconeogenic hormones (glucagon and phenylephrine) to stimulate glucose production (Pryor et al., 1987, Quinlan and Halestrap, 1986).

In a later study Owen and colleagues (1993) determined the effects of the mild respiratory inhibitor DCMU on metabolites and gluconeogenesis and demonstrated raised concentrations of 3-phosphoglycerate, 2-phosphoglycerates and phosphoenolpyruvate but lower concentrations of dihydroxyacetone phosphate, glyceraldehyde-3-P, fructose-1,6 bisphosphate, fructose 6-phosphate and glucose 6-phosphate. They proposed that the inhibition of the respiratory chain by DCMU causes inhibition of gluconeogenesis at the level of 3-phosphoglycerate kinase and proposed that this can be explained by a decrease in ATP/ADP. They concluded that the changes in metabolites of glycolysis and gluconeogenesis caused by DCMU are very similar to those caused by phenformin in a previous study by Cook and colleagues (1973) (Owen and Halestrap, 1993). In this earlier work on phenformin Cook and colleagues (1973) reported that phenformin inhibited gluconeogenesis in the perfused liver from both lactate and dihydroxyacetone but not from xylitol and the effects of phenformin were associated with a more reduced cytoplasmic and mitochondrial NADH/NAD redox state and with a decrease in the ATP/ADP ratio and also with a decrease in the concentration of citrate. They concluded that an effect of phenformin on mitochondrial function and / or the decrease in ATP/ADP ratio may be involved in the inhibition of gluconeogenesis (Cook et al., 1973).

A study by Argaud *et al* (1993) reported inhibition by metformin of gluconeogenesis in isolated hepatocytes from several substrates including lactate/pyruvate, DHA, fructose, glutamine and alanine. This study determined the cell concentrations of various metabolites including ATP and ADP and proposed that metformin causes activation of pyruvate kinase through the decrease in ATP/ADP ratio (Argaud et al., 1993).

Later work from Halestrap's group and El Mir and colleagues reported that the inhibitory effect of biguanides (phenformin and metformin) on the respiratory chain can be explained by inhibition of complex 1 (NADH ubiquinone oxidoreductase) either directly or indirectly (El-Mir et al., 2000, Owen et al., 2000) .

El-Mir *et al* reported an indirect effect of metformin on complex 1. Intact isolated hepatocytes, permeabilized hepatocytes, and isolated liver mitochondrial were used to investigate the inhibitory effect of metformin (0.1-1mM on the respiratory chain and complex 1 (El-Mir et al., 2000). Oxygen uptake was inhibited by 10mM metformin in the presence of the complex 1 substrates, glutamate plus malate, but not with the complex II substrate, succinate. By using an

artificial electron acceptor of complex 1 (decylubiquinone) NADH oxidation was inhibited in mitochondria isolated from liver previously perfused with 10mM metformin, while there was no effect on oxygen consumption when they used decylubiquinol as complex III electron donor. The inhibitory effect of metformin on oxygen consumption was seen when metformin was added to intact hepatocytes but not with permeabilized hepatocytes or isolated liver mitochondria. The authors concluded that the effect of metformin can only be induced in the whole cell and that the effect of metformin causing inhibition of complex 1 is therefore indirect through a signalling pathway. The cytoplasmic and mitochondrial NADH/NAD^+ ratios were increased in hepatocytes treated with 10mM metformin. The conclusions from this study were (i) that metformin indirectly inhibits complex 1 because the effect was not seen when metformin was added to isolated mitochondria (ii) the inhibition by metformin of oxygen uptake was temperature dependent (iii) The effect of metformin on oxygen uptake persisted after metformin was removed (iv) the mechanism of metformin to inhibit the respiratory chain reaction was independent of insulin and calcium signaling pathways (El-Mir et al., 2000).

Halestrap's group (Owen et al., 2000) in contrast with the previous study was able to demonstrate a direct inhibitory effect of metformin (2-5mM) on respiration when metformin was added to either rat hepatocytes, isolated heart mitochondria or submitochondrial particles (SMPs) from heart and liver. They also observed the effects of lower metformin concentrations in studies on the rat hepatoma cell line (H4IIE) incubated with 0.05-0.1mM metformin for 24-60h. By determining oxygen uptake in isolated mitochondria or permeabilized cells incubated with substrates of complex 1 (glutamate plus malate) or Complex II (succinate), they concluded that metformin was targeting Complex 1 and not Complex II or downstream sites in the respiratory chain. From experiments testing the inhibition of respiration at various times after addition of metformin to cells or isolated mitochondria they concluded that the effect of metformin on respiration at the level of complex 1 is both time-dependent and concentration-dependent and that these effects are best explained by the slow uptake of metformin into cells and into mitochondria. This conclusion was supported by experiments on small mitochondrial particles in which complex 1 is present on the outer surface and can therefore oxidise NADH in the medium. In this experimental system the effects of both metformin and phenformin were not time-dependent but required high concentrations of these biguanides. This supported the conclusion that the time-dependency of metformin in isolated mitochondria or intact cells is the result of the slow uptake of the biguanides and the time required for the drug to reach the required intramitochondrial concentration to inhibit complex 1. Metformin (2mM) inhibited gluconeogenesis in rat hepatocytes concurrently with changes in cellular metabolites involving

a decrease in G6P and F6P levels, and an increase in 2- and 3-phosphoglycerate and phosphoenolpyruvate and increases in both the cytosolic and mitochondrial free NADH/NAD ratios. Similar results were obtained in the liver *in vivo* after treating rats with a metformin dose of 200-600 mg/kg body weight. This dose is > 4 fold higher than was used by Wilcock and colleagues (50mg/kg) (Wilcock and Bailey, 1994). The conclusions from this study were that (i) Metformin inhibited respiration at the level of complex 1 after direct addition of metformin to isolated mitochondria or hepatocytes or hepatoma cells (ii) metformin permeability across the mitochondrial membrane is slow (iii) Due to the positive charge of metformin, it accumulated in the mitochondria in accordance with the mitochondrial membrane potential ($\Delta\Psi$) (Owen et al., 2000).

A recent study by Bridges and colleagues (2014) investigated at the enzyme level the molecular mechanism by which biguanides alter the kinetic activity of complex 1. They used the purified enzyme from bovine heart, yeast and E. coli and reported that complex 1 isolated from bovine heart mitochondria (*Bos taurus*) was inhibited by five biguanides and metformin was the weakest inhibitor compared with phenformin and butformin, and proguanyl and cycloguanyl that are used in therapy for malaria. By investigating the effects of metformin on three steps of the complex 1 mechanism, they concluded that (i) metformin stimulated the first step representing NADH oxidation; (ii) metformin had no effect on the second step representing the intramolecular electron transfer; (iii) metformin caused non-competitive reversible inhibition of the reduction of ubiquinone (third step). This effect of metformin on the reduction of ubiquinone differs from the mechanism of canonical inhibitors (rotenone and piercidin) which bind irreversibly and competitively to the ubiquinone binding site. Their conclusion was that metformin works on two sites of complex 1, one site is the reactivity of flavoprotein and the other the ubiquinone to ubiquinol reduction. The first reaction was investigated by use of artificial electron acceptors and the rate of NADH oxidation or hydrogen peroxide production and their finding was the effect of metformin on the flavin site is related to presence or absence of nucleotide binding to the flavin site. Presence or absence of nucleotide has a critical role in stabilizing the active or deactive conformations of the enzyme transition of complex 1 (Galkin et al., 2008, Roberts and Hirst, 2012). They found that the effect of metformin on NADH oxidation or H_2O_2 production was slower if metformin was added during the catalytic phase and it needs prolonged time to achieve the effect. Therefore they concluded that metformin stabilizes the deactive conformation (Bridges et al., 2014).

1.5.2 Role of AMPK in the metformin mechanism

Adenosine monophosphate-activated protein kinase (AMPK), is often described as a cellular energy sensor, because it is activated in conditions of compromised adenine nucleotide phosphorylation potential and its activation is linked to inhibition of anabolic pathways such as *de novo* lipogenesis and stimulation of energy production pathways such as fatty acid oxidation (Kurumbail and Calabrese, 2016). AMPK is a heterotrimeric serine/threonine kinase complex, which consist of three subunits (one catalytic α-subunit and two regulatory subunits β and γ). Changes in adenine nucleotide concentration AMP: ATP and/or ADP: ATP ratio have been shown to increase the activation of AMPK in cells (Kurumbail and Calabrese, 2016, Grahame Hardie, 2016, Hardie, 2015). AMPK has very low activity in its basal un-phosphorylated state. However when phosphorylated on Thr-174 α-1 or Thr-172 α-2 the activity of AMPK increases more than 500-fold. There are two kinases that catalyze the phosphorylation of AMPK, tumour suppressor Liver kinase B-1 (LKB-1) and Ca^{2+}-calmodulin-activated protein kinase kinase beta (CamKKβ) (Hawley et al., 2005, Woods et al., 2005, Grahame Hardie, 2014, Hardie, 2015). LKB-1 is constitutively active, however, binding of AMP to the γ subunit of AMPK stimulates its activation by LKB-1. In addition the β-subunit of AMPK also has a role in the activation of AMPK by LKB-1 in conditions of raised cellular levels of AMP. The activation of AMPK by CamKKβ is regulated by changes in cell calcium ion and not by changes in AMP. The phosphorylated form of AMPK is inactivated by dephosphorylation by protein phosphatases including PP2A and PP2C. Both AMP and ADP inhibit the dephosphorylation of AMPK by protein phosphatase but AMP is 10-fold more effective than ADP at inhibiting dephosphorylation (Steinberg and Carling, 2019). An increase in cell AMP causes activation of AMPK by inhibiting dephosphorylation by the phosphatases, by promoting activation by LKB-1 and also by direct allosteric activation of AMPK independently of phosphorylation (Sanders et al., 2007b). This allosteric activation of AMPK only occurs with AMP and not with ADP and a physiological concentration of AMP can increase AMPK activity allosterically up to 10-fold independently of its effects on phosphorylation (Xiao et al., 2011, Ross et al., 2016). In whole cells the activity of AMPK can be monitored either from the phosphorylation state of the substrates of AMPK (e.g. acetyl CoA carboxylase) or from the phosphorylation of AMPK itself on the threonine residue in the α-subunit. Because of the allosteric activation of AMPK by AMP the former substrate (ACC) is a better indication of the activation of AMPK (Ross et al., 2016).

It has been shown that inducing AMPK activation has a beneficial effect in lipid metabolism by increasing the phosphorylation of acetyl-CoA carboxylase (ACC) which results in inhibition of enzyme activity and also inhibition of lipogenesis and a decrease in cell malonyl-CoA, the

product of ACC, which is an inhibitor of transport of long-chain fatty acids into mitochondria. Accordingly, AMPK activation results in stimulation of β-oxidation of long chain fatty acids (Munday and Hemingway, 1999, Serviddio et al., 2013, Liu et al., 2011). The importance of AMPK activation in metformin's mechanism has been proposed in many studies (Rena et al., 2017, Zhang et al., 2016, Chen et al., 2013)

Soon after the discovery of the inhibition of complex-I by metformin in 2000, Zhou and colleagues (Zhou et al., 2001) proposed that many of the effects of metformin on hepatocytes can be explained by activation of AMPK. They compared the effects of the AMPK activator, AICAR (5-amino-imidazole carboxamide riboside) with different concentrations of metformin (0.02-2mM) for short and long (1, 7, and 39 hours) incubation times on various metabolic functions. High metformin concentrations (0.5-2mM) caused activation of AMPK and inhibition of ACC activity within 1h but lower concentrations of metformin required longer incubation (7h for 50μM and 39h for 10-20μM metformin). The effects of metformin that were attributed to activation of AMPK included: (i) inhibition of ACC activity; (ii) stimulation of fatty acid oxidation; (iii) inhibition of gluconeogenesis; (iv) inhibition of SREBP-1 activity and mRNA expression; (iv) repression of FAS and S14 mRNA levels: (v) stimulation of glucose transport in muscle. This study proposed that the effects of metformin can be explained by activation of AMPK based on: (i) evidence that metformin activates AMPK; (ii) evidence that AICAR similarly to metformin causes both activation of AMPK and inhibition of gluconeogenesis; (iii) evidence that compound C inhibits both the activation of AMPK by metformin and the inhibition of gluconeogenesis (Zhou et al., 2001).

Later work provided further support for the role of AMPK activation in the metformin mechanism through studies on mice that lack LKB-1 (Shaw et al., 2005). In this mouse model metformin at a dose up to 250mg.kg^{-1} did not cause either activation of AMPK or lowering of blood glucose. These findings further reinforced the conclusion that the lowering of blood glucose by metformin is mediated by activation of AMPK. In this study Shaw and colleagues (2005) reported that metformin induced AMPK-phosphorylation via activation of its upstream tumour suppressor gene LKB-1. Liver-selective LKB1 $^{-/-}$ mice (deficient in LKB-1) were generated to investigate the role of LKB-1 in the metformin effect on AMPK-phosphorylation. Inhibition of AMPK-phosphorylation on Thr^{172} was confirmed in liver tissue from LKB-1 $^{-/-}$ mice. In these mice the level of plasma glucose was higher, and lipogenic and gluconeogenic gene expression was increased. High metformin treatment 250mg.kg^{-1} to wild-type and LKB-1 knockdown mice for three days showed that the effect of metformin to phosphorylate AMPK

was abolished in the liver of LKB-1 $^{-/-}$ mice, and metformin had no effect on blood glucose compared to wild-type. The authors reported that the upstream kinase (LKB-1) of AMPK has a pivotal role in metformin's mechanism to lower glucose through regulation of gluconeogenic gene expression. This study provided further support for the role of AMPK in the metformin mechanism (Shaw et al., 2005).

1.5.3 Metformin suppresses gluconeogenic gene expression by an AMPK linked mechanism

Several studies reported that the repression of enzymes of gluconeogenesis by metformin occurs via an AMPK linked mechanism. Some groups proposed that gene suppression by low metformin is independent of complex 1 inhibition through an unknown mechanism for activation of AMPK (He and Wondisford, 2015) . Glucagon which is elevated during fasting and also in Type 2 diabetes (Finan et al., 2019, Dunning and Gerich, 2007) stimulates gluconeogenesis by binding to the glucagon receptor (GR) on hepatocytes, a G-protein coupled receptor which activates adenylyl cyclase causing elevation in cAMP which binds to the regulatory subunits of protein kinase A (PKA) causes dissociation and activation of the catalytic units from inactive to active form (Figure 1-2) (Yang and Yang, 2016). Activation of cAMP-PKA pathway by glucagon phosphorylates the transcriptional factor cAMP-response element binding protein (CREB) at Ser^{133} and dephosphorylates CREB-regulated transcriptional co-activator 2 (CRTC2) which results in the formation of the transcriptional complex CREB-CBP-CRTC2. The latter complex induces the expression of the gluconeogenic transcriptional factor peroxisome proliferator-activated receptor-γ coactivator-1 α (PGC-1α) and its downstream genes glucose 6-phosphatase (G6pc) and phosphoenolpyruvate carboxykinase (PEPCK) (Hanson and Reshef, 1997, Kim et al., 2012, Oh et al., 2013).

Studies by Wondisford's laboratory proposed that metformin inhibits gluconeogenic gene expression by activation of AMPK which phosphorylates CRTC2 and CBP which leads to disassembly of the CREB-CBP-CRTC2 complex and causes inhibition of gluconeogenic gene expression (He et al., 2009, Cao et al., 2014, He et al., 2016a, Meng et al., 2015). He and colleagues (2009) proposed that metformin like AICAR phosphorylated CBP Ser^{436} resulting in dissociation of the CREB-CBP-CRTC2 and inhibited gluconeogenesis by a mechanism mediated by AMPK activation. This effect was also mimicked by AMPK overexpression and the anti-hyperglycaemic effect of metformin was abolished in mice lacking the CBP phosphorylation site (He et al., 2009). Moreover, evidence from the same laboratory has shown that metformin (≤80μM) suppresses glucose production in the presence of exogenous cAMP

and glucagon-stimulated glucose production via AMPK-activation, which regulates the effect of cAMP-PKA pathway in mouse hepatocytes. In this study they reported that low metformin concentration (≤80μM) has the ability to phosphorylate AMPK and inhibit gluconeogenic gene expression in mouse liver (Cao et al., 2014).

SHP is a member of the nuclear receptor family lacking a typical DNA-binding domain and is expressed in liver (Zhang et al., 2011). In liver it represses the binding of CREB-CBP-CRTC2 complex and suppresses the downstream target gluconeogenic genes (PEPCK and G6Pc) (Lee et al., 2007, Chanda et al., 2008). Work from Choi's laboratory (2008 and 2010) proposed that metformin induces SHP expression and suppresses hepatic gluconeogenic gene expression through activation of AMPK that activation of AMPK by metformin causes induction of SHP which inhibits induction of gluconeogenic gene expression by the CREB-CRTC2 complex (Kim et al., 2008). Inhibition of glucose production by metformin persisted with constitutively active CRTC2 but was abolished by SHP knockdown. Additionally, AMPK-mediated suppression of the promoter activity of G6Pc and PEPCK was also abolished by SHP knockdown (Lee et al., 2010).

Fullerton and colleagues (2013) reported that acute metformin treatment to knock-in mice with ACC mutation of the AMPK phosphorylation site (AccKDI) did improve insulin sensitivity and lowered *de novo* lipogenesis. Metformin increased the phosphorylation of ACC in wild-type mice but not in AccKDI, however, metformin increased the phosphorylation of AMPK in both mouse genotypes. This effect was mimicked by A-769662. Inhibition of gluconeogenic genes (G6Pc and PEPCK) by metformin was abolished in AccKDI compared to wild-type mice (Fullerton et al., 2013).

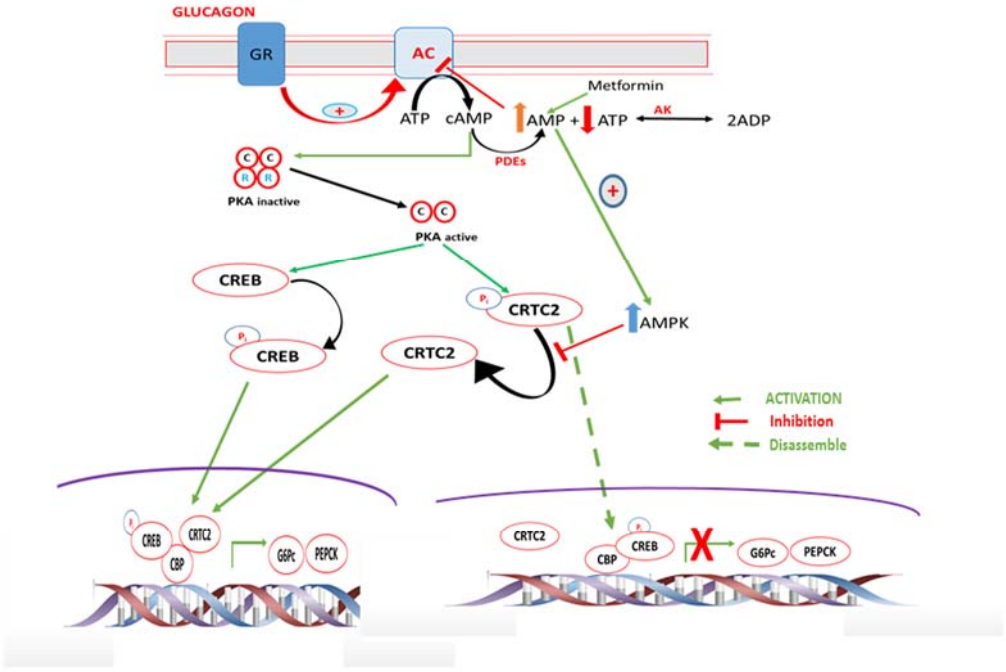

Figure 1-2:- Schematic diagram for the proposed interaction of metformin with glucagon signaling and suppression of gluconeogenic gene expression.

Glucagon binds to its receptor on the cell membrane promoting activation of AC and generation of cAMP. cAMP binds to the R-subunits of the inactive form of PKA resulting in conformational changes in the R-subunit and release of the active C-subunits (Yang and Yang, 2016). The latter subunits phosphorylates the transcription factor CREB and promotes dephosphorylate CRTC2 resulting in the formation of the CREB-CEP-CRTC2 complex. This complex induces the expression of gluconeogenic genes (Hanson and Reshef, 1997, Kim et al., 2012, Oh et al., 2013). Metformin through activation of AMPK counteracts the dephosphorylation of CRTC2 causing the dissociation of CREB-CEB-CRTC2 complex and suppresses the expression of gluconeogenic genes (He et al., 2016b, He et al., 2009).

AC, Adenylyl cyclase; AK, Adenylyl kinase; C, catalytic subunit; CREB, cAMP-response element binding protein; CRTC2, CREB-regulated transcriptional co-activator 2; GR, glucagon receptor; PDEs, phosphodiesterases; R, regulatory subunit.

1.5.4 AICAR is an activator of AMPK and an inhibitor of FBP-1

AICAR is an adenosine analogue that enters the cell through the adenosine transport system and is phosphorylated to 5-aminoimidazole-4-carboxamide-1-β-D-ribonucleotide (ZMP) by adenosine kinase. The intracellular concentration of ZMP increases to millimolar levels after uptake of AICAR and this functions as an AMP mimetic without affecting the intracellular level of ATP, AMP and ADP (Corton et al., 1995, Merrill et al., 1997, Sabina et al., 1985, Vincent et al., 1991). Vincent and colleagues (1991) reported that gluconeogenesis was inhibited by 100-500μM AICAR in rat hepatocytes incubated with different gluconeogenic precursors (lactate plus pyruvate, fructose, and dihydroxyacetone). The inhibition of gluconeogenesis from lactate plus pyruvate as substrate by 500μM AICAR was associated with changes in gluconeogenic metabolites which involved a decrease in F6P, and G6P and an increase in fructose 1,6 bisphosphate. The increase in F1,6-P_2 and the decrease in F6P and G6P were also observed in hepatocytes incubated with fructose or DHA as substrates. This identified a mechanism linked to inhibition of fructose 1,6-bisphosphatase-1 (FBP-1) by ZMP similarly to AMP. Therefore they concluded that the mechanism of inhibition of gluconeogenesis by AICAR is due to inhibition of fructose 1,6-bisphosphatase-1 (FBP-1) (Vincent et al., 1991). A later study by Vincent and colleagues (1992) reported the biphasic effects of AICAR on glucose metabolism in hepatocytes. They showed that lactate production from 15mM glucose was inhibited by 10-100μM AICAR and addition of higher AICAR concentrations (200-500μM) increased the production of lactate. They also showed an inhibitory effect of AICAR on glucokinase and lowering of cell G6P and F6P. In addition fructose 2,6-P_2 a potent activator of PFK-1 was also decreased by AICAR. They concluded that AICAR inhibited glycolysis by inhibition PFK-1 and by inhibition of glucokinase (Vincent et al., 1992).

Activation of AMPK by AICAR was shown in many studies. Sullivan and colleagues (1994) reported that AICAR activates AMPK in a concentration and time-dependent manner in adipocytes (Sullivan et al., 1994). AICAR also activated AMPK in rodent muscle *in vivo* and *in vitro* (Jorgensen et al., 2004, Kjobsted et al., 2015, Musi et al., 2001). Corton *et al* (1995) reported that AICAR mimics the effect of AMP on AMPK and increases AMPK-phosphorylation in hepatocytes resulting in increased phosphorylation and inactivation of, the downstream target of AMPK, 3-hydroxy-3-methylglutaryl-CoA reductase without affecting the nucleotides (ATP, AMP, and ADP) (Corton et al., 1995). The mechanism by which AICAR activates AMPK was linked to activation on the regulatory γ-subunit on AMPK as proposed by Day and colleagues (Day et al., 2007). This subunit has four tandem repeats called cystathionine β-synthase domain (CBS) which makes up the binding site to the adenosine nucleotides on γ-

subunit. Binding of AMP or ZMP to the γ-subunit allosterically activates AMPK on the α-subunit favouring phosphorylation (Oakhill et al., 2012). Lochhead and colleagues (2000) reported that the effect of AICAR on gluconeogenic gene expression from different cell lines and thereby inhibition of gluconeogenesis is mediated by AMPK activation (Lochhead et al., 2000). On the other hand, the study by Hasenour and colleagues (2014) reported an inhibitory effect of AICAR on gluconeogenesis that is not mediated by activation of AMPK. This study investigated the effect of AICAR in the liver of mice with AMPK α1 and 2 deficiency compared with wild-type mice. Inhibition of hepatic glucose production by AICAR was observed in both genotypes (Hasenour et al., 2014).

1.5.5 A-769662 and salicylate are direct activators of AMPK

A-769662 a member of the thienopyridone family has been identified as a direct activator of AMPK (Cool et al., 2006, Sanders et al., 2007a). Cool and colleagues (2006) proposed that activation of AMPK by A-769662 had many beneficial effects in hepatocytes and liver from Sprague Dawley rats. A-769662 increased the phosphorylation of the AMPK substrate (ACC), and inhibited fatty acid synthesis as a result of inhibition of ACC activity and decreased malonyl CoA levels in rat liver. They reported that treating mice with 30mg/kg A-769662 lowered plasma glucose, decreased plasma and liver triglycerides and suppressed the expression of gluconeogenic genes (*Pck1, G6Pc*). They showed that A-769662 increased AMPK activation by a mechanism independent of an increase in AMP but by direct AMPK activation. They reported that metformin (450mg/kg) like A-769662, lowered plasma glucose, liver triglycerides, and liver malonyl CoA in mice (Cool et al., 2006). The mechanism by which A-769662 activates AMPK was described by Sanders and colleagues (2007) by binding to the glycogen binding domain on the β-subunit. A-769662 activates AMPK in purified recombinant AMPK complexes (α1β1γ1 and α2β1γ1) and inhibits the dephosphorylation on Thr^{172}. The inhibition of dephosphorylation on Thr^{172} by A-769662 was also observed in rat liver (Sanders et al., 2007a). A-769662 synergistically with other AMPK activators such as metformin, phenformin, and oligomycin improved AMPK phosphorylation in rat cardiomyocytes more effectively than A-769662 alone (Timmermans et al., 2014).

Salicylates, formed from break down of aspirin and salsalate *in vivo*, similar to A-769662 cause allosteric activation and inhibition of dephosphorylation on the AMPK Thr^{172} by binding to the glycogen binding domain of the β-subunit (Hawley et al., 2012). Metformin is an indirect AMPK activator through changes in adenosine nucleotides (AMP and ATP). Ford and

colleagues (2015) reported that metformin and salicylate in combination caused concentration-dependent phosphorylation of ACC and inhibition of lipogenesis in mouse hepatocytes and liver. These effects were also observed in primary human hepatocytes and insulin resistance was markedly improved in patients treated with metformin and salicylate in combination compared with either drug alone (Ford et al., 2015b).

1.5.6 Metformin activates AMPK through inhibition of complex 1 resulting in increased cellular AMP

Increasing the cellular AMP concentration stimulates the activity of AMPK through binding to the γ-subunit and enhancing LKB-1 to phosphorylate Thr^{172} (Gowans et al., 2013). Zhou and colleagues (2001) reported that metformin activates AMPK in hepatocytes but that it does not directly activate purified AMPK (Zhou et al., 2001). This cannot be explained by direct effect on AMPK or the upstream LKB-1 and CaMKK-β but is best explained by indirect effect through increasing the cellular AMP concentration by inhibition of mitochondrial respiration complex 1 (Hardie, 2006, Hawley et al., 2005, Fogarty et al., 2010). The inhibition of complex 1 by metformin resulted in changes in adenine nucleotides, ATP and AMP, homeostasis. This observation suggested that metformin activated AMPK due to an increase in AMP to ATP ratio secondary to inhibition of complex 1 (Bridges et al., 2014, El-Mir et al., 2000, Owen et al., 2000). Hawley and colleagues (2010) reported that metformin activates AMPK through inhibition of mitochondrial respiration at complex 1. In a human cell line they generated an AMPK-insensitive AMPK-γ2 (R531G) mutant and because the expression of a single subunit is unstable in cells therefore they expressed all the three α, β, and γ complexes (wild type) and investigated the effects of AMPK activators. A-769662 but not AMP increased AMPK activity in both WT and mutant cells indicating that A-769662 activates AMPK on a different site from AMP. All activators increased the phosphorylation and the activity of AMPK in the wild-type cell line and the effects of mitochondrial inhibitors (metformin, phenformin, oligomycin, and DNP) and the AMP mimetic (AICAR) on AMPK activation and phosphorylation, were abolished in cells with mutation in AMP-insensitive site (RG), while A-769662, a direct activator of AMPK, did activate and phosphorylate AMPK in wild-type and mutant RG cells. Mitochondrial inhibitors, except metformin, increased the ADP to ATP ratio in wild-type and in mutant RG cells. Metformin inhibited oxygen uptake in both wild-type and RG mutant cells (Hawley et al., 2010). These results suggest that activation and phosphorylation of AMPK by metformin is due to inhibition of mitochondrial respiration (Hawley et al., 2010, Hardie, 2014)

1.5.7 Inhibition of AMP-deaminase

Activation of AMPK by metformin by inhibiting AMP-deaminase (AMPD) was proposed by Ouyang and colleagues (2011), AMPD catalyses AMP deamination to inosine monophosphate (IMP). In this study both metformin (10mM) and the AMPD inhibitor erytho-9-(2-hydroxy-3-nonyl)-adenine (EHNA) increased glucose uptake and palmitate oxidation in L6 cell. These effects were associated with increased AMPK phosphorylation. They also reported that metformin (10mM) inhibited the activity of purified AMPD from rabbit muscle. The effect of metformin on glucose uptake was abolished by AMPD1 knockdown but not with LKB-1 knockdown in L6 cell. The inhibitor of complex 1, rotenone, like metformin stimulated glucose uptake in L6 cell but without increased fatty acid oxidation (Ouyang et al., 2011). In the later study they reported that both metformin (15mM) and the inhibitor of AMPD (EHNA) increased the cellular concentration of AMP without effecting ATP concentration. They suggested that metformin stimulates glucose uptake by inhibition of AMPD by a mechanism independent of inhibition of complex 1 (Vytla and Ochs, 2013).

1.5.8 Metformin activates AMPK through a lysosomal signalling pathway

It has been reported that activation of AMPK by glucose starvation or by AICAR treatment occurs on the surface of the lysosome. AXIN is a scaffold protein and negative regulator in the Wnt signalling pathway (Song et al., 2016). An increase in AMP concentration drives AXIN to directly tether LKB1 and form the AXIN-AMPK-LKB1 complex. AXIN-knockdown in mice abolished the phosphorylation of AMPK by raised AMP. This established an essential role of AXIN in mediating AMPK activation by LKB1 (Zhang et al., 2013). The lysosomal v-ATPase-Ragulator complex plays a pivotal role in the AMPK activation mechanism by docking the AXIN-AMPK-LKB1 complex on the surface of the lysosome (Zhang et al., 2018). Recently, Zhang and colleagues (2016) reported that metformin activates AMPK via the lysosomal pathway. This study reported that phosphorylation of AMPK by metformin was abolished in mouse liver and hepatocytes lacking AXIN. Moreover, phosphorylation of AMPK by metformin was completely abolished in the liver of mice with specific knockout of LAMTOR1, a protein that is anchored to the lysosomal membrane (Lin and Hardie, 2018), and the effect of metformin on AMPK phosphorylation was also abolished in hepatocytes lacking LAMTOR1. Furthermore, phosphorylation of AMPK by metformin was also abolished in a cell line with knockdown in 6v0c subunit of v-ATPase. These results demonstrated the role of AXIN-LKB1 complex and the lysosomal pathway in mediating the metformin mechanism to activate AMPK (Zhang et al., 2016). Additionally, metformin abolished complex formation of mTORC1 in MEF cells indicating that metformin inactivates mTORC1. Mechanistic Target Of Rapamycin

Complex 1 (mTORC1) is a complex formed from the protein kinase mTOR and the non-catalytic polypeptide RAPTOR. It has an important role to regulate catabolic and anabolic process (Chao and Avruch, 2019). Together metformin activates AMPK phosphorylation by a mechanism involving activation of ANIX-LKB1-v-ATPase-Ragulator pathway and dissociation the mTORC1 resulting in switch off of anabolic metabolism (Zhang et al., 2016).

1.5.9 AMPK-independent mechanisms

The generation of an AMPK deficient mouse provided an animal model to test for AMPK-independent mechanisms. (Foretz et al., 2010, Guigas et al., 2006). Guigas and colleagues (2006) reported that metformin inhibited glucose phosphorylation by abolishing the translocation of glucokinase from the nucleus to cytoplasm through a mechanism independent on AMPK activation and in association with lowering of cellular ATP. In this study the effect of metformin was compared with the AMP mimetic 5-aminoimidazol-4-carboxamide-1-β-D-ribofuranoside (AICAR) and oligomycin (an ATP-synthase inhibitor) in rat and mouse hepatocytes. Metformin like AICAR inhibited glucose phosphorylation in rat hepatocytes. This effect cannot be explained by AMPK activation because both AICAR and metformin inhibited glucose phosphorylation in AMPK-deficient mouse hepatocytes. The inhibition of glucose phosphorylation was associated with depletion in ATP with AICAR, metformin, and oligomycin. The inhibition by AICAR was stronger than could be explained by ATP depletion in rat hepatocytes and in hepatocytes from WT mice (Guigas et al., 2006)

Furthermore, Foretz and colleagues (2010) investigated the effect of metformin in mice lacking either hepatic AMPK or LKB1. The rate of gluconeogenesis was increased in LKB1-deficient mice, but not in AMPK-deficient mice, compared with wild type. They reported that the inhibition of glucose production by metformin (0.25-2mM) was increased in LKB1-deficient and AMPK-deficient hepatocytes compared with hepatocytes from wild type mice. In addition, metformin suppressed the expression of G6pc mRNA in hepatocytes from all mouse genotypes. They reported that metformin lowered the ATP level *in vivo* and *in vitro*. Therefore, they concluded that the inhibition of glucose production by metformin in hepatocytes is not mediated by AMPK activation, but is due to lowering in ATP (Foretz et al., 2010).

1.5.10- Indirect inhibition of adenylate cyclase

Although a major complication of type 2 diabetes is insulin resistance, in recent years there has also been focus on the role of raised blood glucagon in type 2 diabetes. This has led to therapies that target glucagon signalling such as glucagon-like peptide-1 (GLP-1) (D'Alessio, 2011). A role of metformin on glucagon signalling has been proposed by Miller and colleagues (2013). Glucagon binds to its receptor in the plasma membrane of hepatocytes and causes activation of adenylyl cyclase which results in phosphorylation of protein kinase A (PKA) by the second-messenger cyclic AMP (cAMP) which leads to an increase in hepatic glucose production (Jiang and Zhang, 2003). Miller and colleagues reported that metformin exerts its anti-hyperglycaemic effect through inhibition of glucagon signalling. Mouse hepatocytes were used to investigate the effect of biguanides (metformin and phenformin) on glucagon signalling. Phenformin attenuated the increase in PKA caused by glucagon in hepatocytes. Moreover, the levels of AMP and ADP were increased in hepatocytes untreated and treated with glucagon in the presence of 250-500μM metformin and >125μM metformin abolished the effect of glucagon but not the effect of a membrane-permeable cAMP analogue (SP-8Br-cAMPS-AM) to stimulate gluconeogenesis. The inhibition of glucose production by metformin was abolished in hepatocytes with overexpression of a dominant-negative PKA regulatory subunit which prevents cAMP binding. This indicated that the effect of biguanides is at a signalling step upstream of PKA activation. Metformin 250mg/kg increased the accumulation of AMP in the liver of fasted mice after 60 minutes. Phenformin (250-500μM) also increased the accumulation of AMP in hepatocytes. They suggested that metformin inhibited gluconeogenesis by increasing AMP accumulation and inhibition of the glucagon stimulation of adenylyl cyclase activation. This mechanism was confirmed to be AMPK-independent from experiments on hepatocytes from AMPK-deficient mice (Miller et al., 2013)

1.5.11 Indirect inhibition of fructose 1,6-bisphosphatase (FBP-1)

A recent study by Hunter and colleagues (2018) reported that the effect of metformin on inhibition of gluconeogenesis is through inhibition of fructose 1,6-bisphosphatase as a secondary effect of increased AMP concentration causing allosteric inhibition of FBP-1. In this study, the effect of metformin was investigated in the liver of mice with a mutation (Knock-in) in FBP-1 that makes it insensitive to AMP. Metformin up to 10mM had no direct inhibitory effect on FBP-1, and also it had no effect on AMP-deaminase 1 (AMPD1). They observed that FBP1-KI mice had no differences in plasma glucose, gluconeogenesis rate, and the activities of gluconeogenic and glycolytic enzymes were similar in both mouse genotypes with significant changes in G6Pc and GK at mRNA level but not at protein level. The effects of MB05032 (an

AMP mimetic FBP1 inhibitor) and AICAR (an AMP-mimetic ZMP) on blood glucose and blood lactate formation were more pronounced in wild-type mice than in FBP1-KI mice, and plasma glucagon increased with AICAR in wild-type but not in FBP1-KI mice. AICAR increased the phosphorylation of AMPK and ACC in both mouse genotypes. In both wild-type mice and in FBP1-KI mice 250 mg per kg metformin concentration raised hepatic AMP to ATP ratio and decreased ATP, resulting in AMPK activation and ACC phosphorylation. In this study they created metformin-euglycaemic clamp study by infusion of two different metformin concentrations (1.875mg/kg per min, and 3.75mg/kg per min.) and variable glucose infusion for 2h to reach euglycaemia in both mouse genotypes. The low (1.875mg/kg per min) metformin dose did not increase the rate of glucose disposal in either mouse genotype, while high metformin (3.75mg/kg per min) increased the glucose disposal rate in wild type mice but not in FBP1-KI mice. The anti-hyperglycaemic effect of 250mg/kg metformin in wild type mice fed with high-fat diet was abolished in FBP1-KI mice fed with high-fat diet. They showed that the level of fructose 6-phosphate was decreased, and the level of fructose 1,6-bisphosphate was increased in the liver of wild type mice, but not in FBP1-KI mice, treated with metformin. This study concluded that metformin lowered hepatic glucose production by inhibiting FBP1 as a secondary effect to the increase in hepatic AMP. Although, the authors did not completely exclude FBP-1 independent mechanisms because they noticed a small but significant lowering of plasma glucose by metformin in FBP1-KI mice (Hunter et al., 2018)

1.5.12 Inhibition of mitochondrial glycerol-3-phosphate dehydrogenase

A recent study by Madiraju and colleagues (2014) reported that the metformin inhibitory effect on gluconeogenesis and lowering of plasma glucose appeared 30 minutes after treating rats with either 20mg/kg or 50mg/kg metformin (intravenous IV administration). This study criticized previous studies that used metformin concentrations higher than the relevant therapeutic metformin dose (Wilcock and Bailey, 1994). They reported that the decrease in plasma glucose and rapid increase in plasma lactate were observed in rats infused with a monoguanide for 20 minutes without any change in hepatic gluconeogenic gene expression but with increased AMPK activity. However, an AMPK activator (A-769662) did not lower plasma glucose and endogenous glucose production in rats. This suggested that inhibition of glucose production by metformin is not mediated by AMPK activation. Due to a massive increase in plasma lactate that cannot be explained by differences in activity of enzymes which regulate pyruvate metabolism they proposed that the increase in plasma lactate by metformin might be due to an increase in cytosolic redox state (increase the lactate to pyruvate ratio). Treating rats with 20mg/kg and 50mg/kg metformin rapidly lowered plasma glucose and inhibited endogenous

glucose production with concomitant increase in the lactate to pyruvate ratio in plasma and liver. The more reduced cytoplasmic redox state by metformin was associated with a decrease in the 3-hydroxybuytyrate to acetoacetate ratio suggesting a more oxidised mitochondrial redox state in liver. This study proposed that inhibition of gluconeogenesis occurs in the absence of inhibition of complex 1. Moreover, Metformin had no effect on either the protein expression of gluconeogenic enzymes (PEPCK and pyruvate carboxylase; PC), cAMP response element binding protein (CREB) or on phosphorylation of AMPK and its downstream target ACC. Acute and chronic metformin treatment caused increased plasma glycerol level indicating either inhibition of conversion of glycerol to glucose or increased glycerol production. They proposed that metformin inhibited glucose production from glycerol by a mechanism linked to alteration in the redox state and that the more reduced cytoplasmic and more oxidised mitochondrial redox states by metformin can be explained by inhibition of the transfer of NADH equivalents from the cytoplasm to mitochondria (Madiraju et al., 2014).

The malate-aspartate (MAS) and the glycerophosphate (GPS) shuttles have been identified as the main shuttles that transfer NADH reducing equivalents (Bremer and Davis, 1975, Garrib and McMurray, 1986). The MAS is a reversible shuttle involving two enzymes (malate dehydrogenase and aspartate aminotransferase), present in both the cytoplasm and mitochondria together with the carrier proteins (aspartate-glutamate carrier and malate- α-ketoglutarate carrier). This shuttle works to transfer NADH reducing equivalent formed in cytoplasm to mitochondria via reducing oxaloacetate to malate in the cytoplasm catalyzed by cytoplasmic malate dehydrogenase. Malate enters the mitochondrial matrix through the antiporter transport system (malate- α-ketoglutarate carrier) and exchanges with oxo-ketoglutarate to cytoplasm. Mitochondrial malate dehydrogenase oxidises malate to oxaloacetate in mitochondria and reduces NAD^+ to NADH. The inner mitochondrial membrane is impermeable to oxaloacetate, which is transaminated by mitochondrial aspartate aminotransferase with glutamate as co-substrate to aspartate and α-ketoglutarate. Aspartate is exported from the mitochondria on an electrogenic transporter (aspartate-glutamate carrier) in exchange for glutamate. The transport mechanism is dependent on mitochondrial membrane potential and is very sensitive to depolarization of the mitochondria. In the cytoplasm oxaloacetate is regenerated from aspartate by cytoplasmic aspartate aminotransferase to complete the malate-aspartate shuttle (McKenna et al., 2006, Minarik et al., 2002). The GPS is the other shuttle, it couples the conversion of dihydroxyacetone phosphate (DHAP) to glycerol 3-phosphate (G3P) generating NAD^+ in cytoplasm through cytoplasmic glycerophosphate dehydrogenase (cGPDH) with the metabolism of G3P by mitochondrial glycerophosphate

dehydrogenase (mGPDH). The latter enzyme is embedded in the outer surface of inner mitochondrial membrane to generate DHAP. mGPDH is a Flavin-linked mitochondrial dehydrogenase which transfers the reducing equivalent via FAD^+ to form FADH and transfers electrons to ubiquinone which is reduced to ubiquinol bypassing the first step in complex 1 (McKenna et al., 2006, Mracek et al., 2013, Chowdhury et al., 2005). These two enzymes together form the GPS. However, cGPDH is not rate-limiting for glycerophosphate shuttle (Mracek et al., 2013, Iossa et al., 1995).

The role of the MAS was excluded because metformin had no effect on the activity of either malate dehydrogenase or aspartate aminotransferase. Madiraju and colleagues (2014) reported that metformin did not affect the activity of purified cytoplasmic glycerophosphate dehydrogenase but inhibited the activity of purified mitochondrial glycerophosphate dehydrogenase by 50%. Moreover, they reported that 50μM metformin inhibited oxygen uptake in isolated mitochondria from 10mM glycerol 3-phosphate. Furthermore, they reported that glucose production was inhibited by either 100μM metformin or short interfering RNA (siRNA) for knockdown of mGPDH in rat hepatocytes incubated with 10mM lactate plus 1mM pyruvate but not with 1mM lactate plus 10mM pyruvate as substrates. The authors suggested that the inhibition of gluconeogenesis by both metformin and mGPDH knockdown involves a redox-dependent mechanism. They proposed that inhibition of mGPDH abolished the conversion of glycerol to glucose and caused an increase in cytoplasmic NADH which leads to inhibition of the conversion of lactate to pyruvate by lactate dehydrogenase and glucose production from reduced substrates (lactate and pyruvate) but not from oxidised substrates (dihydroxyacetone, alanine, and pyruvate) which was inhibited by both 100μM metformin and siRNA for mGPDH knockdown. This inhibition of glucose production by 100μM metformin and siRNA for mGPDH knockdown was associated with an increase in cell G3P in hepatocytes. The increase in cell G3P was also confirmed in liver of rats treated with 50mg/kg. They reported that knockdown of mGPDH but not cGPDH like metformin also caused inhibition of glucose production and a more reduced cytoplasmic redox state and a more oxidised mitochondrial redox state and mGPDH knockdown abolished the effects of metformin on glucose production and redox states. These results suggested that the metformin inhibition of glucose production from reduced gluconeogenic precursors is by inhibition of mGPDH. (Madiraju et al., 2014).

Recently, Madiraju and colleagues (2018) further confirmed that the metformin inhibitory effect is through a redox-dependent mechanism because metformin inhibited gluconeogenesis from lactate but not from alanine *in vivo*. Accordingly, they concluded that metformin disrupted

the glycerophosphate shuttle either directly or indirectly and inhibited glucose production from glycerol and lactate as a result in a more reduced cytoplasmic redox state (increase NADH to NAD^+) (Madiraju et al., 2014, Madiraju et al., 2018). The caveats to this mechanism are: first, it predicts that inhibition of gluconeogenesis by metformin is a redox-dependent, whereas other mechanisms predict inhibition of gluconeogenesis by a redox-independent mechanisms (Miller et al., 2013, Hunter et al., 2018). Second, it predicts a more oxidised mitochondrial redox state (decrease NADH to NAD^+ ratio) as opposed to a more reduced mitochondrial redox state (increase NADH to NAD^+ ratio) through inhibition of complex 1 (El-Mir et al., 2000, Fulgencio et al., 2001, Owen and Halestrap, 1993, Hunter et al., 2018) and a more reduced cytoplasmic redox state. However, this mechanism has been challenged by others based on three considerations: first, the MAS is thought to have a more prominent role in the liver than the GPS on both man and mouse (Saheki et al., 2007). Second, GAPDH consumes NADH generated in cytoplasm during gluconeogenesis (Baur and Birnbaum, 2014). Third, a recent study reported that the effect of metformin to inhibit glucose production from 5mM lactate in the perfused rat liver required a minimum concentration of metformin of 400µM rather than 100 µM (Calza et al., 2018).

1.6 Substrate and inhibitors used in this thesis

The present thesis explored the different mechanisms that have been proposed to explain the inhibition of gluconeogenesis by metformin, with particular emphasis of the mitochondrial redox state and the role of the NADH shuttles (Figure 1-3). Octanoate was used as a source of mitochondrial acetyl-CoA. Octanoate enters the mitochondria as the free acid and is then converted to octanoyl-CoA and metabolized by β-oxidation to generate acetyl-CoA, which is then further metabolized by ketogenesis to form acetoacetate, which is reduced by hydroxybutyrate dehydrogenase to 3-hydroxybutyrate. The activity of hydroxybutyrate dehydrogenase in the mitochondrial matrix is high and near-equilibrium. The ratio of 3-hydroxybutyrate to acetoacetate therefore reflects the NADH/NAD in the mitochondrial matrix. The rate of production of acetoacetate and 3-hydroxybutyrate was determined as a measure of octanoate β-oxidation (Ferre et al., 1983) and the ratio of 3-hydroxybutyrate to acetoacetate as a measure of changes in the mitochondrial redox state (Williamson et al., 1967) (Table 1-1)

To test the role of inhibition of Complex 1, the first reaction of the respiratory chain that catalyses the NADH oxidation, rotenone was used as an irreversible inhibitor of complex I. Rotenone inhibits the reduction of ubiquinone by binding irreversibly and competitively to the ubiquinone binding site (Heinz et al., 2017). To investigate mechanisms linked to a more oxidized mitochondrial NADH/NAD redox state, 2,4-dinitrophenol (DNP) was used to dissipate the proton gradient. The decrease in proton motive force by DNP results in a more rapid rate of electron transport and thereby in a decrease in the mitochondrial NADH/ NAD redox state. The transmitochondrial proton gradient that is generated by the electron transport chain at the level of Complex I, III and 1V drives electrogenic transport mechanisms across the mitochondrial inner membrane e.g. the ATP/ADP transporter and transport of inorganic phosphate (Pi) and also ATP synthase (Complex V) and the Nicotinamide nucleotide transhydrogenase (NNT). High concentrations of DNP cause total dissipation of the proton gradient and rapid ATP depletion. Measurement of cell ATP in experiments with inhibitors of the respiratory chain or uncoupler enables use of the low concentrations of mitochondrial inhibitors that have small to minimal effects on the proton gradient. This is particularly important in the use of rotenone and DNP which cause ATP depletion at elevated concentration (Lou et al., 2007).

To study gluconeogenesis we used either dihydroxyacetone which is phosphorylated by triokinase to DHAP an intermediate of the glycolytic and gluconeogenic pathways and represents an oxidised precursor or glycerol and xylitol which are reduced substrates that enter the pathway after NAD linked oxidation (Eggleston and Krebs, 1969, Flynn and McKay, 1972). Xylitol is converted to xylulose catalysed by the NAD-dependent xylitol dehydrogenase (Cook et al., 1973) and glycerol is phopshorylated by glycerokinase to glycero 3-phosphate and then further converted to DHAP either by the NAD-dependent cytoplasmic glycerophosphate dehydrogenase or by the mitochondrial glycerophosphate dehydrogenase (Mracek et al., 2013)

To investigate the role of inhibition of the GPS and MAS in metformin mechanism two shuttle inhibitors were used Figure 1-3. Gpi, the GPS inhibitor, inhibits mGPDH activity by binding at a single, allosteric binding site (Orr et al., 2014). AOA, the MAS inhibitor, is an inhibitor of pyridoxal phosphate dependent enzymes (Rognstad and Clark, 1974). AOA has been used in a very large number of studies and with a very wide range of concentrations. But some studies from the lab of Veech showed that in liver AOA is metabolized to various toxic products (glycolate and glyoxalte) if used at high concentrations. Therefore, in this study AOA was used

at the lowest concentration that causes an increase in the lactate to pyruvate ratio (Harris et al., 1982).

Table 1-1: Schematic table of medium metabolites assayed as measures of metabolic pathway or redox state.

Substrate	Medium metabolites	Composite metabolite equation	Pathway or redox state	Ref
Octanoate	Acetoacetate, 3-Hydroxybutyrate	Acetoacetate + 3-Hydroxybutyrate	Octanoate β-oxidation	(Ferre et al., 1983)
		Hydroxybutyrate/acetoacetate	Mitochondrial NADH/NAD redox state	(Williamson et al., 1967)
DHA, xylitol, glycerol	Lactate, pyruvate	Lactate + Pyruvate	Glycolysis	
		Lactate / Pyruvate	Cytoplasmic NADH/NAD redox state	(Williamson et al., 1967)
	Glucose	Glucose	Gluconeogenesis	
		Glucose + Lactate + Pyruvate	Total substrate metabolism	(Taleux et al., 2009)
		Glucose / (2G + L +P)	Fractional partitioning of substrate to glucose vs glycolysis	

Two strains of C57BL/6J were used in this study that have either an intact Nnt gene (C57BL/6JolaHsd) or deletion of the Nnt gene (C57BL/6J). The inbred mouse strain C57BL/6J commonly known as Black 6 was developed at the Jackson Laboratory, Bar Harbor, Maine, 1946. The C57BL/6J strain that is currently available from the Jackson Laboratory and from Charles River carries a homozygous spontaneous deletion in the Nnt gene (Freeman et al., 2006, Toye et al., 2005). Nnt encodes the nicotinamide nucleotide transhydrogenase (Table 1-2) which is an integral protein of the inner mitochondrial membrane and couples hydride transfer from NADH to $NADP^+$ to proton translocation across the inner mitochondrial membrane. The Black Six strain was transferred from the Jackson Laboratory to the UK in 1974 and to Olac, UK in 1984 and to Harlan Laboratories (Envigo) in 1985. The strain now designated C57BL/6JOlaHsd strain available from Envigo, UK and derived from the original Black 6 strain does not carry the Nnt gene deletion but carries a deletion in the Scna (Alpha synuclein). These mice do not show increased expression of either beta-synuclein or gamma-synuclein and spatial

learning in these mice is not affected (Specht and Schoepfer, 2001). These mice also carry a deletion in the Mnrn1 gene. Mulitmerin 1 is a platelet and endothelial cell adhesive protein that binds to collagen. These mice and have impaired platelet adhesion and impaired thrombus formation (Reheman et al., 2010). Genetic concordance between the two strains in 98.5%. Unless otherwise indicated mice of the C57BLJOlaHsd strain were used.

Table 1-2: Genetic differences between two strains of C57BL/6J mice used in this thesis.

Mouse strains	Supplier	Gene deletion			
		Nnt	Scna	Mnrn1	~~Rd8~~
C57BL/6J	Charles River	Yes	No	No	~~No~~
C57BL/6JOlaHsd	Harlan/Envigo	No	Yes	yes	~~N0~~

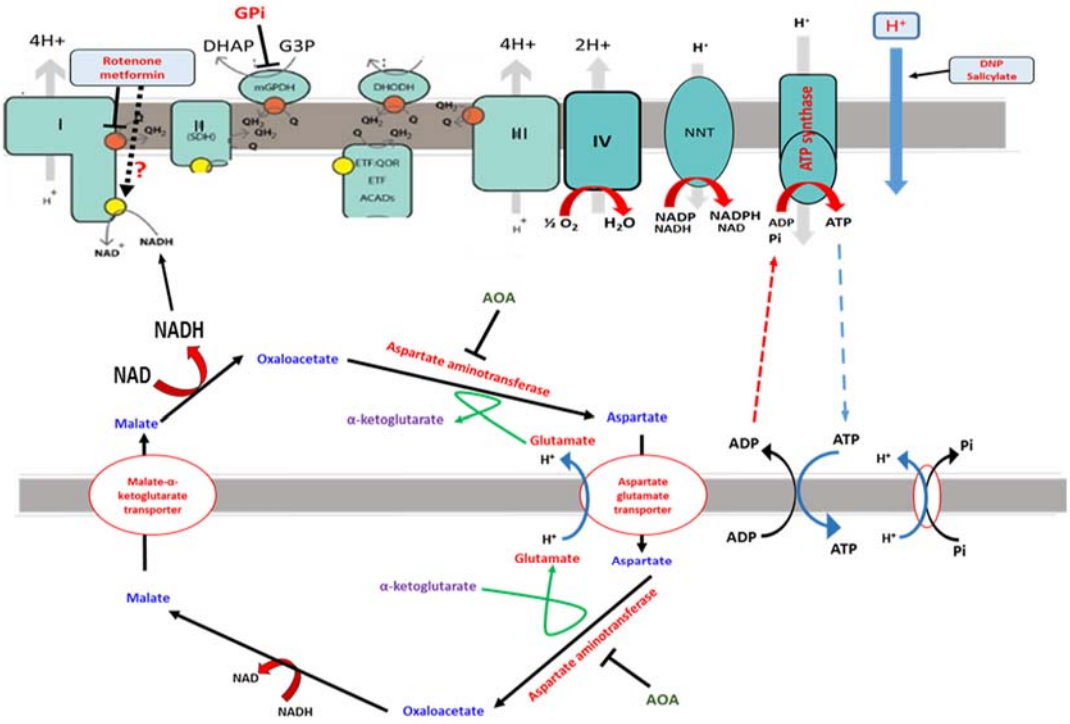

Figure 1-3: Schematic diagram for the electron transport chain and NADH shuttles and proposed action of inhibitors of mitochondrial function used in this thesis. Rotenone inhibitor of complex 1, Gpi inhibitor of mGPDH, DNP and salicylate uncouplers of the mitochondrial proton gradient, and AOA inhibitor of aspartate aminotransferase.

Modified form (Wong et al., 2017)

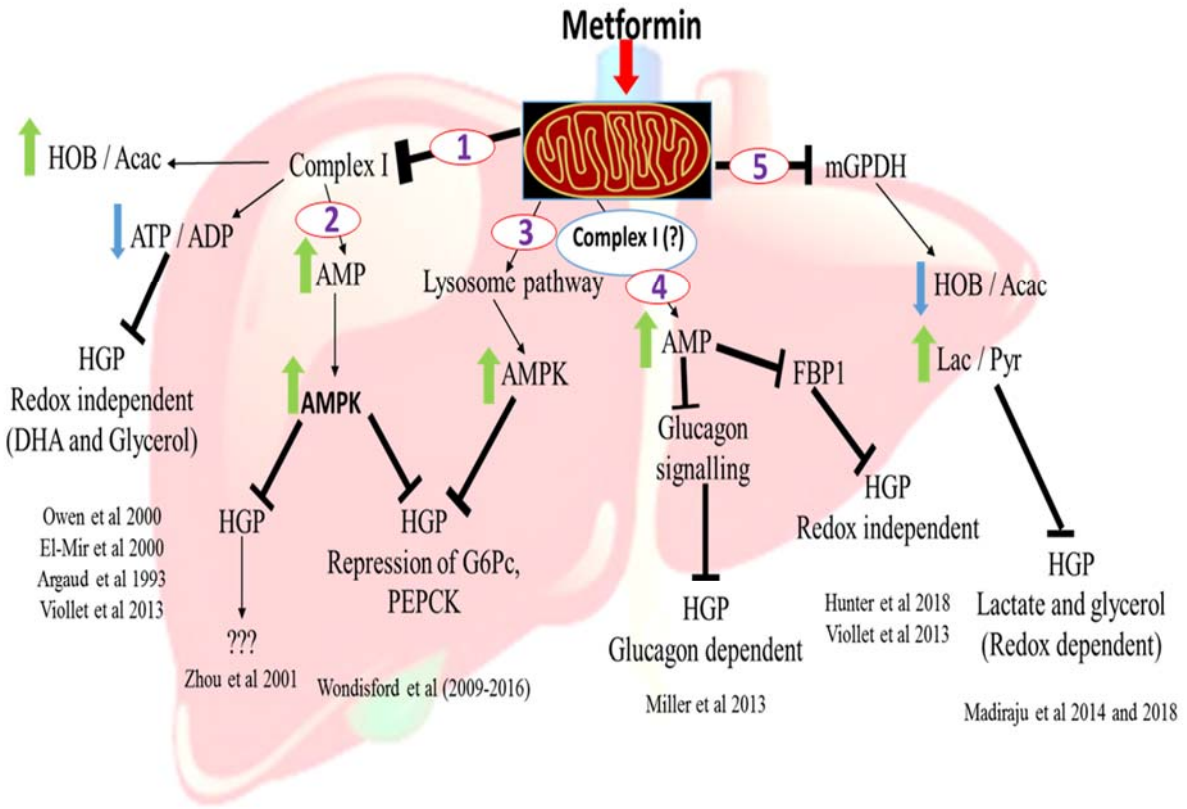

Figure 1-4: Schematic diagram of the proposed mechanisms for inhibition of gluconeogenesis by metformin.

Metformin accumulates in mitochondria in accordance with mitochondrial trasmembrane potential because of its positive charge. The proposed mechanisms include: (1) Inhibition of complex 1, the first complex of the respiratory chain resulting in an increase in NADH/NAD ratio and a decrease in the transmitochondrial proton gradient and a decrease in ATP/ADP ratio and raised AMP; (2) raised AMP causes activation of AMPK which has been reported to inhibit gluconeogenesis and expression of gluconeogenic genes; (3) activation of AMPK has also been reported to occur independently of inhibition of complex 1 through either inhibition of AMP-deaminase or through a lysosomal pathway; (4) raised AMP can inhibit gluconeogenesis independently of activation of AMPK by at least two pathways involving either inhibition of adenylate cyclase or inhibition of FBP-1 (5) metformin may inhibit gluconeogenesis from lactate and glycerol by inhibition of mGPDH resulting in a more oxidised mitochondrial redox state and a more reduced cytoplasmic redox state.

1.7 Hypothesis and Aims of the study

Previous studies on the mechanism by which metformin inhibits gluconeogenesis through a rapid acute effect that is independent of changes in gene expression have focused on each of four mechanisms (Figure 1-4). (1) Inhibition of gluconeogenesis through inhibition of Complex 1 resulting in a decrease in ATP/ADP ratio (Owen et al., 2000). (2) Activation of AMPK leading to acute inhibition of gluconeogenesis. This was supported by inhibition by AICAR and counteraction of the metformin effect by compound C (Zhou et al., 2001). (3) Inhibition of gluconeogenesis by an AMPK independent mechanism (Foretz et al., 2010, Hunter et al., 2018, Miller et al., 2013). This is supported by an inhibitory effect of metformin in hepatocytes from AMPK deficient mice. (4) A redox-dependent mechanism for inhibition of gluconeogenesis that occurs only with reduced but not oxidised substrates and that occurs in conditions of a more oxidised mitochondrial redox state. This mechanism is explained by direct inhibition by metformin of mGPDH (Madiraju et al., 2014). This mechanism was supported by demonstrating a more oxidised mitochondrial redox state by metformin *in vivo* but not *in vitro* and by demonstration of inhibition of gluconeogenesis from reduced substrates *in vitro* and *in vivo* (Madiraju et al., 2014, Madiraju et al., 2018).

Each of the earlier studies focused on testing one of the above mechanisms. It is recognized that metformin may exert its effects over a wide range of concentrations and by different mechanisms at low and high metformin, but that only mechanisms that occur at concentrations of metformin that are within the therapeutic range (portal vein concentration of 20-80 μM, or cellular dose of 1-2 nmol metformin / mg) are relevant for understanding the therapeutic mechanisms (He and Wondisford, 2015, Wilcock and Bailey, 1994).

This thesis tested three hypotheses for the mechanism(s) by which metformin causes acute inhibition of gluconeogenesis: (1) involvement of Complex 1 inhibition; (2) involvement of AMPK activation or AMPK-independent mechanisms; (3) direct inhibition of mGPDH. The focus of this thesis was to test the lowest effective metformin concentrations that are relevant to the therapeutic range.

A further aim of this thesis was to test whether inhibition of the malate-aspartate shuttle and / or the glycerophosphate shuttle mimics the mechanism of action of metformin.

Chapter 2

Materials and Methods

Chpater. 2 **Materials and Methods**

2.1 Materials

2.1.1 Biochemical reagents

Chemicals and reagents used in this study were purchased from manufacturers listed in Table 2-1

Table 2-1: Chemicals and reagents

Chemicals/Reagents	Suppliers	Cat. No.
A-769662	Tocris Biosciences	3336
Acetoacetate	Sigma	A-8509
Adenosine 5-Triphosphate	Sigma	A-3377
ATA	Sigma	A1895
AOA	Sigma	C13408
Bradford protein assay dye reagent	Bio-rad	500-00006
Bovine serum albumin	Sigma	A2153
Chlorogenic acid derivative (1-[2-(4-chloro-phenyl)-cyclopropylmethoxy]-3,4-dihydroxy-5-(3-imidazo[4,5-b]pyrudin-1-y1-3-phenyl-acryloyloxy)-cyclohexanecarboxlic acid S4048	Gift from Dr. D. Schmoll, Aventis, Pharma GnbH, Frankfurt, Germany	
Developer and replenisher	Sigma	P7042-5GA
Dihydroxyacetone	Sigma	PHR1430
DL- Dithiothereitol (DTT)	Sigma	D-6052
DL-Glycerol 3-phosphate	Sigma	G6126
Eagles' Minimum Essential Medium (1X)	Gibco, Invitrogen	21430

ECL detection Kit	Thermo scientific	32106
Fixer and replenisher	Sigma	P7167-5GA
Folin-Ciocalteau's Phenol Reagent	Sigma	F9252
Glucose-free media	Gibco, Invitrogen	A-14430
Glutamine	Sigma	G3126
Glucose	BDH	28450
Glycerol	Sigma	G-7893
Glucose 6 phosphate	Sigma	G7879
Glycerol 3-phosphate	Sigma	G7886
HEPES	Lonza	17-737F
Lactate	Sigma	L7022
LightCycler Master SYBR	Promega	A600A
Metformin	Sigma	D5035
mGPDH inhibitor (Gpi)	Vitas-M Laboratory	STK017597
NAD	CalBiochem	481911
NADH	CalBiochem	481913
NADP	CalBiochem	481972
Non-essential amino acid (100X)	Gibco, Invitrogen	11140-035
Phenylmethanesufonyl Fluoride (PMSF)	Sigma	P7626
Protein inhibitor	Sigma	P8340
Primer random	Roche	11034731001
Pyruvate	Sigma	P2256

Rotenone	Sigma	R8875
Resazurin Sodium Salt	Sigma	R7017
Salicylate	Sigma	S2679
Sodium Octanoate	Sigma	C5038
Trizol	Ambion	15596018
Xylitol	Sigma	X3375
3-hydroxybutyrate	Sigma	19F-0596
5-chloro-2-[N-(2,5dichlorobenzene sulfonamide)]-benzoxazole (FBPi)	Calbiochem/Santa cruz	344267
[2-^{3}H] glucose	Perkin Elmer	NET238C005MC
[5-^{3}H] glucose	Perkin Elmer	NET531005MC

Enzymes used in this study were purchased from manufacturers listed in Table 2-2

Table 2-2: Enzymes

Enzymes	Suppliers	Cat. No
Diaphorase, cloned from *Clostridium Kluveri*	Sigma	D-2197
DNase I recombinant, RNase-free	Roche	04716728001
Glucose 6-phosphate dehydrogenase (G6PDH)	Roche	11452221
Glycerol 3-phosphate dehydrogenase	Roche	21866325
Hexokinase	Roche	11819023
Lactate dehydrogenase	Roche	19938121
M-MLV reverse transcriptase	Promega	M1708
3-hydroxybutyrate dehydrogenase	Roche	10113620

2.1.2 Adenoviral vectors

Adenoviral vectors were purchased from manufacturers listed in Table 2-3

Table 2-3: Adenoviral vectors

Adenoviral vectors	Suppliers	RefSeq
Ad-m-GPD2 (overexpression) ADV-279685	Vector BIOLABS	BC021359
Ad-m-GPD2-shRNA (Knockdown) shADV-279685	Vector BIOLABS	NM-010274
PFK-KD S32SD, T55V		(Arden et al., 2012, Wu et al., 2004)

2.1.3 Antibodies

Commercial antibodies were purchased from manufacturers listed in Table 2-4

Table 2-4: Antibodies

Antibodies	HOST	Suppliers	Cat. No.
ACC-ser-79 (phosph.)	Rabbit	Cell signalling	11818
GPD2 Ab	Rabbit polyclonal	Proteintech	17219-1-AP
GAPDH	Mouse	Hytest	ABIN153387

2.1.4 Primers for Real time RT-PCR

Primers were designed using the online (https://lifescience.roche.com/en_gb/brands/universal-probe-library.html#assay-design-center) Roche Universal ProbeLibrary Assay.

Primers were synthesized by Sigma (Table 2-5)

Table 2-5: Primers for Real-time RT-PCR

	Primers
ChREBP-β	For: TCTGCAGATCGCGTGGAG Rev: CTTGTCCCGGCATAGCAAC
FGF21 A	For: AGATGGAGCTCTCTATGGATCG Rev: GGGCTTCAGACTGGTACACAT
G6Pc	For: TGGTAGCCCTGTCTTTCTTT Rev: TCAGTTTCCAGCATTCACAC
Gpd2	For: ACTACCTGAGTTCTGACGTTGAAG Rev: TAACAAGGGGACGGATACCA
Gapdh	For: GAC AAT GAA TACGGCTACAGCA Rev: GGC CTC TCTTGCTCAGTGTC
Txnip	For: AACATCCCAGATACCCCAGA Rev: GTGGGGCTCTCTAGTCTGTGA

2.2 Animals

Adult male Wistar rats (body wt. 180-250 g body wt.) and adult male C57BL/6JOlaHsd mice (20-30 g, body wt.) were purchased from Envigo Bicester UK. Adult male C57BL6/JCrl mice were purchased from Charles River UK. The C57BL6/JCrl stain has a deletion in the Nnt gene (Kraev, 2014). Rats and mice were housed in the Comparative Biology Centre. They were allowed free access to standard rodent chow and water *ad libitum* on a 12 h light / 12 h dark cycle at 20 ± 2ºC and at a controlled relative humidity of 50 ± 10%. All procedures for housing of animals and for isolation of hepatocytes conformed to Home Office Regulations and were approved by the University Ethics Committee and by appropriate Home Office Licenses.

2.3 Rat hepatocyte isolation.

The liver isolation was by a modification the two-step collagenase perfusion technique described by Seglen (1976) (Seglen, 1976). The perfusion apparatus consisted of 2 separate peristaltic pumps (set at a flow rate of 25-30 ml/min) with a tubing system containing a bubble trap, for the first and second perfusion buffers. The perfusion buffers were maintained at 37^0C in a water bath. The first perfusion buffer contained 148 mM NaCl, 10mM Hepes, 6.7mM KCl, 6mM glucose, 0.2mM EGTA, 10µg/ml phenol red, pH 7.4. The second buffer contained 144mM NaCl, 20mM Hepes, 6.7mM KCl, 6mM glucose, 1mM $CaCl_2$, 10µg/ml phenol red, 30mg / 100ml collagenase (Sigma Collagenase Type IV, *Clostiridium histolyticum* C5138). For isolation of rat hepatocytes, the rat was euthanized by isoflurane overdose. After laparotomy, the portal vein was exposed and two loose sutures were placed round the portal vein. This was then cannulated with a 14Ga plastic cannula. The thoracic cage was opened and a 14Ga cannula was inserted through the right atrium into the inferion vena cava and secured tightly to allow outflow of perfusate from the liver. The first perfusion system was connected to the portal cannula and the liver was perfusion with the first calcium free buffer for 15 min. This was followed by the second perfusion buffer which was recirculated by connection of a tube to the outflow cannula from the heart. The liver was perfused for 15-20 min, until digested was evident from the characteristic swelling of the liver. The liver was then dissociated in MEM and filtered through a 200 micron mesh and the cell suspension was sedimented 3 times at 50 g (90-120 sec). The supernatant containing non-viable hepatocytes and non-parenchymal cells was discarded and the pellet was suspended in MEM to a cell density of ~ 0.5 million cells/ml and the cells were seeded in multi-well plates at a density of approximately 10^5 cells /cm^2. The cell culture plates (Greiner), were coated with 0.1%w/v gelatin and allowed to dry before seeding with hepatocytes.

2.4 Mouse hepatocyte isolation

The mouse was anaesthetized in a 2-litre chamber containing 8 ml of isoflurane (IsoFlo 100%, Zoetis UK Ltd). After 2 min the mouse was weighed, injected intraperitoneally with 300 µl heparin (Sigma H9399; 3mg (9000U) / ml sterile 150 mM NaCl) and then returned to the isoflurane chamber. After 4 min from first exposure to isoflurane the mouse was removed from the chamber attached to the dissection tray, wiped in 70% ethanol and dissected to expose the heart and liver. A suture was placed below the heart under the vena cava. The heart was then gripped with fine forceps from the right atrium and stretched upwards and a 20Gauge x 32 mm i.v. catheter (Versatus, SR+DU2032PX) was inserted into the inferior vena cava. The needle insert was then removed and when the cannula filled with blood, the suture was tied securely, and the portal vein was cut approximately 1 cm distal to the liver. The cannula was then connected to a first peristaltic pump linked to calcium-free perfusate (containing per liter: 8000mg NaCl, 400mg KCl, 130mg KH_2PO_4, 76mg EGTA, 20mg phenol red, 10 mM HEPES, pH 7.4). The liver was perfused at 5 ml / min for 6 min. The cannula was then connected to a calcium plus collagenase Hanks medium buffered with 5mM $NaHCO_3$, 20mM HEPES and containing 10 mg/100 ml collagenase (Sigma Collagenase Type IV, *Clostiridium histolyticum* C5138) and it was perfused for between 15 and 20 min. On termination of the perfusion the liver was transferred to a petri dish and gently dissociated in ~ 40 ml Minimum Essential Medium. The medium used for washing and cell culture was MEM with Earle's salts (Gibco 21430-020), supplemented with Non-Essential Amino acids (Gibco #11140-035); 2mM glutamine; penicillin (75mg/l) and streptomycin sulphate (50mg/l) (designated MEM). The cell suspension was filtered through a 200-micron mesh, sedimented at 50g (2 min) and the pellet was washed at 50 g 2 min. The pellet was suspended in Minimum Essential Medium (as above) but supplemented with 5% vol/vol newborn calf serum (Gibco, Heat inactivated #26010-074), 10 nM dexamethasone and 10 nM insulin. Cell viability was checked with Trypan Blue (Lonza 19-942E) by mixing equal volumes of cell suspension and Trypan Blue and checking for dye exclusion. The final cell suspension was diluted to ~ 0.5 million cells/ml.

2.5 Hepatocyte culture

The multi-well plates used for monolayer culture of both rat and mouse hepatocytes were coated with 0.1% gelatin. A 2% solution of gelatin was heated filter sterilized and aliquoted. Aliquots were diluted 20 times to 0.1%w/w and multi-well plates were filled with 0.5-1ml of the diluted gelatin. After 20 min this was aspirated and the plates were allowed to dry. Rat or mouse hepatocytes were seeded at a density of approximately 10^5 cells /cm^2 in MEM containing 2mM glutamine, penicillin (75mg/l) and streptomycin sulphate (50mg/l), and 4% vol/vol newborn calf serum. The plates were placed in an incubator at 37°C equilibrated with 5%CO_2 / air and the cells were left to attach for between 2h and 4h. After cell attachment the medium was aspirated and replaced by serum-free medium containing 10nM dexamethasone and 1nM insulin and the cells were cultured overnight.

2.6 Treatment of hepatocytes with adenoviral vectors

Treatment of hepatocytes with adenoviral vectors was started at approximately 1.5-2 hours after plating and was for 4-4.5 hours. Adenoviral vectors were diluted in MEM containing glutamine, penicillin and streptomycin but without serum or added hormones. For expression of Gpd2, the stock concentration of Ad-m-Gpd2 (ADV-279685) was 2.4 x 10^{10} PFU/ml (Plaque forming units per ml). This was diluted in MEM at 1:500 and 1:1500 to 5 and 1.6 x 10^7 PFU. For knock-down of mGpd2 the vector Ad-m-GPD2-shRNA (shADV-279685) was diluted at 1:100. For expression of a kinase deficient variant of PFK2/FBP2, an adenoviral vector encoding the liver isoform with two mutations (S32D, T55V) was used (Wu et al., 2004, Arden et al., 2012). Within approximately 2h of seeding of hepatocytes, the medium was gently aspirated and MEM containing the adenoviral vector was added at a volume of 0.38 ml for 12-well plates and 0.18 ml for 24-well plates. The hepatocytes were incubated with the adenoviral vector for between 4 and 4.5 h and the medium was then changed to serum-free MEM containing 10nM dexamethasone and 1nM insulin.

2.7 Incubation with metformin for metabolic studies

For all experiments with metformin, the hepatocyte monolayers were cultured overnight in MEM containing 10nM dexamethasone and 1nM insulin. Incubations for metabolic studies were performed either in MEM (Gibco 21430) which contains 5mM glucose or in glucose-free DMEM (Gibco A-14430). The overnight medium was aspirated and replaced by either MEM or DMEM containing the metformin concentrations (0.1-0.5mM) indicated and the cells were incubated for 2h to allow cell accumulation of the metformin. The medium was then replaced with fresh medium with substrates and the same metformin concentrations as were present in the 2h pre-incubation. For experiments with the AMPK activator A-769662 (Cool et al., 2006) and Gpi an inhibitor of mGPDH (Orr et al., 2014), these were also added during the 2h pre-incubation and the final incubation.

2.8 Incubations for determination of the mitochondrial redox state

The mitochondrial NADH/NAD redox state can be determined from the ratio of 3-hydroxybutyrate / acetoacetate which is in equilibrium with the mitochondrial NADH / NAD ratio through the 3-hydroxybutyrate dehydrogenase equilibrium (Williamson et al., 1967) Table 1-2. In this study hepatocytes were incubated in medium containing sodium octanoate which is metabolised to 3-hydroxybutyrate and acetoacetate, and the medium was collected at the end of the incubation for enzymatic assay of 3-hydroxybutyrate and acetoacetate. After pre-incubation of hepatocytes in either MEM or glucose-free media (DMEM) containing the metformin concentrations indicated, the medium was then replaced with fresh medium containing octanoate, substrates, and other additions for 1 hour. The incubations were terminated after 60 min. The medium was collected into a 96-well plate and acidified with 0.2 volumes of 0.6M perchloric acid. The samples were kept on ice for analysis of acetoacetate and 3-hydroxybutyrate within 2 h. The hepatocytes were snap frozen in liquid nitrogen and stored at -80^{0}C, for later analysis of cell protein and metabolites.

2.8.1 Enzymatic assays for acetoacetate and 3-hydroxybutyrate.

Acetoacetate and 3-hydroxybutyrate were assayed using 3-hydroxybutyrate dehydrogenase by monitoring fluorometrically the decrease or increase in NADH, respectively (Agius et al., 1986) (Ex 340 nm, Em 460 nm, cutoff filter 420 nm) using a Spectramax M5e plate reader (Molecular Devices).

$$\text{Acetoacetate} + \text{NADH} + \text{H}^{+} \xrightarrow{\text{3-hydroxybutyrate dehydrogenase}} \text{3-hydroxybutyrate} + \text{NAD}$$

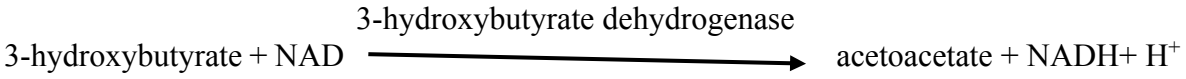

Standards for acetoacetate and 3-hydroxybutyrate were prepared in either MEM or DMEM at concentrations of 20, 50, 100, 200 and 500 µM from a freshly prepared aqueous stock of 10mM. These standards were acidified with 0.6M prechloric acid in parallel with the samples. For the acetoacetate assay, the assay reagent contained 0.4M potassium phosphate buffer (prepared from equimolar KH_2PO_4 and K_2HPO_4), 0.1mM NADH, and 3-hydroxybutyrate dehydrogenase (7.5µg/ml). Sample or standard (in duplicate) was added at 30µl to a white plate followed by 150µl of main reagent and the fluorescence was determined after 30-60 min. For the 3-hydroxybutyrate assay, the assay reagent contained 0.1M Tris, pH 9.3, 200µM NAD, and 3-hydroxybutyrate dehydrogenase 7.5µg/ml. Sample or standard (in duplicate) was added at 30µl to a white plate followed by 150µl of main reagent and the fluorescence was determined after 20-40 min. Sample concentrations were determined from the standard curve (5 concentrations) which was generally linear or quadratic using Softmax Pro Software. For inhibitors with potential interference in the assay, additional blank incubations with inhibitors were run in parallel. The formation of ketone bodies (acetoacetate + 3-hydroxybutyrate) was calculated from the total volume of incubation medium (0.3ml / well) and was expressed as nmol of ketone bodies formed per mg of cell protein, based on the cell protein per well which was determined by the Lowry assay.

2.9 Incubations for determination of glucose production

After overnight culture in MEM, the hepatocytes were incubated for 4h in glucose-free DMEM. The overnight medium was aspirated the cells were washed with 150mM NaCl and incubated for 2h in glucose-free DMEM containing the metformin concentrations indicated. After the 2h pre-incubation, media were aspirated and replaced by fresh glucose- free DMEM containing substrates and other additions for 2h. The incubations were terminated after 120 min. The medium was collected into two separate 96-well plates, one used for determination glucose production and lactate assays and the second one for pyruvate assay after heated in hot plate at 70^0C for 5min to destroy lactate dehydrogenase. Samples were kept on ice for analysis of glucose production within 1h. The remaining samples were stored at 4^0C for less than 16h before lactate and pyruvate assay done.

Total metabolism of DHA, xylitol or glycerol was calculated from the production of glucose plus pyruvate plus lactate expressed as C3 units. Glucose production was expressed either as nmol/ mg of cell protein or as a fraction of total metabolism to glucose, pyruvate and lactate.

2.9.1 Enzymatic assays for glucose, lactate and pyruvate

2.9.1.1 Glucose

Glucose was determined enzymatically by the hexokinase, glucose 6-phosphate dehydrogenase assay (Stappenbeck et al., 1990). From the increase in the absorption of NADPH produced by glucose 6-phosphate dehydrogenase at 340nm using a Spectramax M5[e]

$$\text{Glucose + ATP} \xrightarrow{\textit{Hexokinase}} \text{Glucose 6-P + ADP}$$

$$\text{Glucose 6-P + NADP} \xrightarrow{\textit{G6PDH}} \text{6-phosphogluconate + } H^+ \text{ +NADPH}$$

Standards for glucose were prepared in glucose-free DMEM at concentrations of 25, 50, 100, 200, and 400µM from freshly prepared aqueous stock 10mM. The assay was done on untreated medium. The assay reagent contained 50mM Tris/acetate pH 7.5, 20mM $MgCl_2$, 400µM NADP, 400µM ATP, hexokinase 0.375 µg/ml, and G6PDH 0.5µg/ml. Sample or standard (in duplicate) was added at 20µl to a transparent plate followed by 180µl of main reagent and the absorption was determined after 5-15 min. Sample concentrations were determined from the standard curve (5 concentrations) which was generally linear using Softmax Pro Software.

2.9.1.2 Lactate and pyruvate assay

Lactate and pyruvate were assayed using lactate dehydrogenase by monitoring fluorometrically the increase or decrease in NADH, respectively (Agius et al., 1986) (Ex 340 nm, Em 460 nm, cutoff filter 420 nm) using a Spectramax M5e plate reader (Molecular Devices).

$$\text{Lactate + } NAD^+ \xleftrightarrow{\textit{LDH}} \text{Pyruvate + NADH + } H^+$$

$$\text{Pyruvate + NADH + } H^+ \xleftrightarrow{\textit{LDH}} \text{Lactate + } NAD^+$$

Standards for lactate and pyruvate assays were prepared in either MEM or glucose-free DMEM at concentrations of 50, 100, 200, 500, and 1000µM (lactate) and 20, 50, 100, 200, and 500µM (pyruvate) from freshly prepared aqueous stock of 10mM. For the lactate assay, untreated medium was used. The main reagent contained 0.1M Tris/HCl /1% hydrazine, 200µM NAD, 10µg/ml LDH. Sample or standard (in duplicate) was added at 30µl to a white plate followed by 150µl of main reagent and the fluorescence was determined after 30-60 min. For pyruvate assay, samples and standard were heated at 70^0C for 5 min. The assay main reagent contained (0.4M K-Phosphate (KH_2PO_4 plus K_2HPO_4), 100µM NADH, 0.0015µg/ml. Sample or standard (in duplicate) was added at 30µl to a white plate followed by 150µl of main reagent and the fluorescence was determined after 5-30 min. Sample concentrations were determined from the standard curve (5 concentrations) which was generally linear or quadratic using Softmax Pro Software. For inhibitors with potential interference in the assay, additional blank incubations with inhibitors were run in parallel. The formation of pyruvate plus lactate was calculated from the total volume of incubation medium (0.3ml / well) and was expressed as nmol of pyruvate plus lactate formed per mg of cell protein, based on the cell protein per well which was determined by the Lowry assay.

2.10 Glucose phosphorylation and glycolysis

Glucose phosphorylation was measured from detritiation of [2-^{3}H] glucose and glycolysis was measured from detritiation of [5-^{3}H] glucose (Hue, 1981). [2-^{3}H] glucose or [5-^{3}H] glucose 1.5µCi/ml were reconstituted in MEM and incubated with hepatocytes for 3h. Then media were collected and acidified with 0.1 volume of 1M HCl. Acidified sample (100µl) were transferred into 500µl Eppendorf tube, and placed inside a 5ml scintillation tube containing 0.75ml water and stoppered. For blank correction 100µl MEM containing 1.5µCi/ml [2-^{3}H] glucose or [5-^{3}H] glucose had not been incubated with the cells was treated similar to samples. The samples were incubated at room temperature for 3 days to allow the ^3H_2O to equilibrate with the water in the outer tube. Determination of the amount of ^3H_2O in 0.75ml was measured by on a liquid scintillation analyzer after addition of 3ml of scintillation cocktail (Gold star scintillation cocktail GS1, Meridian Biotechnologies). Results are expressed as nmol of glucose metabolised to ^3H_2O per 3h per mg of protein.

Calculation

$$\text{Specific activity (SA)} = \frac{(\text{dpm}/\mu\text{l})}{\text{nmol glucose}/\mu\text{l}} = \text{dpm/nmol}$$

$$= \frac{\textbf{dpm samples – dpm (blank)}}{\textbf{SA (dpm/nmol)}} \times \frac{\textbf{Total volume / well}}{\textbf{volume taken for assay}} \times \frac{\textbf{1}}{\textbf{Recovery}} \times \frac{\textbf{1}}{\textbf{Protein (mg well)}}$$

= nmol of glucose detritiated per 3h per mg cell protein

$$\text{Recovery factor} = \frac{^3H_2O \text{ in Eppendorf}}{^3H_2O + 0.75\text{ml } H_2O \text{ (total recovery)}}$$

2.11 Mitochondrial glycerophosphate dehydrogenase activity

Mitochondrial GPDH activity was determined by the exogenous electron acceptor 2,6-dichlorophenol-indophenol (DCIP) on hepatocyte monolayers that were snap-frozen in liquid nitrogen and stored at -80^{o}C until analysis. This assay is based on oxidation of G3P by DCIP. The decrease in DCIP absorbance per minute at 600nm reflects the activity mGPDH. The main reagent of the assay contained 200mM sucrose, 50mM KPi pH7.6, 200µM DCIP, and 25mM DL-G3P (Dawson and Thorne, 1969).

2.12 Cell metabolites: ATP, G6P and G3P

After collection of the medium on termination of the incubations, the cells were snap frozen in liquid nitrogen and stored at -80^{0}C until analysis. They were extracted in 2.5% (w/v) 5-sulphosalicylic acid. Samples were transferred to microcentrifuge tube and centrifuged for 10 min 13,000g at 4^{O}C. The supernatants (150µl) were neutralized with 30µl KOH/KPi (3M KOH + 1M K_2HPO_4) in a 96 well plate and neutralized samples were used to measure cell metabolites.

2.12.1 Adenosine 5-tri-phosphate

ATP was determined using an endpoint chemiluminescence assay. This assay is based on measuring of emitted light produced from the oxidation of luciferin to oxyluciferin catalyzed by luciferase (see principle of reaction below).

$$\text{ATP + D-Luciferin + } O_2 \xrightarrow{\text{Luciferase}} \text{Oxyluciferin + AMP + PPi + } CO_2 \text{ + Light}$$

ATP standards were prepared in 2.5% SSA at final concentrations of 2, 5, 10, 20, 40µM from a freshly prepared stock of 1mM ATP. They were neutralized similarly to the cell extracts. Sample or standard in duplicate (20µl) was added to a white 96-well plate followed by 100µl of main reagent. This contained the Luciferin/Lucifease (Sigma FL-AAB) made up according manufacturer's instructions and aliquoted in 50µl aliquots. The main reagent contained an aliquot reconstituted in buffer containing 0.1M Tris acetate, pH7.5, 10mM magnesium acetate, 1.8mM EDTA. Luminescence was measured within 5 minutes using the Spectramax and ATP was determined from the standard curve which was linear.

2.12.2 Glucose 6-phosphate

Glucose 6-P was determined using fluorimetric enzyme assay (Zhu et al., 2009). This method is based on the oxidation of glucose 6-P by glucose 6-P dehydrogenase (G6PDH) to yield NADPH, which is coupled to reduction of resazurin in the presence of diaphorase to produce resorufin (see principle of reaction below). Resorufin is highly fluorescent and can be detected by excitation at 530 nm and emission 590 nm with a cut off of 570 nm using a Spectramax M5^{e} fluorimeter.

$$\text{Glucose 6-P + NADP} \xrightarrow{G6PDH} \text{6-phosphogluconate +NADPH + } H^{+}$$

$$\text{NADPH + Resazurin} \xrightarrow{Diaphorase} \text{NADP + Resorufin}$$

G6P standards were prepared in 2.5% SSA at final concentrations of 2, 5, 10, 20, 50µM from a freshly prepared stock of 1mM G6P. They were neutralized similarly to the cell extracts.

Sample or standard in duplicate (40µl) was added to a white 96-well plate followed by 160µl of main reagent. The main reagent contained 50mM Tris/acetate pH 8.0, 2mM $MgCl_2$, 0.2mM NADP, 0.02mM resazurin, 0.275µg/ml glucose 6-phosphate dehydrogenase, 0.45µg/ml diaphorase. Fluorescence was measured within 30 minutes using the Spectramax and G6P was determined from the standard curve which was quadratic.

2.12.3 Glycerol 3-phosphate

Glucose 3-P was determined using an endpoint fluorimetric enzyme assay (Zhu et al., 2009). This method is based on the oxidation of glycerol 3-P by glycerol 3-P dehydrogenase (G3PDH) to yield NADH, which is coupled to reduction of resazurin in the presence of diaphorase to produce resorufin (see principle of reaction below). Resorufin is highly fluorescent and can be detected by excitation at 530nm and emission 590nm with a cut off of 570nm using a Spectramax M5^{e} fluorimeter.

$$\text{Glycerol 3-P} + \text{NAD}^+ \xrightarrow{G3PDH} \text{DHAP} + \text{NADH} + \text{H}^+$$

$$\text{NADH} + \text{Resazurin} \xrightarrow{Diaphorase} \text{NAD} + \text{Resorufin}$$

G3P standards were prepared in 2.5% SSA at final concentrations of 2, 5, 10, 20, 50µM from a freshly prepared stock of 1mM G3P. They were neutralized similarly to the cell extracts. Sample or standard in duplicate (40µl) was added to a white 96-well plate followed by 160µl of main reagent. The main reagent contained 0.1M Tris/HCl; pH 9.3, 0.4mM NAD, 0.02mM resazurin, 9µg/ml glycerophosphate dehydrogenase, and 0.5µg/ml diaphorase. Fluorescence was measured within 60 minutes using the Spectramax and G3P was determined from the standard curve which was quadratic.

2.13 Cellular protein determination

2.13.1 Lowry assay

Cellular protein was determined spectrometrically by the Lowry assay. Cells were extracted with 0.1M NaOH. The principle of this reaction is that an active constituent of Folin-phenol reagent, phosphomolybdic-tungstic acid, is reduced by protein to form a coloured complex which can be measured at 750nm. A combination of start and main reagents are used in the assay. The assay main reagent containing (10% (w/v) Na_2CO_3 in 0.5M NaOH, water, 2% (w/v) Na^+/K^+ tartrate, and 1% (w/v) $CuSO_4.5H_2O$ in a ratio 10:40:1:1) is activated with Folin and Ciocalteu's phenol diluted with distilled water in a 1:1 (v/v) ratio. BSA standards (0.2, 0.4, 0.6, 1.0, 1.5, and 2.0mg/ml) were prepared in 0.1M NaOH and used as standard curve.

2.13.2 Bradford assay

Protein for western blot was determined spectrometrically by Bradford assay. This assay involves the binding of the dye Coomassie blue to peptide residues that form a coloured complex and measured at 595nm. Samples were diluted 1:20 with 0.05% Triton X-100. The main reagent (Bio-rad protein assay dye reagent, 500-00006) was diluted 1:5 (v/v). BSA standard (25, 50, 100, 150, 200, 300, and 500µg/ml) were prepared in 0.05% Triton X-100 and used for the standard curve.

2.14 Protein and mRNA expressions

2.14.1 Western blotting

Monolayer hepatocytes were snap frozen in liquid nitrogen and stored at -80°C. Hepatocytes were extracted in extraction buffer containing (100mM KCl, 10mM EDTA, 20mM Kpi, 0.5mM PMSF, 0.5 benzamidine, 1mM DTT, 5µl Caliculin A, 5µl protease inhibitor, and 4.1ml water). Extracted samples were transferred into Eppendorf tubes, sonicated for 5 seconds and then centrifuged for 10 min. at 12,000g. The Bradford assay was used to determine sample protein in supernatant (see 2.13.2) and samples were diluted (4 vol:1 vol) with 4x SDS loading buffer containing (0.5M Tris; pH 6.8, 10% SDS (w/v), 3% glycerol (v/v), 1% bromophenol blue (w/v), mercaptoethanol 400µl, and 2ml water). Samples were denatured at 95°C for 5 min. 20-40µg protein was loaded onto gel (4% stacking, and either 8% running SDS-polyacrylamide for ACC-p, or 12% running SDS-polyacrylamide for mGPDH). Electrophoresis was performed for 15min at 90 volts, and then for 45 min at 180 volts (PowerPac basic power supply, 164-5050, Bio-rad). Protein was transferred to PVDF membrane (Thermo-scientific 0.2µm, 88520, Germany) by transfer equipment for 4h (Power PAC 200, Bio-rad). Membrane was blocked by

blocking buffer to avoid non-specific protein binding membrane for 1h at room temperature. Blocking buffer was either 5% BSA for ACC-P or 5% dried milk (Marvel) in TBST. After blocking the membrane was incubated with primary antibody (1:1000) in blocking buffer and incubated overnight. The membrane was washed with TBST (5x 5 min) and then incubated with 1:5000 diluted secondary antibody (horseradish peroxidise-linked anti-IgG, Rabbit) for 1h at room temperature, followed by further washing with TBST (5x 5 min). Bands were visualized using the enzyme chemiluminescence (ECL) detection system (Pierce ™ ECL Thermo-scientific, USA) according to the manufacturer's instructions and then membrane was exposed to ECL X-ray film (CLX Posure™ Film Thermo-scientific, Belgium) in a dark room for few seconds, followed by developing the X-ray film with developer and replenisher (Carestream, USA) and fixer and replenisher (Carestream, USA).

2.14.2 Semi-quantitative real-time RT-PCR

In this study determination of mRNA level was performed by semi-quantitative real-time PCR (RT-PCR). By using Trizol reagent to extract RNA from mouse hepatocyte monolayers (24-well plates). After incubation monolayer hepatocytes were washed once with 1X saline (150mM NaCl) and 250µl Trizol reagent was added per well and vigorously scraped. Then the trizol reagent was transferred into Eppendorf tubes and incubated for 5 min at room temperature, 50µl of chloroform then added and samples shaken vigorously for 15 seconds. After 2 min room temperature incubation samples were centrifuged for 15 min at 12,000g, 4ºC and the aqueous upper phase transferred into new Eppendorf tubes. Isopropanol (100µl) was added to each tube and mixed thoroughly and incubated for 10 min. at room temperature. After incubation samples were centrifuged at 12,000g, 4ºC for 10 min. The supernatant was removed and pellets were washed with 75% ethanol (diluted with pure H_2O, Sigma-Aldrich, UK), and centrifuged for 5 min at 7,500g, 4ºC. Ethanol was aspirated and samples left in fume hood to dry for 10 min. Pellets were re-suspended in 10µl H_2O and incubated for 10 min at 55ºC. Samples were incubated for 10 min at 37ºC with RNase free DNase I to remove the genomic DNA, and then samples incubated at 75ºC for 10 min for denaturation of the enzyme. The RNA was quantified by NanoDrop 2000 (Scientific).

cDNA preparation

Primer random hexamer (0.5µg/ml) was added to 1µg RNA and samples were incubated for 10 min at 70ºC, followed by 50 min incubation with reverse transcriptase mixture (RT-mix) containing (1X MMLV buffer, dNTP, M-MLV reverse transcriptase, H_2O) at 37ºC, followed by incubation at 70ºC for 15 min. The final concentration of cDNA was 25ng/µl. RT-PCR carried out with 50ng of cDNA, in a final volume of 10µl PCR reaction mixture containing (1X lightCycler FastStart DNA Master SYBR, 0.5µM of forward and reverse primer, and H_2O). RT-PCR was programmed with the following parameters: i) initial incubation at 50ºC for 2 min; ii) denaturation at 95ºC for 15 seconds and 60ºC for one minute. The expression level were quantified using the ΔΔCt method.

2.15 Statistical analysis

Results are expressed as means±SEM. Statistical analysis was performed with the student's paired t-test or ANOVA (one-way and two-way, Post hoc test Bonferroni). A P value <0.05 was considered to be statistically significant.

CHAPTER 3: RESULTS 1

ROLE OF THE MITOCHONDRIAL REDOX STATE AND AMPK ACTIVATION IN MEDIATING THE EFFECT OF METFORMIN ON GLUCONEOGENESIS IN HEPATOCYTES

Chpater. 3 Role of the mitochondrial redox state and AMPK activation in mediating the effect of metformin on gluconeogenesis in hepatocytes

3.1 Aims and rationale

Metformin has been prescribed for T2D patients in Europe since the 1950s and in the US since 1994. The beneficial effects of metformin include lowering of glucose output by the liver, increased insulin sensitivity of peripheral tissues, and reduced absorption of glucose by the gut (Tran et al., 2015). In spite of that the molecular mechanism of metformin remains incompletely understood (Pernicova and Korbonits, 2014). The first mechanism of metformin that was identified as a possible explanation for the inhibition of hepatic glucose production was the inhibition of complex 1 of the respiratory chain. Complex 1 (NADH-ubiquinone oxidoreductase) is the first of five complexes in the respiratory chain. It catalyses the oxidation of NADH to NAD with transfer of two electrons to ubiquinone which is reduced to ubiquinol. This is coupled to the pumping of four protons from the inside of mitochondria to mitochondrial intermembrane space (Hirst, 2013, Das, 2006, Vinogradov and Grivennikova, 2016). Inhibition of complex 1 results in an increase in the mitochondrial NADH/NAD redox state which can be measured from the ratio of 3-hydroxybutyrate /acetoacetate (HOB / Acac ratio) through the hydroxybutyrate dehydrogenase equilibrium. Early studies on metformin reported that metformin treatment *in vivo* and also in isolated hepatocytes results in an increase in the HOB / Acac ratio (a more reduced mitochondrial NADH/NAD redox state). Inhibition of complex 1 was confirmed from studies on isolated mitochondria incubated with substrates that are metabolised by complex 1 (Owen et al., 2000, El-Mir et al., 2000). More recent work by Bridges *et al.* (2014) showed a direct inhibition of complex 1 by reversible binding of metformin to the ubiquinone site (Bridges et al., 2014). Furthermore, metformin caused a more reduced mitochondrial redox state (increase NADH / NAD ratio) in other tissues such as skeletal muscle homogenate (Brunmair et al., 2004), neurons (El-Mir et al., 2008), human endothelial cells (Detaille et al., 2005), pancreatic β-cells (Hinke et al., 2007), kidney (von Morze et al., 2018).

It has been reported that inhibition of complex 1 by biguanides is associated with cellular energy stress (increase in AMP:ATP and ADP:ATP ratios) (Cook et al., 1973, Evans et al., 1983). Alteration in the cellular AMP:ATP ratio results in activation (increase in Thr^{172} phosphorylation) of the energy sensor AMPK. AMPK-activation can occur by many molecules such as: the 5-aminoimidazole-4-carboxamide ribonucleoside metabolite ZMP, A-769662, and 991 activator or drugs such as salicylate. AICAR is converted by phosphorylation to the purine

precursor (ZMP), ZMP mimics the effect of AMP and binds to γ-subunit, while A-769662 and 991 bind to the β-subunit. Similar to A-769662, salicylate also activates AMPK by binding to the β-subunit (Hardie et al., 2016, Jacquel et al., 2018, Ducommun et al., 2014). Biguanides have been shown to activate AMPK by an indirect mechanism through inhibition of ATP production (Hawley et al., 2010, Hawley et al., 2012). Early studies reported that metformin inhibited *de novo* lipogenesis in rat hepatocytes through the phosphorylation of acetyl-CoA carboxylase (ACC) and also that metformin inhibits glucose production (Zhou et al., 2001, Zang et al., 2004). ACC is one of the downstream targets of AMPK (Kristensen et al., 2015, Winder et al., 1997). The activation of AMPK by metformin occurred with (0.5-2mM) metformin concentrations (Zang et al., 2004, Sajan et al., 2013). However, a recent study by Cao *et al* (2014) reported that a lower metformin concentration (~80μM) increased the phosphorylation of AMPK on the α-subunit and inhibited hepatic glucose production (Cao et al., 2014). Moreover, activation of the cAMP/PKA pathway antagonized the effect of metformin on lowering hepatic glucose production. PKA signalling increased the phosphorylation of AMPK-α at Ser^{485} and abolished the phosphorylation of the AMPK-α subunit at Thr^{172}. The latter effect was reversed by salicylate by blocking the phosphorylation of AMPK at Ser^{485} and activation of the phosphorylation on Thr^{172} (He et al., 2016a). It has been reported that metformin and salicylate synergistically improve lipid metabolism in insulin resistant mice through activation of AMPK. The effect of salicylate on AMPK is not on α-subunit but on β-subunit similar to A769662, whereas the effect of metformin is by raised AMP which binds the α-subunit (Ford et al., 2015b, Hayward et al., 2016, O'Brien et al., 2015).

On the other hand, evidence for AMPK-independent mechanisms was reported by Guigas *et al.* (Guigas et al., 2006) and Fortez *et al*. using hepatocytes from AMPK deficient mice (Foretz et al., 2010). The study by Guigas *et al* 2006 reported that metformin lowered glucose phosphorylation in rat and mouse hepatocytes. Glucose phosphorylation was inhibited by 2-3mM metformin in mouse hepatocytes from wild-type and AMPK deficient mice lacking α1 and α2 subunits. The inhibition of glucose-phosphorylation by metformin was associated with decreased in cell ATP. They concluded that metformin inhibited glucose phosphorylation, independently of AMPK, by lowering cellular ATP (Guigas et al., 2006). Furthermore, Fortez *et al*. (2010) reported that the cellular ATP level was depleted in mice hepatocyte treated with metformin (0.25-1mM) and the ratio of AMP/ATP was significantly increased with metformin concentrations of 0.25-1mM. The decrease in gluconeogenesis from lactate, pyruvate, and

DHA by metformin was explained by the decrease in ATP by an AMPK-independent mechanism (Foretz et al., 2010).

A recent study reported a more oxidised mitochondrial redox state in the liver by (20-50mg/kg) metformin treatment. They also reported that 20mg/kg metformin lowered endogenous glucose production. Moreover, they reported that 100μM metformin lowered glucose production in isolated hepatocytes incubated with reduced substrates (Lactate and glycerol) but not with oxidised substrates (DHA, pyruvate, and alanine) as gluconeogenic precursors. However, the effect of 100μM metformin in isolated hepatocytes on the mitochondrial redox state was not tested (Madiraju et al., 2014). In the kidney, metformin showed a more reduced (increase in NADH / NAD ratio) mitochondrial redox state with 125mg/kg metformin (von Morze et al., 2018) and more oxidised (decrease in NADH / NAD ratio) mitochondrial redox state with 50mg/kg metformin (Qi et al., 2018). The more oxidised mitochondrial redox state by metformin in isolated hepatocytes has not been reported.

The aims of this chapter were:

(i) To test the hypothesis that metformin has a biphasic effect on the mitochondrial redox state.

(ii) To test whether metformin inhibits gluconeogenesis from oxidised and reduced substrates in conditions associated with a more oxidised mitochondrial redox state.

(iii) To test whether AMPK activation can explained the metformin mechanism.

(iv) To test the effect of metformin on G6P and glucose phosphorylation in conditions with no change in cell ATP.

3.2 Results

3.2.1 Biphasic effect of metformin on the mitochondrial redox state: more oxidised at low metformin.

The effect of metformin (100-500µM) on the mitochondrial redox state was measured in mouse and rat hepatocytes using octanoate (0.125-0.25mM) as the substrate for β-oxidation. Octanoate enters the mitochondria as the free acid and is converted into octanoyl-CoA inside mitochondria. Unlike long-chain fatty acids mitochondrial oxidation of octanoate is not regulated by malonyl-CoA and AMPK. The final products of octanoate β-oxidation are acetoacetate and 3-hydroxybutyrate (McGarry and Foster, 1980). The sum of acetoacetate plus 3-hydroxybutyrate production is a measure of octanoate β-oxidation and the ratio of 3-hydroxybutyrate / acetoacetate (HOB/Acac) is a measure of the mitochondrial NADH/NAD^+ state (Eaton, 2002, McGarry and Foster, 1980). Throughout this study a protocol was used involving pre-incubation with metformin for 2h before incubating in medium with substrate for either 1 h or 2h. Using this protocol when the concentration of metformin in the pre-incubation was between 100 and 500 µM, the cell content of metformin was between 1 nmol /mg cell protein (100 µM) and > 5 nmol/mg protein (500µM) (Al-Oanzi et al., 2017). Previous studies in mice given an oral load of metformin corresponding to 50mg/kg body weight showed a peak metformin content in the liver corresponding to 1-2 nmol/mg protein (Wilcock and Bailey, 1994). Using our protocol, a concentration of 100 µM metformin gives a cell metformin content after 2 hours pre-incubation corresponding to the peak level in liver (1-2 nmol/mg protein).

In this study the ratio of 3-hydroxybutyrate / acetoacetate was significantly increased by high metformin (500µM) in both mouse hepatocytes (Figure 3-1A) and rat hepatocytes (Figure 3-1C) and also by the complex 1 inhibitor (rotenone), as expected. However at 100µM metformin the 3-hydroxybutyrate / acetoacetate ratio was significantly decreased indicating a more oxidised mitochondrial NADH/NAD redox state in both mouse and rat hepatocytes. The effect of low metformin (100µM) was mimicked by dinitrophenol (DNP) in both rat (Figure 3-1C) and mouse (Figure 3-3 B) hepatocytes. The similar effects of the complex 1 inhibitor and high metformin (500µM) on the mitochondrial redox state are consistent with inhibition of complex 1 by high metformin (corresponding to a cell load of > 5 nmol/mg metformin content) (Al-Oanzi et al., 2017). On the other hand, the effect of low metformin (100µM) cannot be explained by inhibition of complex 1 due to the opposite effects of 100µM metformin and rotenone on the NADH/NAD^+ (3-hydroxybutyrate / acetoacetate ratio). Possible explanations

for the decrease in ratio by 100 μM metformin are either a decrease NADH production or other mechanisms such as stimulatory effects of metformin on respiratory chain (increase the NADH oxidation). Both high metformin (500μM) and rotenone decreased the rate of 3-hydroxybutyrate plus acetoacetate production in mouse hepatocytes (Figure 3-1B) with a small not significant decrease in rat hepatocytes (Figure 3-1D). The rate of 3-hydroxybutyrate plus acetoacetate production was increased by low metformin (100μM) in both mouse (Figure 3-1B) and rat hepatocytes and also by the uncoupler (DNP) (Figure 3-1D). This implicates an effect of metformin on the respiratory chain mimicking the uncoupler which causes a more oxidised NADH/NAD ratio as a result of the decrease in proton gradient which leads to an increase in fatty acid oxidation. When the effects of low metformin and DNP were tested in the presence of rotenone (shaded bars) (Figure 3-3 A and B), only DNP lowered the 3-hydroxybutyrate / acetoacetate ratio (figure 3-3 B), suggesting that the metformin effect is either upstream of the rotenone site or alternatively abolished by rotenone through other mechanisms. Cell ATP was maintained in cells treated with all metformin concentrations tested in this study (Figure 3-2 A and B). This does not exclude small localized changes in free ATP/ADP ratio in the cytoplasm as was reported by Owen & Halestrap (2000) in conditions of maintained total cell ATP.

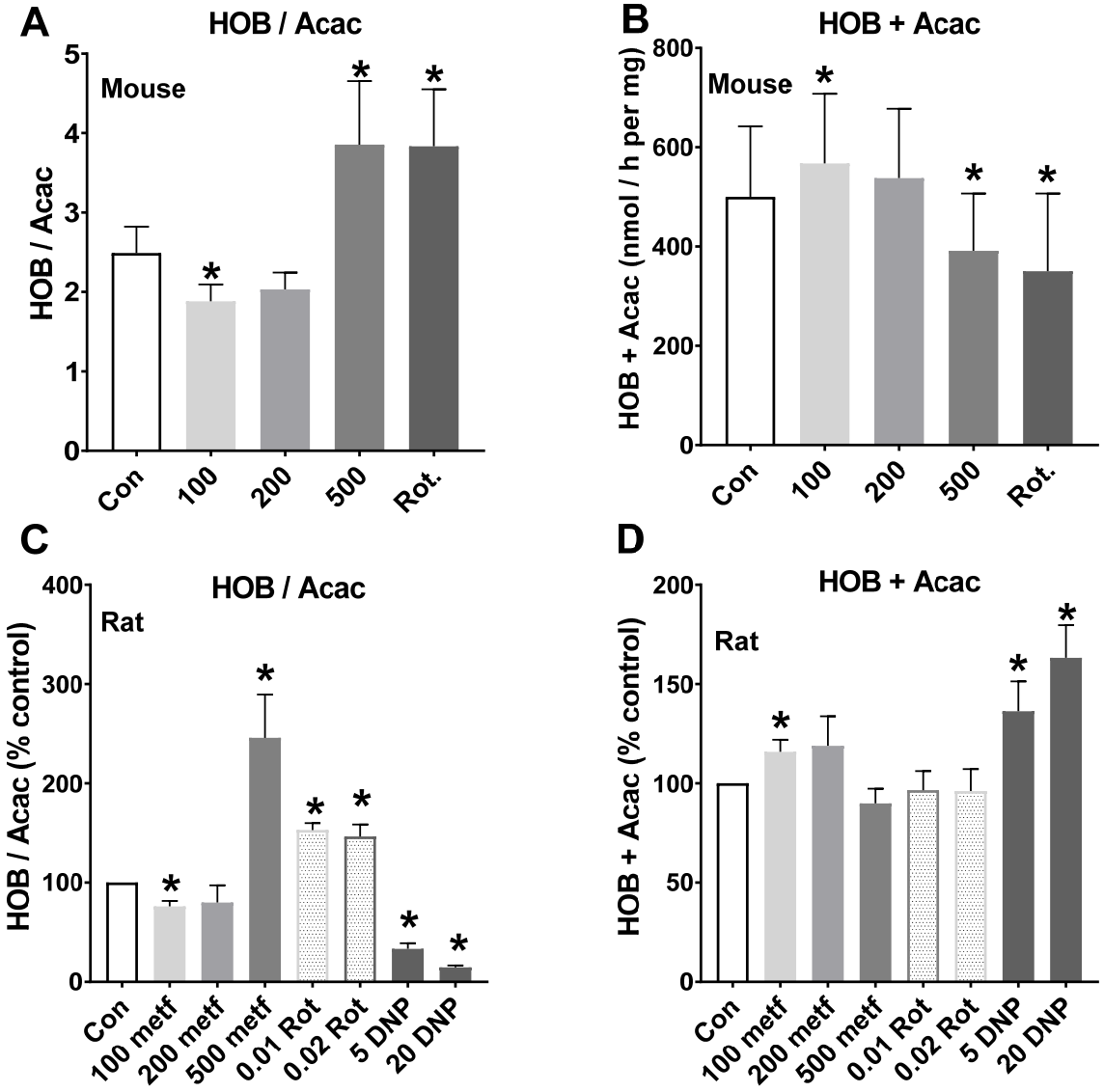

Figure 3-1: Low metformin and DNP cause a more oxidised mitochondrial redox state.

Mouse (A-B) and rat (C-D) hepatocytes were pre□incubated for 2h in MEM with the metformin concentrations (100-500μM) indicated. The medium was then replaced with fresh MEM containing 25mM glucose, 0.25mM octanoate and the other conditions indicated for 1h to achieve cell content of metformin between 1nmol/mg protein (100μM) and > 5nmol/mg protein (500μM). The medium was collected for analysis of acetoacetate (Acac) and 3-hydroxybutyrate (Gardner et al.). A and C ratio of 3□ hydroxybutyrate / acetoacetate; B and D total production of 3□hydroxybutyrate + acetoacetate. Results are Means ± SEM for n= 8-14.

***P < 0.05 relative to control.**

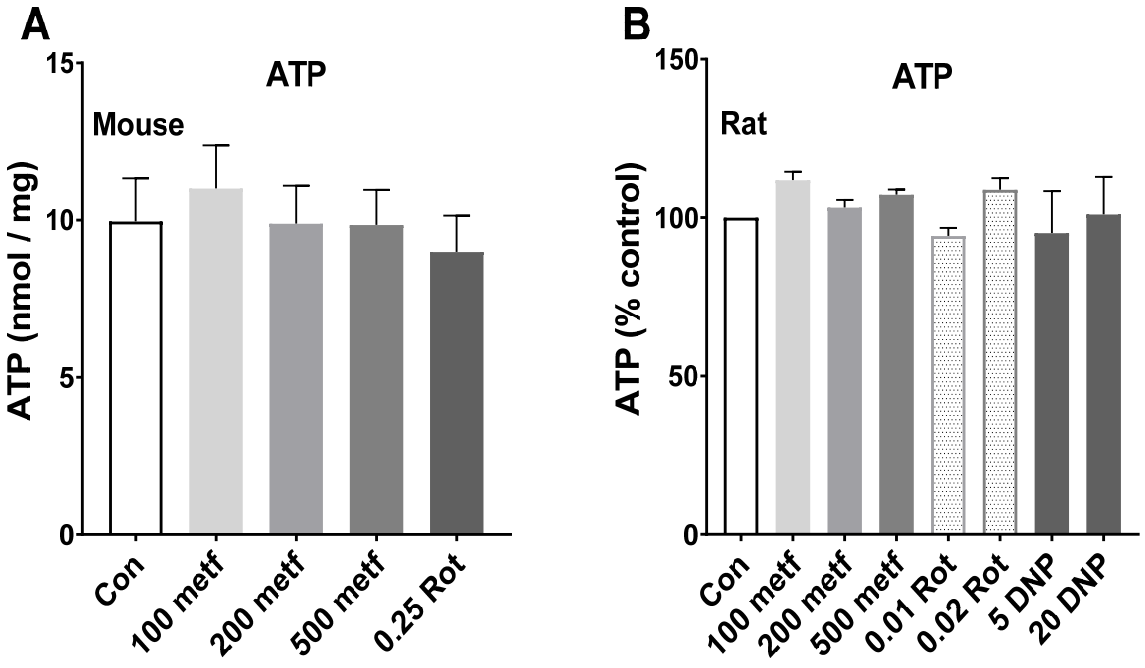

Figure 3-2: Cell ATP for conditions in figure 3-1.

Cells were snap-frozen for ATP analysis after the medium was collected for 3-hydroxybutyrate and acetoacetate assays in figure 3-1. **Means ± SEM for n= 8-14.**

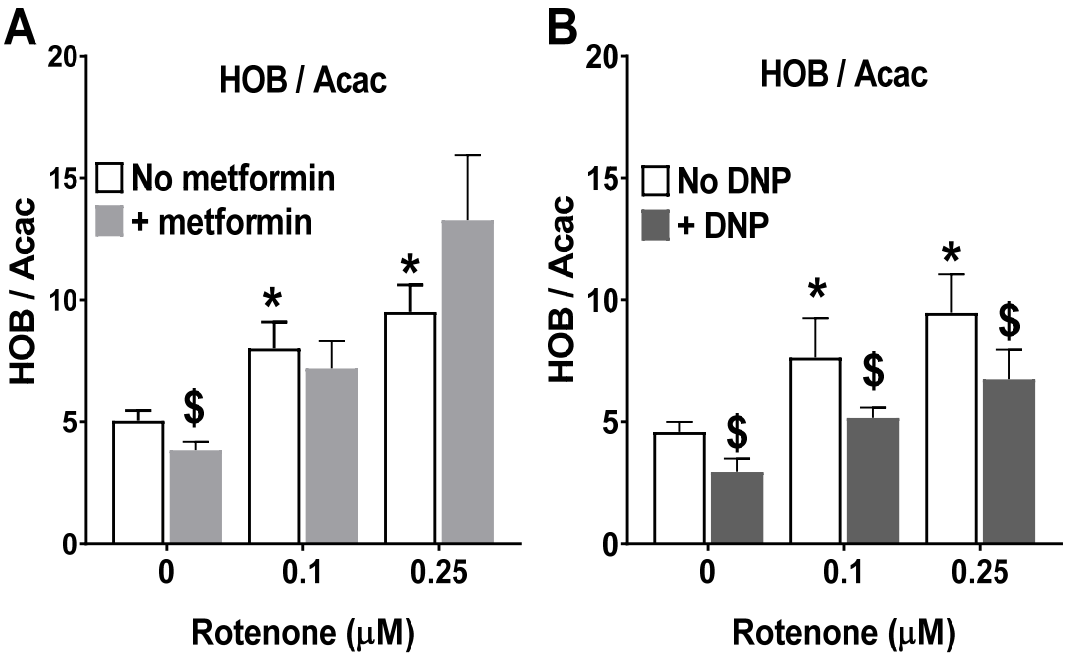

Figure 3-3: DNP causes a more oxidised mitochondrial redox state in the presence of rotenone

Mouse hepatocytes cultured for 3h after cell plating and then incubated for 2h without (white bars) or with (shaded bars) either 100μM metformin (A) or 20 μM DNP (B), and then for further 1h in fresh MEM containing 25mM glucose plus 0.125mM octanoate and the conditions indicated. The medium was collected for analysis of 3-hydroxybutryate and acetoacetate. Mean ±SEM for n=5-7.

* P<0.05 relative to respective control.

$ P<0.05 effect of metformin or DNP.

3.2.2 High but not low metformin activates AMPK

Previous studies have proposed that activation of AMPK by metformin may occur through either inhibition of complex 1 resulting in raised AMP/ATP ratio or also through other mechanisms (Gouaref et al., Cao et al., 2014, He et al., 2016a, Zhang et al., 2016, He and Wondisford, 2015). We next determined the effect of low (100μM) and high (500μM) metformin on AMPK activation from the phosphorylation of the AMPK downstream target (acetyl-CoA carboxylase ACC-P) and used the AMPK activators, A-769662 (10-20μM) and salicylate (500 μM) as reference controls. As discussed in the introduction salicylate similar to A769662 binds to the glycogen binding domain of the β-subunit and causes activation and phosphorylation on the AMPK Thr^{172} (Hawley et al., 2012). Salicylate was also shown to activate AMPK synergistically with metformin (Ford et al., 2015a). in this study the effect of salicylate was tested both alone and in combination with low metformin in mouse hepatocytes incubated with 25mM glucose. There was no effect on ACC-P by low 100μM metformin concentration. While the high (500μM) metformin and A-769662 (10-20μM) caused increased in ACC-phosphorylation. Salicylate (500μM) known as AMPK activator similar to A-769662 (Hawley et al., 2012) did not have a statistically significant effect on ACC-phosphorylation when present alone, but it caused a significant increase in ACC-P in combination of 100μM metformin (Figure 3-4). The significant increase in ACC phosphorylation by the combined effects of low metformin and salicylate could be due to the different mechanisms of AMPK activation because salicylate binds to the β-subunit whereas metformin may cause a small elevation in AMP which binds to the catalytic α-subunit. Synergism between metformin and salicylate in causing activation of AMPK has been reported previously (Ford et al., 2015b).

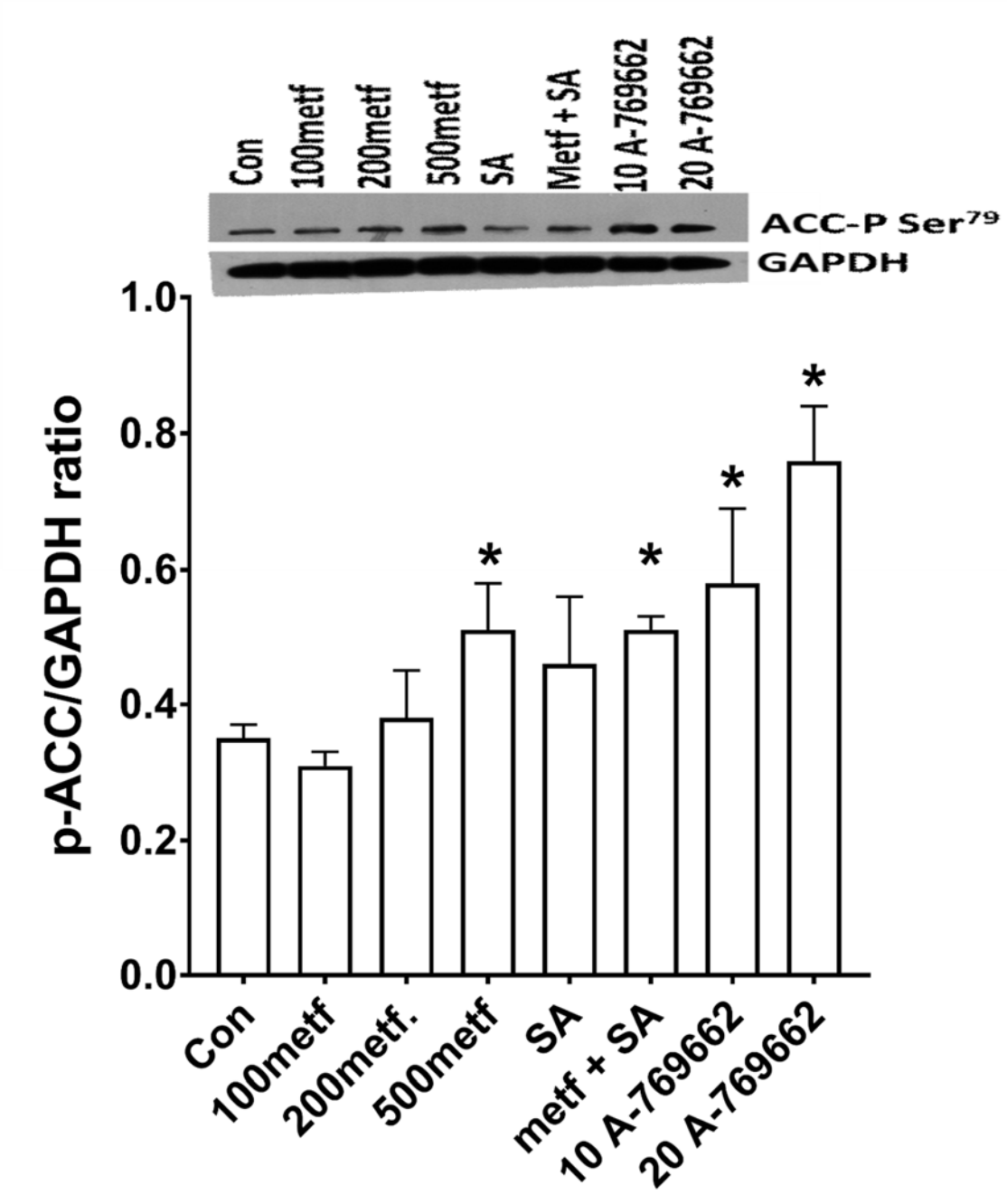

Figure 3-4: High but not low metformin concentration mimics the effect of the AMPK-activator, A-769662, on ACC-phosphorylation.

After overnight culture hepatocytes monolayers were incubated for 2h with metformin (100, 200 or 500µM), 500µM SA, 100µM metformin plus 500µM salicylate, and A-769662 in MEM. The medium was then replaced with fresh MEM containing 25mM glucose and the additions indicated for 1h. Results are expressed as ratio to GAPDH and the value are Means ± SEM.

*P<0.05 relative to control.

3.2.3 Inhibition of gluconeogenesis from oxidised and reduced substrates by low metformin is not mimicked by the AMPK activator A-769662

The above studies show opposite effects of low and high metformin on the mitochondrial redox state and activation of AMPK only by the high metformin concentration which caused inhibition of complex 1. We next tested whether the low metformin dose that causes a more oxidised redox state but not phosphorylation of ACC (Figure 3-4), inhibits gluconeogenesis from oxidised (dihydroxyacetone, DHA) and reduced (xylitol and glycerol) substrates. The rate of glucose production was significantly higher from the oxidised substrate DHA than from the reduced substrate glycerol (Figure 3-5A). Metformin significantly lowered the rate of hepatic glucose production from oxidised (DHA) and from reduced (xylitol and 0.25mM glycerol) substrates (Figure 3-5 A) and increased glycolysis (increased the rate of pyruvate plus lactate production) (Figure 3-5 B) without affecting total metabolism of DHA and xylitol (Figure 3-5 D). While there was no effect of metformin on glycolysis from glycerol. The effect of metformin with 0.25mM glycerol was associated with a decrease in total glycerol metabolism which might explain the effect of metformin on inhibition of gluconeogenesis from 0.25mM glycerol (Figure 3-5 D). Accordingly, metformin lowered the fractional partitioning of oxidised (DHA) and reduced (xylitol) substrates to glucose relative to glycolysis (Figure 3-5 C).

Having confirmed that low metformin (100μM) inhibits the production of glucose from DHA and the fractional partitioning of DHA to glucose relative to glycolysis without increased the phosphorylation of the AMPK substrate (ACC) we next tested the effect of the AMPK-activator on hepatic glucose production in mouse hepatocytes incubated with either oxidised (DHA) or reduced (xylitol) substrates. With DHA as substrate, metformin (100-200μM) inhibited glucose production by (22 and 27%, respectively) (291±13.7, and 274±20.7 vs 373±15.8, respectively) (Figure 3-6 A) and increased the production of pyruvate plus lactate (980±34.9 and 1147±84.7 vs 862±25.3, respectively) (Figure 3-6 B) without effecting total DHA metabolism (1583±52 and 1722±96.95 vs 1642±51.25, respectively) (Figure 3-6 D). Metformin decreased the fractional partitioning of DHA to glucose relative to glycolysis (38± 1.32 and 32.43± 2.31 vs 44.94± 1.1) (Figure 3-6 C). The AMPK activator, A-769662 had the opposite effect to metformin (Figure 3-6 A-D). It favored gluconeogenesis rather than glycolysis and increased the fractional partitioning to glucose relative to glycolysis

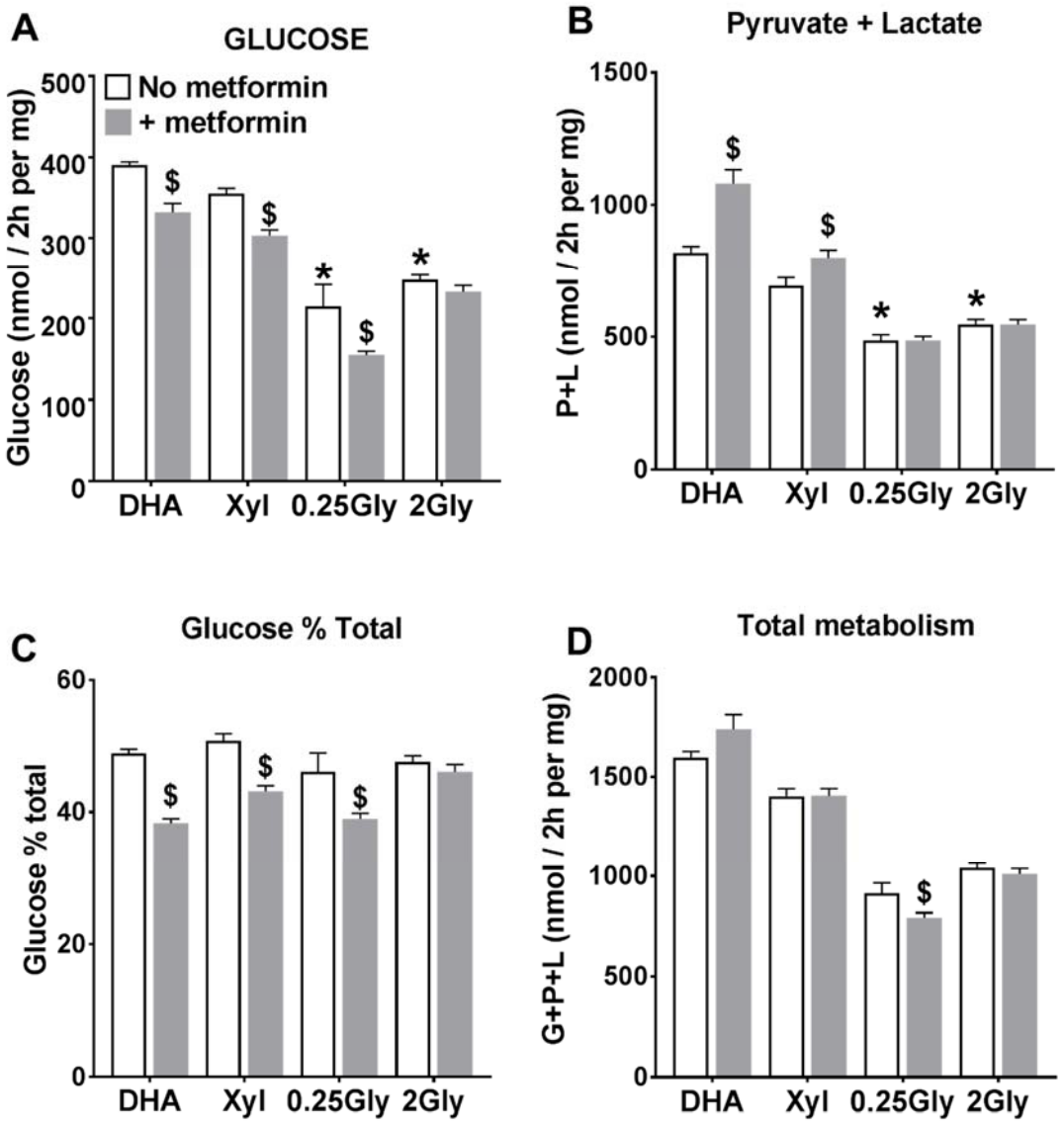

Figure 3-5: Effects of metformin on glucose production from oxidised and reduced substrates.

After overnight culture, mouse hepatocytes were pre-incubated for 2h in glucose-free DMEM without or with 100µM metformin. The medium was then replaced by fresh glucose-free DMEM containing either 5mM DHA, 2mM xylitol (Xyl) or glycerol at 0.25mM or 2mM. After 2h the medium was collected for determination of glucose (A), pyruvate and lactate (B) glucose production percentage (C), and total metabolism (D). Results are representing as mean±SEM for triplicate plates from one hepatocytes preparation.

*** P<0.05 relative to DHA;**

$ P<0.05 effect of metformin.

(51±2.6 vs 45±1.1), and lowered glycolysis (765±60 vs 862±25.3) without effecting total DHA metabolism (1571±80 vs 1642±51.3).

Although salicylate is known to activate AMPK by binding the same subunit as A-769662 (Hawley et al., 2012), in this study 500μM salicylate did not mimic the effect of A-769662 on glycolysis or the fractional partitioning to glucose relative to glycolysis. The studies on phosphorylation of ACC had shown that salicylate is a weaker activator of AMPK than A-769662 (Figure 3-4). The combination of metformin and salicylate had no extra effect on glucose production (335±22 vs 373± 16). However, the combination of metformin and salicylate inhibited the fractional partitioning of DHA to glucose relative to glycolysis (37.2±1.7 vs 45±1.1) and increased glycolysis (1251±68 vs 862±25.3) with concomitant increase in total DHA metabolism (1983±83 vs 1642±51.2) (Figure 3-6 A-D). Salicylate is also an uncoupler and causes lowering of cell ATP (Smith et al., 2016). In this study salicylate was used at highest concentrations that do not cause ATP depletion (0.5mM). At this concentration, salicylate did not cause significant activation of AMPK, therefore salicylate was not further used in the rest of this study. The cellular ATP level was monitored in parallel and was unchanged (Figure 3-6 E). With xylitol as substrate, the effect of 100μM metformin on hepatic glucose production was less pronounced (278±42.4 vs 325±32; 14%) (Figure 3-7 A) compared with DHA (22%) (Figure 3-6 A). Inhibition of the rate of glucose production by metformin was associated with an increase in glycolysis (613±88.2 vs 524±36.6) (Figure 3-7 B) and decrease in the fractional partitioning of xylitol to glucose relative to glycolysis (55±9 vs 67±6) (Figure 3-7 C) without changing total xylitol metabolism (1046±63 vs 988±32) (Figure 3-7 D). The AMPK activator A-769662 had no effect on gluconeogenesis, glycolysis, and the fractional partitioning of xylitol to glucose relative to glycolysis (Figure 3-7 A-D). There was no change in ATP with the various treatments (Figure 3-7 E). Cumulatively, the above results indicated that the low metformin dose that causes a more oxidised mitochondrial redox state lowers the rate of glucose production from both oxidised (DHA) and reduced (xylitol) gluconeogenic precursors. The metformin effect is not mimicked by activation of AMPK because the AMPK-activator A-769662 which causes similar phosphorylation of ACC-P as high metformin did not inhibit glucose production from the oxidised substrate DHA.

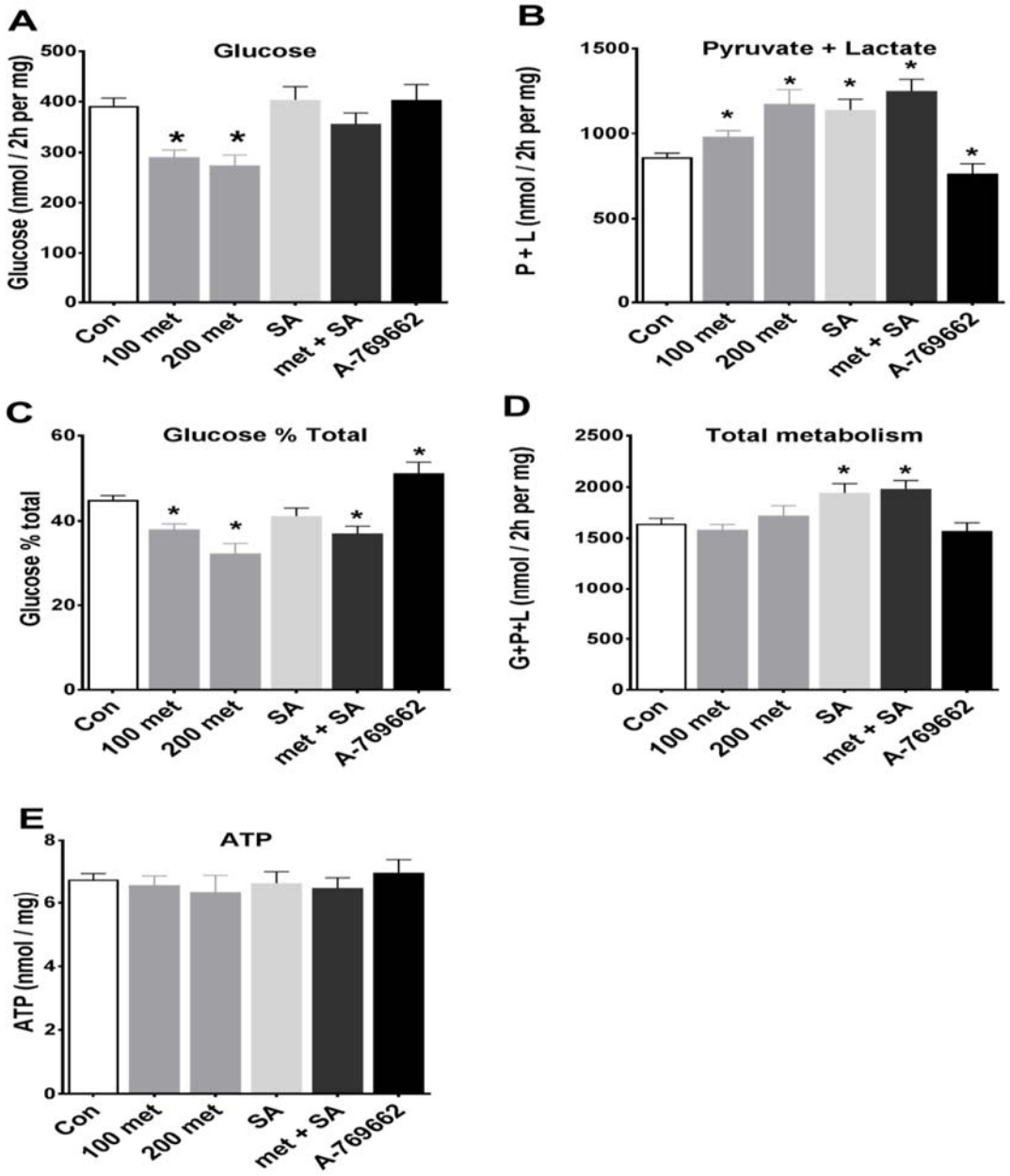

Figure 3-6: Metformin lowers gluconeogenesis from dihydroxyacetone DHA: the effect of metformin is not mimicked by either the AMPK activator, A-769662, or by salicylate (SA).

After overnight culture mouse hepatocyte monolayers were incubated with metformin, 500µM SA, 100µM metformin plus 500µM salicylate, and 10µM A-769662 in glucose-free DMEM for 2h. The medium was then replaced by glucose-free DMEM containing 5mM DHA and other additions as indicated (µM) and incubated for 2h. (A) Glucose production, (B) pyruvate plus lactate (C) glucose production percentage (D) total DHA metabolism. Results are Means ±SEM, n=11.

***P <0.05 (One-way ANOVA) relative to control with no addition.**

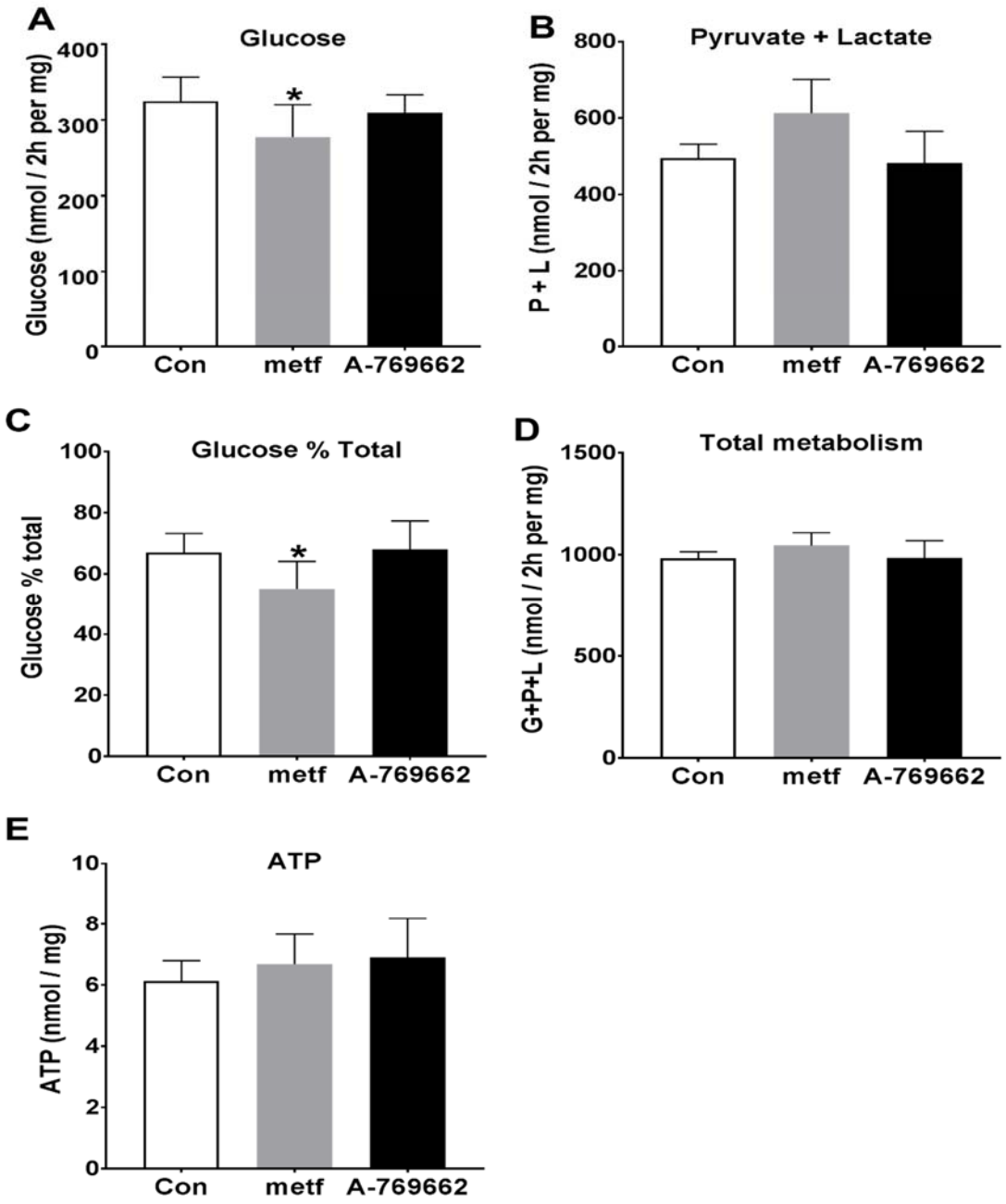

Figure 3-7: Metformin lowers gluconeogenesis from xylitol and the fractional partitioning of xylitol to glucose relative to glycolysis.

After overnight culture mouse hepatocyte monolayers were incubated with 100μM metformin, and 10μM A-769662 in glucose-free DMEM for 2h. The medium was then replaced by glucose-free DMEM containing 2mM xylitol and other additions as indicated (μM) and incubated for 2h. (A) Glucose production, (B) pyruvate plus lactate (C) glucose production percentage (D) total DHA metabolism (E) cell ATP level. Results are Means ±SEM, n=5.

***P <0.05 relative to control with no addition**.

3.2.4 Metformin lowers G6P with both DHA and high glucose as substrates- an effect mimicked by rotenone and DNP

Previous studies reported an AMPK-independent mechanism for the effects of metformin on both gluconeogenesis and lowering of cell G6P in conditions associated with lowering of ATP (Foretz et al., 2010, Guigas et al., 2006). A proposed mechanism for the lowering of G6P was inhibition of glucose phosphorylation (Guigas et al., 2006). In this study metformin inhibited gluconeogenesis in conditions of maintained ATP, we therefore next tested the effects of metformin on cell G6P with either DHA (mouse hepatocytes) or with high glucose (25mM) in mouse and rat hepatocytes in comparison with the AMPK activator (A-769662), salicylate, rotenone, and the uncoupler (DNP).

Because cell G6P is very low in a glucose-free medium we used the chlorogenic acid derivative, S4048 an inhibitor of G6P translocase (G6PT) to block hydrolysis of G6P to glucose (van Dijk et al., 2001, Hemmerle et al., 1997). With DHA as substrate, low metformin lowered the cellular G6P level (1.6±0.3 vs 2.4±0.2), while activation of AMPK by A-769662 had no effect on G6P (2.3±0.2 vs 2.4±0.2). Cell ATP was unchanged with both conditions (Figure 3-8 A-B).

With high glucose (25mM), metformin (100-500μM) caused a concentration-dependent lowering in the cellular G6P level in mouse (Figure 3-8 C) and rat (Figure 3-8 E) hepatocytes. This effect was mimicked by the complex 1 inhibitor (rotenone), salicylate plus metformin, and the uncoupler (DNP) (Figure 3-8 C,E), while there was no effect on G6P level by A-769662 or salicylate alone. Cell ATP was unchanged with all conditions (Figure 3-8 F). Collectively, (1) metformin lowered the cellular G6P level with both DHA and glucose, without lowering cell ATP. (2) The effect of metformin on cell G6P was mimicked by the complex 1 inhibitor (rotenone) and the uncoupler (DNP) but not by the AMPK activator. This suggests a mechanism linked to mitochondrial function but not AMPK activation that results in lowering of G6P in conditions of maintained ATP.

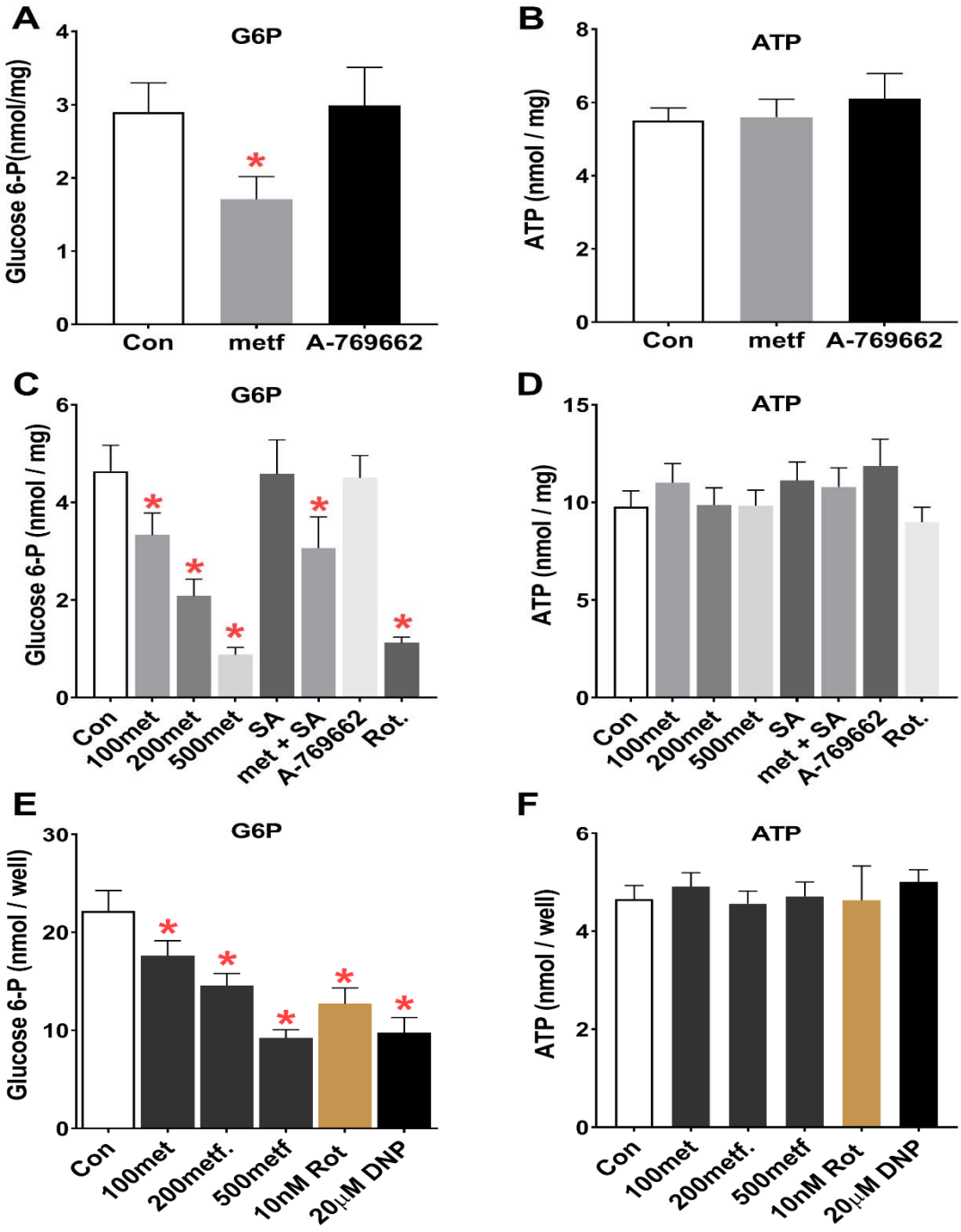

Figure 3-8: Metformin lowers cell G6P in a concentration-dependent manner.

After overnight culture hepatocytes monolayers (A-D mouse, E-F rat) were incubated with either glucose-free DMEM for (A and B) or MEM (C-F) and (100-500μM) metformin, 500μM SA, 100μM metformin plus 500μM salicylate, and (10μM) A-769662 for 2h. The medium was changed with either glucose-free DMEM containing (5mM DHA and 0.2μM S4048; A and B) or MEM (25mM glucose and 0.2μM S4048 and 0.25mM octanoate; C-F) with the conditions indicated for either 1h (MEM) or 2h (GFM). (A, C and E) G6P level and (B, D and F) ATP. Results are Means ±SEM, for 5-6 individual experiments.

***P <0.05 relative to control with no addition.**

3.2.5 Metformin lowers G6P at high glucose without inhibition of glucose phosphorylation

Previous studies on hepatocytes from AMPK deficient mice showed that the lowering of G6P by high metformin (3mM) could be explained by inhibition of glucose phosphorylation (Guigas et al., 2006). The effects of metformin (200-1000μM), 20μM DNP and 10μM A-769662 on glucose phosphorylation and glycolysis were determined in rat hepatocytes incubated with 25mM glucose containing 1.5μCi/ml of [2-^{3}H] glucose for glucose phosphorylation or [5-^{3}H] glucose for glycolysis. The results showed that activation of AMPK by A-769662 significantly inhibited both glucose phosphorylation (19±2.4 vs 31±3) (Figure 3-9 A) and glycolysis (18±1.8 vs 26±4) (Figure 3-9 B). However there was no effect on glucose phosphorylation by metformin up to 1000μM or the uncoupler (20μM DNP) (33±3, 32±3, 27±1.6 and 30.5±2.0 vs 31±3), also they did not affect glycolysis (27±4.0, 24.4±2.8, 22.2±2.7 and 30.7±3.6 vs 25.8±4) (Figure 3-9 A and B) and cell ATP was unchanged (Figure 3-9 C).

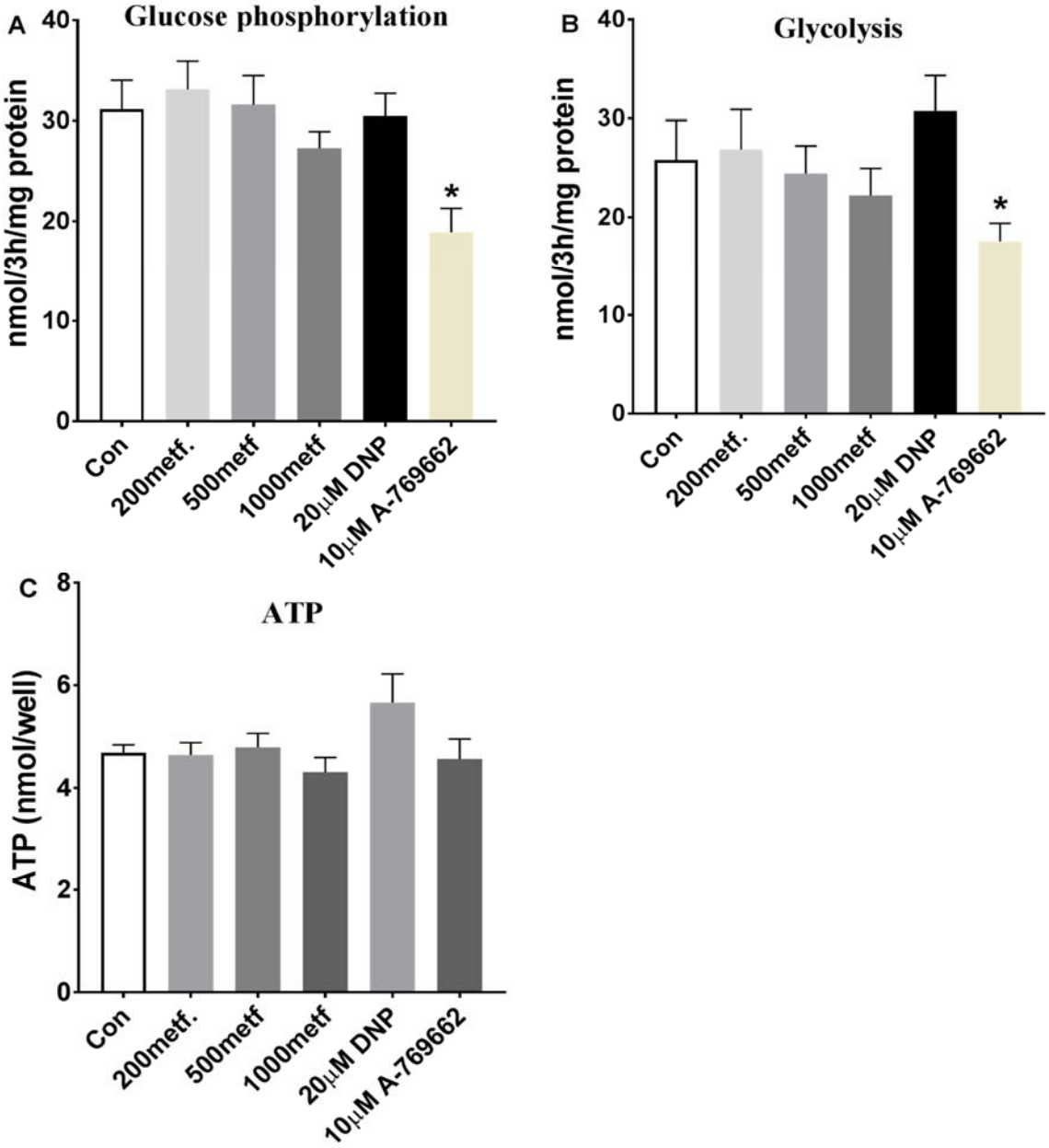

Figure 3-9: The AMPK activator A769662, but not metformin inhibits glucose phosphorylation and glycolysis in hepatocytes.

After overnight culture rat hepatocyte monolayers were incubated in MEM with metformin and A-769662 for 2h. the medium was changed with fresh MEM containing 25mM glucose, and either [2-^{3}H] glucose (A) or [5-^{3}H] glucose (B) and the hepatocytes were incubated for 3h for determination of glucose phosphorylation and glycolysis, respectively from the formation of $^{3}H_2O$. Rates of glucose phosphorylation and glycolysis are expressed as nmol/h/well (A and B). Cell ATP (C) is expressed as nmol/well. Results are Means ± SEM for n=4 individual hepatocytes preparation (A and C); n=3 individual hepatocytes preparation (B).

*** P< 0.05 relative to control with no addition**

3.2.6 Hepatocytes from NNT-deficient mice have higher G6P but similar redox state changes with metformin

The above results showed that metformin lowered the cellular G6P level in mouse and rat hepatocytes and this effect was mimicked by the complex 1 inhibitor (rotenone) and the uncoupler (DNP). One of the mechanisms linked to complex 1 inhibitor and uncoupling is a decrease in the mitochondrial proton gradient. Two mechanisms that are driven by the proton gradient are generation of ATP by ATP synthase (Complex V) and the activity of nicotinamide nucleotide transhydrogenase (NNT) which catalyzes the synthesis of NADPH from NADH and $NADP^+$ coupled to the transfer of protons across the mitochondrial membrane into the mitochondria.

NNT is one of two major mechanisms that generate NADPH in mitochondria, the other being isocitrate dehydrogenase (ICDH) (Ronchi et al., 2013, Rydstrom, 2006). Malic and the pentose phosphate pathway generate NADPH in the cytoplasm and various shuttles can transfer NADPH between the mitochondria and cytoplasm (Guay et al., 2013). A possible mechanism for the decrease in G6P by metformin, rotenone and DNP is by inhibition of NNT and increase the metabolism of G6P by the pentose phosphate pathway. To test this hypothesis we used hepatocytes from two mouse genotypes (wild-type, $NNT^{+/+}$) and (NNT-deletion, $NNT^{-/-}$). The hepatocytes were incubated with high glucose (25mM) in the presence of G6P transport inhibitor (S4048). Hepatocytes from the NNT-deletion mouse (C57Bl6J) showed higher G6P level comparing to wild-type mice (Figure 3-10 A). The concentration dependent lowering of G6P by metformin was similar in hepatocytes from both genotypes (Figure 3-10 A). The cellular ATP level was unchanged in all conditions (Figure 3-10 B). To further investigate the role of NNT in the metformin mechanism, hepatocytes from wild-type and NNT-deletion mouse were incubated with high glucose (25mM) in the presence of 0.25mM octanoate to measure the 3-hydroxybutryate / acetoacetate ratio and ketone body formation. Both genotypes had the same 3-hydroxybutryate / acetoacetate ratio (Figure 3-10 C) and rate of formation of ketone bodies (Figure 3-10 D). The biphasic effect of metformin was shown in both wild-type and NNT-deletion hepatocytes a more oxidised with 100µM metformin and a more reduced with 500µM metformin. With the complex 1 inhibitor and 500µM metformin the mitochondrial redox state was more reduced in hepatocytes from both genotypes (Figure 3-10 C). The formation of ketone bodies was increased by low 100µM metformin in both wild-type and

NNT-deleted hepatocytes, while high 500μM metformin and rotenone decreased the production of ketone body (Figure 3-10 D)

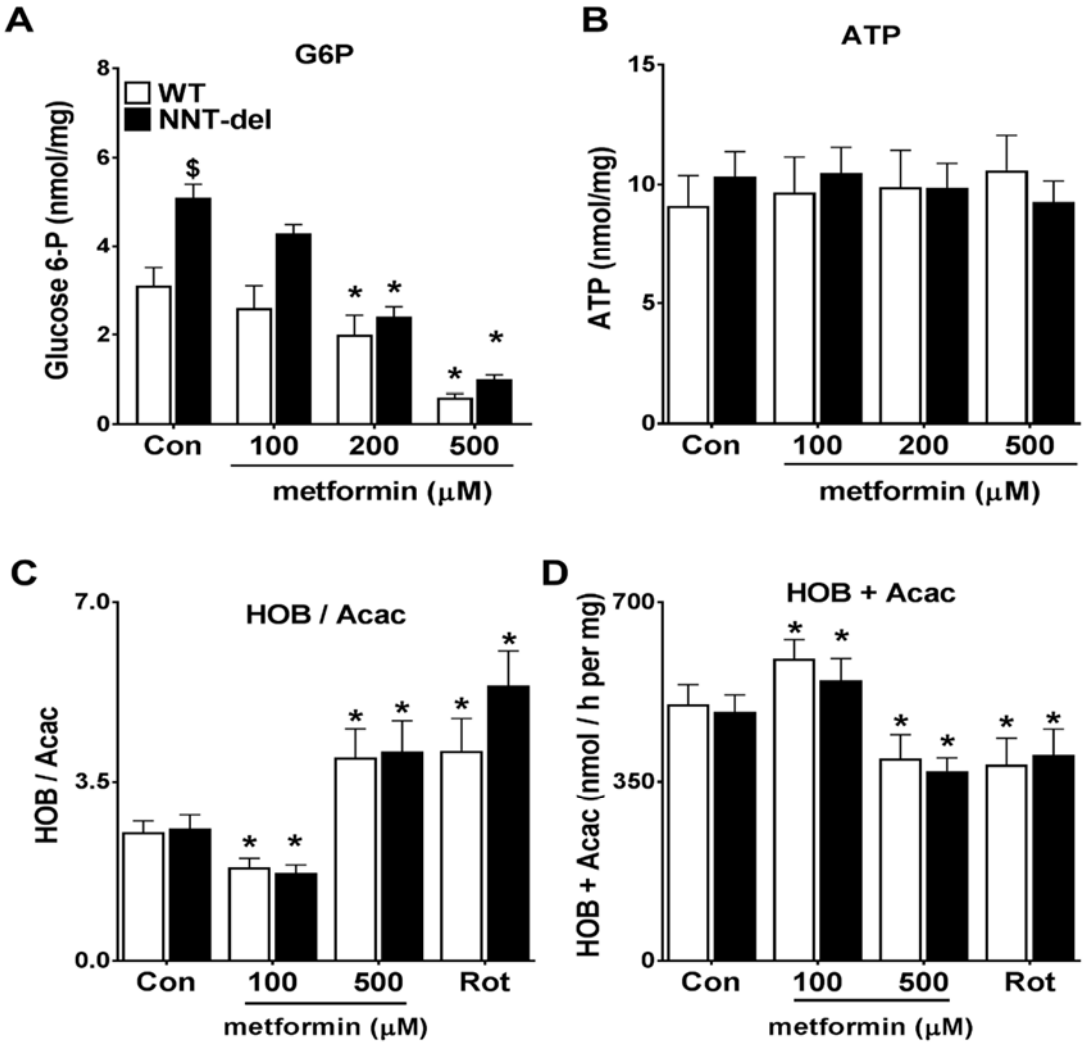

Figure 3-10: Cell G6P is higher in hepatocytes from NNT-deficient mice than in hepatocytes from wild-type mice.

After overnight culture mouse hepatocyte monolayers were incubated with metformin in MEM for 2h. The medium was replaced by MEM with 25mM glucose, 0.25mM octanoate in the presence (A-B) or absence (C-D) of 0.2μM S4048 with other conditions as indicated for 1h. *(A) Cell* **G6P level, (B) Cell ATP level, (C)** *3*-**hydroxybutyrate / acetoacetate ratio** *(D) 3*-**hydroxybutyrate plus acetoacetate. Results are Means ± SEM for n=3 individual hepatocytes preparation (A and B); n=6 individual hepatocytes preparation (C and D).**
*** P< 0.05 relative to control with no addition**

$ P<0.05 effect of NNT-deletion.

3.2.7 NNT-deficiency does not affect the metformin inhibition of gluconeogenesis from DHA and xylitol

Hepatocytes from NNT$^{-/-}$ mice and NNT$^{+/+}$ (Wild-type) mice were used to test the effect of metformin on gluconeogenesis from oxidised (DHA) or reduced (xylitol) substrates.

With both DHA and xylitol as substrate, hepatocytes from NNT$^{-/-}$ mice had lower rates of production of pyruvate plus lactate (Figure 3-11 B and Figure 3-12 B) but similar rates of glucose production (Figure 3-11 A and Figure 3-12 A) to hepatocytes from wild-type mice. Metformin (100µM) caused similar inhibition of glucose production in hepatocytes form NNT$^{-/-}$ mice as in wild-type hepatocytes (Figure 3-11 A and Figure 3-12 A). The activator of AMPK (A-769662) unlike metformin did not inhibit glucose production and in incubations (Figure 3-11 A and Figure 3-12 A), with xylitol it increased the fractional partitioning of xylitol to glucose (Figure 3-12 C). Total glucose plus pyruvate plus lactate production was significantly lower in hepatocytes from NNT$^{-/-}$ mice with a concomitant decrease in pyruvate plus lactate (Figure 3-11 B,D and Figure 3-12 B,D). Metformin lowered gluconeogenesis and the fractional partitioning of DHA in hepatocytes from both wild-type and NNT$^{-/-}$ mice (Figure 3-11 A and C), with negligible increase in glycolysis (Figure 3-11 B) without affecting total glucose plus pyruvate plus lactate formation (Figure 3-11 D). The activator of AMPK A-769662 (10µM) did not affect glucose production from wild-type hepatocytes and NNT$^{-/-}$ hepatocytes, but there was a trend to increase the fractional partitioning of DHA to gluconeogenesis relative to glycolysis in both mouse genotypes (Figure 3-11 A-D). The ATP level was unchanged with all conditions (Figure 3-11 E).

With xylitol as substrate, NNT$^{-/-}$ hepatocytes favoured gluconeogenesis rather than glycolysis and the fractional partitioning to glucose was slightly increased compared with hepatocytes from wild-type mouse concomitant with a trend to lower total glucose plus pyruvate plus lactate. The effect of 100µM metformin on hepatic glucose production was similar in both wild-type and NNT$^{-/-}$ hepatocytes (Figure 3-12 A) and metformin favoured glycolysis relative to gluconeogenesis, however, in NNT$^{-/-}$ hepatocytes metformin did not significantly increase pyruvate plus lactate formation (Figure 3-12 B). A-769662 (AMPK activator) unlike metformin favoured gluconeogenesis (Figure 3-12 A) rather than glycolysis by increased partitioning to glucose relative to glycolysis (Figure 3-12 C) and lowered pyruvate plus lactate production (Figure 3-12 B) with negligible effect on total glucose plus pyruvate plus lactate in hepatocytes from both wild-type and in NNT$^{-/-}$ mice (Figure 3-12 D). These effects were not associated with ATP depletion in both mice genotypes (Figure 3-12 E). These results suggested

that NNT might have a role in gluconeogenesis, but it does not mediate the mechanism of lowering glucose production by metformin.

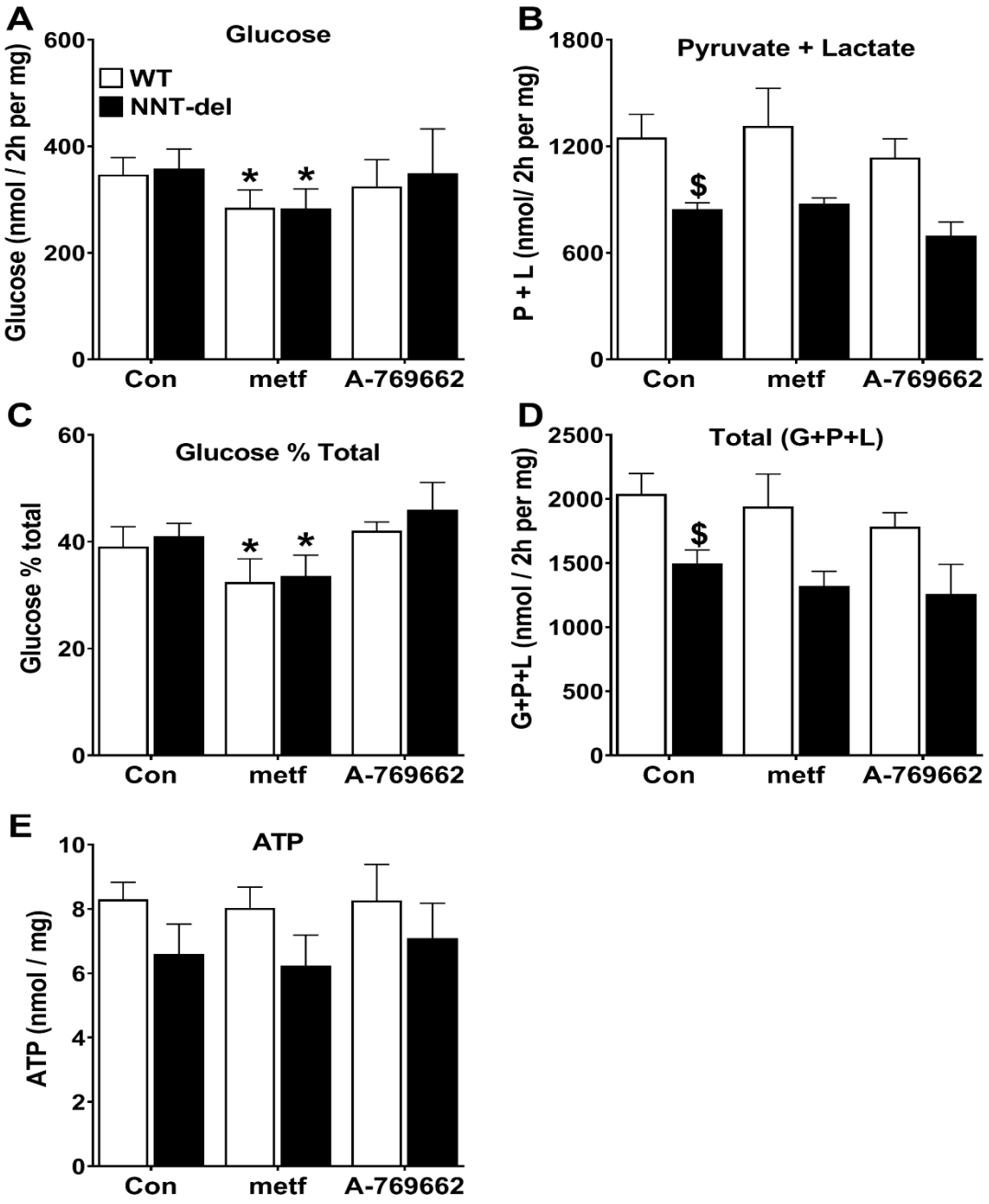

Figure 3-11: Metformin inhibits gluconeogenesis in hepatocytes from oxidised (DHA) substrate in both mouse genotypes.

After overnight culture mouse hepatocyte monolayers were pre-incubated with 100µM metformin and 10µM A-769662 in glucose-free DMEM for 2h. The medium was then replaced by glucose-free DMEM containing 5mM DHA and other additions as indicated for 2h. (A) Glucose production; (B) pyruvate plus lactate formation; (C) glucose production percentage; (D) total metabolism; (E) cell ATP level. Results are Means ±SEM, n=6.

***P <0.05 relative to control.**

$ P<0.05 effect of NNT-deletion.

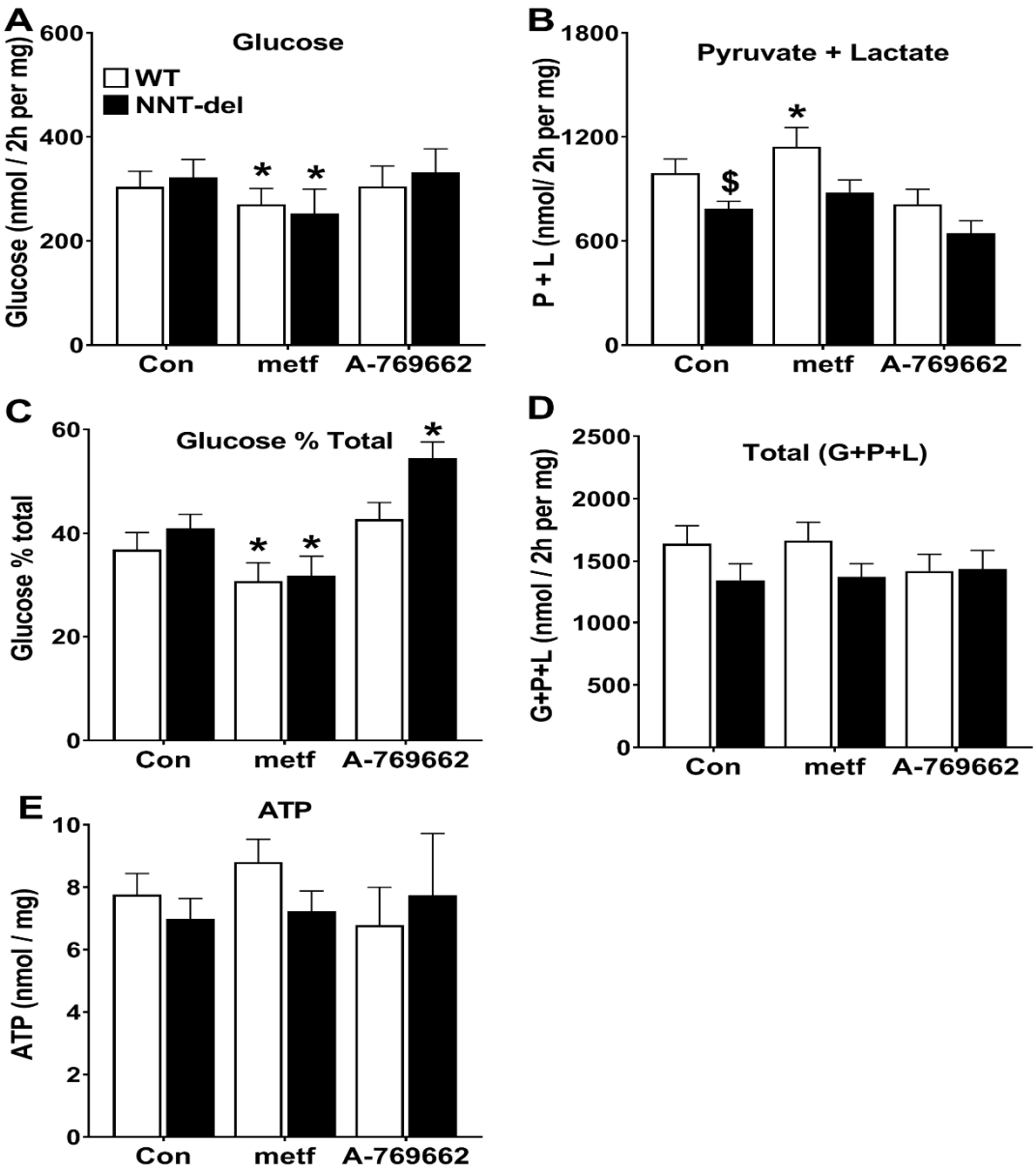

Figure 3-12: Metformin inhibits gluconeogenesis in hepatocytes from reduced (xylitol) substrate in both mouse genotypes.

Monolayer hepatocytes pre-incubated similar to figure 3-11, and then incubated with 2mM xylitol for further 2h in free-glucose DMEM with indicated conditions. (A) glucose production; (B) pyruvate plus lactate formation; (C) glucose production percentage, (D) total metabolism; (E) cell ATP level. Results are Mean±SEM, n=4.

***P<0.05 relative to control.**

$ P<0.05 effect of NNT-deletion.

3.3 Discussion

There remains little consensus on the mechanism by which metformin inhibits hepatic glucose production. The major mechanisms that have been proposed include: (1) Inhibition of complex 1 and thereby the mitochondrial respiratory chain which has a high control strength on gluconeogenesis through compromised energy status (El-Mir et al., 2000, Owen et al., 2000, Miller et al., 2013). (2) Activation of AMPK through either inhibition of complex 1 which results in a raised AMP / ATP or through other mechanisms (Zhou et al., 2001). However this mechanism has been challenged because metformin inhibited gluconeogenesis in mice lacking AMPK and its upstream LKB (Foretz et al., 2010). (3) Various mechanisms have been proposed to explain the AMPK independent inhibition of gluconeogenesis. These include a raised cell AMP which inhibits glucagon signalling (Miller et al., 2013) and also FBP-1 (Hunter et al., 2018) and also a redox dependent mechanism linked to inhibition of mGPDH. This mechanism proposes a more reduced cytoplasmic redox state and a more oxidised mitochondrial redox state. A key caveat of this mechanism is that it proposes inhibition of gluconeogenesis from reduced but not from oxidised substrates.

A key problem with the above diverse mechanisms is that some of these mechanisms are observed only at a high dose of metformin that may not be of therapeutic relevance. A recent study showed that 20-50mg/kg metformin causes a more oxidised redox state in rat liver and inhibits hepatic glucose production. *In vitro* study on hepatocytes reported that 100µM metformin lowered gluconeogenesis from reduced (lactate and glycerol) but not from oxidised (DHA and pyruvate). However, this study did not show whether 100µM metformin makes the mitochondrial redox state more oxidised or more reduced in isolated hepatocytes (Madiraju et al., 2014). In the present study the metformin concentration and exposure time used in hepatocytes resulted in cellular metformin levels (1-2nmol/mg) that are relevant to the therapeutic dose after metformin (50mg/kg or 3gm/60kg) treatment (Wilcock and Bailey, 1994, Al-Oanzi et al., 2017). The main findings of this chapter are

1- Metformin has a biphasic effect on the redox state: a more oxidised at low (100µM) metformin concentration and a more reduced at high (500µM) metformin.
2- Metformin (100µM) inhibits gluconeogenesis from the oxidised and reduced substrates. This effect is not associated with a decrease in ATP and was not mimicked by AMPK activation.

3- Metformin (100μM) lowers G6P without inhibition of glucose phosphorylation or lowering ATP.
4- The metformin effect on G6P is mimicked by rotenone and DNP but is not due to NNT inhibition.

These effects are discussed below. Previous studies on the effects of metformin (1-10mM) on the mitochondrial redox state in isolated hepatocytes have reported either an increase in the ratio of 3-HOB/Acac or no effect (Owen et al., 2000, Gouaref et al., 2017). The more reduced NADH/NAD ratio was explained by inhibition of complex 1 as shown in studies on isolated mitochondria (El-Mir et al., 2000, Owen et al., 2000) or the purified enzyme (Bridges et al., 2014). In the present study we found a more reduced NADH/NAD redox state with rotenone (as expected) and at 500μM metformin but not at lower metformin concentrations. The cellular metformin content at 500μM metformin is about 5 nmol/mg cell protein (Al-Oanzi et al., 2017). This is higher than the maximum metformin level in the liver after a therapeutic dose (50mg/kg metformin). This supports the conclusion by Madiraju *et al*. (2014) that inhibition of complex 1 does not occur at a therapeutic dose of metformin but only at higher doses. Madiraju *et al.* (2014, 2018) reported from studies *in vivo* that a therapeutic dose of metformin causes a more oxidised mitochondrial redox state. However, studies *in vivo* cannot rule out an indirect mechanism for example that is caused by changes in hormones or circulating levels of fatty acids. The present study demonstrates for the first time that treatment of hepatocytes with a low concentration of metformin (100μM) causes a more oxidised redox state. This concentration of metformin results in cellular accumulation of the drug to the same level (1-2 nmol/mg) as occurs *in vivo* after a 50mg/kg dose (Al-Oanzi et al., 2017). This supports the conclusion of Madiraju and colleagues (2014) that at a therapeutic level the effect of metformin on hepatocytes is a more oxidised mitochondrial redox state. At least 4 mechanisms can be considered for the more oxidised mitochondrial NADH/NAD redox state by 100μM metformin. First, this could be due to inhibition of production of NADH within mitochondria. Second, it could be due to an increase in activity of the respiratory chain which oxidies NADH by complex 1 with the transfer of electrons to ubiquinone and then down the electron transport chain. Two other possibilities are the inhibition of the transfer of reducing equivalents from the cytoplasm to mitochondria by either the malate-aspartate or the glycerophosphate shuttles (Madiraju et al., 2014, Bridges et al., 2014). The present experiments allow us to exclude the first mechanism that metformin inhibits the production of NADH in mitochondria. The rate of ketone body production was measured from 3-hydroxybutyrate plus acetoacetate. The use of

medium chain fatty acid, octanoate, as ketogenic precursor was made up depending on (i) that the mitochondrial uptake of octanoate is independent of carnitine palmitoyltransferase I (McGarry and Foster, 1980, Pegorier et al., 1989) (ii) its ability to form ketone body is high (Barrena et al., 2009). Octanoate is metabolized in the mitochondria by β-oxidation to acetyl-CoA, resulting in the production of NADH and FADH2. The acetyl-CoA formed from octanoate is then converted to acetoacetate and 3-hydroxybutyrate (Ferre et al., 1981). Low metformin caused an increase in the sum of acetoacetate plus 3-hydroxybutyrate production. This indicates an increase in total β-oxidation of octanoate and therefore in the production rate of NADH. The more oxidised state (lower NADH/NAD) at 100μM metformin is therefore associated with increased rather than decreased production of NADH. The opposite situation occurred at high metformin which caused an increase in the mitochondrial NADH/NAD ratio (increase in HOB/Acac) but a decrease in production of HOB plus Acac and therefore in the production rate of NADH. These opposite changes in the production rate of NADH and in the ratio of NADH/NAD suggest that the effect of metformin on the mitochondrial redox state may be the primary mechanism and that the stimulation (low metformin) or inhibition (high metformin) on β-oxidation of octanoate is secondary to the change in the redox state.

The second aim of this chapter was to test whether the metformin effect on gluconeogenesis is dependent on whether the substrate is oxidised (DHA) or reduced (xylitol or glycerol). Previous studies using high metformin concentrations reported inhibition of gluconeogenesis that was independent of the redox state of the substrate (Fulgencio et al., 2001, Gouaref et al., 2017) However, more recent work using 100μM metformin reported inhibition of gluconeogenesis from reduced substrates (glycerol and lactate) but not from oxidised substrates (pyruvate and DHA) (Madiraju et al., 2014). The present study showed that the low metformin dose that caused a more oxidised mitochondrial NADH/NAD redox state inhibited gluconeogenesis from both oxidised (DHA) and reduced (xylitol) substrates. This inhibition cannot be explained by inhibition of complex 1 because of the more oxidised mitochondrial redox state. It also cannot be explained by AMPK activation, because the small molecule activator of AMPK that caused strong phosphorylation of ACC did not mimic the effect of metformin on gluconeogenesis. In addition the low dose of metformin unlike A-769662 or 500μM metformin did not cause phosphorylation of acetyl-CoA carboxylase. This finding agrees with the recent studies that reported significant AMPK activation after a metformin dose of 250mg/kg (Hunter et al., 2018) but not after a dose of 50 mg/kg (Madiraju et al., 2014, Madiraju et al., 2018). Based on the cellular accumulation studies showing that with 500μM metformin cellular

accumulation occurs to >5 nmol/mg whereas with 100μM cellular accumulation occurs to < 1-2 nmol/mg which is similar to the peak level in the liver after 50mg/kg (Wilcock and Bailey, 1994, Al-Oanzi et al., 2017), the present findings support the following conclusions. First, that there is negligible activation of AMPK at a therapeutic dose of metformin (100μM) but significant activation at a 5-fold higher dose. Second, that activation of AMPK by A-769662 to a comparable level as occurs at high metformin (500μM or 5 nmol/mg) does not mimic the metformin inhibition of gluconeogenesis or the lowering of G6P. Third that the inhibition of gluconeogenesis by the low dose of metformin that causes a more oxidised mitochondrial redox state is independent of whether the gluconeogenic precursors are reduced (xylitol) or oxidised (DHA).

Previous studies reported lowering of G6P by metformin both *in vivo* (Owen et al., 2000) and also in isolated hepatocytes (Fulgencio et al., 2001, Guigas et al., 2006, Owen et al., 2000) incubated with high metformin concentrations (2-10mM). The hepatocyte studies were performed with either gluconeogenic precursors (Fulgencio et al., 2001, Owen et al., 2000) or with high glucose (Guigas et al., 2006) and in the latter study an AMPK-independent mechanism involving inhibition of glucose phosphorylation was proposed (Guigas et al., 2006). The aims of the present study were to determine whether the lowering of G6P occurs at a therapeutic dose of metformin (1-2 nmol/mg) and whether this effect involves interactions of metformin with multiple metabolic pathways. G6P is generated by glucose phosphorylation, gluconeogenesis and glycogenolysis and it is metabolised by several pathways including glycogen synthesis, glycolysis and the pentose pathway. Lowering of G6P by metformin could involve inhibition of G6P production by glucose phosphorylation and / or gluconeogenesis and / or stimulation of G6P metabolism by one or more pathways. In this study we show that the low dose of metformin lowers G6P with both DHA and high glucose as substrate and that the latter cannot be explained by inhibition of glucose phosphorylation. This suggests either that a single G6P consuming pathway (for example the pentose pathway or glycolysis) could explain the G6P lowering effect of metformin with both DHA and high glucose or alternatively that effects of metformin on two or more pathways could explain the effect with DHA and high glucose. Because the lowering of G6P by metformin was mimicked by rotenone which decreases the mitochondrial proton gradient by inhibiting the electron transport and proton pumping and also by DNP which dissipates the proton gradient, we tested the hypothesis that the metformin effect on G6P could be explained by inhibition of NNT activity which is dependent on the proton gradient. Although hepatocytes from NNT deficient mice had a raised

G6P, metformin caused a similar lowering of G6P as in wild-type hepatocytes. Although we cannot rule out inhibition of NNT by metformin, we can conclude that metformin causes substantial lowering of G6P by a mechanism that is independent of inhibition of NNT and also independent of activation of AMPK and inhibition of complex 1. A possible mechanism that could explain the lowering of G6P by DNP and rotenone but not by AMPK activators is the depolarization of the mitochondria which is expected to occur with rotenone by inhibition of the respiratory chain and by DNP by dissipation of the proton gradient and by metformin through accumulation inside the mitochondria, or binding to the mitochondrial membranes or other mechanisms (Won et al., 2015, Khailova et al., 2017). Depolarization of mitochondria might be expected to affect various mechanisms that are dependent on the mitochondrial potential. Candidate mechanisms include the malate aspartate shuttle which is dependent on the mitochondrial potential and inhibited by the mitochondrial depolarization (Berry et al., 1992, Davis et al., 1980, LaNoue et al., 1974, Sibille et al., 1995) also the adenine nucleotide translocator which exchanges cytoplasmic ADP^{3-} for mitochondrial ATP^{4-} (Maldonado et al., 2016, Zorova et al., 2018). Inhibition of this transporter by mitochondrial depolarization would be expected to cause an increase in the cytoplasmic ADP/ATP ratio as shown by Owen *et al.* (Owen et al., 2000). Although metformin did not decrease the total cell ATP content, we cannot exclude small changes in cytoplasmic ADP/ATP ratio through inhibition of the adenine nucleotide translocator by mitochondrial depolarization.

This study shows that metformin lowered the cell G6P level in a concentration-dependent manner in mouse and rat hepatocytes. G6P is an intermediate of glycolysis and gluconeogenesis and several other pathways. Glucose is phosphorylated by glucokinase to G6P, this reaction involves consumption of ATP. The lowering effect of metformin on G6P can be explained by either (i) a decrease in the rate of glucose phosphorylation or (ii) increase in the downstream metabolism of G6P either toward glycolysis or the pentose phosphate pathway. In this study we show that the decrease in G6P by metformin is not associated with either depletion in ATP or inhibition of the rate of glucose phosphorylation. Accordingly, lowering of G6P by metformin cannot be explained by inhibition of glucose phosphorylation or by changing energy state of hepatocytes. Interestingly, G6P level was lowered by the complex 1 inhibitor (rotenone) and the uncoupler (DNP) similar to metformin, indicating that the lowering effect might be due to mitochondrial depolarization. One possible mechanism linked to mitochondrial depolarization and affecting the proton gradient is the mitochondrial nicotinamide nucleotide transhydrogenase (NNT) which catalyses the formation of NADPH

from NADH and $NADP^+$. The hypothesis of inhibition of NNT by metformin to lower G6P and gluconeogenesis was tested in mouse hepatocytes from $NNT^{-/-}$ and wild-type mice. We concluded that the effect of metformin in both genotypes was similar, and metformin has biphasic effect on the mitochondrial redox state in wild-type and $NNT^{-/-}$ hepatocytes. Metformin inhibits the rate of gluconeogenesis in both genotypes from DHA (oxidised) and xylitol (reduced) as substrates. Therefore, we excluded the hypothesis of inhibition of NNT by metformin.

3.4 Summary:

This study has shown that:

1- Metformin has a biphasic effect on the mitochondrial NADH/NAD redox state: a more oxidised at low metformin and a more reduced at high metformin concentration. These effects of metformin are not explained by inhibition and stimulation respectively of mitochondrial production of NADH and suggest either a direct effect of metformin on the respiratory chain or an effect on the transfer of reducing equivalents into mitochondria.

2- Low metformin causes inhibition of glucose production from both oxidised and reduced substrates and lowers G6P with both DHA and high glucose

3- High (500µM or > 5nmol/mg) but not low (100µM or < 2 nmol/mg) metformin causes AMPK activation.

4- AMPK activation with an allosteric activator of the beta-subunit does not mimic the metformin inhibition of glucose production or the lowering of G6P.

5- Rotenone and DNP mimic the metformin effect on G6P but deletion of NNT does not abolish the metformin effect. This implicates a role for the mitochondrial proton gradient or electrochemical potential on the flux through metabolic pathways linked to G6P.

CHAPTER 4: RESULTS 2

ROLE OF THE MALATE-ASPARTATE SHUTTLE (MAS) AND THE GLYCEROPHOSPHATE SHUTTLE (GPS) IN GLUCONEOGENESIS

Chpater. 4 Role of the malate-aspartate shuttle (MAS) and the glycerophosphate shuttle (GPS) in gluconeogenesis

4.1 Aims and rationale

The work in the previous chapter provided evidence that inhibition of gluconeogenesis by low concentrations of metformin occurs in association with a more oxidised mitochondrial redox state and therefore cannot be explained by inhibition of Complex 1. It also shows that it cannot be explained by activation of AMPK. Two mechanisms have been proposed to explain inhibition of gluconeogenesis by AMPK independent mechanisms. A recent study reported that metformin indirectly inhibits FBP-1 via increases in the concentration of AMP. This study showed that FBP-1 is not a direct target for metformin however, the lowering of blood glucose is attenuated in a mouse model of a knock-in mutation in FBP-1 which makes the enzyme insensitive to inhibition by AMP. This study suggests that the effect of metformin is at least in part due to raised levels of AMP and independently of AMPK (Hunter et al., 2018). The other mechanism for inhibition of gluconeogenesis by metformin proposes that is linked to direct inhibition of mGPDH and to transfer of reducing equivalents from the cytoplasm to mitochondria. This hypothesis proposes that the inhibition of gluconeogenesis by metformin is linked to a more oxidised mitochondrial redox state and a more reduced cytoplasmic redox state (Madiraju et al., 2014)

Two shuttles control the transfer of the NADH reducing equivalents form the cytoplasm to mitochondria, the malate-aspartate shuttle (MAS) and the glycerophosphate shuttle (GPS) as described in chapter one. Early studies reported that inhibition of the MAS by 0.2-2mM AOA lowered gluconeogenesis from reduced substrates (lactate, glycerol, and xylitol) but not from oxidised (pyruvate, and DHA) substrates in hepatocytes (Arinze et al., 1973, Rognstad and Clark, 1974). However, genetic deletion of citrin, a carrier of aspartate-glutamate in mitochondria, that is expressed in liver, kidney, heart and small intestinal and is an essential component of the MAS to transfer aspartate out of mitochondria (Kobayashi et al., 1999, Iijima et al., 2001, Begum et al., 2002) had little effect on lowering of blood glucose. In contrast genetic knock-out of both the GPS by deletion of mGPDH and of citrin, in the double knock-out citrin/mGPDH model resulted in greater lowering of blood glucose compared with the citrin knock-out model. In addition knock-out of mGPDH alone in mice showed either no effect on plasma glucose compared to wild-type mice (Saheki et al., 2007) or a small decrease in fasting plasma glucose compared with control littermates (Brown et al., 2002). These genetic studies together indicate that in mouse models both shuttles can compensate when either shuttle is

genetically deleted. On the other hand Madiraju and colleagues (2014) reported that treatment of rat hepatocytes with siRNA to knock-down mGPDH abolished hepatic glucose production from reduced (lactate and glycerol) but not oxidised (pyruvate DHA and alanine) substrates and that metformin similarly inhibited gluconeogenesis from reduced substrates (lactate and glycerol) but not oxidised substrates. This effect of metformin was explained by non-competitive inhibition of mitochondrial glycerophosphate dehydrogenase. From studies *in vivo* the authors proposed that the metformin effect is associated with a more oxidised mitochondrial redox state (decrease NADH / NAD^+ ratio) and a more reduced cytoplasmic redox state (increase NADH / NAD^+ ratio). This effect was explained by inhibition of transfer of NADH from the cytoplasm to mitochondria by inhibition of the GPS. Madiraju and colleagues (2014 and 2018) claimed that the more reduced cytosolic redox state prevented the conversion of lactate to pyruvate and glycerol 3-phosphate (G3P) to dihydroxyacetone phosphate (DHAP) lowering glucose production from these substrates. Inhibition of the MAS was excluded because metformin had no effect on malate dehydrogenase activity (Madiraju et al., 2014, Madiraju et al., 2018). However this mechanism of inhibition of the GPS by metformin for explaining the inhibition of gluconeogenesis has been challenged because the malate-aspartate shuttle is thought to have a more prominent role in the liver than the glycerophosphate shuttle in man (Baur and Birnbaum, 2014) and also in the mouse as shown by the genetic models of mGPDH and citrin knock-out (Saheki et al., 2007).

Regulation of mGPDH in liver is controlled acutely by calcium and chronically by altered thyroid states (Scholz et al., 2000, Gellerich et al., 2010, Hunt et al., 1970). Several studies showed that up- and down-regulation of mGPDH is linked to levels of thyroid hormones (L-3,3'-5 triiodothyronine T3 and thyroid-stimulation hormone) (Hunt et al., 1970, Sellinger and Lee, 1964, Hamatani et al., 1991, Costante et al., 1990). Comte and colleagues (1990) reported that raised thyroid hormone level causes an increase in mitochondrial glycerophosphate dehydrogenase and an increase in the rate of gluconeogenesis in rat hepatocytes from 2mM glycerol, 10mM lactate, and 10mM pyruvate. This increment was associated with lowering of cell G3P level. While hypothyroidism caused an increase in cell G3P level and inhibited hepatic glucose production (Comte et al., 1990). Furthermore, the rate of hepatic glucose production was measured in hepatocytes from thyroidectomized rats that were untreated or treated with T3. Hepatocytes from hypothyroid rats had low mGPDH activity and rates of glucose production treatment with T3 hormone to hypothyroid rats reversed the effect on glucose production and mGPDH activity (Kneer and Lardy, 2000). Evidence for a link between glucose

production from glycerol and the activity of mGPDH, was provided by studies on hepatocytes from the Lou/C rat which has high levels of expression of the thyroid hormone receptor and of activity of mGPDH and of raised gluconeogenesis compared with Wistar rats. This model is also characterized by high rates of octanoate oxidation to 3-hydroxybutyrate plus acetoacetate and a more oxidised mitochondrial redox state (Taleux et al., 2009).

Although several studies have reported an association between raised mGPDH and gluconeogenesis in hepatocytes from hyperthyroid animals no study has investigated the effect of direct stimulation of mGPDH in hepatocytes on gluconeogenesis.

The aims of this chapter were:

(i) To test whether inhibition of the GPS or the MAS mimics the effect of metformin on the mitochondrial redox state.
(ii) To test whether the inhibition of gluconeogenesis by metformin can be explained by inhibition of either the GPS or the MAS shuttles.
(iii) To test the role of mGPDH in gluconeogenesis.
(iv) To test the hypothesis that the effect of metformin on gluconeogenesis can be explained by altered regulation at PFK-1 and/or FBP1.

4.2 Results

4.2.1 Inhibition of the GPS, but not the MAS, makes the mitochondrial redox state more oxidised similar to low metformin

The first aim of this chapter was to test whether inhibition of the MAS with AOA or the GPS with the Gpi mimics the metformin effect on the mitochondrial redox state. Mouse hepatocytes were incubated with (100-500µM) metformin, 200µM aminooxyacetate (AOA) (an inhibitor of malate-aspartate; MAS), (20-40µM) Gpi (STK017597; an inhibitor of mitochondrial glycerophosphate dehydrogenase; mGPDH), and 0.25µM rotenone (complex 1 inhibitor). Octanoate was used as the substrate as in the previous experiments to measure both the mitochondrial redox state and the rate of fatty acid β-oxidation. The results from these experiments showed that Gpi, the inhibitor of the GPS, similar to low metformin (100µM) caused a more oxidised mitochondrial (NADH / NAD ratio) redox state, while inhibition of the MAS by AOA had no effect on the mitochondrial redox state (Figure 4-1 A). This indicates that a more oxidised redox state can arise as a result of inhibition of the GPS but not by inhibition of the MAS. Although the Gpi caused a more oxidised redox state, unlike metformin it did not stimulate β-oxidation as determined from the 3-hydroxybutyrate / acetoacetate ratio (Figure 4-1 B).

The more oxidised (decrease in NADH / NAD ratio) mitochondrial redox state causes by 100µM metformin was associated with a more reduced cytoplasmic (increase NADH / NAD ratio) redox state based on an increase in the lactate to pyruvate ratio. The uncoupler DNP had a negligible effect on the cytoplasmic redox state, while inhibition of the malate-aspartate shuttle by AOA and inhibition of complex 1 by rotenone like metformin made the cytoplasmic redox state more reduced (increase NADH / NAD ratio) (Figure 4-1 C). These results show (i) the biphasic effect of low and high metformin on the mitochondrial NADH / NAD ratio (ii) a more oxidised mitochondrial redox state with Gpi similar to low metformin (iii) lack of effect of the MAS inhibitor on the mitochondrial redox state. Collectively, like low metformin, the inhibition of the GPS caused a more oxidised mitochondrial redox state but without increasing the rate of 3-hydroxybutyrate plus acetoacetate production.

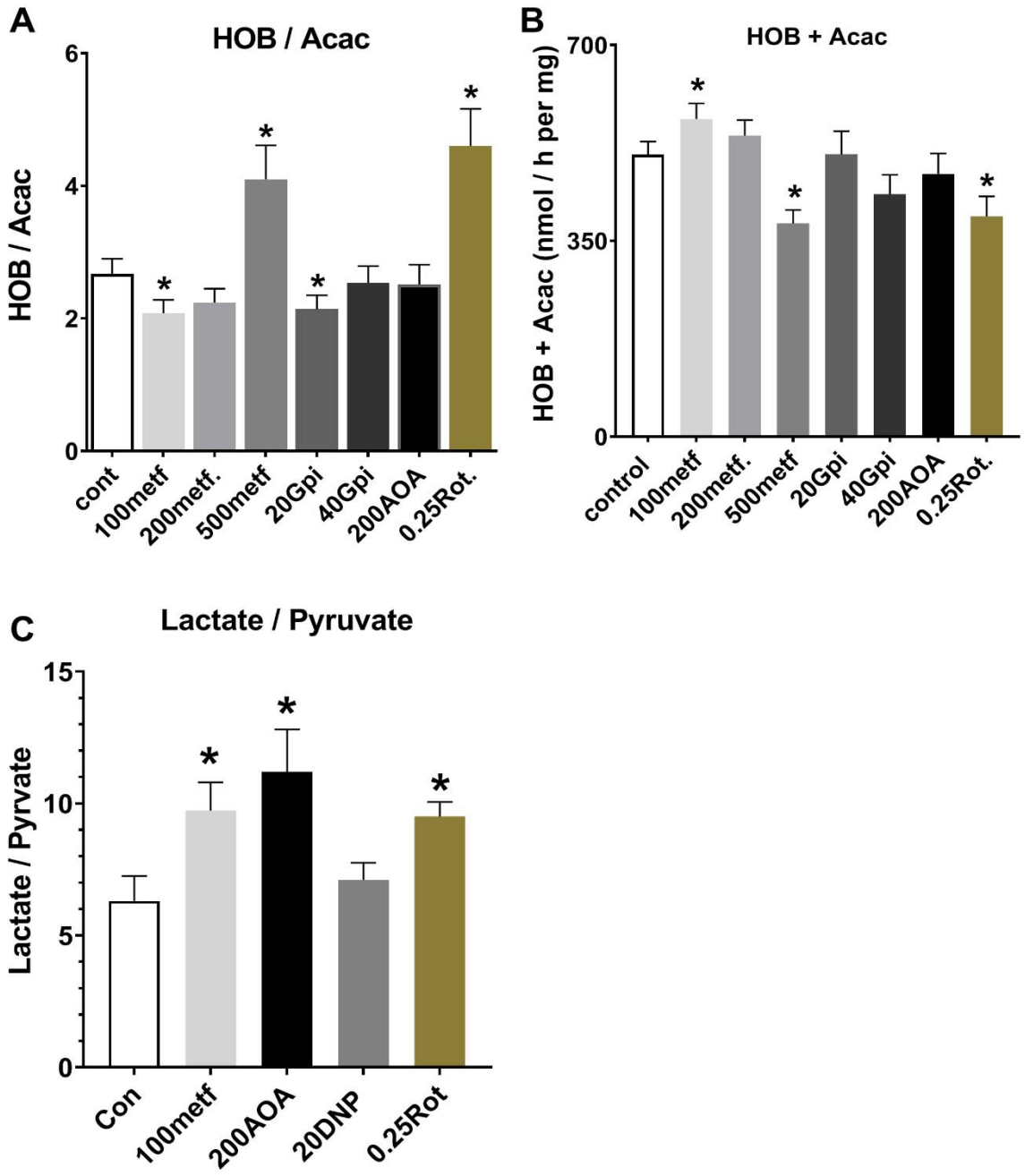

Figure 4-1:- Inhibition of the Glycerophosphate shuttle mimics the effect of low metformin on the mitochondrial redox state.

After overnight culture mouse hepatocyte monolayers were incubated for 2h with metformin and GPi in MEM. The medium was then replaced with fresh MEM containing 25mM glucose and 0.25mM octanoate and the additions indicated (µM) for 60 min. (A) HOB/Acac ratio. (B) HOB + Acac production. (C) lactate/pyruvate ratio. Results are mean±SEM. (A and B n=9, C=5 individual experiments).

*** P<0.05 relative to control.**

4.2.2 Inhibition of the MAS or the GPS does not mimic the metformin effect on gluconeogenesis

The above results suggest that inhibition of mitochondrial glycerophosphate dehydrogenase is a possible explanation for a more oxidised mitochondrial redox state, as occurs with low metformin. Therefore, the next aim was to test whether the inhibition of gluconeogenesis by low metformin can be mimicked by inhibition of the GPS or the MAS. The effect of mGPDH inhibitor (Gpi) and the malate-aspartate shuttle inhibitor (AOA) on gluconeogenesis were compared with the effect of low 100μM metformin in hepatocytes incubated with DHA (oxidised) and xylitol (reduced) as gluconeogenic substrates. The effect of AOA as an inhibitor of the MAS is well documented (Berry et al., 1994). However, Gpi has been shown to be effective on isolated mitochondria but has not been tested previously in hepatocytes (Orr et al., 2014).

With the oxidised substrate DHA, metformin inhibited gluconeogenesis by 22% (291±14 vs 373±16) (Figure 4-2 A). The inhibition of the rate of glucose production by (100μM) metformin was associated with increased production of pyruvate plus lactate formation (980±35 vs 862±25) (Figure 4-2 B), without affecting total DHA metabolism to glucose plus lactate plus pyruvate (Figure 4-2 D) and with a decrease in the fractional partitioning to glucose and an increase in the lactate to pyruvate ratio (5.0±0.4 vs 4.0±0.3) (Figure 4-2 C) and decreased the cellular G3P level (4.2±0.8 vs 6.5±0.8) (Figure 4-3 B). The level of ATP was unchanged by metformin (Figure 4-3 C). AOA had no effect on gluconeogenesis from DHA (344±26 vs 373±16), and similarly Gpi also had no effect (363±20 vs 373±16) (Figure 4-2 A). Unlike metformin, AOA and Gpi did not increase pyruvate plus lactate formation and did not decrease the fractional partitioning of DHA to glucose (Figure 4-2B, C). They also did not affect total DHA metabolism (Figure 4-2 D). AOA caused a large increase in the lactate to pyruvate ratio and Gpi had smaller affect than AOA (Figure 4-3 A). An increase in the lactate to pyruvate ratio by AOA was shown previously (Berry et al., 1994). This is consistent with inhibition of the transfer of reducing equivalents from the cytoplasm to mitochondria. Cellular G3P was increased by AOA but not by 20μM Gpi (Figure 4-2 B).

With xylitol as substrate, similar to the results of oxidised substrate, metformin lowered glucose production (359±37 vs 421± 53) (Figure 4-4 A), and increased the production of lactate plus pyruvate (1363±137 vs 1200±106) (Figure 4-4 B) and favoured glycolysis rather than gluconeogenesis by lowering the fractional partitioning of xylitol to glucose (37.8±1.1 vs

47.0±1.1) (Figure 4-4 C) without changing total xylitol metabolism (2299±204 vs 2300±221) (Figure 4-4 D). As expected, both the lactate to pyruvate ratio and cell G3P were higher with xylitol (Figure 4-5 A and B) than with DHA (Figure 4-3 A and B) (Vincent et al., 1989). Low metformin increased the lactate to pyruvate ratio and decreased the cell G3P (Figure 4-5 A and B). Inhibition of gluconeogenesis by low metformin was mimicked by 200µM AOA (370±54 vs 421±53) but not by Gpi (418±44 vs 421±53) (Figure 4-4 A). Inhibition of gluconeogenesis by AOA was associated with inhibition of total xylitol metabolism and with a decrease in the fractional partitioning of xylitol to glucose (Figure 4-5 A and B). Gpi like AOA, inhibited total xylitol metabolism (Figure 4-4 D). Both AOA and Gpi increased the ratio of lactate to pyruvate by more than metformin did (Figure 4-5 A). Unlike metformin, AOA increased the cell G3P level in hepatocytes incubated with xylitol as substrate (Figure 4-5 B). Cell ATP was unchanged in most conditions except with Gpi where there was a trend to lower cell ATP (Figure 4-5 C). Collectively, the above results suggested that (i) metformin lowers gluconeogenesis and the fractional partitioning to glucose relative to glycolysis from both oxidised and reduced substrates with a concomitant increase in the lactate to pyruvate ratio and decrease in cell G3P. (ii) AOA caused a more reduced cytoplasmic redox state by increase the lactate to pyruvate ratio more than metformin. However, AOA did not mimic the effect of metformin on lowering gluconeogenesis from oxidised substrate (DHA), but it decreased total xylitol metabolism and increased cell G3P. (iii) Gpi caused a more oxidised mitochondrial redox state like low metformin but did not mimic the effect of the low metformin on glucose production (iv) the lowering effect of Gpi on ATP level from reduced substrate might explain the inhibition of total xylitol metabolism by Gpi. (v) Gpi did not increase cell G3P, but it raised the lactate to pyruvate ratio to a less extent than AOA. The greater effect of AOA compared with the Gpi on the lactate to pyruvate ratio with both DHA and xylitol as substrates might be because of a greater contribution of the MAS compared to the GPS in transfer of NADH reducing equivalent from cytoplasm to mitochondria in hepatocytes or because the Gpi causes only partial inhibition of mGPDH in hepatocytes. This inhibitor has been extensively characterized and validated in isolated mitochondria (Orr et al., 2014) but uptake by hepatocytes has not been demonstrated.

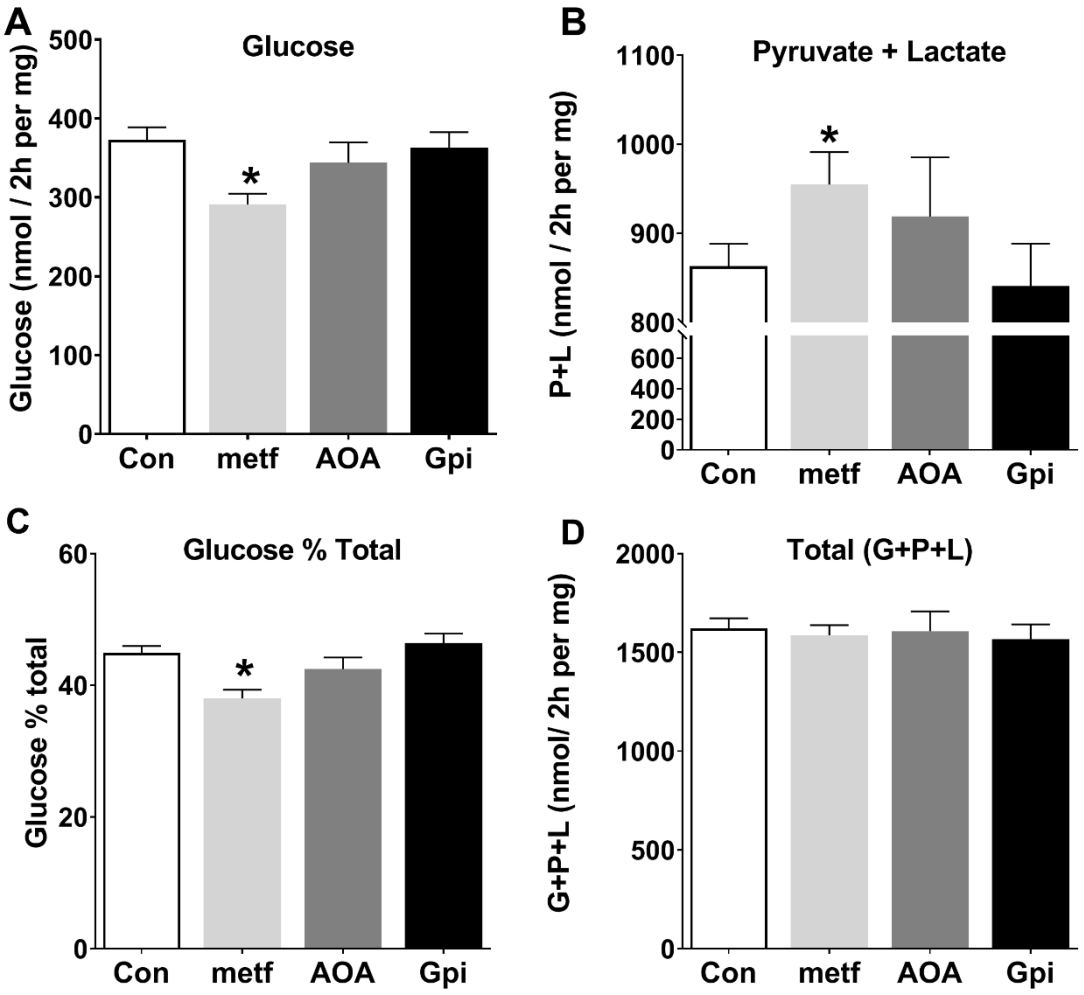

Figure 4-2: Inhibition of the malate-aspartate and the glycerophosphate shuttles did not mimic the effect of metformin on gluconeogenesis from DHA.

After overnight culture mouse hepatocyte monolayers were pre-incubated with 100µM metformin and 20µM Gpi in glucose-free DMEM for 2h. The medium was then replaced by glucose-free DMEM containing 5mM DHA and other additions (metformin, Gpi and 200µM AOA) and incubated for 120 min. (A) glucose production, (B) lactate plus pyruvate production, (C) glucose production percentage, (D) total glucose plus pyruvate plus lactate production. Results are Mean±SEM for n=11 individual experiments.

*** P<0.05 relative to control**.

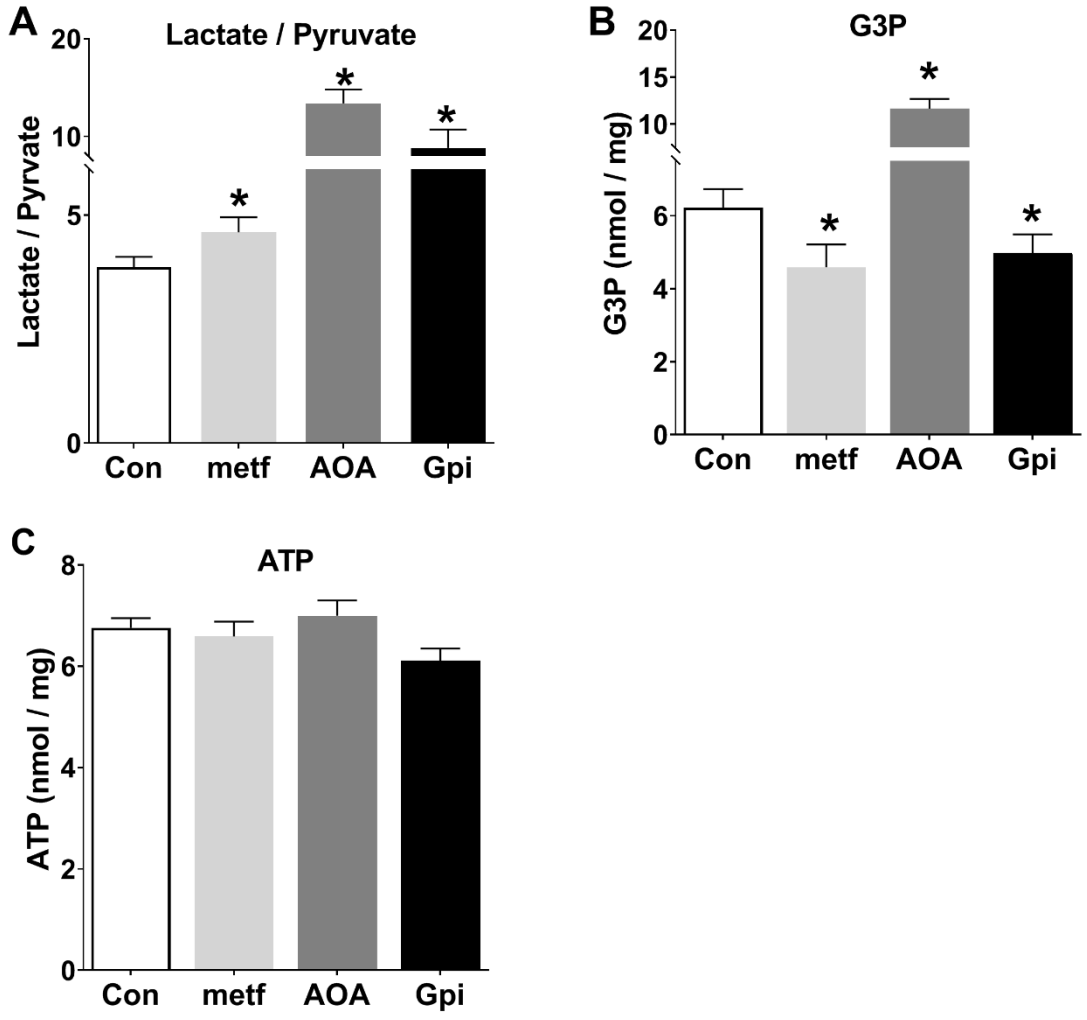

Figure 4-3: Metformin opposite from the MAS inhibitor lowers G3P level in hepatocytes in incubation with DHA.

After overnight culture mouse hepatocyte monolayers were pre-incubated with metformin (100µM) and Gpi (20µM) in glucose-free DMEM for 2h. The medium was then replaced by glucose-free DMEM containing 5mM DHA and other additions (metformin, Gpi and 200µM AOA) and incubated for extra 2h then the medium was collected to analysis lactate and pyruvate. The cells were snap-frozen to analysis G3P and ATP (A) lactate to pyruvate ratio; (B) cell G3P; (C) ATP level. Results are Mean±SEM for n=11 individual experiments.

*** P<0.05 relative to control**.

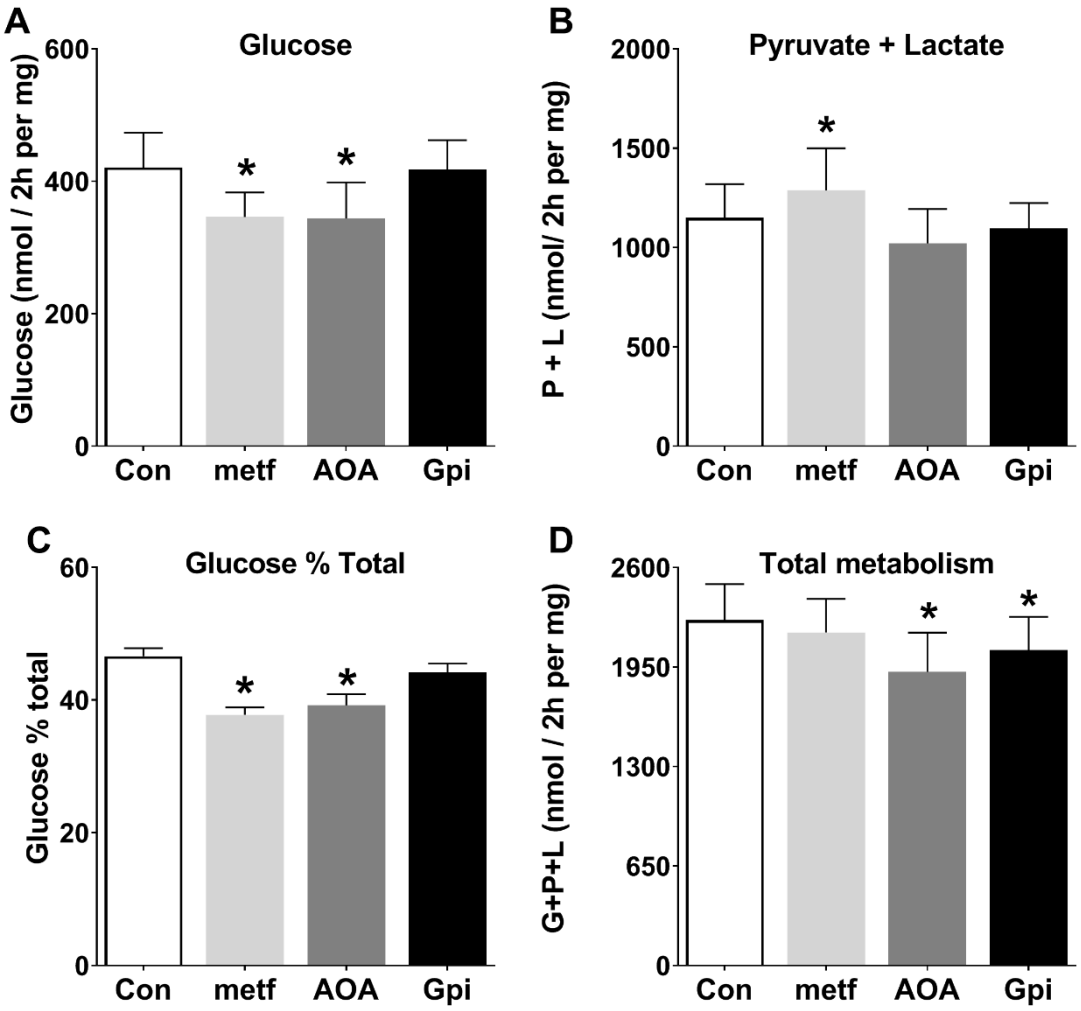

Figure 4-4: AOA inhibits total xylitol metabolism and partitioning of substrate towards gluconeogenesis.

After overnight culture mouse hepatocyte monolayers were pre-incubated with metformin (100µM) and Gpi (20µM) in glucose-free DMEM for 2h. The medium was then replaced by glucose-free DMEM containing 2mM xylitol and other additions (metformin, Gpi and 200µM AOA) and incubated for 120 min. (A) glucose production, (B) lactate plus pyruvate production, (C) glucose production percentage, (D) total glucose plus pyruvate plus lactate production. Results are Mean±SEM for n =7 individual experiments.

*** P<0.05 relative to control**

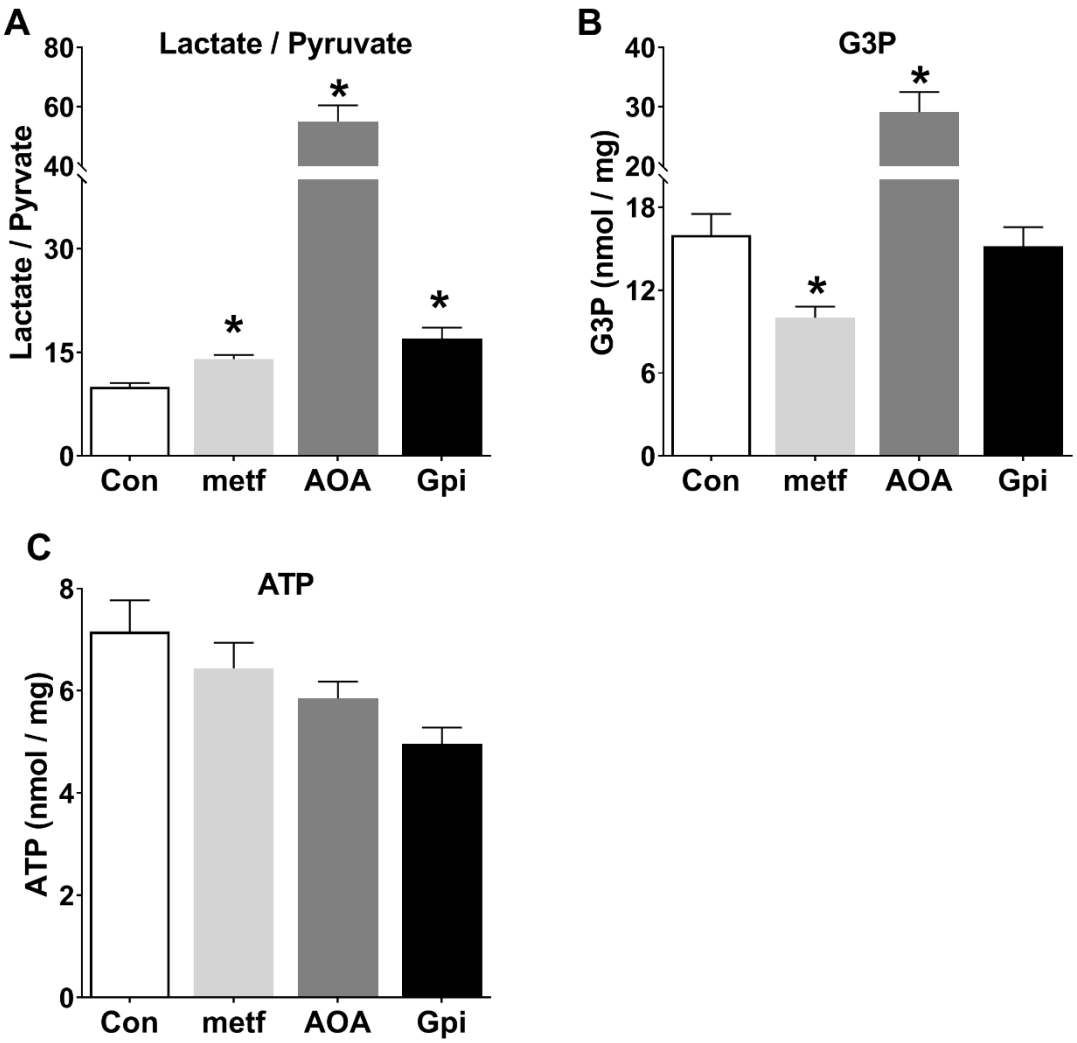

Figure 4-5: AOA raises G3P level opposite from low metformin in hepatocytes in incubation with xylitol.

After overnight culture mouse hepatocyte monolayers were pre-incubated with 100µM metformin and 20µM Gpi in glucose-free DMEM for 2h. The medium was then replaced by glucose-free DMEM containing 2mM xylitol and other additions (metformin, Gpi and 200µM AOA) and incubated for extra 2h then the medium was collected to analysis lactate and pyruvate. The cells were snap-frozen to analysis G3P and ATP (A) lactate to pyruvate ratio; (B) cell G3P; (C) ATP level. Results are Mean±SEM for n=7 individual experiments.

*** P<0.05 relative to control**.

4.2.3 DNP like metformin favours glycolysis rather than gluconeogenesis

The above results showed that the inhibitor of the MAS caused a more reduced cytoplasmic NADH / NAD redox state but had no effect on the mitochondrial redox state, whereas the inhibitor of the GPS caused a more reduced cytoplasmic and a more oxidised mitochondrial redox states similarly to 100µM metformin. Neither of these inhibitors mimicked the inhibition of gluconeogenesis from DHA by metformin. Therefore, the effect of 100µM metformin on gluconeogenesis cannot be explained by inhibition of the MAS or GPS. Previous results showed that uncoupling the mitochondrial membrane with 2,4-dinitrophenol (DNP) like 100µM metformin causes a more oxidised mitochondrial (decrease NADH / NAD ratio) redox state. We next investigated the effect of the uncoupler (20µM DNP) on glucose production from DHA in hepatocytes and compared this with 100µM metformin. DNP like 100µM metformin inhibited the rate of gluconeogenesis (Figure 4-6 A) and favoured glycolysis (Figure 4-6 B) by decreasing the fractional partitioning of DHA to glucose relative to glycolysis (Figure 4-6 C) without inhibition total DHA metabolism (Figure 4-6 D). Inhibition of gluconeogenesis by DNP was associated with lowered cell G3P and mimicked the effect of metformin (Figure 4-7 B), however, the lactate to pyruvate ratio was unchanged by DNP (Figure 4-7 A). ATP level was unchanged with all conditions (Figure 4-7 C). Collectively, the above results suggested that (i) DNP like metformin lowers gluconeogenesis and the fractional partitioning to glucose relative to glycolysis from DHA. (ii) However DNP did not mimic the effect of metformin on the lactate to pyruvate ratio but decreased cell G3P.

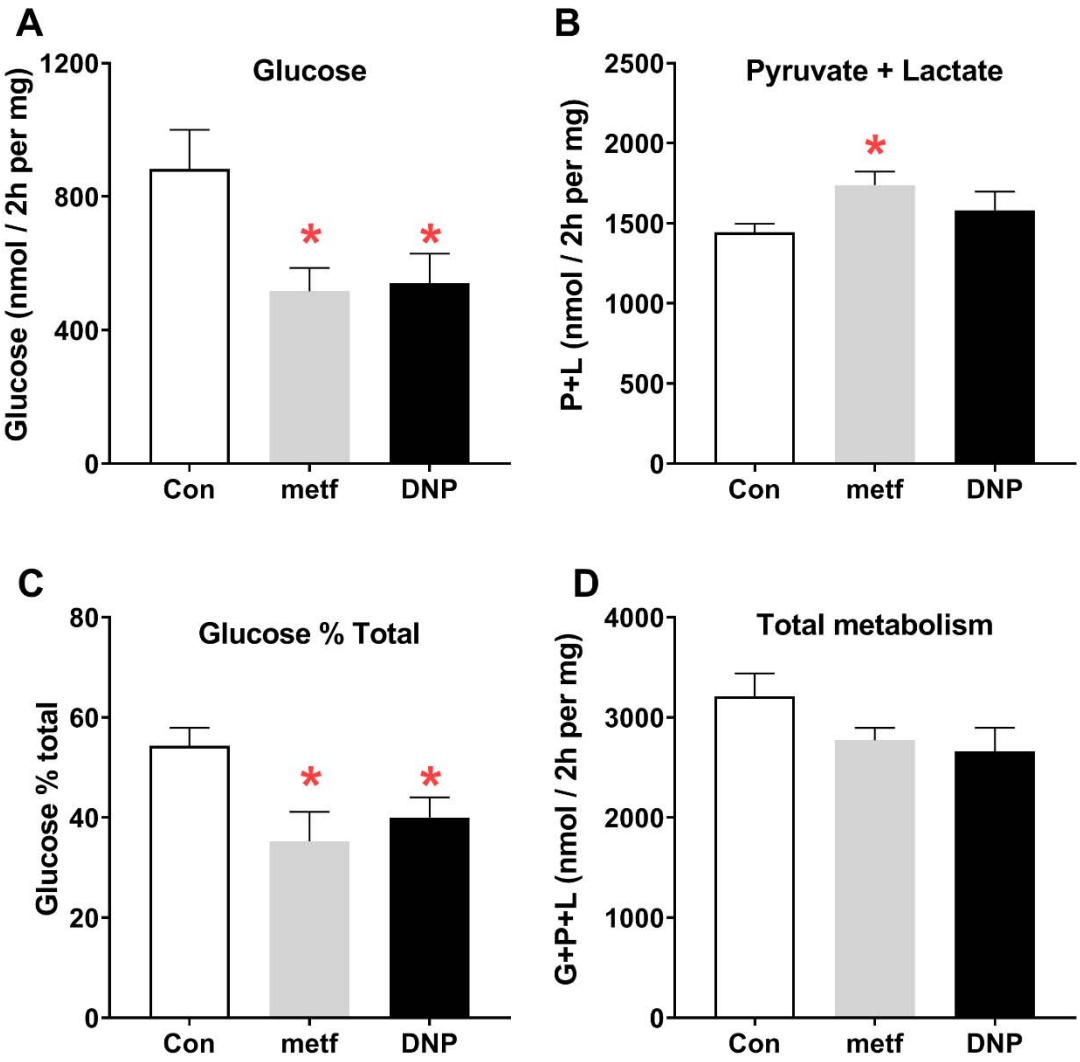

Figure 4-6: The mitochondrial uncoupler DNP, mimics the effect of metformin on gluconeogenesis.

After overnight culture mouse hepatocyte monolayers were pre-incubated with 100 µM metformin in glucose-free DMEM for 2h. The medium was then replaced by glucose-free DMEM containing 5mM DHA and either 100 µM metformin or 20 µM DNP for extra 120 min. (A) glucose production, (B) pyruvate plus lactate production, (C) glucose production percentage, (D) total glucose plus pyruvate plus lactate production. Results are Mean±SEM. n=2 individual experiments.

*** P<0.05 relative to control**

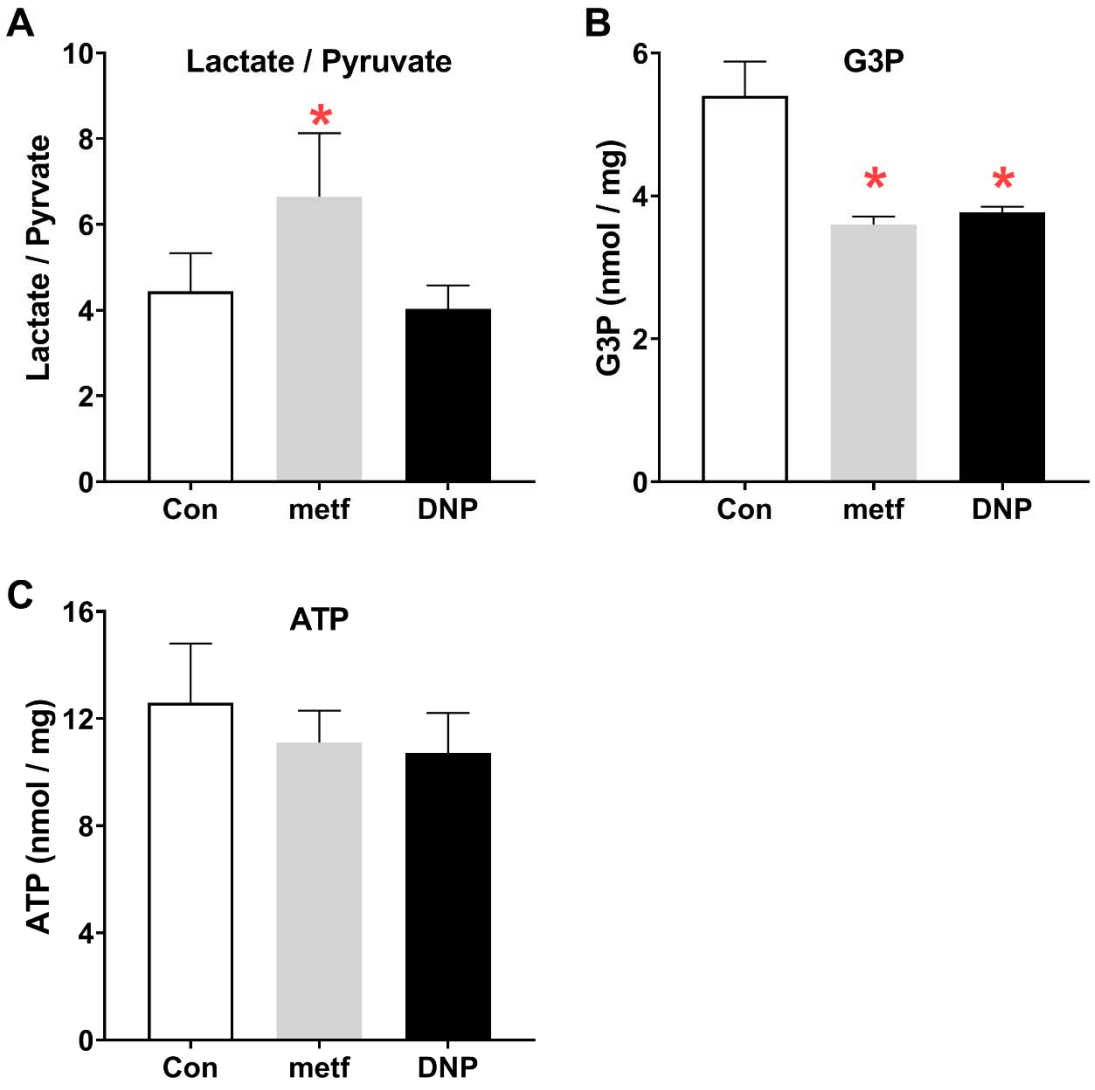

Figure 4-7: DNP similar to low metformin (100µM) lowers G3P.

After overnight culture mouse hepatocyte monolayers were pre-incubated with metformin (100µM) in glucose-free DMEM for 2h. The medium was then replaced by glucose-free DMEM containing 5mM DHA and either 100µM metformin or 20µM DNP and incubated for extra 2h then the medium was collected to analysis lactate and pyruvate. The cells were snap-frozen to analysis G3P and ATP. (A) lactate to pyruvate ratio; (B) cell G3P; (C) ATP level. Results are Mean±SEM for n=2 individual experiments.

*** P<0.05 relative to control.**

4.2.4 Gpi but not metformin inhibits the activity of mitochondrial glycerophosphate dehydrogenase (mGPDH)

The inhibition of gluconeogenesis by low metformin has been proposed to be due to inhibition of mitochondrial glycerophosphate dehydrogenase (mGPDH) (Madiraju et al., 2014). Because the Gpi reported by Orr *et al.* (2014) is currently the best characterized inhibitor of mGPDH activity in mitochondria from skeletal muscle by using dichlorophenol indophenol (DCIP) as electron acceptor (Orr et al., 2014), the next aim was to compare the inhibition of mGPDH enzyme activity in permeabilized hepatocytes by Gpi (10-80µM) and metformin using DCIP as electron acceptor. Inhibition of mGPDH activity by Gpi (10-80µM) was confirmed in hepatocytes (Figure 4-8 A) as previously reported (Orr et al., 2014). While metformin 0.1-5mM did not inhibit the activity of mGPDH in permeabilized hepatocytes (Figure 4-8 B).

To further test the role of the GPS in gluconeogenesis and glycolysis adenoviral vectors for shRNA mGPDH knock-down (SH) and mGPDH overexpression in mouse hepatocytes were used. Measuring the mRNA expression by qPCR confirmed knock-down and overexpression by the two vectors respectively (Figure 4-9 A). Measurement of mGPDH protein by Western blotting confirmed protein overexpression but not protein knock-down (Figure 4-9 B). The enzyme activity measurements (Figure 4-9 C) also confirmed an increase in enzyme activity by overexpression but not a decrease by the shRNA. The lack of protein knock-down by the shRNA vector is best explained by the long half-life of mGPDH protein (Mracek et al., 2013). In the rest of this study the overexpression vector was used (at 2 titers) to study the effect of an increase in mGPDH activity of glucose production and glycolysis. Increased mGPDH activity was associated with a decrease in cell G3P level confirming that the overexpressed mGPDH was functionally active in hepatocytes (Figure 4-9 D).

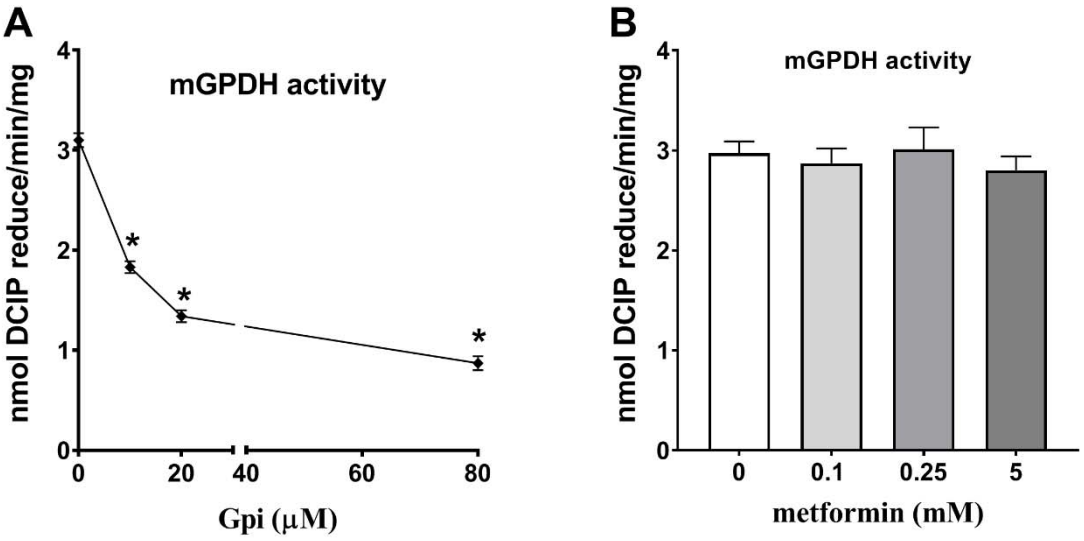

Figure 4-8: Inhibition of mGPDH activity by Gpi but not by metformin.

Activity of endogenous mGPDH assayed in permeabilised hepatocytes with the concentrations of GPi (A) or metformin (B) indicated.

*** P < 0.05 relative to control.**

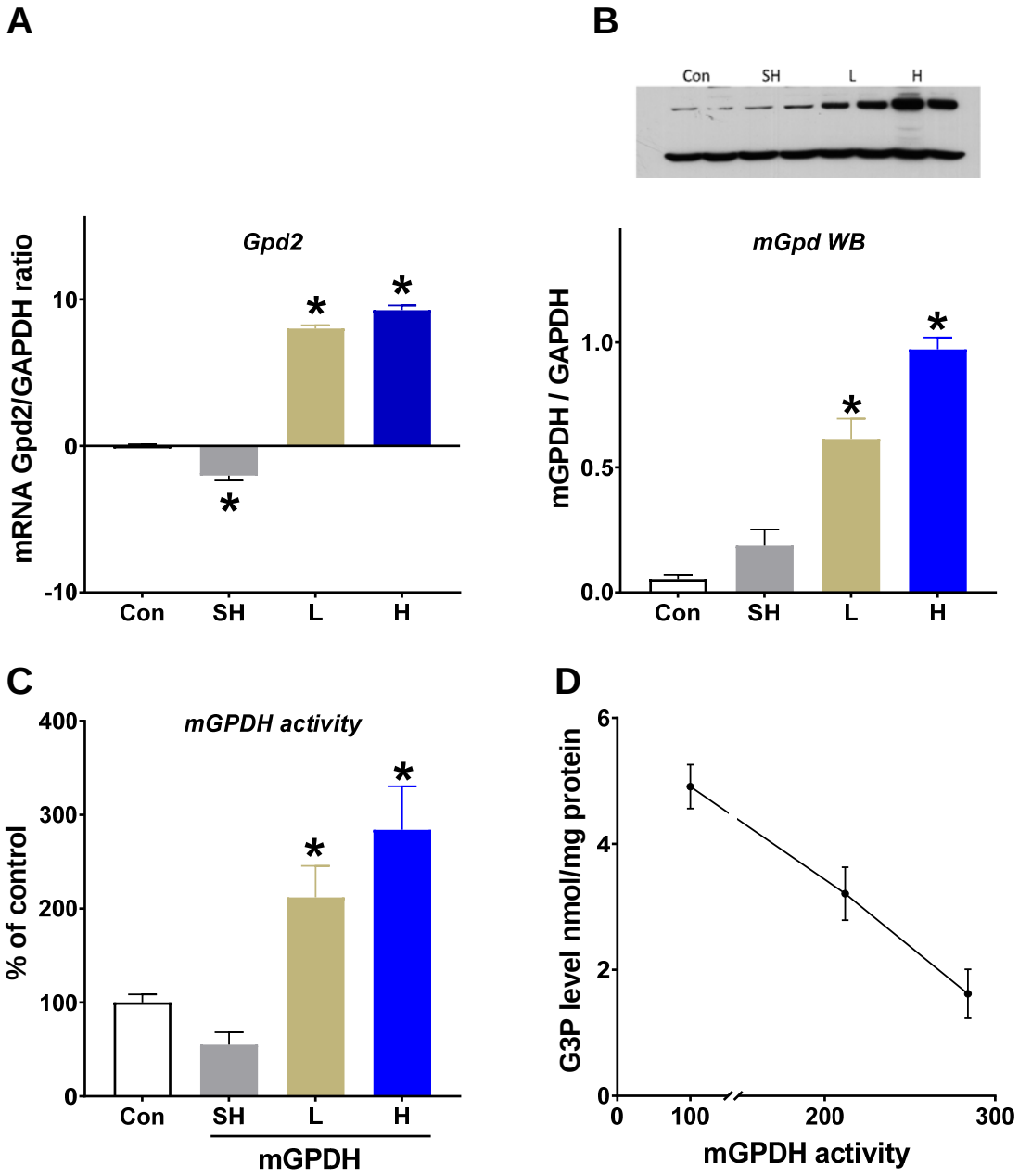

Figure 4-9: Adv-SH-mGpd2 suppresses mGPDH mRNA but not protein expression and enzyme activity

Monolayer hepatocytes were cultured for 2h for cell attached. Then cells either untreated (Con) or treated with 8 x 10^8 PFU/ml Adv-SH-mGpd2 (SH) for Gpd2 knock-down or with Adv-mGpd2 at 1.6 (L) or 4.8 (H) x 10^7 PFU/ml for mGPDH overexpression for 4-5h. The medium was replaced with new fresh MEM and incubated for 24h. (A) Gpd2/Gapdh mRNA expressed relative to untreated control. (B) Immunoactivity of mGPDH/GAPDH. (C) mGPDH enzyme activity. D G3P level vs mGPDH activity. Means ± SEM for n= 4 and for (D) n=7 experiments.

***P<0.05 relative to control with expressed endogenous mGPDH only.**

4.2.5 Overexpression of mGPDH lowers cell G3P level with a wide range of substrates

We investigated the effect of mGPDH overexpression using two titers of adenovirus vector (Low; L and High; H) for increasing mGPDH by around 2-fold and 3-fold relative to the endogenous activity (Figure 4-9 C). This increase in mGPDH activity was first compared on cell G3P in hepatocytes incubated with glycerol, high glucose, DHA and xylitol as substrates. Cell G3P levels were highest with glycerol, followed by glucose and xylitol and DHA (Figure 4-10 A-D; white bars). Overexpression of mGPDH by 2-fold and 3-fold caused a large decrease in G3P with all substrates tested (Figure 4-10 A-D; shaded bars). The decrease in the concentration of G3P, the substrate of mGPDH, confirms that the overexpressed mGPDH is functionally active in hepatocytes.

The highest G3P level was noticed in hepatocytes incubated with glycerol. High dose mGPDH overexpression lowered cellular G3P level from 0.25mM and 2mM glycerol by 91% and 88%, respectively. The effect with low dose was concomitant with less inhibition in cell G3P level compared with the high dose (54% and 69%, respectively) (Figure 4-10 A).

With high glucose (25mM) as substrate, the high titre of adenovirus for mGPDH overexpression caused a marked (90%) lowering of in cell G3P level and the low titer associated with 62% lowering of the cell G3P level (Figure 4-10 B). With xylitol as substrate, both low and high titers of adenovirus showed about similar lowering effect on cell G3P level in hepatocytes (83 and 91%, respectively) (Figure 4-10 C). With oxidised (DHA) substrate, the level of cell G3P was the lowest compared with other substrates. But the effect of mGPDH overexpression was also clear with high dose virus (67%) with less inhibition at the low dose virus (35%) (Figure 4-10 D).

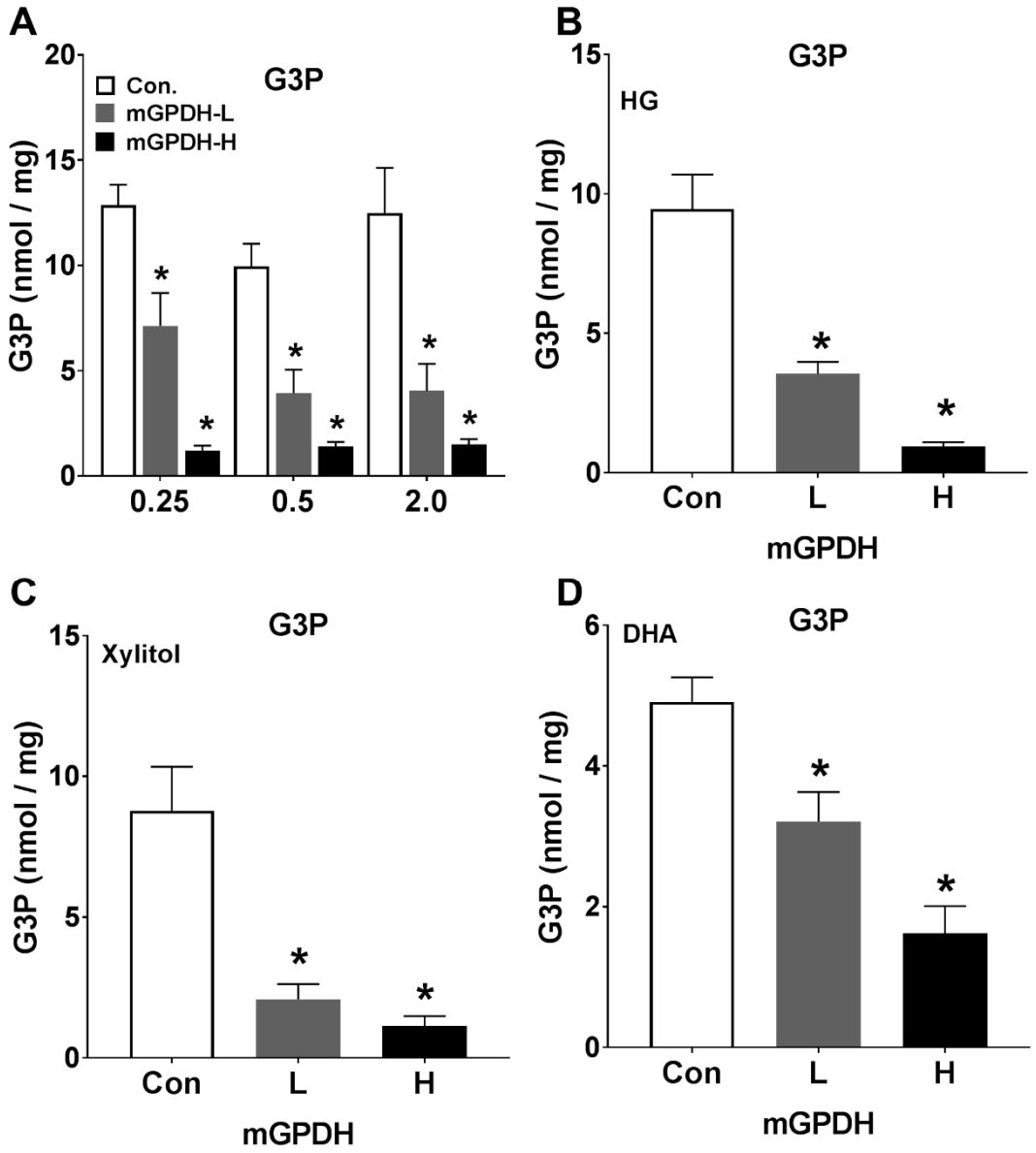

Figure 4-10: mGPDH overexpression lowers cell G3P with glucose and gluconeogenic precursors.

Hepatocytes were either untreated (Con) or treated with Adv-Gpd2 for mGPDH overexpression at 1.6 x 10^7 (L) or 4.8 x10^7 (H) PFU/ml. After overnight culture, they were incubated with either MEM containing 25mM glucose (HG), for 1h (B) or with glucose-free DMEM containing either glycerol (A), 2mM xylitol (C) or 5mM DHA (D) for 120 min. Results are Mean±SEM. (A) Glycerol (0.25-2mM); n=4, (B) 25mM glucose; n=11 (C) 2mM xylitol; n= 4 (D) 5mM DHA; n=13 individual experiments.

*** P<0.05 relative to no treatment (control).**

4.2.6 Overexpression of mGPDH associates with a more reduced mitochondrial NADH / NAD redox state

mGPDH couples the oxidation of cytoplasmic G3P to DHAP with the transfer of electrons via reduction of FAD to FADH to the respiratory chain (Mracek et al., 2013). The previous results (Figure 4-1) showed that the mGPDH inhibitor caused a more oxidised mitochondrial NADH/NAD redox state. We next determined the effect of mGPDH overexpression on the mitochondrial redox state in incubations with 0.125mM octanoate and either high glucose (25mM), or DHA or glycerol. The mitochondrial redox state was highest with 25mM glucose compared with DHA and glycerol (2.5±0.2 HG (Figure 4-11), 1.6±0.43 DHA (Figure 4-13), 0.7±0.14 0.5mM glycerol, and 0.8±0.15 2mM glycerol (Figure 4-14)).

With 25mM glucose as substrate, the effects of either Gpi (Figure 4-11A and B) or AOA (Figure 4-11 C-D) on the 3-hydroxybutyrate to acetoacetate ratio were tested in combination with mGPDH overexpression. Total production of ketone bodies was unchanged in all experimental conditions tested (Figure 4-11 B and D). However, the mitochondrial NADH / NAD redox state as determined from the ratio of 3-hydroxybutyate to acetoacetate was more reduced with mGPDH overexpression and more oxidized in the presence of the mGPDH inhibitor (Figure 4-11 A) but was not affected by inhibition of the MAS with AOA (Figure 4-11 C). This concurs with previous results that changes in GPS but not MAS affect the mitochondrial redox state (Figure 4-1). The cytoplasmic redox state as determined from the lactate / pyruvate ratio was increased by both the mGPDH inhibitor and also by the MAS inhibitor in cells expressing only endogenous mGPDH (Figure 4-12 A and C). However, in cells overexpressing mGPDH there was no effect of the MAS shuttle inhibitor on the lactate / pyruvate ratio (Figure 4-12 B). These results suggest that during overexpression of mGPDH, the GPS can compensate for the inhibition of the MAS by AOA. The lack of effect of the Gpi (20µM) on the lactate / pyruvate ratio in cells overexpressing mGPDH may be because this compound is a weak inhibitor in cellular assays as shown in other experiments where an increase in G3P was observed at 80µM Gpi (Figure 4-20 B and Figure 4-22 B) but not at 20µM (Figure 4-3 B and Figure 4-5 B). Cell ATP was measured in parallel and there was no significant change in cell ATP (figure 4-12 B and D). Overexpression of mGPDH also caused an increase in the 3-hydroxybutryate to acetoacetate in incubations with DHA and octanoate (Figure 4-13 A) and glycerol and octanoate (Figure 4-14 A) similar to the results with high glucose and octanoate.

Cumulatively, these results show that the mitochondrial redox state is dependent on flux through the GPS but not through the MAS. In principle therefore the more oxidised mitochondrial redox state caused by low metformin can be due to inhibition of the GPS but not to inhibition of the MAS.

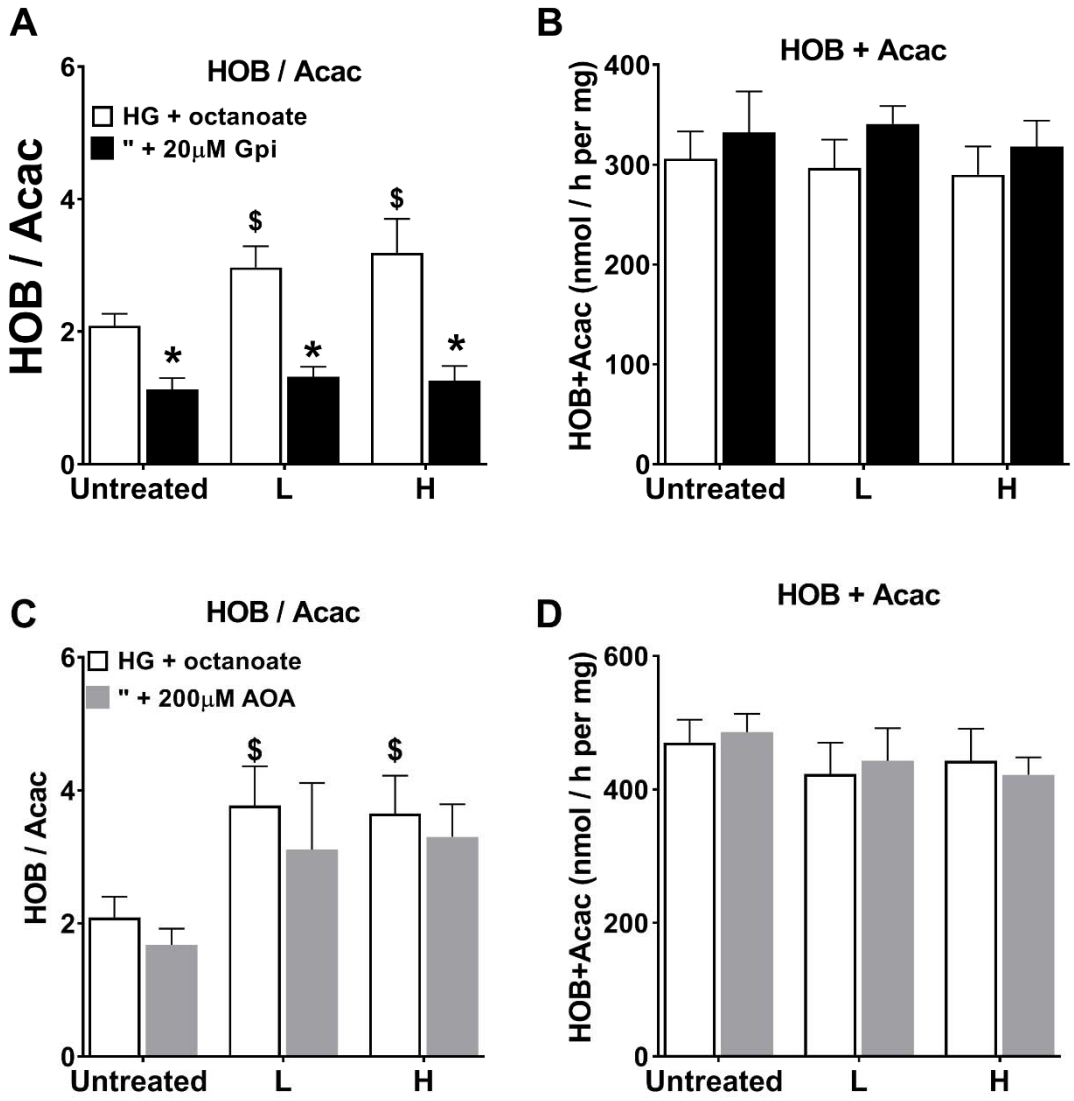

Figure 4-11: Opposite effects of Gpi and mGPDH overexpression on the mitochondrial redox state.

Hepatocytes were treated similar with Adv-Gpd2 to overexpress mGPDH as in figure 4-9. (A-B) After overnight culture, they were pre-incubated for 2h with the Gpi in MEM as indicated and then the medium was changed to fresh MEM containing 25mM glucose and 0.125mM octanoate for 1h with either 20μM Gpi (A and B) or 200μM AOA (C and D). The medium was collected to determine 3-hydroxybutyrate and acetoacetate. Cells were snap-frozen for ATP analysis. (A and C) 3-hydroxybutyrate to acetoacetate ratio; (B and D) 3-hydroxybutyrate plus acetoacetate production. Results are Mean±SEM for n= 11.

*** P<0.05 relative to respective control.**

$ P<0.05 effect mGPDH overexpression.

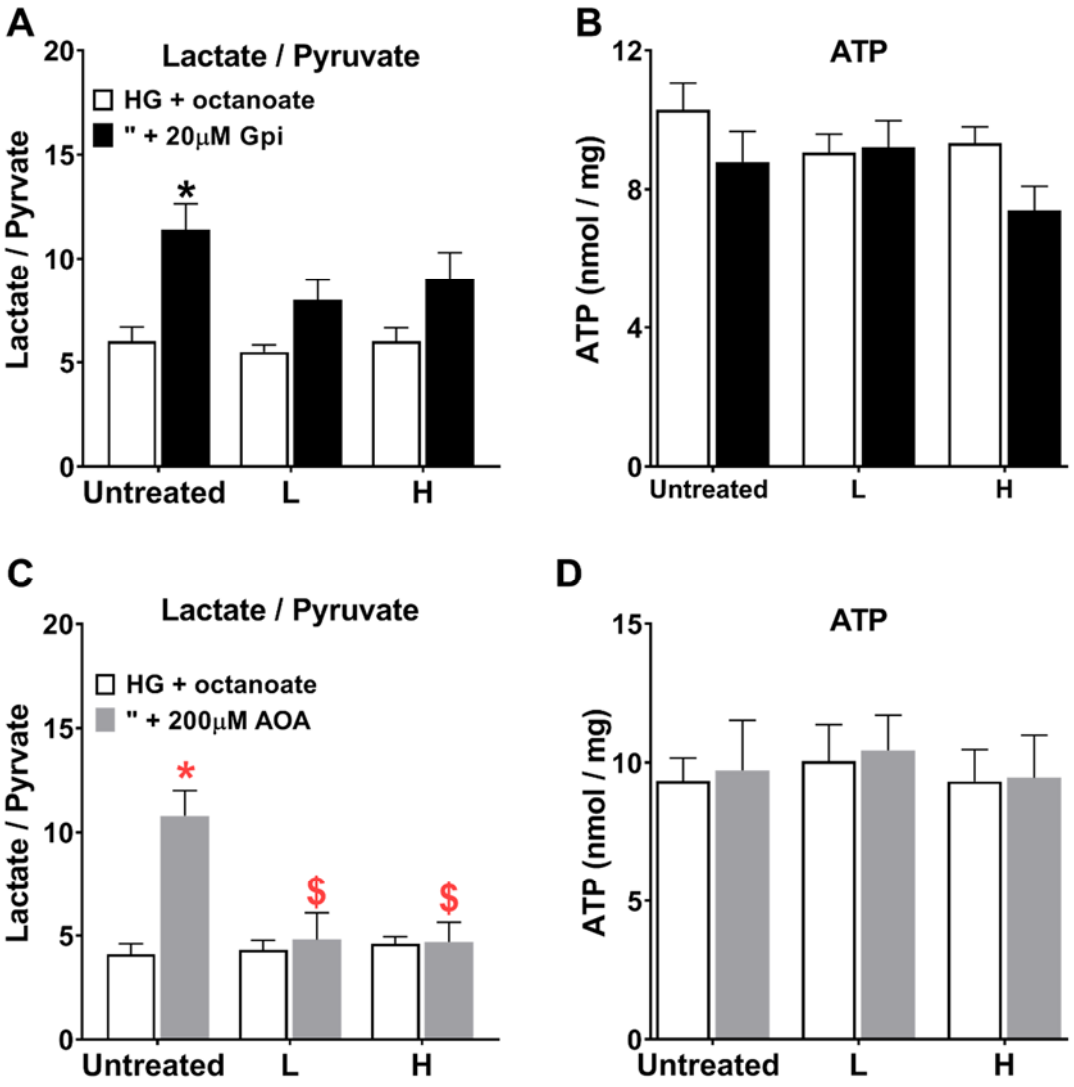

Figure 4-12: mGPDH overexpression can compensate for the inhibition of the MAS

Hepatocytes were treated similar with Adv-Gpd2 to overexpress mGPDH as in figure 4-9. (A-B) After overnight culture, they were pre-incubated for 2h with the Gpi in MEM as indicated and then the medium was changed to fresh MEM containing 25mM glucose and 0.125mM octanoate for 1h with either 20µM Gpi (A and B) or 200µM AOA (C and D). The medium was collected to determine lactate and pyruvate. Cells were snap-frozen for ATP analysis. (A and C) lactate to pyruvate ratio; (B and D) cell ATP. Results are Mean±SEM for n= 11.

*** P<0.05 effect of Gpi or AOA relative to respective control.**

$ P<0.05 effect of mGPDH overexpression (relative to corresponding value without overexpression).

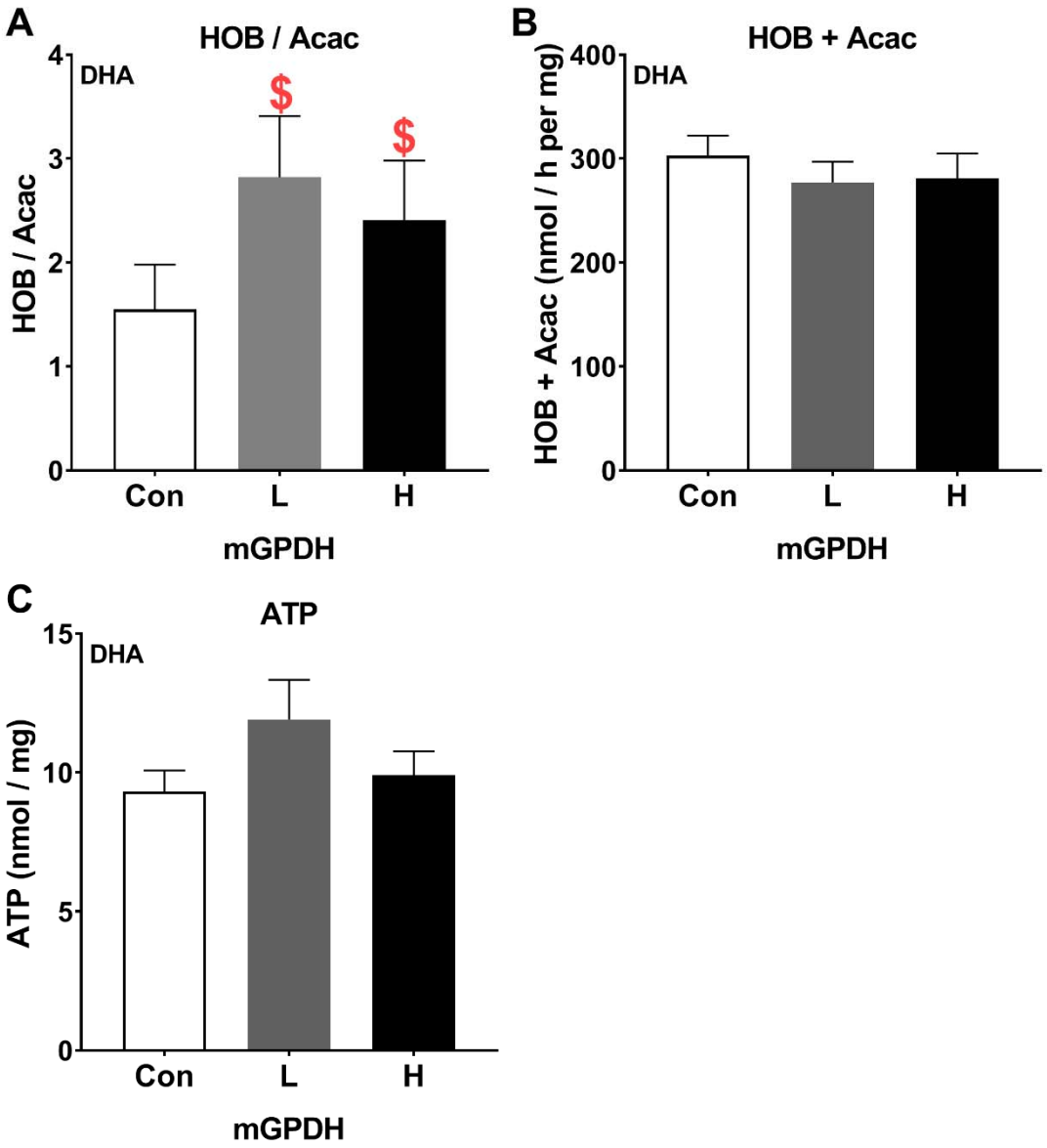

Figure 4-13: mGPDH overexpression causes a more reduced mitochondrial redox state form DHA as substrate

Hepatocytes were treated similar with Adv-Gpd2 to overexpress mGPDH as in figure 4-9. After overnight culture, they were incubated for 1h with glucose-free DMEM containing 5mM DHA and 0.125mM octanoate. The medium was collected to determine 3-hydroxybutyrate and acetoacetate. Cells were snap-frozen for ATP analysis. (A) 3-hydroxybutyrate to acetoacetate ratio; (B) 3-hydroxybutyrate plus acetoacetate production; (C) cell ATP. Results are Mean±SEM for n= 5.

$ P<0.05 effect of mGPDH overexpression (relative to corresponding value without overexpression).

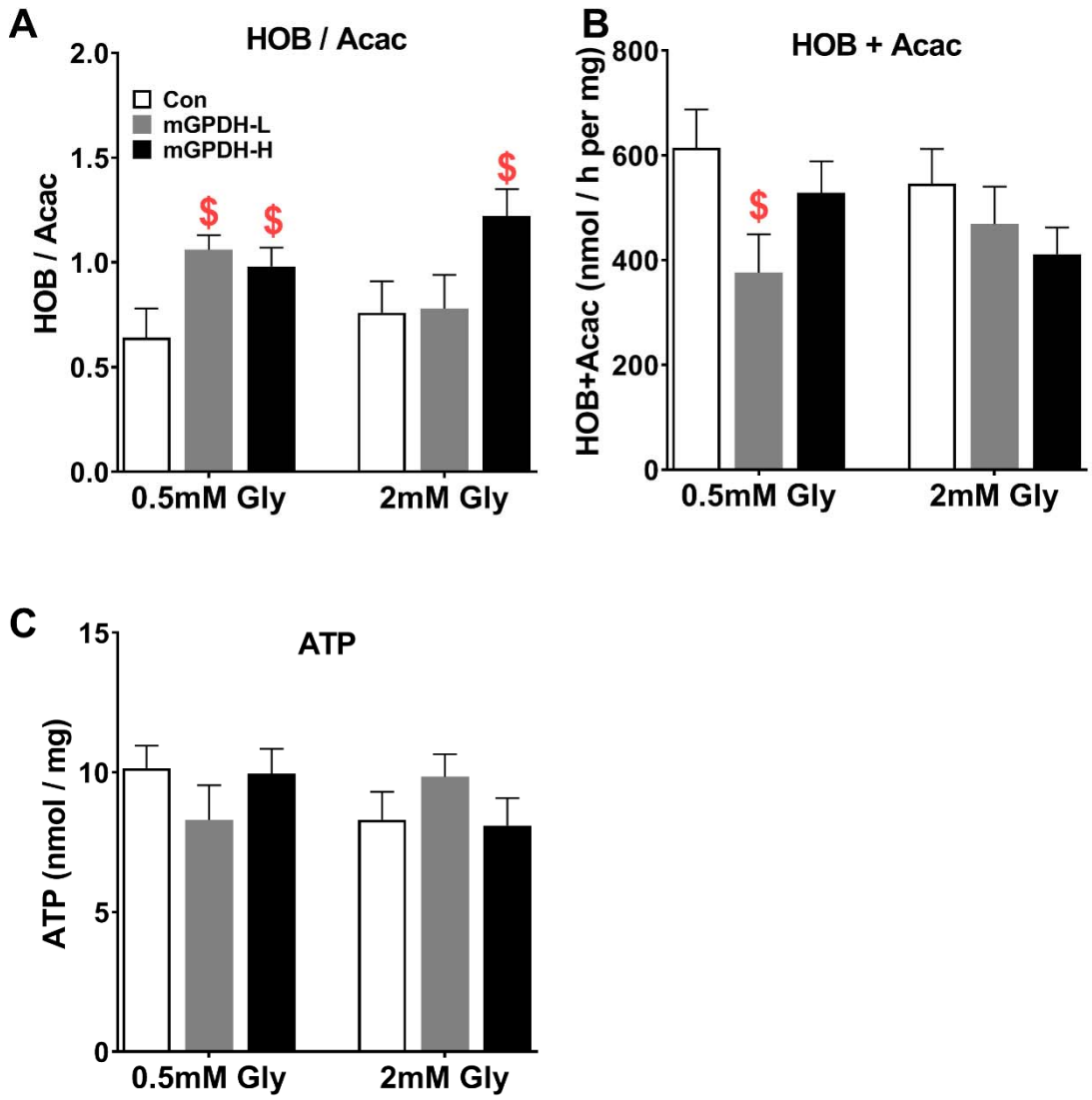

Figure 4-14: mGPDH overexpression causes a more reduced mitochondrial redox state form glycerol as substrate

Hepatocytes were treated similar with Adv-Gpd2 to overexpress mGPDH as in figure 4-9. After overnight culture, they were incubated for 1h with glucose-free DMEM containing glycerol as indicated and 0.125mM octanoate. The medium was collected to determine 3-hydroxybutyrate and acetoacetate. Cells were snap-frozen for ATP analysis. (A) 3-hydroxybutyrate to acetoacetate ratio; (B) 3-hydroxybutyrate plus acetoacetate production; (C) cell ATP. Results are Mean±SEM for n= 5.

$ P<0.05 effect of mGPDH overexpression (relative to corresponding value without overexpression).

4.2.7 Stimulation of the GPS by overexpression of mGPDH favours glycolysis from oxidised and reduced substrates

If the inhibition of gluconeogenesis by metformin were due to inhibition of the GPS, then one would expect overexpression of mGPDH to have an opposite effect from metformin on glucose production. Therefore, the aim of this experiment was to test the effects of mGPDH overexpression on metabolism of oxidised (DHA) and reduced (xylitol and glycerol) substrates. With DHA, mGPDH overexpression did not affect total DHA metabolism but favoured DHA partitioning to glycolysis by increasing pyruvate plus lactate formation (1372±87 vs 1089±57) and decreased partitioning to glucose by 15-24% (28±0.7 HD and 32±0.6 :LD vs 37±1.1, 24%). The lactate to pyruvate ratio was raised by mGPDH overexpression (Figure 4-15 A-F). In the additional presence of octanoate rates of glucose production were higher by 48% (311±14 vs 459±46) (Figure 4-15 A and Figure 4-16 A) but the effects of mGPDH overexpression were otherwise similar (Figure 4-16 B, C and E).

With xylitol as substrate (Figure 4-17 A-F) the effects of mGPDH overexpression were tested in the absence (white bars) or presence of 200µM AOA (shaded bars). As shown previously (Figure 4-4 D), AOA inhibits total xylitol metabolism and causes a very large increase in the lactate to pyruvate ratio indicating a major role of the MAS in transfer of reducing equivalents to mitochondria with the reduced substrate. Overexpression of mGPDH had no effect on total xylitol metabolism (Figure 4-17 D) or on glucose production (339 ± 23 and 355 ± 36 vs 322 ±40, respectively) (Figure 4-17 A) and glycolysis (1134±78 and 1281±109 vs 1115±76, respectively) (Figure 4-17 B). However, it partially reversed the large increase in the lactate / pyruvate ratio caused by AOA (Figure 4-17 E) but not the inhibition of total xylitol metabolism.

With glycerol (0.5mM and 2mM), unlike with xylitol, overexpression of mGPDH increased total glycerol metabolism (Figure 18 D) and this effect was associated with increased glycolysis (Figure 4-18 B) and decreased partitioning to glucose (Figure 4-18 C). Cumulatively mGPDH overexpression: (i) increased total metabolism of glycerol but not DHA or xylitol; (ii) it had only a modest effect in reversing the increase in the lactate / pyruvate ratio caused by inhibition of the MAS with xylitol and did not decrease the lactate / pyruvate ratio in other substrate conditions; (iii) it favoured partitioning of DHA and glycerol to glycolysis rather than glucose production and thereby mimicked the effects of metformin.

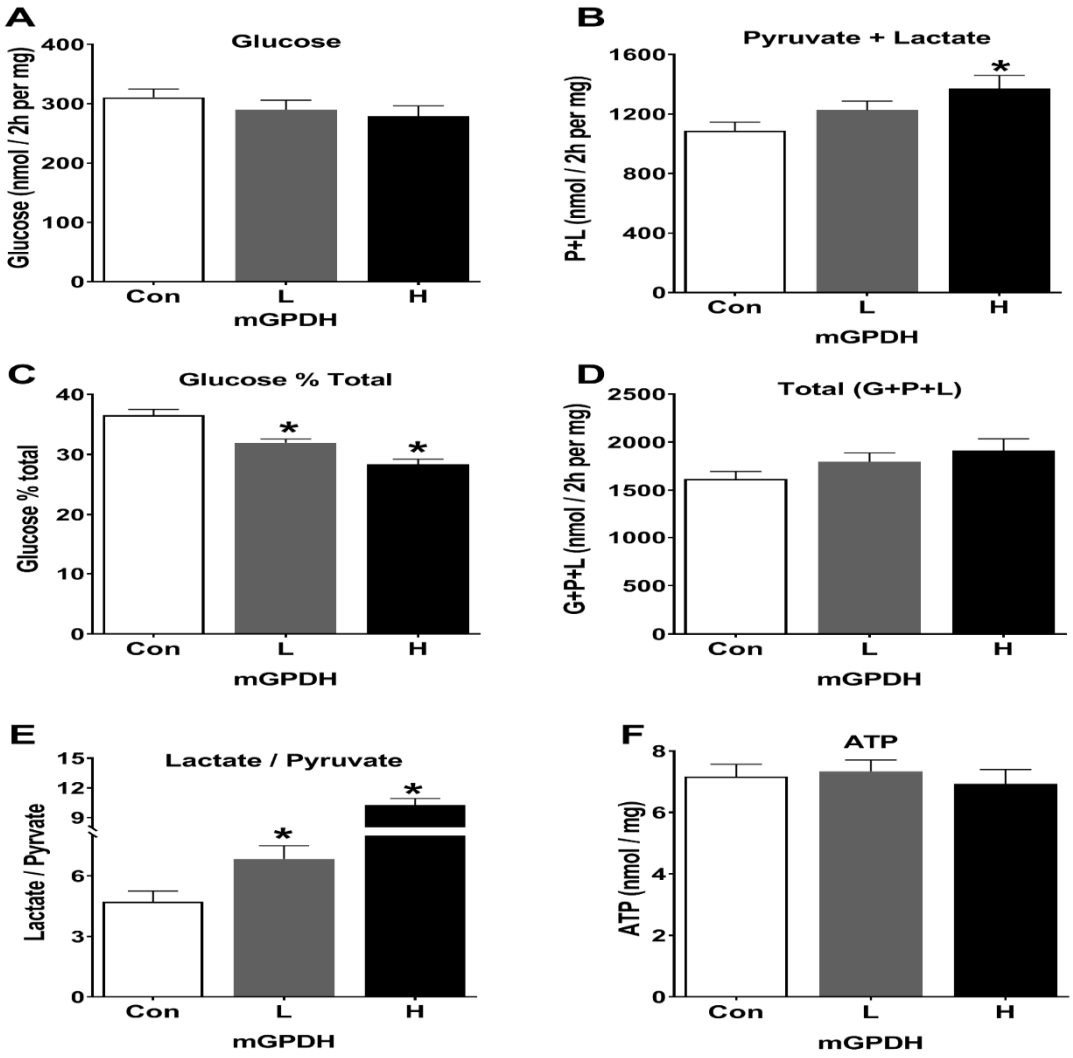

Figure 4-15: mGPDH overexpression favours glycolysis with DHA as substrate.

Hepatocytes were treated with Adv-Gpd2 to overexpress mGPDH as in figure 4-9. After overnight culture, they were incubated in glucose-free DMEM with 5mM DHA for 2h. the medium was collected to measure (A) glucose production; (B) pyruvate plus lactate formation; (C) glucose percentage from total metabolism; (D) total metabolism; (E) lactate to pyruvate ratio. Cells were snap-frozen for ATP analysis (F). Results are Mean±SEM for n=11.

*** P<0.05 relative to control. (ONE-WAY ANOVA)**

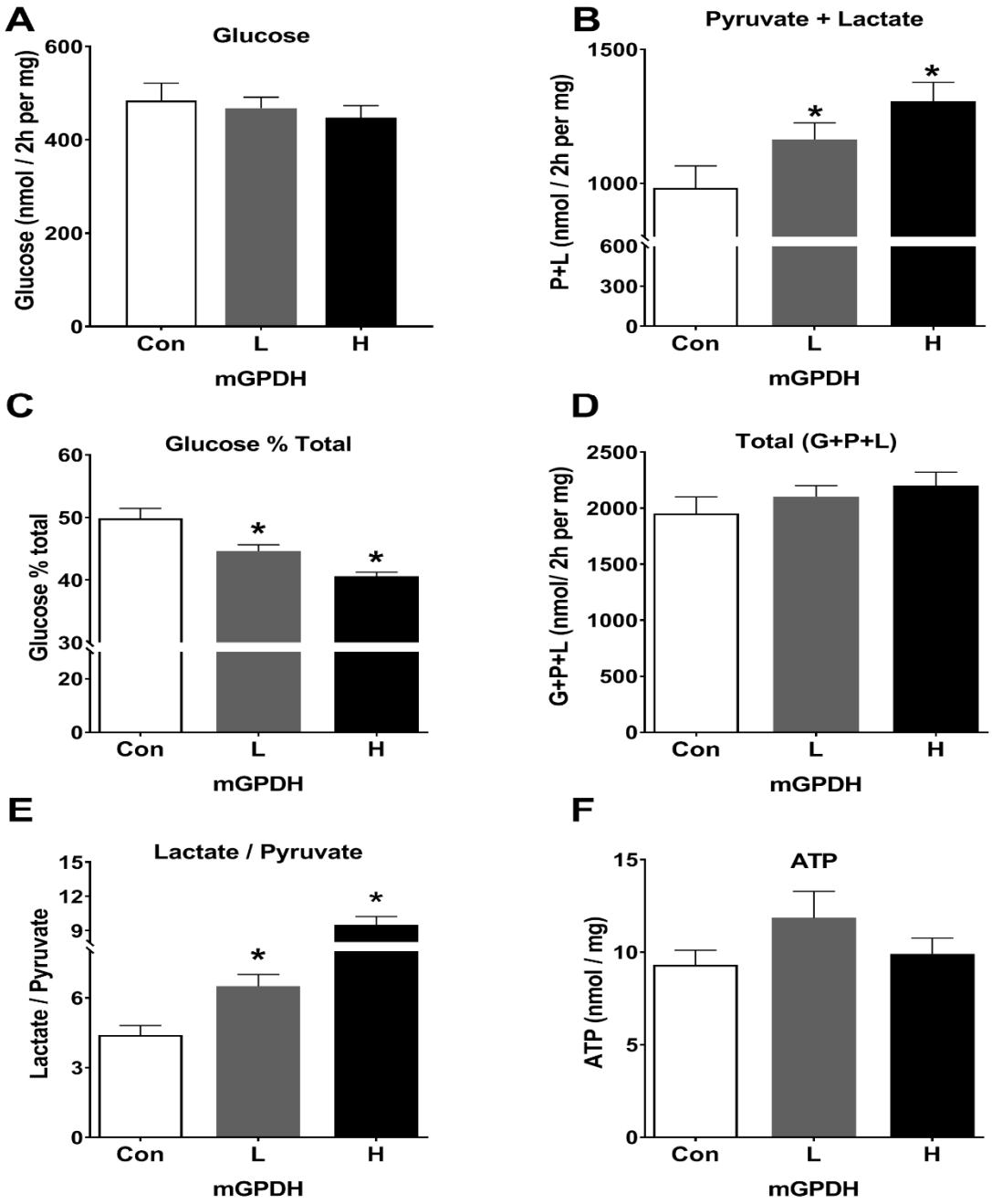

Figure 4-16: mGPDH overexpression favours glycolysis with DHA and octanoate as substrate.

Hepatocytes were treated with Adv-Gpd2 to overexpress mGPDH as in figure 4-9. After overnight culture, they were incubated in glucose-free DMEM with 5mM DHA and 0.125mM octanoate for 2h. the medium was collected to measure (A) glucose production; (B) pyruvate plus lactate formation; (C) glucose percentage from total metabolism; (D) total metabolism; (E) lactate to pyruvate ratio. Cells were snap-frozen for ATP analysis (F). Results are Mean±SEM for n=11.

*** P<0.05 relative to control. (ONE-WAY ANOVA)**

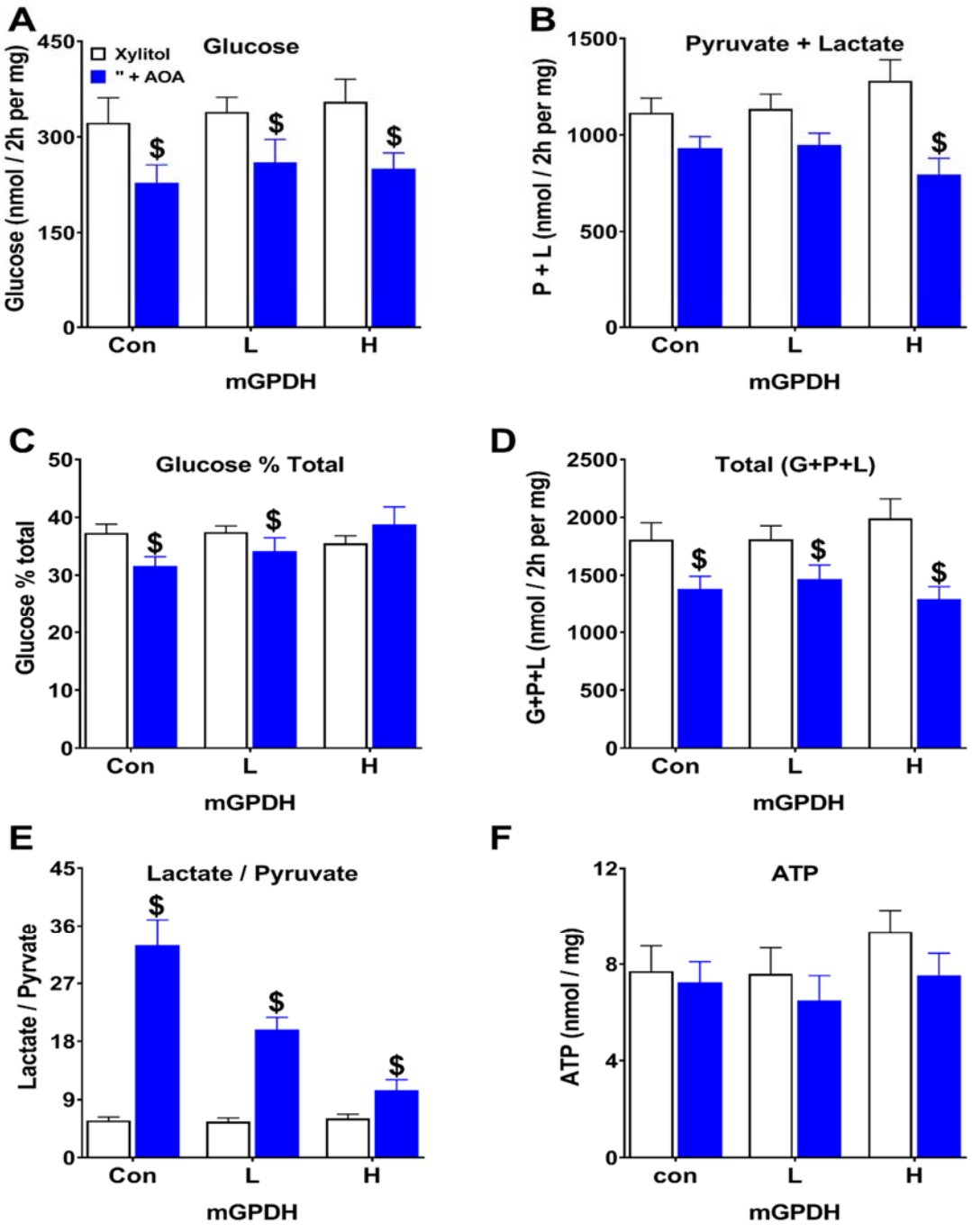

Figure 4-17: Overexpression of mGPDH inhibits glucose production from xylitol as substrate.

Hepatocytes were treated with Adv-Gpd2 to overexpress mGPDH as in (figure 4-9). After overnight culture, they were incubated in glucose-free DMEM with 2mM Xylitol in the absence (white bars) or presence (shaded bars) of 200µM AOA for 2h the medium was collected to measure (A) glucose production; (B) pyruvate plus lactate formation; (C) glucose percentage from total metabolism; (D) total metabolism; (E) lactate to pyruvate ratio. Cells were snap-frozen for ATP analysis (F). Results are Mean±SEM for n=4.

$ P<0.05 effect of AOA.

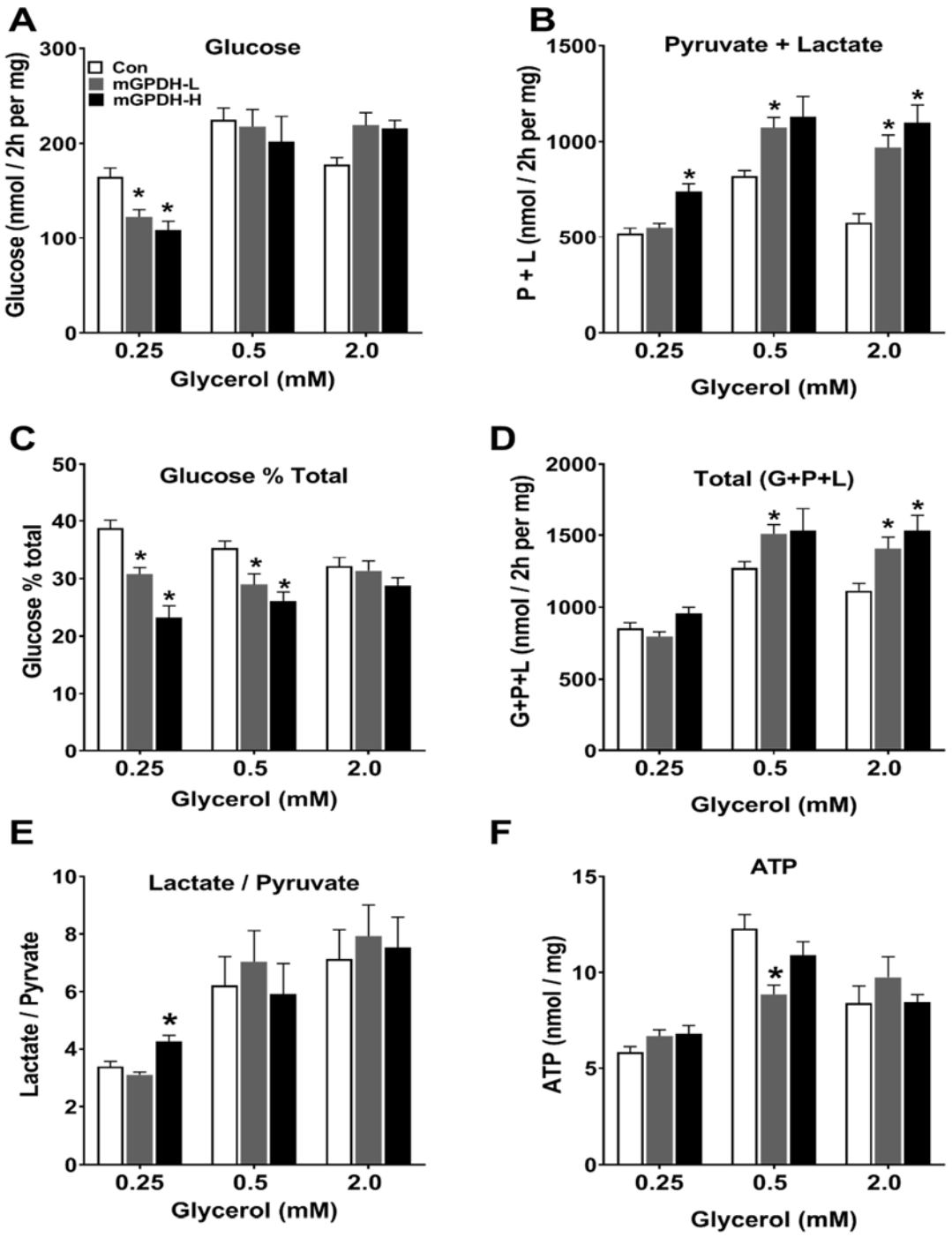

Figure 4-18: Overexpression of mGPDH increases total glycerol metabolism.

Hepatocytes were treated with Adv-Gpd2 to overexpress mGPDH as in (figure 4-9). After overnight culture, they were incubated in glucose-free DMEM with glycerol as indicated for 2h the medium was collected to measure (A) glucose production; (B) pyruvate plus lactate formation; (C) glucose percentage from total metabolism; (D) total metabolism; (E) lactate to pyruvate ratio. Cells were snap-frozen for ATP analysis (F). Results are Mean±SEM for n=5.

*** P<0.05 relative to respective control.**

4.2.8 Overexpression of mGPDH attenuates the effect of metformin on gluconeogenesis from oxidised substrate

Having confirmed that mGPDH like metformin favoured partitioning of DHA to glycolysis rather than glucose, we next tested whether mGPDH overexpression attenuated the effect of metformin on gluconeogenesis from DHA and glycerol. The effect of 50-100μM metformin, 80μM Gpi, and 200μM AOA were tested in hepatocytes expressing endogenous mGPDH only and in hepatocytes with mGPDH overexpression incubated with DHA and glycerol as gluconeogenic substrate. With DHA as substrate, the effects of low metformin on gluconeogenesis and glycolysis were attenuated in cells overexpressing mGPDH (Figure 4-19 A and B shaded bars), Gpi and AOA had no effect on gluconeogenesis and glycolysis (Figure 4-19 A and B; shaded bars). The effects of the Gpi and AOA but not low metformin on the lactate / pyruvate ratio were not attenuated in cells overexpressing mGPDH (Figure 4-20 A). With glycerol as substrate, Gpi inhibited total glycerol metabolism (Figure 4-21 D; white bars). Overexpression of mGPDH reversed the inhibition of glycerol metabolism by the Gpi (Figure 4-21 D; shaded bars) and reversed the raised in cell G3P (Figure 4-22 B)

Collectively, these results show that overexpression of mGPDH abolishes or attenuates the effects of metformin in causing: (i) lowering of cell G3P (ii) metabolism of DHA and glycerol towards glycolysis rather than glucose production; (iii) an increase in the lactate/pyruvate ratio. This suggests a possible link between the metformin mechanism and flux through the GPS.

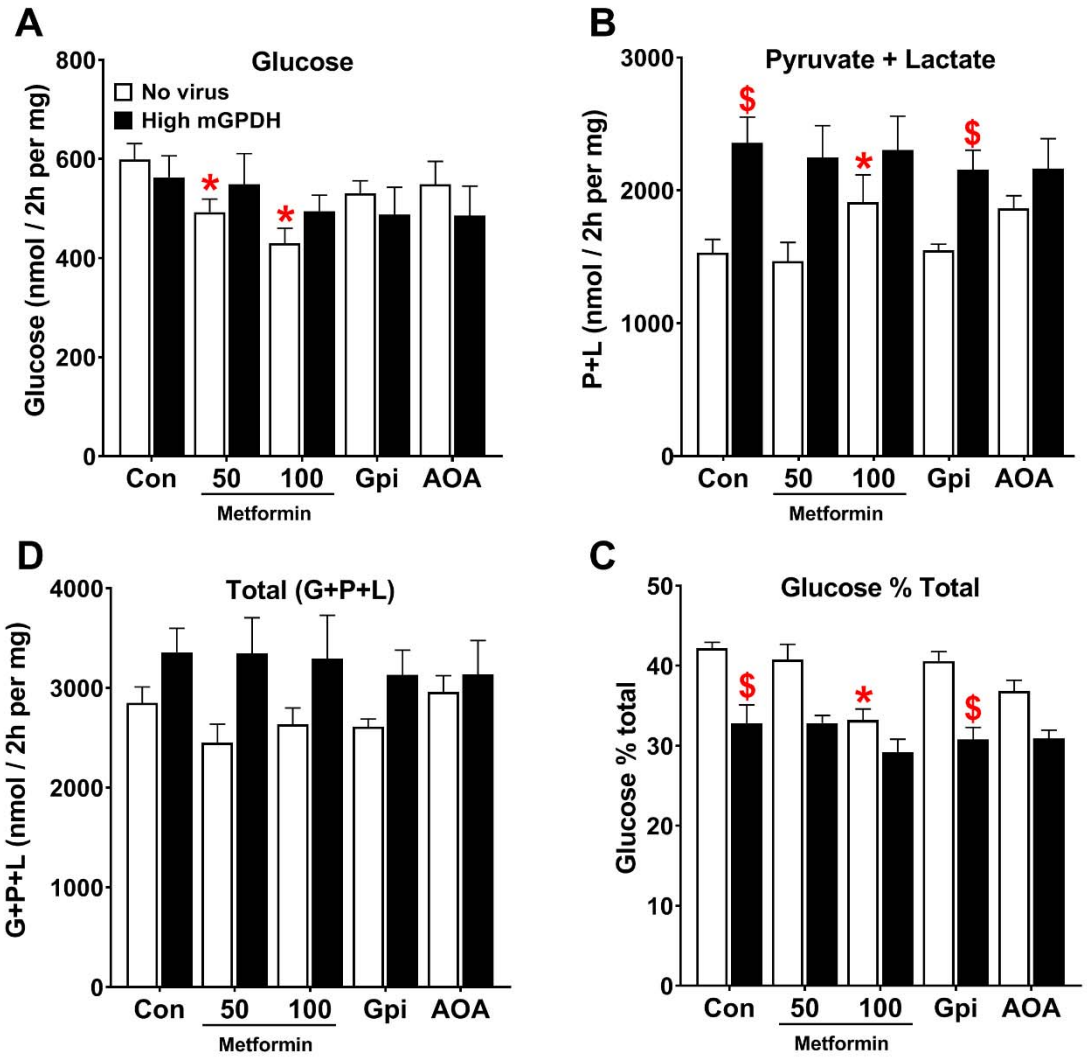

Figure 4-19: mGPDH overexpression attenuates the effect of metformin on glycolysis from DHA.

Hepatocytes were either untreated (Con) or treated with Adv-Gpd2 4.8 x10^7 PFU/ml for mGPDH overexpression (High dose; H). After overnight culture, they were pri-incubated in glucose-free DMEM with 100µM metformin and 80µM Gpi for 2h. the medium was then replaced by glucose-free DMEM containing 5mM DHA and metformin, Gpi, 200µM AOA for 2h the medium was collected to measure (A) glucose production, (B) pyruvate + lactate formation, (C) glucose production percentage, (D) total metabolism. Cells snap-frozen for ATP analysis. Results are Mean ± SEM. n=3 individual experiments.

*** P<0.05 relative to respective control.**

$ P<0.05 effect of mGPDH overexpression

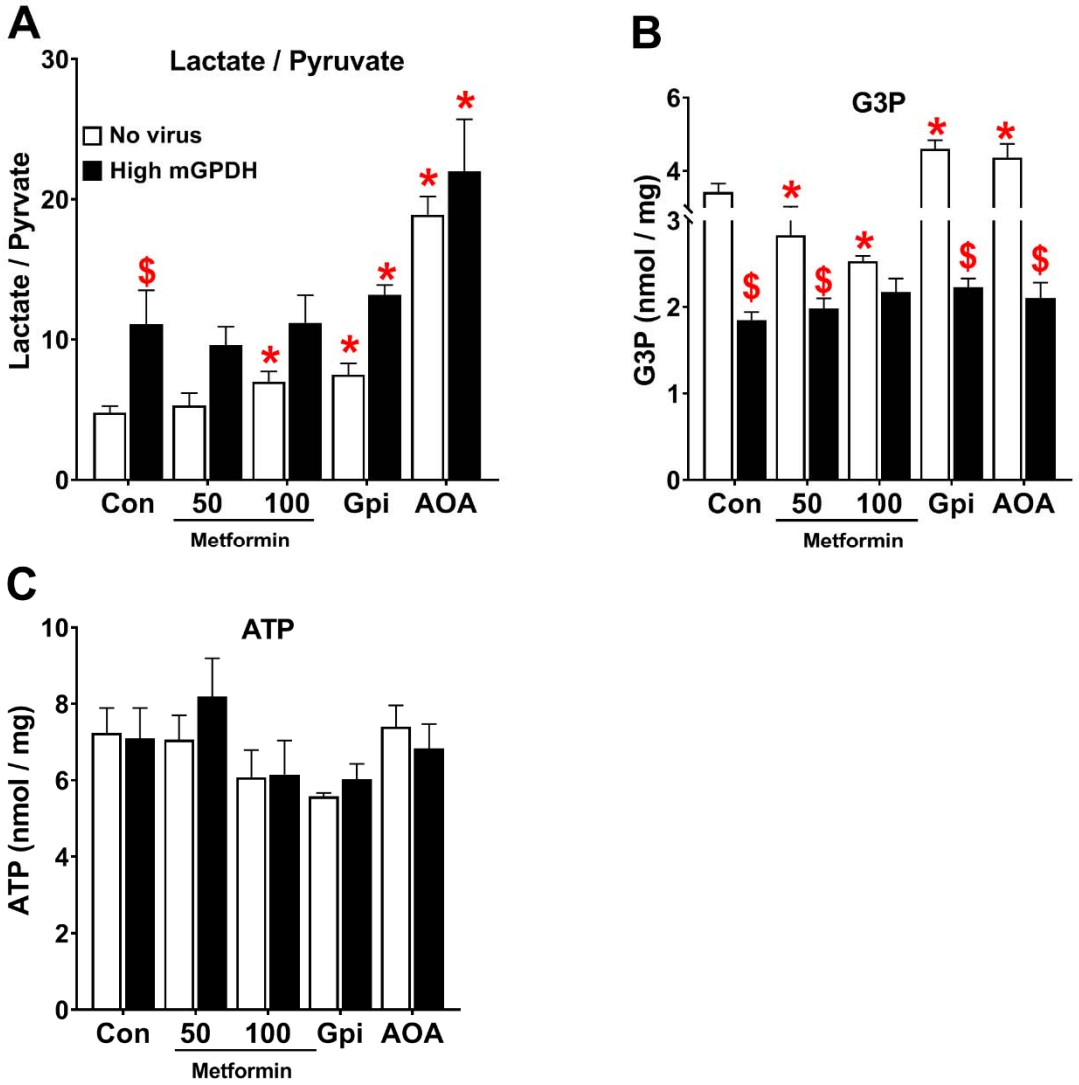

Figure 4-20: mGPDH overexpression reverses the increased in G3P by Gpi and AOA in incubation with DHA

Hepatocytes treated as in figure 4-19. Cells snap-frozen for G3P and ATP assays. (A) Lactate to pyruvate ratio; (B) cell G3P; (C) cell ATP. Results are Mean ±SEM for n=3 individual experiments.

*** P<0.05 relative to respective control.**

$ P<0.05 effect of mGPDH overexpression

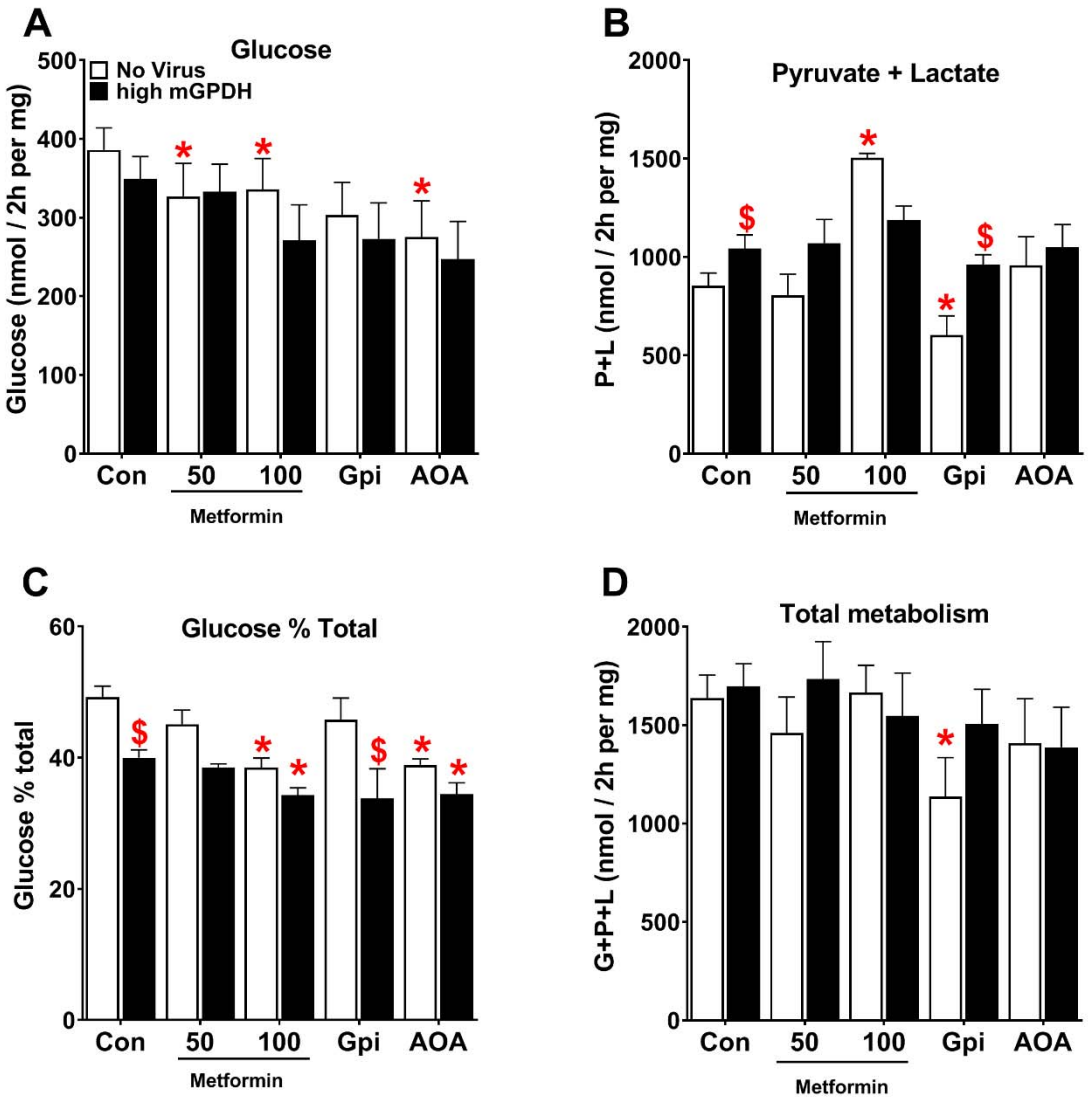

Figure 4-21: Inhibition of mGPDH by Gpi decreases total glycerol metabolism: effect corrected by mGPDH overexpression.

Hepatocytes were treated with Adv-Gpd2 to overexpress mGPDH as in figure 4-19. After overnight culture, they were pre-incubated in glucose-free DMEM with 100µM metformin and 80µM Gpi for 2h. The medium was then replaced by glucose-free DMEM containing 2mM glycerol and metformin, Gpi, 200µM AOA for 2h the medium was collected to measure (A) glucose production, (B) pyruvate + lactate formation, (C) glucose production percentage, (D) total metabolism. Cells snap-frozen for ATP analysis. Results are Mean ± SEM. n=3 individual experiments.

*** P<0.05 relative to respective control.**

$ P<0.05 effect of mGPDH overexpression

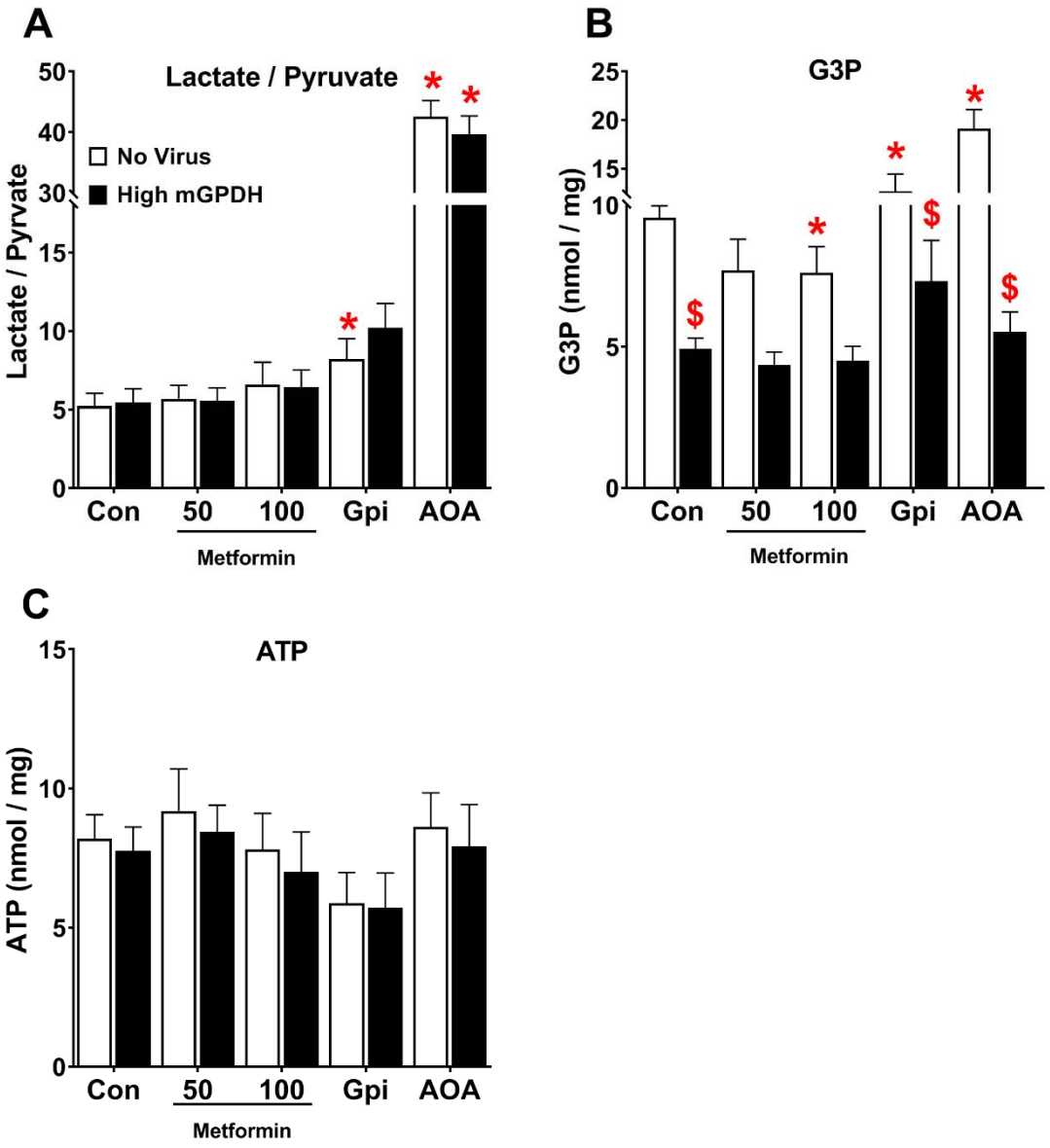

Figure 4-22: mGPDH overexpression attenuates lowering cell G3P by low metformin in incubation with glycerol

Hepatocytes treated as in figure 4-21. Cells snap-frozen for G3P and ATP assays. (A) Lactate to pyruvate ratio; (B) cell G3P; (C) cell ATP. Results are Mean ±SEM for n=3 individual experiments.

*** P<0.05 relative to respective control.**

$ P<0.05 effect of mGPDH overexpression.

4.2.9 Overexpression of mGPDH lowers cell G6P and mimics metformin

The above studies show that metformin increases the production of pyruvate and lactate and lowers G3P in cells expressing endogenous mGPDH but not in cells with mGPDH overexpression. G3P has been identified as an allosteric inhibitor of PFK1 (Claus et al., 1982). The stimulation of glycolysis by metformin and also by overexpression of mGPDH could be due to either an effect of the GPS on the cytoplasmic (NADH/NAD) redox state or to activation of PFK1 by the lower cell G3P. We found little or no evidence for a more reduced cytoplasmic redox state as determined from the lactate/pyruvate ratio with mGPDH overexpression because the lactate / pyruvate ratio was either unchanged (Figure 4-11 A) or increased (Figure 4-15 E). If the stimulation of glycolysis by mGPDH overexpression is due to activation of PFK1 then overexpression of mGPDH would be expected to lower cell G6P. We next tested the effects of mGPDH overexpression on cell G6P in hepatocytes incubated with high glucose, glycerol or DHA and compared this with the effect of 100μM metformin. Cell G6P level was highest with 25mM glucose (Figure 4-23 A) and lowest with 2mM glycerol (Figure 4-23 B). Overexpressing of mGPDH lower cell G6P with all substrate conditions (Figure 4-23 A-C). This shows that the activity of mGPDH has a major effect not only on lowering cell G3P but also G6P, and is consistent with the hypothesis that the stimulation of glycolysis by both metformin and mGPDH could be explained by the lowering of G3P which is an inhibitor of PFK1.

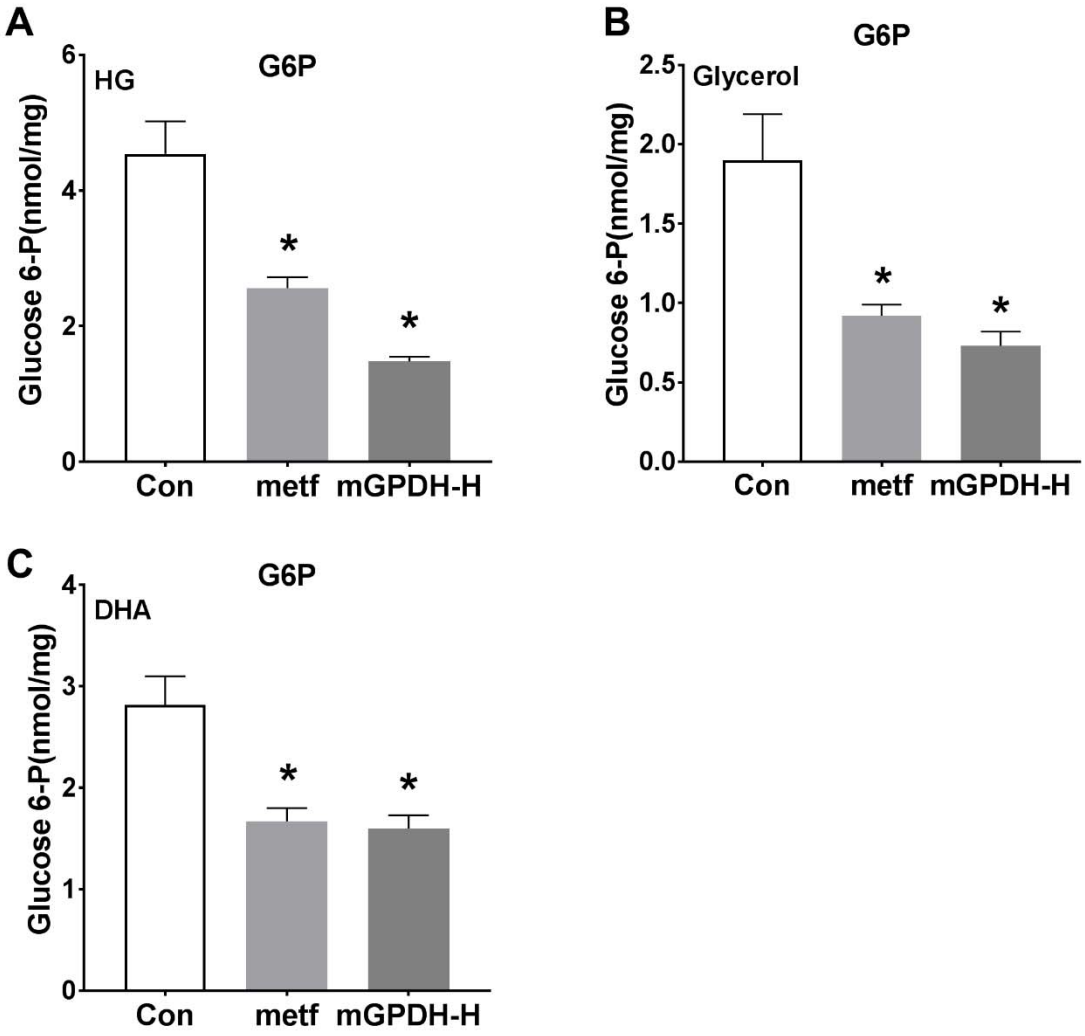

Figure 4-23: mGPDH overexpression mimics the metformin effect on cellular G6P.

Hepatocytes were treated with Adv-Gpd2 to overexpress mGPDH as in figure 4-9. After overnight culture they were pre-incubated in MEM with 100µM metformin as indicated for 2h. The medium was then replaced by fresh MEM containing 0.2µM S4048 and either (HG) 25mM glucose (A) for 1h, or 2mM glycerol (B), 5mM DHA (C) for 2h and 100µM metformin. Results are Mean±SEM. n=3 individual experiments.

*** P<0.05 relative to control with no virus (One-way ANOVA).**

4.2.10 Overexpression of mGPDH but not inhibition of the MAS mimics metformin on G6Pc gene expression

Metformin affects gene expression through either AMPK-dependent or AMPK-independent (Foretz et al., 2010) and counteracts the effects of high glucose on gene regulation by lowering G6P and other metabolites (Al-Oanzi et al., 2017). Because overexpression of mGPDH lowers both cell G6P and G3P similarly to metformin we next compared the effects of low metformin on mRNA levels of 4 genes that have previously been shown to be regulated by metformin with overexpression of mGPDH which lowers both G6P and G3P and with AOA which causes a large increase in G3P and also in the cytoplasmic redox state. High glucose caused a 2-fold increase in mRNA levels of G6pc, TXNIP, ChREBP-β and FGF21 (Figure 4-24 A-D) as expected from previous studies (Ma et al., 2006) and xylitol which causes a larger increase in G3P than glucose caused a 3-5 fold increase in expression of these genes (Figure 4-25 A-D). AOA markedly enhanced the gene induction by xylitol (Figure 4-25 A-D), whereas overexpression of mGPDH mimicked the counter regulatory effect of metformin on G6pc and TXNIP (Figure 4-24 A and B) but not on ChREBP-β and FGF21 (Figure 4-24 C and D). These results suggest that changes in metabolites that are influenced by the GPS and MAS are involved in gene regulation by high glucose and xylitol.

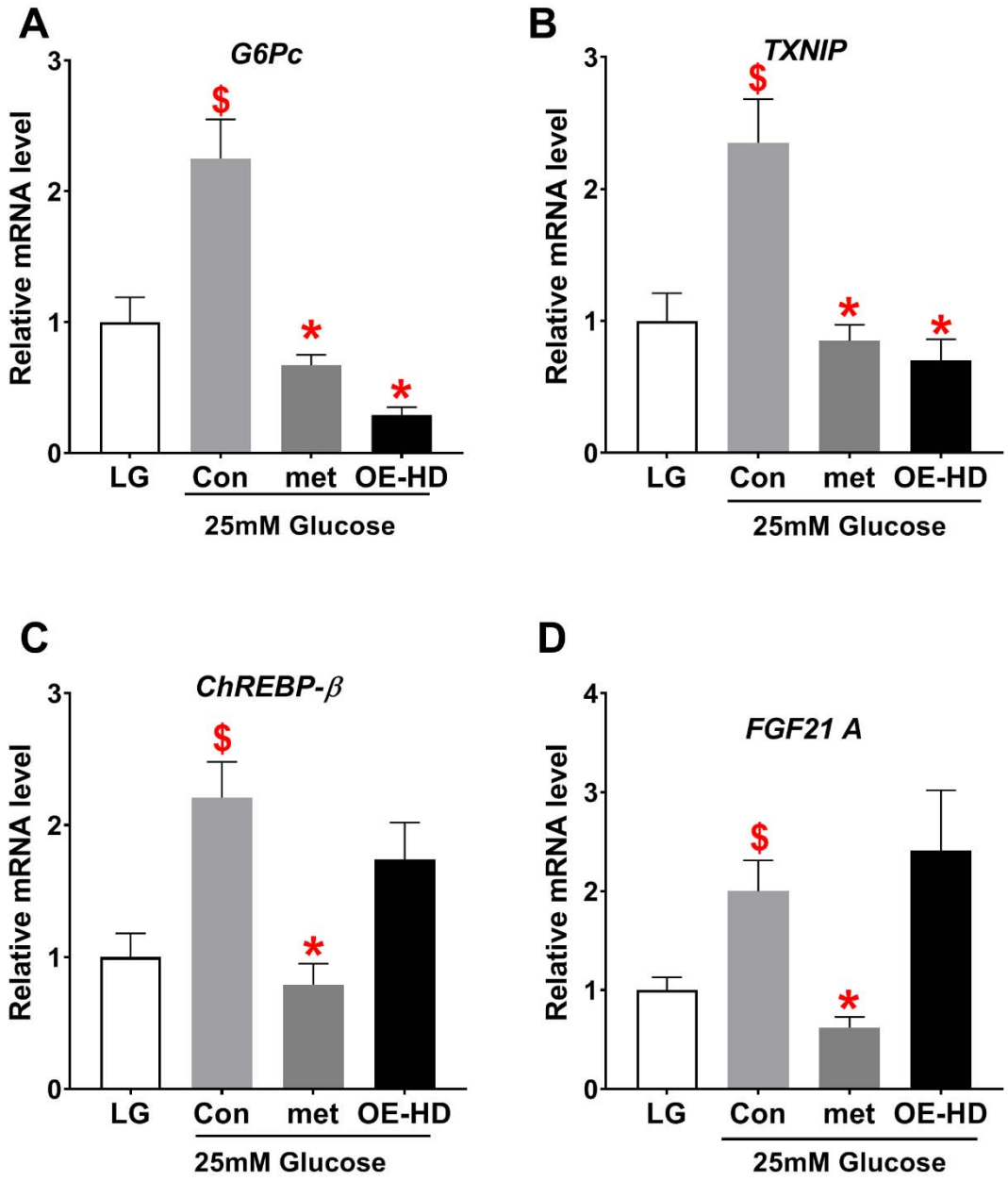

Figure 4-24: Overexpression of mGPDH like metformin suppresses G6Pc gene expression.

Mouse hepatocytes were either untreated or treated with Ad-m-Gpd2 4.8 x10^7 PFU/ml for overexpression of mGPDH (High dose; H). After overnight culture they were pre-incubated in MEM with 100µM metformin as indicated for 2h. The medium was then replaced by fresh MEM and incubated with 25mM glucose and metformin for further 4h. Total RNA was extracted in Trizol for mRNA analysis. n=4 individual experiments.

$ P<0.05 relative to low 5mM glucose (LG).

*** P<0.05 relative to high glucose (HG).**

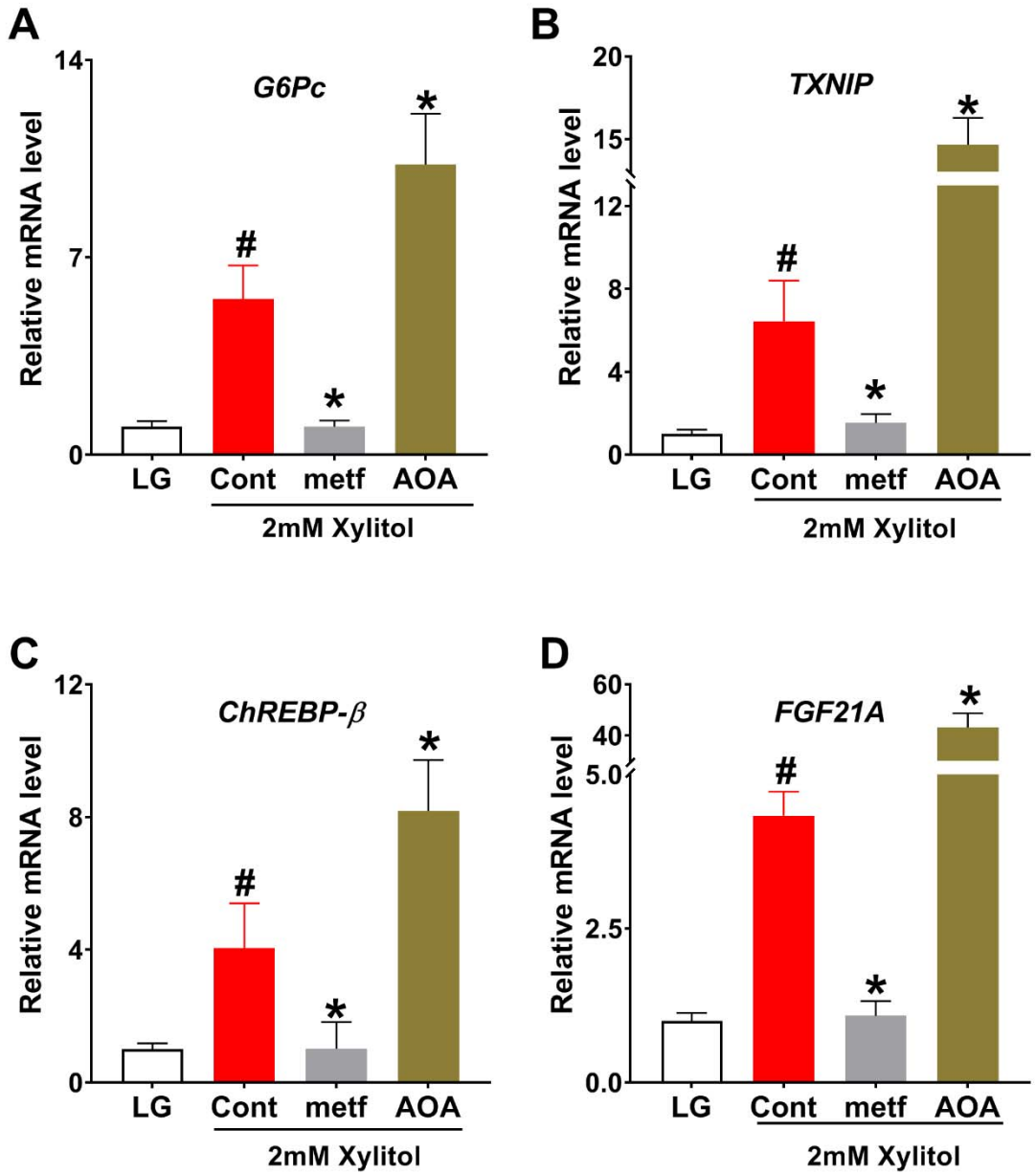

Figure 4-25: metformin opposite from AOA suppresses gluconeogenic genes

Mouse hepatocytes were either untreated or treated with Ad-m-Gpd2 4.8 x10^7 PFU/ml for overexpression of mGPDH (High dose; H). After overnight culture they were pre-incubated in MEM with 100µM metformin as indicated for 2h. The medium was then replaced by fresh MEM containing 2mM xylitol and metformin and 200µM AOA for further 4h. Total RNA was extracted in Trizol for mRNA analysis. n=4 individual experiments.

 # P<0.05 relative to low 5mM glucose (LG).

*** P<0.05 relative to xylitol with no treatment.**

4.2.11 Octanoate favours gluconeogenesis rather than glycolysis from oxidised and reduced substrates

The previous results showed that inhibition of the MAS and GPS does not mimic the inhibition of gluconeogenesis by 100μM metformin. Moreover, overexpression of mGPDH mimicked the stimulation of glycolysis by metformin. In this study we compared the effect of metformin on gluconeogenesis in the absence and presence of octanoate which has been shown previously to stimulate gluconeogenesis and inhibit glycolysis either by increasing citrate which is an inhibitor of PFK1 (Hers and Hue, 1983) or by direct inhibition of PFK-1 by octanoyl-CoA (Jenkins et al., 2011). Our first aim was to investigate whether octanoate abolished the effect of metformin on gluconeogenesis. Hepatocytes were incubated with either (0.125mM) or (0.25mM) octanoate in the presence of the oxidised substrate DHA, and with 0.125mM octanoate in the presence of reduced substrate xylitol as gluconeogenic precursor. Octanoate increased the rate of gluconeogenesis from both DHA (Figure 4-26 A) and xylitol (Figure 4-28 A) and increased the fractional partitioning of DHA (Figure 4-26 C) and xylitol (Figure 4-28 C) to glucose rather than glycolysis. The increase in gluconeogenesis by octanoate was associated with inhibition in pyruvate plus lactate formation (Figure 4-26 B and Figure 4-28 B) without significant effect on total metabolism (Figure 4-26 D and 4-28 D). Octanoate increased the lactate to pyruvate ratio (Figure 4-27 A and Figure 4-29 A) as expected (Sibille et al., 1995) and lowered the cell G3P level from oxidised (DHA) (Figure 4-27 B) but not from reduced (xylitol) substrate (Figure 4-29 B). With DHA as substrate, low octanoate (0.125mM) did not affect the inhibitory effects of metformin on gluconeogenesis but high octanoate (0.25mM) attenuated the inhibition of glucose production (Figure 4-26 A) but did not abolish the effect of metformin on the pyruvate plus lactate formation (Figure 4-26 B) and fractional partitioning of DHA to glucose (Figure 4-26 C). Metformin increased the lactate to pyruvate ratio (Figure 4-28 A) and lowered cell G3P with 0.125mM but not with 0.25mM octanoate (Figure 4-28 B), while the effects of metformin were abolished by octanoate (0.12mM) in incubation with 2mM xylitol (Figure 4-28 A-D). Interestingly, inhibition of the MAS by AOA in the presence of octanoate favored gluconeogenesis rather than glycolysis by increasing the fractional partitioning of both DHA and xylitol to glucose relative to glycolysis and inhibited pyruvate plus lactate formation with concomitant inhibition in total metabolism (Figure 4-26 and Figure 4-28 A-D). AOA and octanoate had additive effects on the lactate / pyruvate ratio (Figure 4-27 A and Figure 4-29 A), and the increase in G3P by AOA was attenuated in the presence of octanoate (Figure 4-27 B).

Collectively, (i) octanoate had opposite effects from metformin on gluconeogenesis from DHA and xylitol, which are suggestive of inhibition of PFK1 or activation of FBP1. (ii) Addition of octanoate did not abolish the effects of low (100μM) metformin on gluconeogenesis.

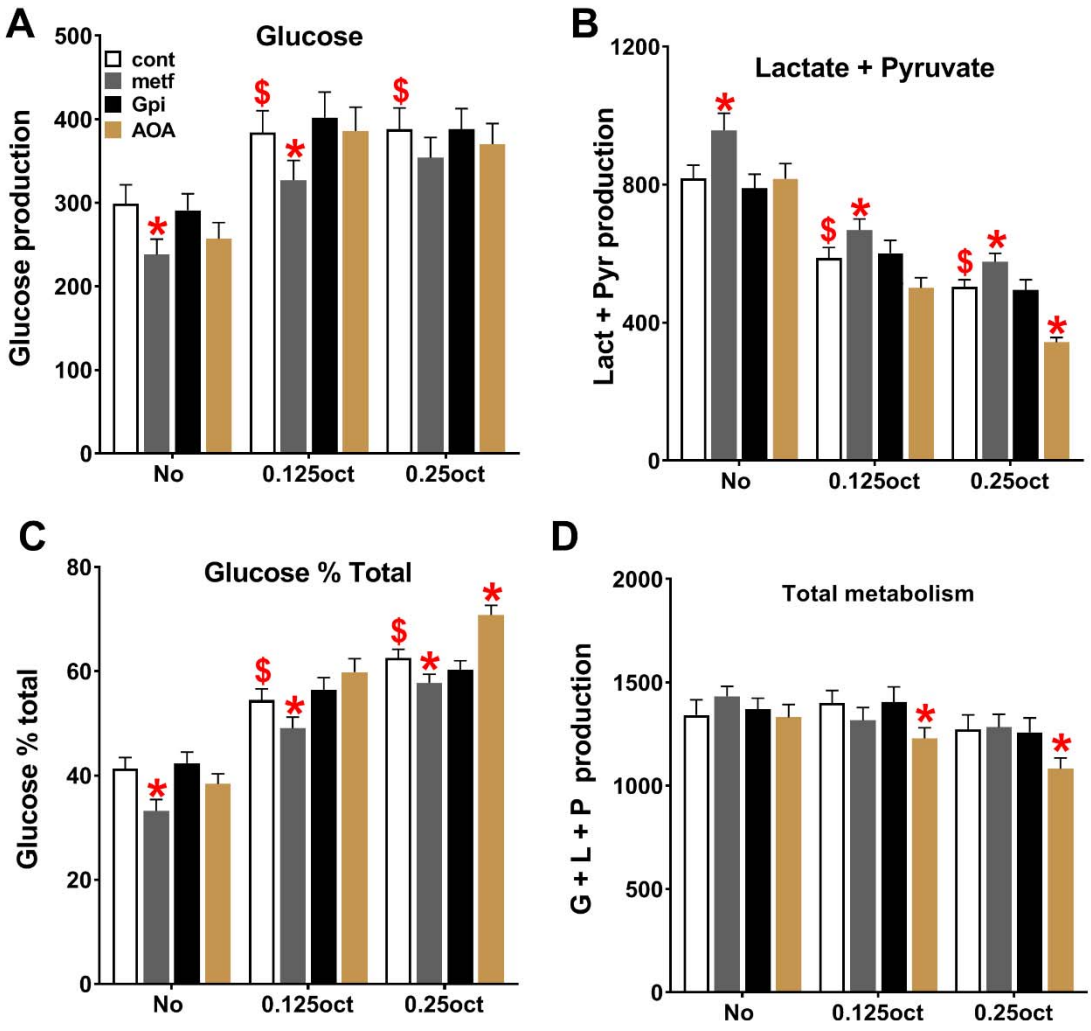

Figure 4-26: High octanoate concentration attenuates the effect of metformin on gluconeogenesis from the oxidised substrate, DHA.

After overnight culture mouse hepatocyte monolayers were pre-incubated with 100µM metformin, 20µM Gpi in glucose-free DMEM for 2h. The medium was then replaced by glucose-free DMEM containing 5mM DHA plus either 0.125mM or 0.25mM octanoate and other additions (100µM metformin, 20µM Gpi, and 200µM AOA) and incubated for further 2h and medium was collected to measure (A) glucose production, (B) lactate plus pyruvate formation, (C) glucose production percentage, (D) total DHA metabolism. Results are Mean±SEM for n=7 individual experiments.

*** P<0.05 relative to respective control.**

$P<0.05 effect of octanoate.

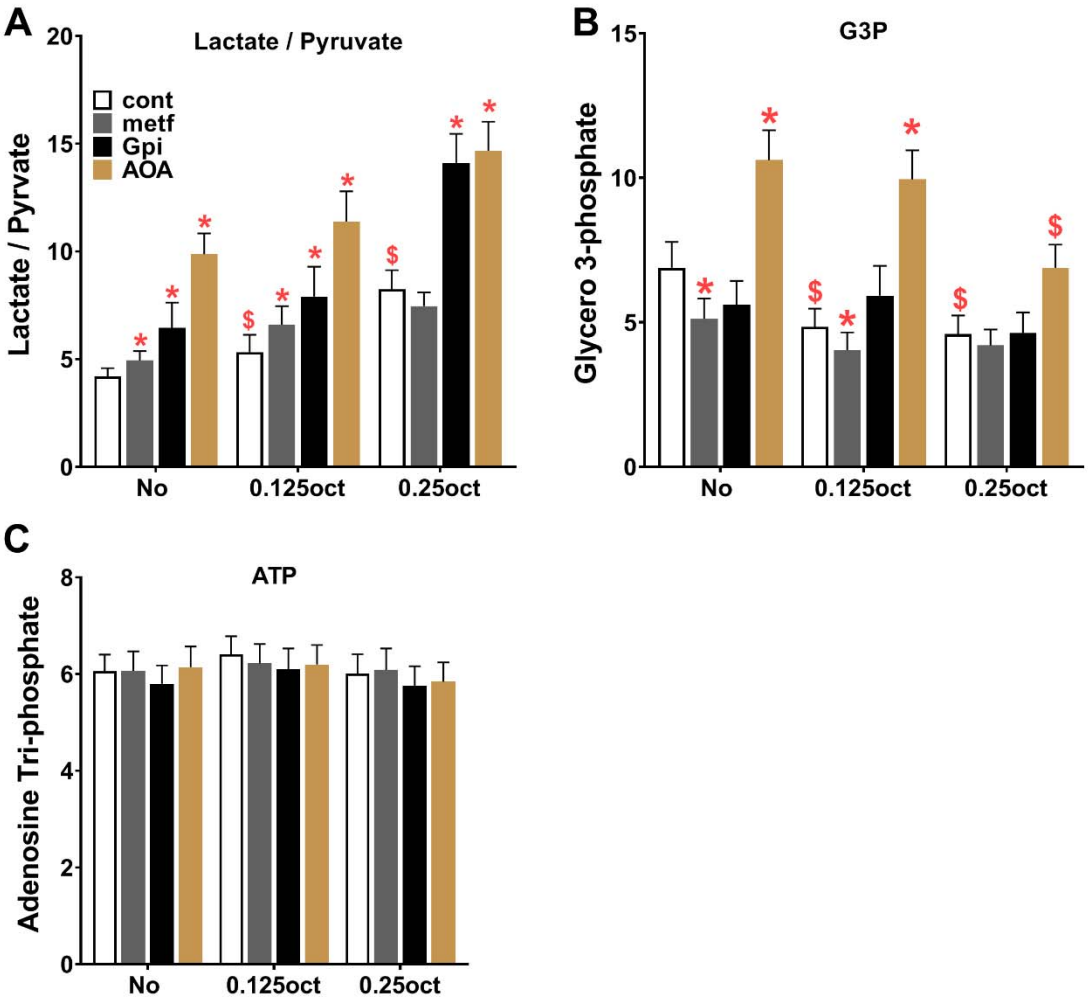

Figure 4-27: Octanoate lowers cell G3P in incubation with oxidised substrate, DHA.

Hepatocytes were incubated as in figure 4-26, medium was collected and cells were snap-frozen for G3P and ATP analysis (A) lactate to pyruvate ratio; (B) cell G3P; (C) cell ATP. Results are Mean±SEM for n=7 individual experiments.

*** P<0.05 relative to respective control.**

$P<0.05 effect of octanoate.

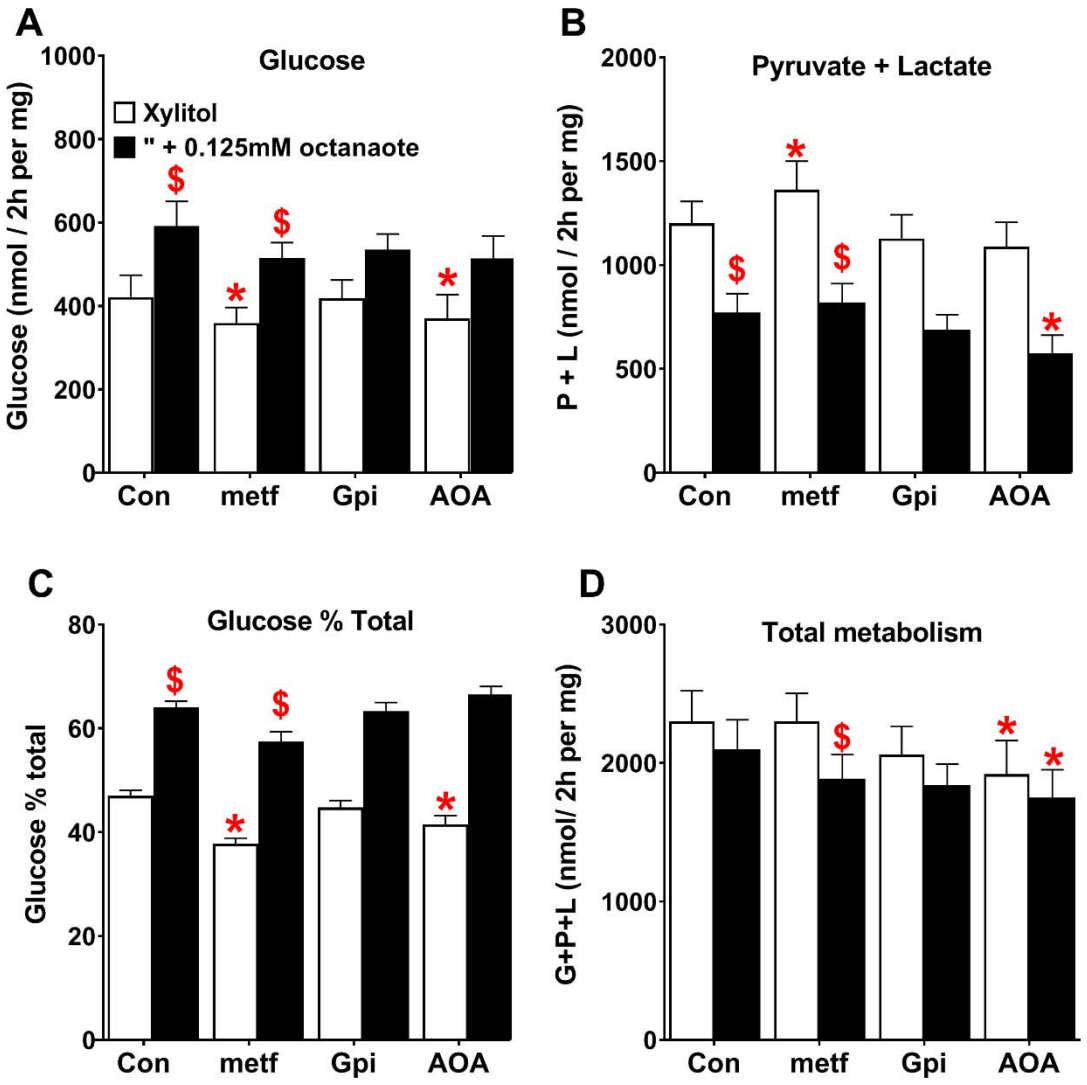

Figure 4-28: Octanoate increases gluconeogenesis and abolishes the metformin inhibitory effect on gluconeogenesis from the reduced substrate, xylitol.

After overnight culture mouse hepatocyte monolayers were pre-incubated with 100µM metformin, 20µM Gpi in glucose-free DMEM for 2h. The medium was then replaced by glucose-free DMEM containing 2mM xylitol plus 0.125mM octanoate and other additions (100µM metformin, 20µM Gpi, and 200µM AOA) and incubated for further 2h and medium was collected to measure (A) glucose production, (B) lactate plus pyruvate formation, (C) glucose production percentage, (D) total DHA metabolism. Results are Mean±SEM. n=4 individual experiments.

*** P<0.05 relative to respective control.**

$P<0.05 effect of octanoate.

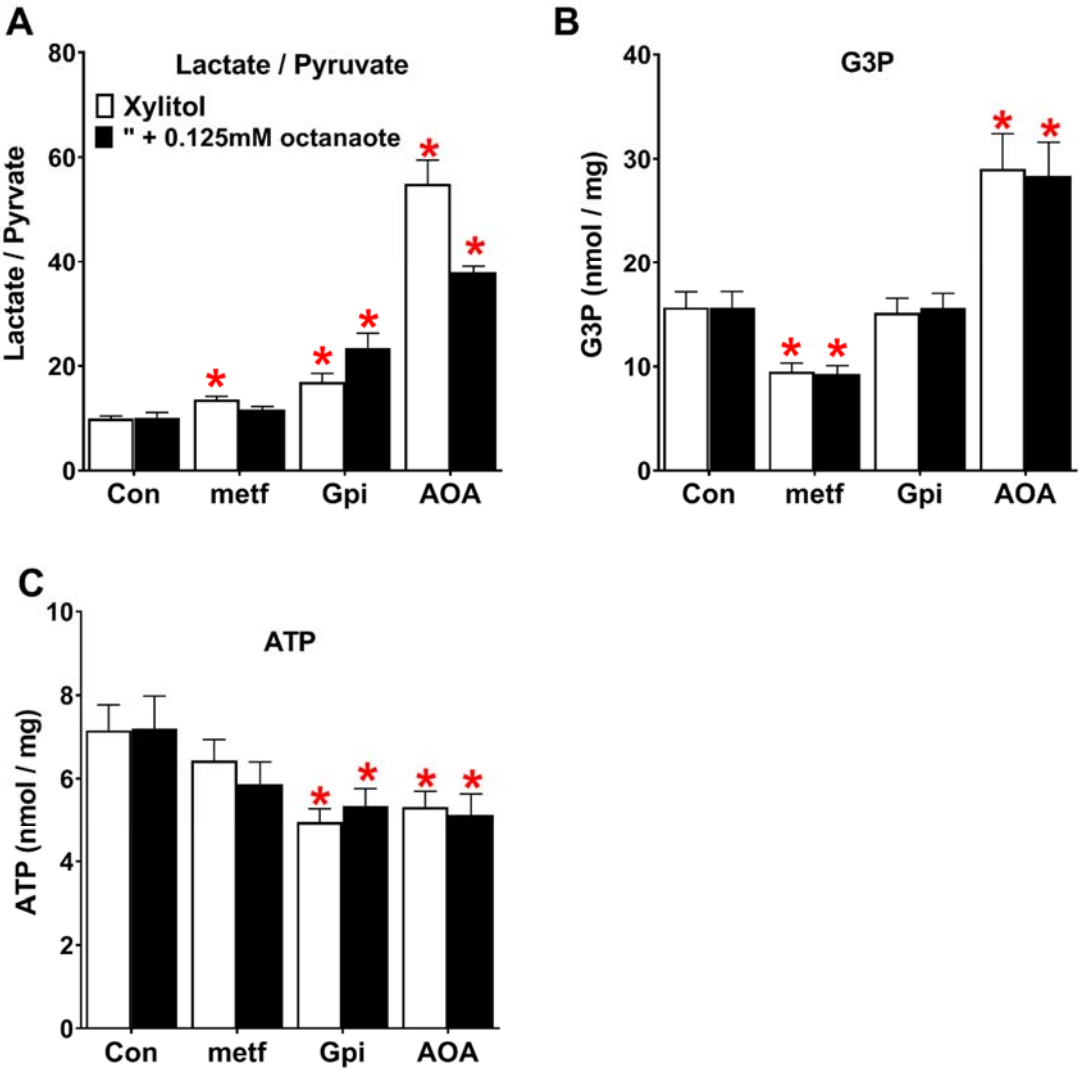

Figure 4-29: Octanoate abolishes the effect of metformin on the lactate to pyruvate ratio from the reduced substrate, xylitol.

Hepatocytes were incubated as in figure 4-28, medium was collected and cells were snap-frozen for G3P and ATP analysis (A) lactate to pyruvate ratio; (B) cell G3P; (C) cell ATP. Results are Mean±SEM for n=4 individual experiments.

*** P<0.05 relative to respective control.**

$P<0.05 effect of octanoate.

4.2.12 Activation of AMPK by octanoate but not by low metformin

The above results showed that octanoate stimulates gluconeogenesis. Next, we investigated the effect of octanoate on ACC-phosphorylation, the AMPK substrate, to test whether the increase in gluconeogenesis by octanoate can be explain by a decrease in AMP (which is a potent inhibitor of FBP1 and activator of PFK1). Addition of octanoate increased ACC-phosphorylation, indicating AMPK activation. This suggests increased AMP with octanoate most likely through acyl-CoA synthase which produces acyl CoA plus AMP, as reported previously (Kawaguchi et al., 2002). There was lower phosphorylation of ACC by 100µM metformin in combination with octanoate relative to octanoate alone (Figure 4-30). This may be due to accelerated clearance of octanoate by 100µM metformin. Cumulatively, octanoate increased the activation of AMPK suggesting an increase in AMP, which is expected to stimulate glycolysis by PFK-1 activation and inhibit gluconeogenesis by FBP-1 inhibition. Therefore other mechanisms must be involved in the stimulation of gluconeogenesis, such as an increase in citrate or direct inhibition of PFK-1 by octanoyl-CoA (Jenkins et al., 2011).

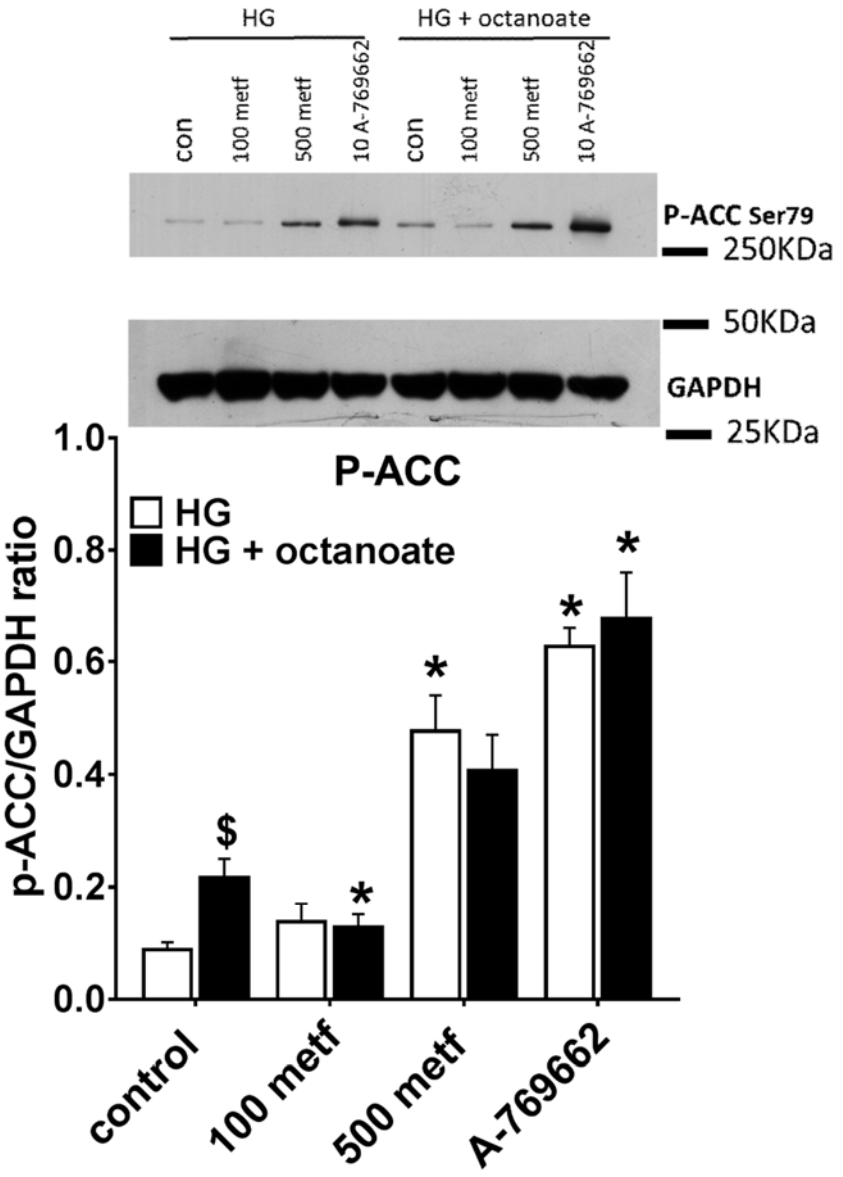

Figure 4-30: Octanoate but not low metformin increases ACC-phosphorylation.

After overnight culture mouse hepatocyte monolayers were incubated with MEM for 2h. The medium was then replaced with MEM containing 25mM glucose without (white bars) or with (shaded bars) 0.125mM octanoate 1hr. (100 and 500µM metformin, 10µM A-769662 were presented in both incubation). Results are representative immunoblotting and densitometry for n=4 individual experiments.

***P<0.05 relative to respective control.**

$P<0.05 octanoate effect.

4.2.13 Inhibition of PFK-1 attenuates the metformin effect on gluconeogenesis

The above result shows opposite effects of metformin and octanoate on gluconeogenesis which may be due to regulation at the level of PFK1 and / or FBP1. We next tested whether inhibition of PFK and activation of FBP1 is a candidate mechanism for the effect of low metformin on glycolysis and gluconeogenesis. We depleted fructose 2,6-P_2 a potent activator of PFK-1 and inhibitor of FBP1 (Hers and Hue, 1983) by expressing a kinase-deficient variant (PFK-KD) of the bifunctional enzyme PFK2/FBP2 (Arden et al., 2012) and compared 100µM metformin with AMPK activator A-769662 (10µM) in hepatocytes that were untreated or treated with Adv-PFK-KD. Cells treated with PFK-KD to deplete the PFK1 activator showed inhibition of glycolysis as expected (Figure 4-31 B) and increased glucose production and partitioning of DHA to glucose (Figure 4-31 A and C), without a change in total DHA metabolism (Figure 4-31 D) and with lowering of cell G3P (Figure 4-32B). The effects of low metformin (100µM) on the increased partitioning of substrate towards glycolysis and on lowering of G3P were abolished in the presence of PFK-KD (Figure 4-31 C and Figure 4-32 B). Similar results were obtained on gluconeogenesis and glycolysis when hepatocytes were incubated with db-cAMP, which is expected to inhibit the kinase activity as occurs with glucose (Payne et al., 2005) and deplete fructose 2,6-P_2. It is noteworthy that db-cAMP causes via activation of PKA phosphorylation of the liver isoform of PFK2/FBP2 resulting in inhibition of the kinase activation of the bisphosphatase but PKA also phosphorylates several other enzymes such as phosphorylase kinase and glycogen synthase and therefore regulates several metabolic pathways including glycogen synthesis and degradation. The liver isoform of PFK2/FBP2 (PFKFB1) when phosphorylated by PKA on a serine residue at the N-terminus functions as a bisphosphatase (Rider et al., 2004) causing depletion of F2,6-P_2 as occurs during overexpression of the kinase-deficient variant of PFKFB1. The similar effect of db-cAMP compared with PFK-KD are consistent with the major role of the liver isoform PFK2/FPBP2 in mediating the acute stimulation of gluconeogenesis by glucagon. db-cAMP increased the partitioning of substrate to gluconeogenesis and abolished the effect of metformin (Figure 4-33 C; shaded bars). The AMPK activator (A-769662) inhibited pyruvate plus lactate formation and had no effect on gluconeogenesis (Figure 4-31 A and B; white bars) in untreated hepatocytes, or in cells treated with PFK-KD or db-cAMP (Figure 4-31 and Figure 4-33 ; shaded bars). A-769662 increased the lactate to pyruvate ratio in untreated hepatocytes (Figure 4-32 A; white bars). In hepatocytes treated with PFK-KD or db-cAMP the effect of A-769662 on the lactate / pyruvate ratio was attenuated (Figure 4-32 A and Figure 4-34 A; shaded bars).

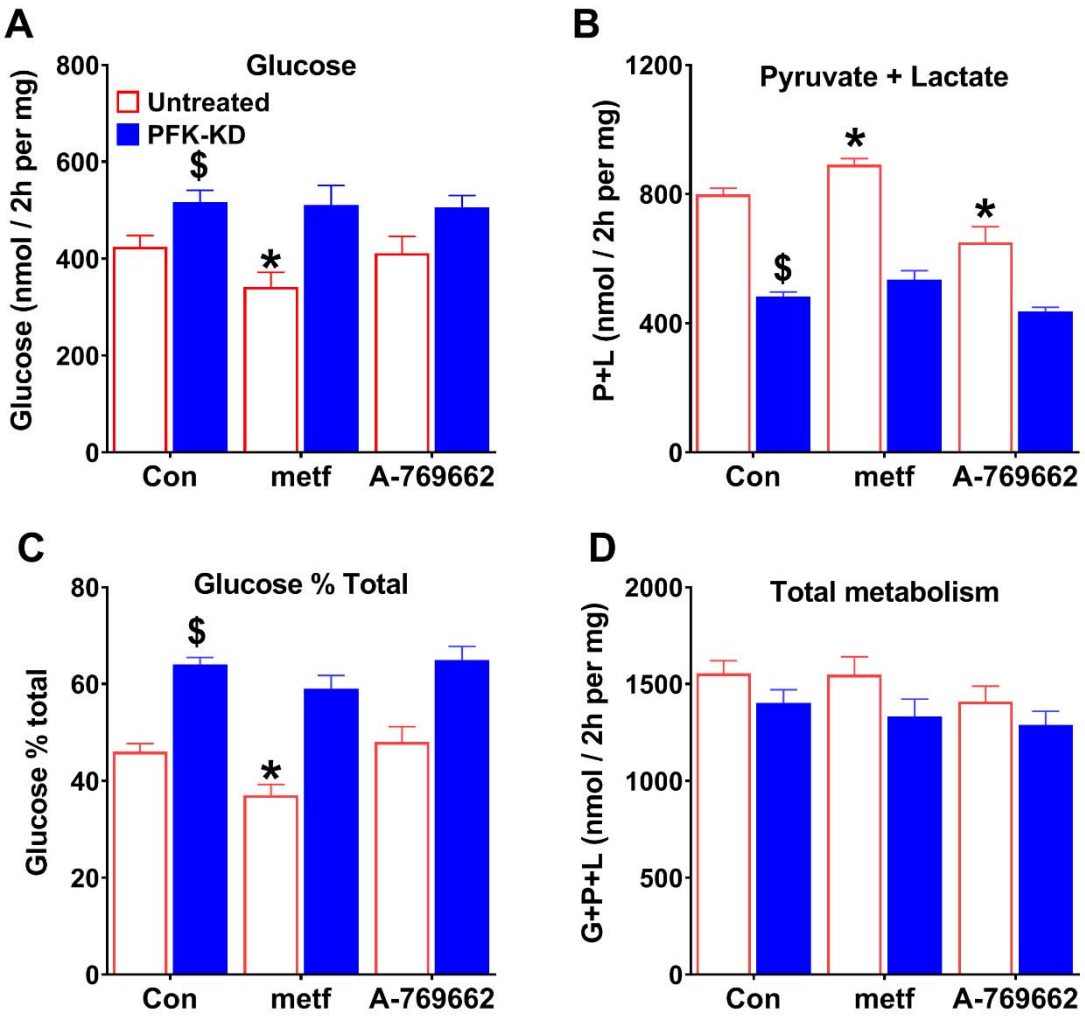

Figure 4-31: PFK-KD abolishes the effect of metformin on gluconeogenesis from DHA.

Hepatocytes were either untreated (open bars) or treated (shaded bars) with an adenovirus vector for expression of PFK-KD to deplete cell fructose 2,6-P_2. After overnight culture mouse hepatocyte monolayers were incubated with in glucose-free DMEM for 2h. The medium was then replaced by glucose-free DMEM containing 5mM DHA and incubated for further 2h (100µM metformin and 10µM A-769662 present in both incubation) medium was collected to analysis (A) glucose production, (B) pyruvate plus lactate formation (C) glucose production percentage, (D) Total metabolism. Results are Means ±SEM for n= 8.

***P <0.05 relative to respective control.**

$ P<0.05 effect of PFK-KD.

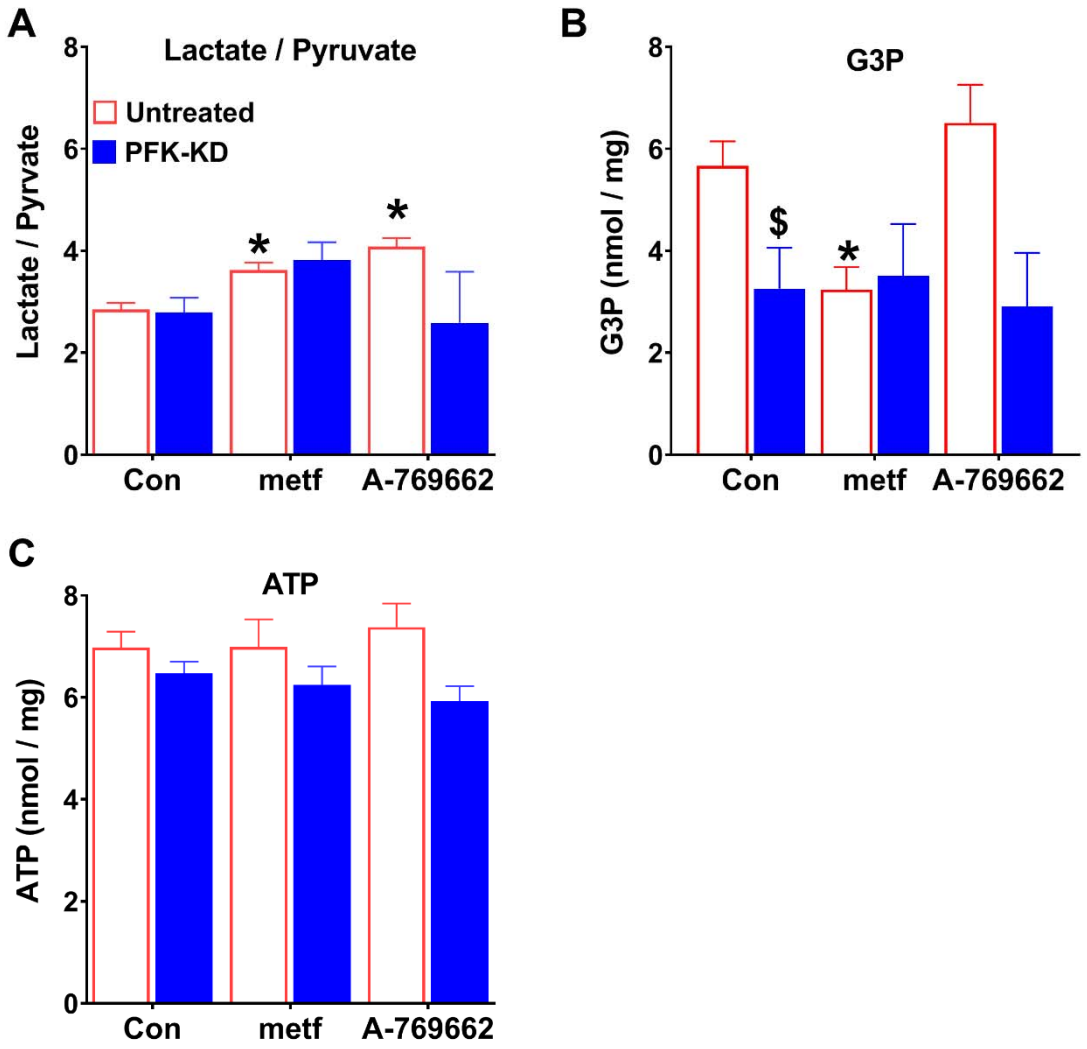

Figure 4-32: PFK-KD attenuates the effects of metformin on the lactate to pyruvate ratio and G3P.

Hepatocytes were treated similar to (Figure 4-31), medium was collected and cells were snap-frozen for G3P and ATP analysis (A) lactate to pyruvate ratio; (B) cell G3P; (C) cell ATP. Results are Means ±SEM for n= 8.

***P <0.05 relative to respective control.**

$ P<0.05 effect of PFK-KD.

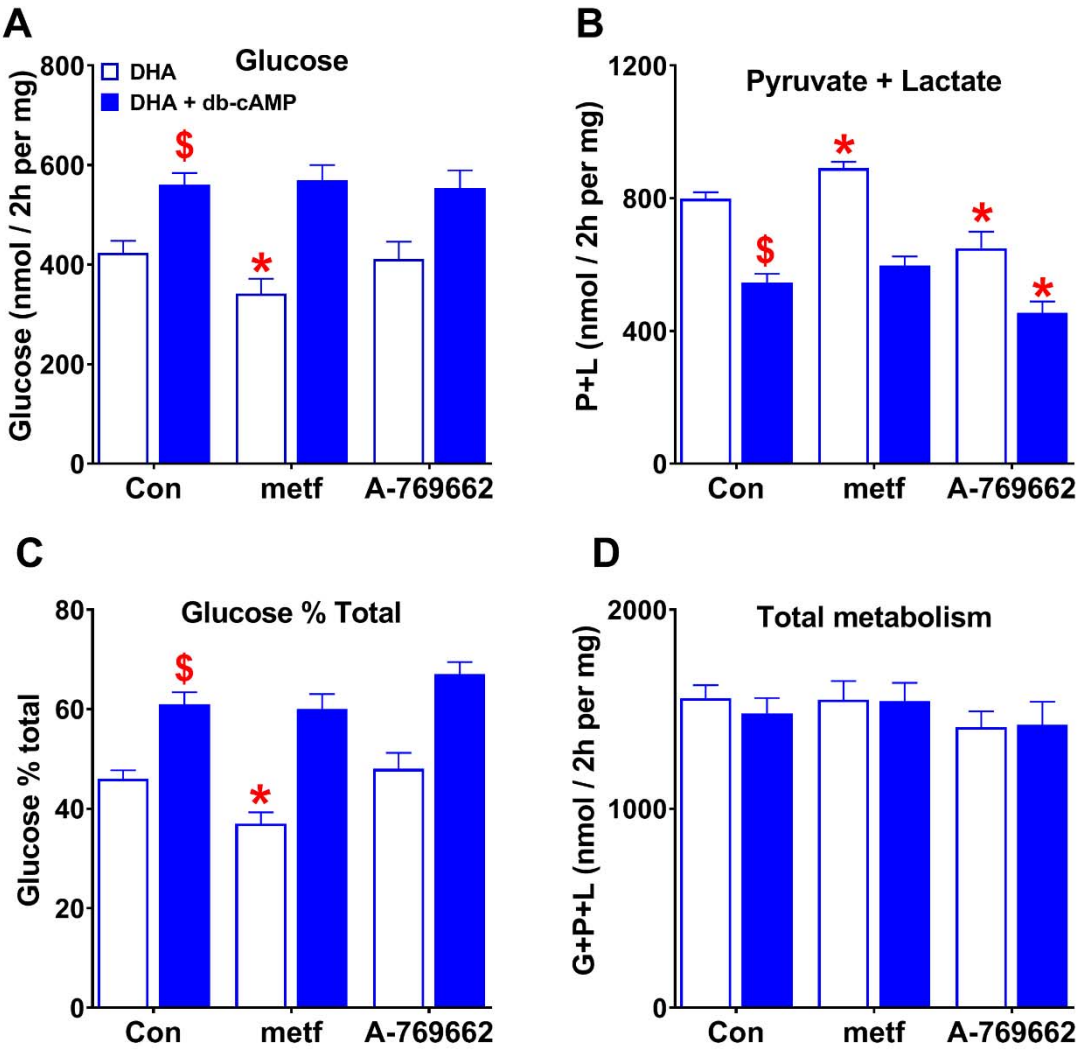

Figure 4-33: db-cAMP abolishes the effect of metformin on DHA metabolism.

After overnight culture mouse hepatocyte monolayers were incubated in glucose-free DMEM for 2h. The medium was then replaced by glucose-free DMEM containing 5mM DHA plus 10µM db-cAMP and incubated for further 2h (100µM metformin or 10µM A-769662 present in both incubation) medium was collected to measure (A) glucose production, (B) pyruvate plus lactate formation (C) glucose production percentage, (D) Total metabolism. Results are Means ±SEM for n= 8.

***P <0.05 relative to respective control.**

$ P<0.05 relative effect of db-cAMP.

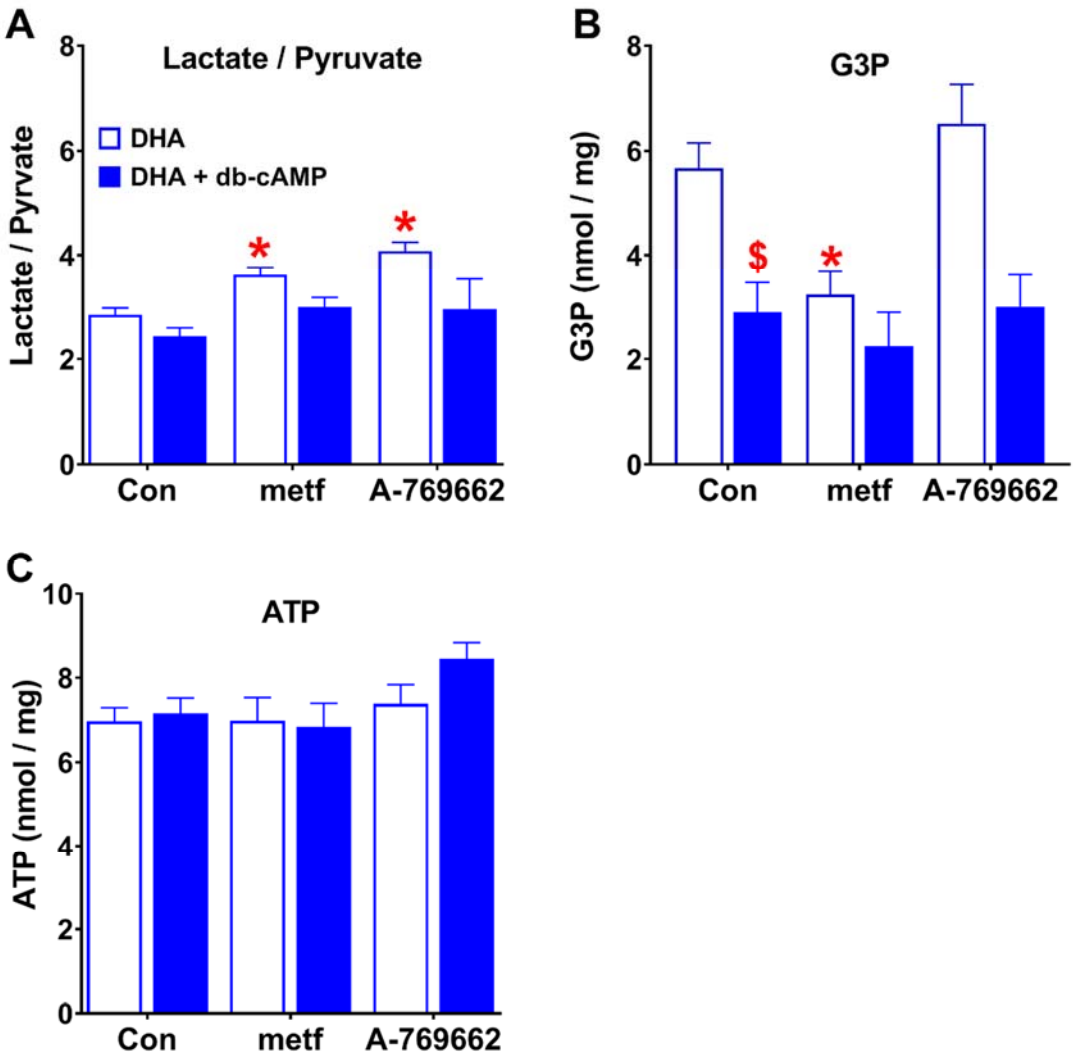

Figure 4-34: db-cAMP abolishes metformin inhibitroy effect on G3P.

Hepatocytes were treated as in figure 4-33, medium was collected and cells were snap-frozen for G3P and ATP analysis (A) lactate to pyruvate ratio; (B) cell G3P; (C) cell ATP. Results are Means ±SEM for n= 8.

***P <0.05 relative to respective control.**

$ P<0.05 effect of db-cAMP.

4.2.14 Inhibition of fructose-1,6-bisphosphatase-1 (FBP1) mimics low metformin on gluconeogenesis

Fructose 1,6-bisphosphatase-1 (FBP1) was recently proposed as the target for metformin (Hunter et al., 2018). To selectively target FBP1 or PFK1, we next used an FBP1 inhibitor that binds to the AMP site (Dang et al., 2009) and a citrate analogue PFK1 inhibitor (aurintricaboxylic acid, ATA), which antagonizes activation of PFK1 by AMP and fructose 2,6-P_2 (McCune et al., 1989). Hepatocytes were incubated with DHA and 0.2μM S4048 to raise cell G6P, which is otherwise below detection limits in hepatocytes incubated in glucose-free medium. The chlorogenic acid derivative S4048 is a very potent inhibitor of the G6P transporter. This inhibitor has no effect on cell G6P in hepatocytes incubated at basal glucose but it raises G6P with high glucose or gluconeogenic precursors (Al-Oanzi et al., 2017, Harndahl et al., 2006), and it suppresses but does not abolish glucose production. The FBP1 inhibitor (FBPi) like metformin inhibited gluconeogenesis, but unlike metformin it did not stimulate glycolysis (Figure 4-35 A-B). Cell G6P was lowered by FBPi and increased with the PFK1 inhibitor (ATA) (Figure 4-36 B), which also increased glucose production and the fractional partitioning of DHA to glucose relative glycolysis with concomitant inhibition of pyruvate plus lactate formation, (Figure 4-35, white bars). The inhibition of glucose production and lowering of cell G6P by low (100μM) metformin were abolished by both FBP1 and PFK1 inhibitors (Figure 4-35 and Figure 4-36; shaded bars). Cumulatively, this points to a significant contribution of allosteric control of PFK1 and FBP1 in the partitioning of DHA metabolism between gluconeogenesis and glycolysis. The attenuation of the metformin effect in the presence of these inhibitors suggests an effect of metformin at PFK1 or FBP1.

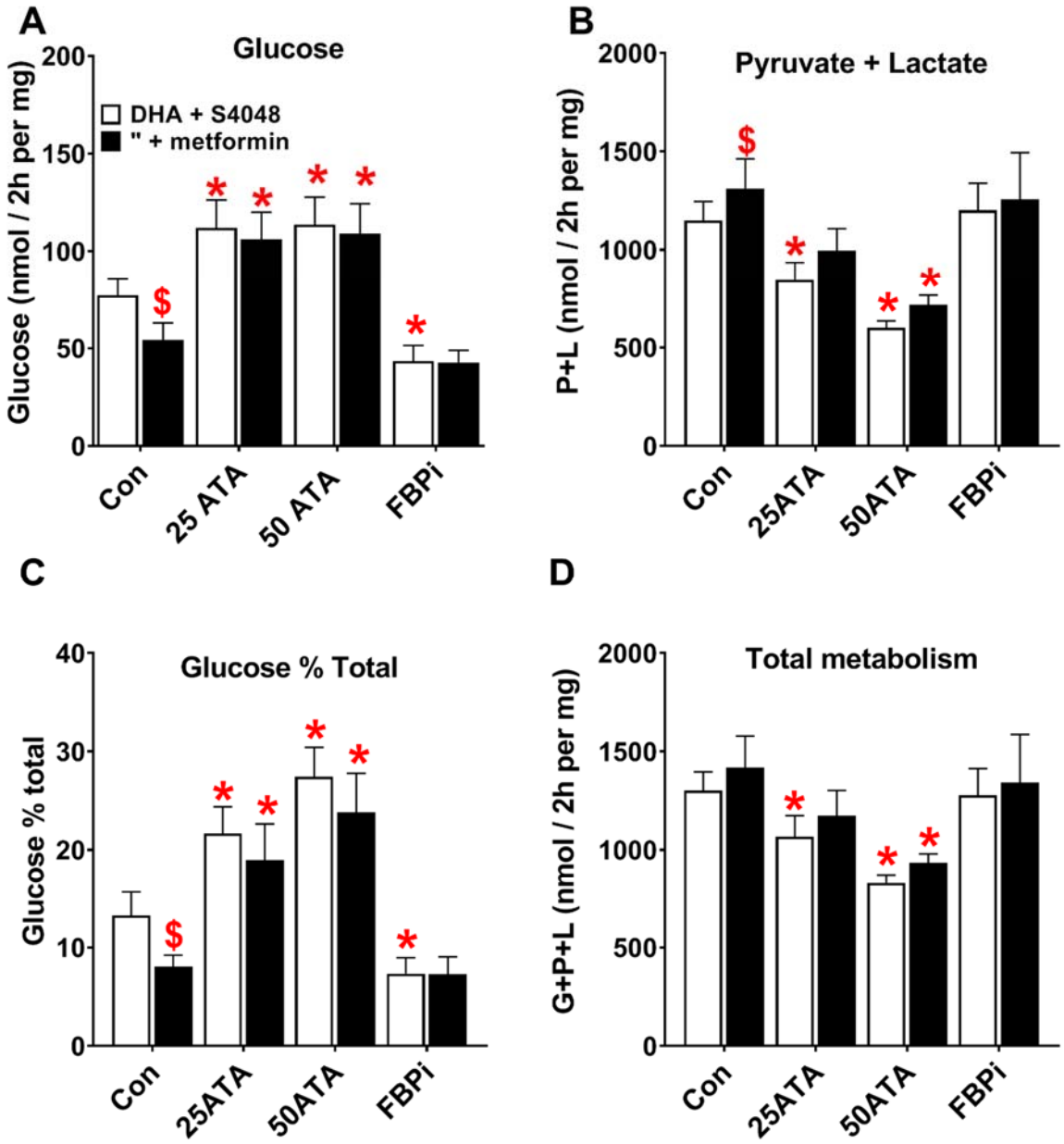

Figure 4-35: Inhibition of PFK-1 or FBP-1 abolishes the effects of metformin on gluconeogenesis from DHA.

Mouse hepatocytes were incubated for 2h in glucose-free media DMEM without (white bars) or with (shaded bars) 100µM metformin and then for further 2h in fresh medium containing 5mM DHA plus 0.2µM S4048 and other additions as indicated ATA at 25 or 50µM and FBPi at 5µM, medium was collected for analysis (A) glucose production, (B) pyruvate plus lactate formation (C) glucose production percentage from total DHA metabolism, (D) total DHA metabolite. Results are Means ±SEM for n=6.

***P <0.05 relative to respective control.**

$ P<0.05 effect of metformin.

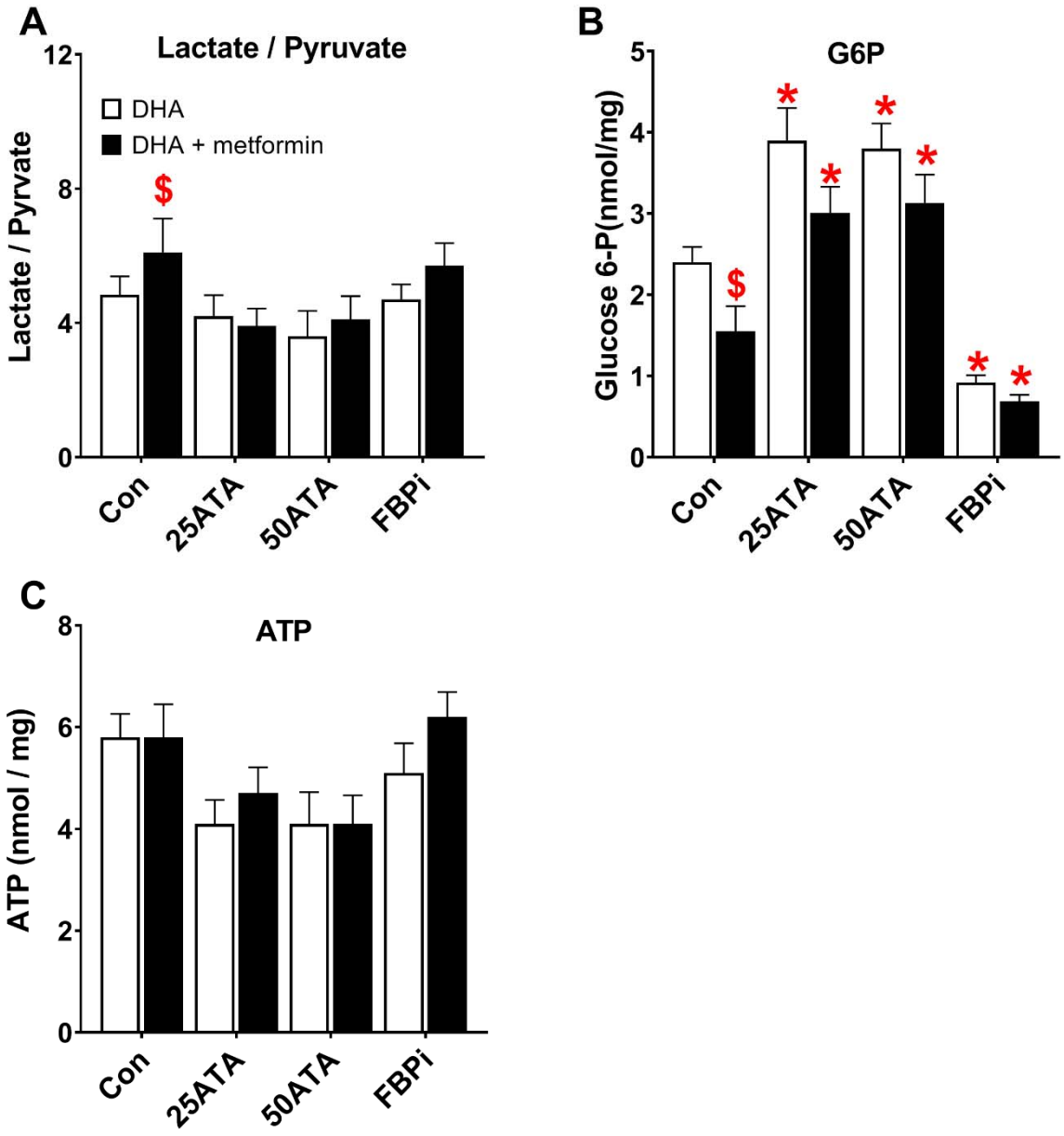

Figure 4-36: Inhibition of PFK opposite from low metformin raises G6P.

Hepatocytes were treated as in figure 4-35, medium was collected and cells were snap-frozen for G6P and ATP analysis (A) lactate to pyruvate ratio; (B) cell G6P; (C) cell ATP. Results are Means ±SEM for n= 6.

***P <0.05 relative to respective control.**

$ P<0.05 effect of metformin.

4.3 Discussion

Two recent reports by Madiraju *et al.* (2014, 2018) on the metformin mechanism concluded that metformin lowered gluconeogenesis by a redox-dependent mechanism. Metformin lowered glucose production from hepatocytes incubated with reduced (lactate and glycerol) but not with oxidised (DHA, pyruvate, and alanine) substrates. It was proposed that the metformin effect on gluconeogenesis in hepatocytes linked to the GPS through inhibition of mGPDH activity (Madiraju et al., 2014). In the second study Madiraju and colleagues (2018) proposed that inhibition of gluconeogenesis *in vivo* by low metformin (20-50 mg/kg) is a redox dependent based on the inhibition of incorporation of [3-^{13}C] lactate but not [3-^{13}C] alanine into glucose in normal and diabetic rats (Madiraju et al., 2018, Madiraju et al., 2014). The role of mGPDH in the metformin mechanism has been challenged because in liver the MAS has more important role than the GPS due to the low activity of GPS (Baur and Birnbaum, 2014).

It is well documented that metformin increases the cytosolic redox state (NADH / NAD^+ ratio; more reduced) *in vitro* (El-Mir et al., 2000, Argaud et al., 1993) and *in vivo* (Madiraju et al., 2018, Madiraju et al., 2014, Qi et al., 2018). NAD^+ is required to maintain glycolysis in cytoplasm of hepatocytes. The MAS and GPS beside the reduction of pyruvate to lactate by lactate dehydrogenase are the major sources in liver to regenerate NAD^+. An early study by Rognstad and Clark (1974) reported that inhibition of gluconeogenesis by low AOA (200µM) was more efficient with reduced (lactate) than oxidised (pyruvate) gluconeogenic substrates (Rognstad and Clark, 1974). The more reduced cytoplasmic redox state caused by low metformin was proposed by Madiraju and colleagues (2014) as the mechanism for the inhibition of gluconeogenesis and supported by studies on hepatocytes showing inhibition of gluconeogenesis from lactate and glycerol but not pyruvate and DHA and by studies *in vivo* showing inhibition of label incorporation from lactate but not alanine (Madiraju et al., 2018). Interestingly a recent study on the perfused liver argues that at low doses of metformin used by Madiraju and colleagues there is no inhibition of gluconeogenesis from lactate in the perfused liver (Calza et al., 2018).

The present study shows that the inhibitory effect of the lowest effect dose of metformin on hepatic glucose production (0.1mM or 1-2nmol/ mg protein) from DHA was associated with a more oxidised mitochondrial redox state (decrease in the 3-hydroxybutyrate / acetoacetate ratio). This effect cannot be explained by inhibition of complex 1 or activation of AMPK (see chapter three), but it might be explained by direct effect on mitochondrial membrane or inhibition of NADH reducing equivalents shuttles (the MAS or GPS). To investigate the role

of the MAS and GPS in the regulation of the cytoplasmic and mitochondrial redox state and gluconeogenesis from oxidised and reduced substrates, two inhibitors of the shuttle were used AOA an inhibitor of the MAS and STK017597 (Gpi) an inhibitor of the GPS. To explore the role of the GPS we also studied the effect of overexpression of mGPDH. The use of AOA especially at a concentration of 200µM to study flux through the MAS is widely documented (Rognstad and Clark, 1974, Berry et al., 1994). Non-specific effects of AOA, such as metabolism to glycolate which is a potential source of H_2O_2 occur at concentrations higher than 500µM. The identification of Gpi as an inhibitor of the mGPDH and accordingly the GPS was reported recently by Orr and colleagues (2014). This inhibitor has not previously been used in hepatocytes.

The main findings of this chapter are;

1- Low metformin (100µM) caused a more reduced cytoplasmic redox state (increase NADH / NAD^+ ratio) similar to inhibition of the GPS by Gpi or the MAS by AOA and it caused a more oxidised mitochondrial redox state (decrease NADH / NAD^+ ratio) similar to the inhibition of the GPS by Gpi or depolarisation of mitochondria by DNP.

2- Low metformin 100µM inhibited the production of glucose in hepatocytes from both oxidised (DHA) and reduced (xylitol and glycerol) substrates by preferential partitioning to glycolysis with concomitant lowering of G3P level. This effect of metformin on gluconeogenesis indicates a redox independent inhibition of gluconeogenesis that cannot be explained by inhibition of the GPS as proposed by (Madiraju et al., 2018, Madiraju et al., 2014) because Gpi did not mimic the inhibitory effect of metformin on gluconeogenesis.

3- DNP caused a more oxidised mitochondrial (decrease NADH / NAD ratio) redox state and mimicked the effect of low metformin on inhibition of gluconeogenesis and on lowering of cell G3P level.

4- Overexpression of mGPDH caused a more reduced mitochondrial redox state (increase in 3-hydroxybutyrate / acetoacetate ratio), but mimicked the effect of metformin on increasing the fractional partitioning of reduced and oxidised substrates to glycolysis relative to gluconeogenesis (increased pyruvate plus lactate formation) with marked lowering of cell G3P.

5- Octanoate, oppositely to metformin, increased the rate of gluconeogenesis form reduced and oxidised substrates and a similar effect was observed by depletion of fructose 2,6-P_2 and by the PFK-1 inhibitor (ATA). The inhibition of PFK-1 antagonized the inhibition of gluconeogenesis by metformin arguing for this highly regulated allosteric enzyme as a likely site for the mechanism of action of metformin.

These effects are discussed below. The more reduced cytoplasmic redox state, as determined by the increase in the lactate to pyruvate ratio in liver and also in plasma by metformin has been widely reported *in vivo* (Madiraju et al., 2014, Madiraju et al., 2018) and *in vitro* (El-Mir et al., 2000, Owen et al., 2000). The more reduced cytoplasmic redox state at high metformin was explained by inhibition of complex 1 as shown in the study by (El-Mir et al., 2000) and at low metformin was proposed to be due inhibition of mGPDH (Madiraju et al., 2014). In the present study we found that low metformin (100µM) caused a more reduced cytoplasmic redox state concomitant with a more oxidised mitochondrial redox state in isolated hepatocytes. This effect of low metformin (100µM) on the cytoplasmic redox state cannot be explained by inhibition of complex 1 and the respiratory chain. The present study demonstrates for the first time that treating isolated hepatocytes with concentrations of metformin that result in cellular accumulation of the drug to the same level (1-2 nmol/mg) as occurs *in vivo* after a 20-50 mg/kg dose make the cytoplasmic redox state more reduced and the mitochondrial redox state more oxidised. This supports the conclusion by Madiraju et al. (2014) that with low therapeutic doses *in vivo* metformin caused a more reduced cytoplasmic redox state but with a more oxidised mitochondrial redox state (Madiraju et al., 2014). Two possible explanations for the more reduced cytoplasmic redox state by 100µM metformin are either inhibition of mGPDH activity (Madiraju et al., 2014), or dissipation of mitochondrial membrane potential with consequent inhibition of the MAS which is strongly dependent on mitochondrial membrane potential (Qiu et al., 2010, Davis et al., 1980). Metformin inhibits the production of glucose from both oxidised and reduced substrates in conditions of a more oxidised mitochondrial redox state and in the absence of activation of AMPK. This supports a complex 1independent and AMPK independent mechanism we therefore compared the metformin effect with inhibition of two shuttles, the GPS and the MAS.

Gpi (an inhibitor of GPS) mimicked the effect of low metformin on the ratio of lactate to pyruvate in hepatocytes, and Gpi like metformin caused a more oxidised mitochondrial redox state, cell G3P level was raised by high (80µM) Gpi . This indicates that inhibition of the GPS

causes a more reduced cytoplasmic redox state and a more oxidised mitochondrial redox state with increase in cell G3P. In this study we found no evidence for inhibition of mGPDH by metformin at concentrations up to 5mM, unlike Gpi (10-80μM), in permeabilized hepatocytes (Figure 4-4 A,B) (Pecinova et al., 2017). In addition studies with the Gpi did not mimic the metformin inhibition of gluconeogenesis. To further explore the functional role of the GPS in the control of gluconeogenesis and glycolysis we overexpressed mGPDH with an adenoviral vector in hepatocytes. This enabled studies into the effect of increased activity of the GPS on the redox state (cytoplasmic and mitochondrial) and gluconeogenesis. Overexpression of mGPDH caused a more reduced mitochondrial redox state (increase in 3-hydroxybutyrate / acetoacetate ratio) concomitant with variable effects on cytoplasmic redox state depending on the substrates, importantly it caused a large decrease in cell G3P with all substrates tested. Collectively, these results indicated that the increased activity of mGPDH was associated with increased activity of the GPS. Overexpression of mGPDH favoured glycolysis by increasing the fractional partitioning of substrates toward glycolysis rather than gluconeogenesis. This effect mimicked the effect of low dose metformin on gluconeogenesis and supports the conclusion that the inhibitory effect of low metformin on glucose production cannot be due to inhibition of the GPS. This effect did not support the conclusion of inhibition of mGPDH by metformin as proposed by Madiraju and colleagues (Madiraju et al., 2014). Furthermore, overexpression of mGPDH abolished the effect of low dose of metformin on gluconeogenesis and the fractional partitioning to glucose. The lowering of G3P by metformin and the uncoupler could be explained by activation of the GPS possibly as a result of a decrease in mitochondrial membrane potential.

The other possible explanation for the more oxidised mitochondrial redox state is that metformin accumulates in the mitochondria or through interaction with the mitochondrial membrane promotes depolarization and secondary to depolarization causes inhibition of the MAS (Davis et al., 1980, Qiu et al., 2010). DNP causes a more oxidised (decrease NADH / NAD ratio) mitochondrial redox state and like metformin also inhibited the rate of gluconeogenesis and the fractional partitioning to glucose. The effects of DNP on gluconeogenesis and glycolysis were in good agreement with previous studies and suggested that inhibition of gluconeogenesis by metformin can be explained by uncoupling of mitochondrial membrane (Sibille et al., 1995, Sibille et al., 1998). AOA inhibited gluconeogenesis and the fractional partitioning of xylitol to glucose relative to glycolysis but this effect was concomitant with inhibition of total xylitol metabolism and partial lowering of

ATP. Because the effect of AOA on cell G3P is opposite to the metformin effect which lowered cellular G3P, other explanation are required for this effect of metformin. One possibility is that the mitochondrial depolarization by metformin may account for the decrease in G3P, because this effect was also seen with DNP.

Previous studies reported that metformin treatment suppressed the gluconeogenic gene expression in liver and hepatocytes (Heishi et al., 2006, Cao et al., 2014). The study by Heishi and colleagues (2006) reported that the anti-hyperglycaemic effect of metformin is positively correlated to suppression of hepatic *G6pc* mRNA. In this study, the authors did not give a clear explanation for the mechanism of suppressing *G6pc* mRNA by metformin (Heishi et al., 2006). The conclusion by Cao et al (2014) was that low metformin suppresses gene expression (*G6pc*) by a mechanism linked to AMPK activation (Cao et al., 2014). In the present study we showed that gluconeogenic genes expression were induced by high 25mM glucose and xylitol whereas low metformin (100μM) and mGPDH overexpression suppressed the gluconeogenic gene expression, while AOA did not suppress gluconeogenic gene expression. Suppression of *G6pc* mRNA by metformin cannot be explained by a mechanism linked to an AMPK activation as proposed by (Cao et al., 2014) because A-769662 an AMPK activator did not inhibit glucose production (Figure 3-4) and lower cell G6P (Figure 3-6 A and B) and cell G3P (Figure 4-18 F; white bar) but it might be through indirect effect of metformin due to inhibition of gluconeogenesis. Collectively, these results supported that the explanation of metformin mechanism is due to mitochondrial depolarisation through accumulation of metformin in mitochondrial matrix rather than direct effect on malate-aspartate shuttle (Davis et al., 1980, Qi et al., 2018, Schafer, 1976)

Octanoate was used as a precursor of ketone bodies (acetoacetate and 3-hydroxybutyrate), (Pegorier et al., 1989, Schonfeld and Wojtczak, 2016, Sanaka et al., 2008) to enable measurement of the mitochondrial redox from the HOB/Acac ratio accumulated in the medium. An advantage of octanoate compared with long-chain fatty acids is that it enters the mitochondria as octanoate rather than octanoyl-CoA by a mechanism independent on carnitine palmitoyltransferase I, and therefore independent of AMPK, which indirectly regulates CPT1 by changes in malonyl-CoA. Stimulation of gluconeogenesis by octanoate is widely documented (González-Manchón et al., 1989), proposed mechanisms include an increase in citrate which inhibits PFK1 and also a direct inhibition of PFK1 by octanoate-CoA (Jenkins et al., 2011). A raised cell G6P level in rat islets is also consistent with inhibition of PFK1 (Montague and Taylor, 1969). As expected, octanoate increased glucose production in

hepatocytes (González-Manchón et al., 1989), this can be explained by inhibition of phosphofructokinase-1 (PFK-1) and / or activation of fructose 1,6-bisphosphatase-1 (FBP-1). PFK-1 is positively regulated by AMP, fructose 2,6-P_2, fructose 1,6-P_2, and P_i and it is negatively by ATP, citrate, and G3P. FBP1 is a rate-limiting enzyme in gluconeogenesis, conversely to PFK-1 it is negatively regulated by AMP, fructose 2,6-P_2, and P_i (Hers and Hue, 1983). In this study we found that octanoate increased ACC phosphorylation which indicates an increase in AMP concentration. The most plausible explanation for the octanoate effect is through inhibition of PFK-1 by increasing the concentration of citrate (Hers and Hue, 1983, Montague and Taylor, 1969, Jenkins et al., 2011). We showed in this study that the increase in gluconeogenesis by 0.125mM octanoate was antagonized by 100μM metformin. This could be explained by increased glycolysis by metformin through changes in allosteric effectors of PFK-1, for example by a decrease in citrate, which was reported to be decreased by metformin (Pelantova et al., 2016) or by the decrease in cell G3P, because both citrate and G3P are considered as potent inhibitors for PFK-1 (Hers and Hue, 1983). In this study cell G3P was decreased by low metformin in conditions of raised glycolysis and decreased gluconeogenesis and likewise G3P was decreased in cells overexpressing mGPDH which showed similar partitioning of DHA towards glycolysis as metformin.

Recent studies have proposed that the mechanism of metformin in lowering glucose production might be linked to increase AMP by AMPK independent mechanisms. Miller and colleagues (2013) proposed a link between raised AMP and inhibition of glucagon signalling through AMP inhibition of adenylyl cyclase (Miller et al., 2013) and Hunter et al (2018) proposed AMP inhibition of FBP1, this was demonstrated in mouse model expressing an AMP-insensitive variant of FBP1 (Hunter et al., 2018). In this study we tested the role of the PFK1/FBP1 site in regulating the direction of DHA flux between gluconeogenesis and glycolysis by using an adenovirus vector to express a bisphosphatase-active kinase-deficient variant of phosphofructokinase 2/fructosebisphosphatase 2 (PFK2/FBP2) (Arden et al., 2012). The increased in gluconeogenesis and decreased in glycolysis in hepatocytes treated with PFK2/FBP2-KD support a major role for the PFK1/FBP1 site in regulation of glycolysis and gluconeogenesis. This was further supported by db-cAMP which is also known to cause acute depletion of fructose 2,6-bisphosphate by phosphorylation of PFK2/FBP2 (Van Schaftingen and Hers, 1981). These results implicate that the molecular target of metformin to lower glucose production might be due to activation of PFK-1 and / or inhibition of FBP-1and this effect could be due to an increase in AMP as proposed by Hunter and colleagues (Hunter et al.,

2018) or lowering the cell G3P as shown in this study or changes in other allosteric effectors such as ATP, ADP, citrate and Pi.

4.4 Summary

This study has shown that:

1. In isolated hepatocytes a low dose of metformin that is within the therapeutic range causes a more oxidised mitochondrial (NADH/NAD) redox state and a more reduced cytoplasmic redox state as has been reported in recent studies *in vivo* with a low dose of metformin. This low metformin dose inhibits gluconeogenesis by a redox-independent mechanism that cannot be explained by inhibition of either the MAS or the GPS but is best explained by allosteric activation of PFK1 resulting in increased partitioning of substrate to glycolysis as opposed to gluconeogenesis. This same mechanism also accounts for the lowering of G6P by metformin with either high glucose or gluconeogenic precursors. This does not exclude an additional role for FBP1 through inhibition by AMP as proposed by Hunter and colleagues (Hunter et al., 2018).

2. Overexpression of mGPDH had three effects a more reduced mitochondrial redox state and markedly lowered cell G3P and also G6P, and preferential partitioning of DHA to glycolysis as opposed to gluconeogenesis. The lowering of G3P is expected to be a contributing factor to the increased glycolysis because G3P is an allosteric inhibitor of PFK1. The recently identified inhibitor of mGPDH (SKT017597) had converse effects from mGPDH overexpression. Inhibition of the MAS had no effect on the mitochondrial redox state despite causing a more reduced cytoplasmic redox state and it did not mimic the metformin effect on partitioning of DHA metabolism between glycolysis and gluconeogenesis.

3. The more oxidised mitochondrial redox state caused by metformin cannot be explained by inhibition of the GPS because it is associated with lowering of G3P. It is best explained by a primary effect of metformin on mitochondrial membrane potential. Depolarisation of mitochondria by metformin as proposed in other studies could explain the more oxidised mitochondrial redox state, the increase in octanoate oxidation and the more reduced cytoplasmic redox state, through inhibition of the MAS which is dependent on mitochondrial membrane potential.

4. The lowering of G3P by metformin and by the uncoupler is tentatively explained by increased flux through the GPS as a result of mitochondrial depolarization. The effects of metformin and of mGPDH overexpression on both cell G3P and partitioning of DHA between glycolysis and gluconeogenesis are not additive. This supports the conclusions that the lowering of G3P by metformin is best explained by increased flux through the GPS as a result of mitochondrial depolarization and that the decrease in G3P by metformin contributes to the allosteric regulation of PFK1.

5. Metformin and likewise overexpression of mGPDH counteract the induction of G6pc and Txnip genes by high glucose. This effect is best explained by the lowering of G3P and G6P and supports the conclusion that the effects of metformin on gene expression as on gluconeogenesis are in part consequent to the decrease in G6P by activation of PFK-1 and a decrease in G3P through increased flux through mGPDH.

CHAPTER 5

GENERAL DISCUSSION

Chpater. 5 **General discussion**

5.1 General discussion

Metformin is the most commonly prescribed drug to treat type 2 diabetes (Bailey, 2017, Maruthur et al., 2016). The clinical benefits of metformin are: to decrease glucose production from the liver, increase glucose uptake by muscle, and lower the absorption of glucose from the gut. Although the liver is considered to be a major target of metformin, the molecular mechanism of metformin to lower hepatic glucose production remains debated (Foretz et al., 2014, Rena et al., 2013, Rena et al., 2017, He and Wondisford, 2015). The first mechanism that was identified for the acute inhibition of hepatic glucose production was the inhibition of complex 1 of the respiratory chain (NADH:ubiquinone oxidoreductase) with a consequent decrease in the cell ATP/ADP ratio in conjunction with a more reduced mitochondrial and cytoplasmic NADH/NAD redox state as determined from the raised ratios of 3-hydroxybutyrate / acetoacetate and lactate / pyruvate, respectively (Bridges et al., 2014, El-Mir et al., 2000, Owen et al., 2000). This inhibition in gluconeogenesis was explained by inhibition of complex 1 resulting in lowering the ATP / ADP ratio (El-Mir et al., 2000, Owen et al., 2000) and activation of AMP-activated protein kinase (AMPK) (Zhou et al., 2001). A functional role for activation of AMPK by metformin in the lowering of glucose production has been challenged by Foretz and colleagues (2010) when they showed that metformin lowered plasma glucose and inhibited gluconeogenesis in a mouse model lacking liver AMPK (Foretz et al., 2010). Metformin concentrations ~10-100 fold of the therapeutic dose were used in these studies and the effects could be explained by lowering of cell ATP (Gouaref et al., 2017).

Recently, two new metformin mechanisms were proposed by two independent laboratories. Madiraju and colleagues (2014 and 2018) reported that metformin concentrations relevant to therapeutic dose inhibited hepatic glucose production through non-competitive inhibition of mitochondrial glycerophosphate dehydrogenase (mGPDH) in a redox-dependent manner (Madiraju et al., 2014, Madiraju et al., 2018). This mechanism has been challenged because (i) the contribution of the glycerophosphate shuttle to control the cytoplasmic redox state is considered to be low relative to the malate-aspartate shuttle in liver compared with other tissues (Baur and Birnbaum, 2014, Mracek et al., 2013) and (ii) metformin had no effect on gluconeogenesis in the liver perfused with lactate at low therapeutic doses (Calza et al., 2018). The second mechanism by Hunter and colleagues (2018) reported that metformin lowered gluconeogenesis by inhibition of the rate-limiting gluconeogenic enzyme fructose 1,6-bisphosphatase-1 (FBP-1) as a result of increasing liver AMP concentration (Hunter et al.,

2018). Evidence for this was provided from studies *in vivo* using a knock-in mouse model for a variant of FBP-1 that is insensitive to AMP. This thesis aimed to identify the mechanisms involved in the inhibition of gluconeogenesis at the lowest effective concentrations of metformin that result in cellular accumulation in hepatocytes to levels of 1-2nmol/ mg hepatocytes protein (Al-Oanzi et al., 2017), this corresponds to hepatic accumulation in mice treated with a dose of 50 mg/kg, which is considered the equivalent of the therapeutic range.

5.1.1 Inhibition of gluconeogenesis by low metformin cannot be explained by inhibition of complex 1

The first molecular mechanism proposed for the acute inhibition of gluconeogenesis by metformin was by inhibition of complex 1 (El-Mir et al., 2000, Owen et al., 2000), the first complex in the respiratory chain (NADH:ubiquinone oxidoreductase). This was based on evidence for a more reduced mitochondrial NADH / NAD ratio redox state from the increase in 3-hydroxybutyrate to acetoacetate ratio *in vivo* and *in vitro* and studies on intact mitochondria (Bridges et al., 2014, El-Mir et al., 2000, Owen et al., 2000) and also from studies on purified complex 1, demonstrating a direct inhibitory effect of metformin at the ubiquinone site (Bridges et al., 2014). The more reduced mitochondrial redox state caused by metformin was associated with increase in the lactate to pyruvate ratio indicating a more reduced cytoplasmic redox state (increase NADH / NAD ratio) (El-Mir et al., 2000). The above studies that showed a more reduced mitochondrial redox state had used higher metformin concentrations (> 100 mg/kg) than are considered equivalent to the therapeutic dose (50 mg per kg) (Al-Oanzi et al., 2017, Wilcock and Bailey, 1994). Madiraju and colleagues were the first to report that metformin concentrations relevant to the therapeutic dose are associated with a more reduced cytoplasmic redox state as reported previously but also with a more oxidised mitochondrial redox state (Madiraju et al., 2014). On this basis they proposed that metformin inhibits the transfer of reducing equivalents from the cytoplasm to mitochondria.

In agreement with the previous studies, the current study showed that with high metformin concentration 500µM (> 5 nmol/ mg protein) like rotenone, an inhibitor of complex 1, cause a more reduced mitochondrial (increase NADH / NAD^+ ratio) redox state in hepatocytes (El-Mir et al., 2000, Gouaref et al., 2017, Owen et al., 2000). This can be explained by inhibition of complex 1 by metformin at cell loads (> 5 nmol/ mg protein). The rate of total 3-hydroxybutyrate plus acetoacetate production was decreased with 500µM metformin and by

rotenone. This is explained by inhibition of β-oxidation by the increase in mitochondrial NADH/NAD ratio as supported by the stimulation with the uncoupler which causes a more oxidised mitochondrial NADH/NAD.

This thesis is the first to show that metformin tested over a range of concentrations in isolated hepatocytes has a biphasic effect on the mitochondrial redox state, causing a more oxidised redox state at an extracellular concentration of 100μM for 4h which results in cellular accumulation to relevant therapeutic concentrations (1-2nmol/ mg protein) (Al-Oanzi et al., 2017, Wilcock and Bailey, 1994) but a more reduced NADH/NAD state at concentrations ≥ 500uM which result in cellular loads ≥ 5nmol/mg. This suggests that the association of low metformin with a more oxidised redox state reported in recent studies *in vivo* in liver and kidney with 50mg/kg metformin (Madiraju et al., 2014, Madiraju et al., 2018, Qi et al., 2018) can be explained by a direct effect of metformin on the hepatocyte. A recent study in intact mitochondria showed that metformin unlike other diguanides caused NADH oxidation and proposed that metformin uncouples redox and proton transfer domains by complex 1 (Cameron et al., 2018). Other studies have reported that metformin causes mitochondrial depolarization (Dykens et al., 2008). Various mechanisms can therefore be proposed for the effect of low metformin on the decrease in NADH/NAD ratio.

The more oxidised mitochondrial (decrease in NADH / NAD^+ ratio) redox state by metformin (100μM) was associated with an increase in ketone body (3-hydroxybutyrate plus acetoacetate) production. These results implicate that inhibition of complex 1 cannot be the plausible explanation of inhibition for gluconeogenesis by low metformin (100μM) as proposed by Owen and colleagues (Owen et al., 2000) because inhibition of complex 1 associated with a more reduced mitochondrial (NADH / NAD) redox state. Bridges and colleagues (2014) reported that metformin interacts with at least two sites on complex 1, the flavin site and the ubiquinone site. The NADH oxidation, the first reaction of complex 1, was increased by metformin in the presence of an artificial electron acceptor FeCN, while metformin inhibits the ubiquinone reduction in a mechanism similar (but reversible) to the canonical complex 1 inhibitors (rotenone) (Bridges et al., 2014), similar results were also reported by Cameron and colleagues (Cameron et al., 2018). The explanation of accelerating of NADH oxidation by low metformin binding at the flavin site to cause a more oxidised (decrease NADH to NAD ratio) mitochondrial redox state is unlikely because the rate of NADH oxidation is far higher at the flavin site than for ubiquinone reduction (Hirst, 2013). Moreover, the more oxidised mitochondrial redox state by low metformin 100μM concentration was associated with a more

reduced cytosolic (increase NADH / NAD^+ ratio) redox state based on increased in the lactate to pyruvate ratio. The increase in the lactate to pyruvate ratio is probably the most widely documented effect of metformin *in vivo* (Madiraju et al., 2014, Madiraju et al., 2018, Qi et al., 2018, Owen et al., 2000) and *in vitro* (Argaud et al., 1993, El-Mir et al., 2000, Gouaref et al., 2017, Owen et al., 2000). The effect of high metformin causing a more reduced cytoplasmic (increase NADH / NAD ratio) redox state was attributed to inhibition of complex 1 and thereby the respiratory chain as proposed by El-Mir et al. (El-Mir et al., 2000). However, the more reduced cytoplasmic (increase NADH / NAD^+ ratio) redox state by low 100µM metformin cannot be explained by inhibition of complex 1 (because of the more oxidised mitochondrial redox state causes by low 100µM metformin). Some possible explanations for the more oxidised mitochondrial NADH / NAD^+ redox state and the more reduced cytoplasmic NADH / NAD redox state by 100µM metformin: are (i) A direct effect of metformin on the mitochondrial membrane or metformin accumulation in mitochondria causing mitochondrial depolarisation (ii) Inhibition of the malate-aspartate shuttle by attenuation of the electrogenic transport of the malate-aspartate shuttle (MAS) (Schafer, 1976, Owen et al., 2000, Davis et al., 1980, LaNoue et al., 1974) (Berry et al., 1992, Sibille et al., 1995). (iii) Inhibition of the glycerophosphate shuttle as proposed by Madiraju and colleagues (Madiraju et al., 2014, Madiraju et al., 2018).

5.1.2 The AMPK activator A-769662 does not mimic the effect of metformin on gluconeogenesis

As discussed in the introduction several studies provided evidence for AMPK activation causing suppression of gluconeogenic gene expression (G6Pc and PEPCK). In some of these studies inhibition of gluconeogenesis by short-term (2-4 hours) metformin treatment was also suggested to occur through an AMPK dependent mechanism (Cao et al., 2014, Kim et al., 2008, Lee et al., 2010). The mechanism by which metformin inhibited glucose production through activation the cellular energy sensor AMP-activated protein kinase (AMPK) as proposed previously by Zhou and colleagues (Zhou et al., 2001) has been challenged by Foretz and colleagues using hepatocytes from mice lacking AMPK or its upstream LKB-1and the inhibitory effect of metformin was explained by the decrease in hepatic energy state (ATP to AMP and ATP to ADP ratios) independent on AMPK. In the study by Foretz and colleagues they reported that metformin inhibited glucose production and also suppressed the G6Pc mRNA in wild-type and AMPK deficient mice (Foretz et al., 2010).

In the present study significant activation of AMPK, based on increased phosphorylation of ACC-P, the AMPK substrate, was only observed at high concentrations of metformin (≥ 500 µM) that caused inhibition of Complex 1 as shown by the increase in the ratio of 3-hydroxybutyrate to acetoacetate and not at low concentrations of metformin (100µM) that had the opposite effect on the mitochondrial redox state. In incubations with octanoate which itself causes activation of AMPK, a decrease in ACC-P was observed with the low concentration of metformin. The present findings concur with the proposal of Madiraju *et al*, that at the lowest doses of metformin that have been used *in vivo* (20-50 mg/ kg body wt) activation of AMPK is not observed. Although the failure of the present studies to identify activation of AMPK by 100 µM with the present substrate conditions cannot firmly exclude the possibility that low concentrations of metformin may activate AMPK in other substrate conditions, the experiments with A-769662 which activates AMPK but does not inhibit gluconeogenesis or lower G6P, is supporting evidence against a role for AMPK in causing inhibition of gluconeogenesis. Furthermore, it can be proposed that also at high metformin (500 µM) which causes activation of AMPK, the inhibition of gluconeogenesis cannot be explained by activation of AMPK, because of the failure of a direct AMPK activator to inhibit gluconeogenesis.

Although studies with AMPK deficient hepatocytes are generally required to demonstrate unequivocally that a mechanism is AMPK independent (Foretz et al., 2010), the present finding that low concentrations of metformin (100 µM) that inhibit gluconeogenesis and lower G6P also cause lowering of G6Pc suggests that the same metformin mechanism that lowers G6P and is not mimicked by an AMPK activator may also be involved in the repression of G6pc, because this gene is known to be strongly induced by intermediates of glucose metabolism through the transcription factor ChREBP (Arden et al., 2011) (Arden et al., 2012).

5.1.3 Inhibition of mGPDH does not mimic the effect of low metformin

Madiraju and colleagues proposed that the more oxidised mitochondrial NADH/NAD redox state and more reduced cytoplasmic NADH/NAD redox state caused by low metformin (100µM) can be explained by inhibition of mGPDH and thereby the GPS which transfers NADH from the cytoplasm to mitochondria (Madiraju et al., 2014, Madiraju et al., 2018).

In this study we showed that inhibition of mGPDH by Gpi mimics the effect of low metformin (100µM) on the mitochondrial redox state and cytoplasmic redox state. This concurs with the suggestion by Madiraju and colleagues (2014) that inhibition of the GPS could explain the

effects of metformin on the redox state in both mitochondria and cytoplasm. However, in this study the Gpi unlike metformin did not inhibit glucose production from the gluconeogenic substrates and it caused an increase in G3P which contrasts with the decrease caused by low metformin in the presence of gluconeogenic substrates. Moreover, overexpression of mGPDH had opposite effect on the mitochondrial redox state (a more reduced; increase NADH to NAD ratio), and it markedly lowered cell G3P and also G6P. In addition overexpression of mGPDH also favoured glycolysis rather than gluconeogenesis from oxidised and reduced substrates with variable effect on the lactate to pyruvate ratio depending on the substrates. These results indicated that inhibition of gluconeogenesis by metformin is mimicked by overexpression rather than inhibition of mGPDH.

5.1.4 Mitochondrial depolarization may explain the effect of metformin on gluconeogenesis

The other shuttle responsible for transfer of NADH is the MAS. Like 100µM metformin, inhibition of the MAS by aminooxyacetate (200µM AOA) increased the lactate to pyruvate ratio, as expected (Berry et al., 1994). This increase in the lactate to pyruvate ratio was associated with an increase in cell G3P without affecting the mitochondrial redox state. Inhibition of the MAS by AOA was associated with inhibition of total metabolism of reduced substrates (xylitol and glycerol). Although metformin caused a small increase in the lactate to pyruvate ratio it did not cause inhibition of total xylitol metabolism and it lowered rather than raised G3P. Flux through the MAS involves an electrogenic transporter for aspartate and is highly dependent on mitochondrial membrane potential (Wang et al., 2015). A possible explanation for the small increase in the lactate to pyruvate ratio caused by metformin is that it results from mitochondrial depolarisation as reported by others (Dykens et al., 2008) resulting in modest inhibition of the MAS through attenuation of the electrogenic aspartate transport (Berry et al., 1992, Davis et al., 1980, LaNoue et al., 1974, Sibille et al., 1995). As discussed above the most plausible explanation for a more oxidised mitochondrial redox state would be either depolarizing the mitochondrial membrane due to metformin accumulation in mitochondria, or to uncoupling of proton transport as suggested by Cameron and colleagues (Cameron et al., 2018). Uncoupling the mitochondrial membrane by DNP (20µM) like metformin (100µM) caused a more oxidised mitochondrial redox state and lowered the rate of glucose production and also cell G6P and G3P. These findings support the role of depolarisation of mitochondrial membrane by metformin as a possible explanation for the inhibition of the MAS, which is dependent on electrogenic transport (Sibille et al., 1995, Sibille

et al., 1998). The lowering of G3P suggests that mitochondrial depolarization may favour increased flux through the GPS and inhibition of gluconeogenesis by preferential partitioning towards glycolysis which is favoured by increased flux through GPS possibly through the decrease in G3P which is a potent inhibitor of PFK-1 (Hers and Hue, 1983).

5.1.5 The metformin effect on glycolysis and gluconeogenesis is at least in part by selective targeting of PFK-1 by lowering of G3P

Fructose 2,6-bisphosphate was discovered through a search for the mechanism by which glucagon regulates glycolysis and gluconeogenesis in liver. It is one of several allosteric regulators of PFK-1 and FBP-1 and has a major role in metabolic conditions linked to changes in cAMP because phosphorylation of PFK-2/FBP-2 by c-AMP dependent protein kinase inhibits the kinase but not the bisphosphatase activity of PFK-2/FBP-2 causing acute depletion of fructose 2,6-bisphosphate (Van Schaftingen and Hers, 1981, Yamada et al., 2008). However it does not have a role in the stimulation of glycolysis by anoxia, indicating that the other allosteric effectors of PFK-1 and FBP-2 can also have a major physiological role (Hue, 1982). The inhibition of gluconeogenesis by AICAR has been shown to be due to inhibition of FBP1 by an AMP-mimetic mechanism (Vincent et al., 1991). Recent work by Hunter et al (2018) also provided evidence for a role of inhibition of FBP1 by metformin through an AMP-mimetic mechanism. This was supported by evidence that the metformin effect on blood glucose is attenuated in a knock-in mouse model expressing a variant form of FBP1 that is insensitive to AMP (Hunter et al., 2018). We show in this study that selective targeting of the PFK-1/FBP-1 site by depletion of fructose 2,6-bisphosphate had large effects on metabolism of DHA by glycolysis and gluconeogenesis. This is consistent with earlier studies that showed that regulation of both glycolysis and gluconeogenesis resides predominantly at the PFK-1/FBP-1 site. We also found large effects on glycolysis and gluconeogenesis with a selective inhibitor of PFK-1 that mimics citrate inhibition. This inhibitor blocked the metformin effect on glucose production and on cell G6P. Targeting the PFK-1/FBP-1 site seems the most likely site of action of low metformin on the partitioning of flux between glycolysis and gluconeogenesis. G3P was identified as an inhibitor of PFK-1 by Claus and colleagues (Claus et al., 1984). In this study we identify, G3P as one candidate allosteric effector of PFK-1 that can be involved in the increased partitioning of DHA towards glycolysis as opposed to gluconeogenesis. The present study demonstrates probably for the first time the major role of mGPDH in regulating the hepatocyte content of G3P. We propose that the stimulation of glycolysis and inhibition of

gluconeogenesis by overexpression of mGPDH is consistent with the hypothesis that G3P has a potential major role in regulating PFK1.

5.2 Summary

To summarise, this thesis reports for the first time that metformin has a direct biphasic effect on the mitochondrial redox state. A low cell dose of metformin (therapeutic equivalent: < 2nmol / mg) caused a more oxidised mitochondrial NADH / NAD state and an increase in the lactate / pyruvate ratio in isolated hepatocytes, whereas a higher metformin dose (≥5nmol / mg) caused a more reduced mitochondrial NADH / NAD state similar to Complex 1 inhibition by rotenone. The low metformin dose inhibited gluconeogenesis from both oxidised (dihydroxyacetone) and reduced (xylitol) substrates by preferential partitioning of substrate towards glycolysis by a redox-independent mechanism that is best explained by allosteric regulation at phospho-fructokinase-1 (PFK1) and/or fructose bisphosphatase-1 (FBP-1) in association with a decrease in cell glycerol 3-P, an inhibitor of PFK1 and other potential allosteric effectors for example raised AMP rather than by inhibition of transfer of reducing equivalents. At a low pharmacological load, the metformin effects on the lactate / pyruvate ratio and glucose production are explained by attenuation of transmitochondrial electrogenic transport mechanisms with consequent compromised the malate-aspartate shuttle and changes in allosteric effectors of PFK1 and FBP1.

This study also demonstrates that low concentrations of metformin and also overexpression of mGPDH attenuates expression of G6Pc. The effects of metformin on gene expression and lowering of cell G3P in conditions of raised the lactate to pyruvate ratio may result from increased flux through the GPS in conditions of impaired the MAS flux because of mitochondrial depolarisation. This thesis demonstrates also for the first time that increased flux through the GPS mimics the effects of low metformin on both metabolic flux and on control of G6pc gene expression, which is one of the gluconeogenic genes that is regulated by metformin through an AMPK independent mechanism (Foretz et al., 2010).

PUBLICATIONS

Publications from the thesis

ALSHAWI A, AND AGIUS L. (2019). Low metformin causes a more oxidized mitochondrial NADH/NAD redox state in hepatocytes and inhibits gluconeogenesis by a redox-independent mechanism. *J. Biol. Chem.* 294(8): 2839-2853.

AL-OANZI ZH, FOUNTANA S, MOONIRA T, TUDHOPE SJ, PETRIE JL, ALSHAWI A, PATMAN G, ARDEN C, REEVES HL, AGIUS L. (2017). Opposite effects of a glucokinase activator and metformin on glucose-regulated gene expression in hepatocytes. *Diabetes Obes Metab.* 19(8): 1078-1087.

REFERENCES

References

2013. Standards of medical care in diabetes--2013. *Diabetes Care,* 36 Suppl 1, S11-66.

ABDUL-GHANI, M., DEFRONZO, R. A., DEL PRATO, S., CHILTON, R., SINGH, R. & RYDER, R. E. J. 2017. Cardiovascular Disease and Type 2 Diabetes: Has the Dawn of a New Era Arrived? *Diabetes Care,* 40, 813-820.

AGIUS, L., CHOWDHURY, M. H., DAVIS, S. N. & ALBERTI, K. G. 1986. Regulation of ketogenesis, gluconeogenesis, and glycogen synthesis by insulin and proinsulin in rat hepatocyte monolayer cultures. *Diabetes,* 35, 1286-93.

AL-OANZI, Z. H., FOUNTANA, S., MOONIRA, T., TUDHOPE, S. J., PETRIE, J. L., ALSHAWI, A., PATMAN, G., ARDEN, C., REEVES, H. L. & AGIUS, L. 2017. Opposite effects of a glucokinase activator and metformin on glucose-regulated gene expression in hepatocytes. *Diabetes Obes Metab,* 19, 1078-1087.

ARDEN, C., PETRIE, J. L., TUDHOPE, S. J., AL-OANZI, Z., CLAYDON, A. J., BEYNON, R. J., TOWLE, H. C. & AGIUS, L. 2011. Elevated glucose represses liver glucokinase and induces its regulatory protein to safeguard hepatic phosphate homeostasis. *Diabetes,* 60, 3110-20.

ARDEN, C., TUDHOPE, S. J., PETRIE, J. L., AL-OANZI, Z. H., CULLEN, K. S., LANGE, A. J., TOWLE, H. C. & AGIUS, L. 2012. Fructose 2,6-bisphosphate is essential for glucose-regulated gene transcription of glucose-6-phosphatase and other ChREBP target genes in hepatocytes. *Biochem J,* 443, 111-23.

ARGAUD, D., ROTH, H., WIERNSPERGER, N. & LEVERVE, X. M. 1993. Metformin decreases gluconeogenesis by enhancing the pyruvate kinase flux in isolated rat hepatocytes. *Eur J Biochem,* 213, 1341-8.

ARINZE, I. J., GARBER, A. J. & HANSON, R. W. 1973. The regulation of gluconeogenesis in mammalian liver. The role of mitochondrial phosphoenolpyruvate carboxykinase. *J Biol Chem,* 248, 2266-74.

BAILEY, C. J. 1992. Biguanides and NIDDM. *Diabetes Care,* 15, 755-72.

BAILEY, C. J. 2017. Metformin: historical overview. *Diabetologia,* 60, 1566-1576.

BARRENA, H. C., GAZOLA, V. A. F. G., FURLAN, M. M. D. P., GARCIA, R. F., DE SOUZA, H. M. & BAZOTTE, R. B. 2009. Ketogenesis evaluation in perfused liver of diabetic rats submitted to short-term insulin-induced hypoglycemia. *Cell Biochemistry and Function: Cellular biochemistry and its modulation by active agents or disease,* 27, 383-387.

BARZILAI, N., GROOP, P. H., GROOP, L. & DEFRONZO, R. A. 1995. A novel mechanism of glipizide sulfonylurea action: decreased metabolic clearance rate of insulin. *Acta diabetologica,* 32, 273-278.

BAUR, J. A. & BIRNBAUM, M. J. 2014. Control of gluconeogenesis by metformin: does redox trump energy charge? *Cell Metab,* 20, 197-199

BEGUM, L., JALIL, M. A., KOBAYASHI, K., IIJIMA, M., LI, M. X., YASUDA, T., HORIUCHI, M., DEL ARCO, A., SATRUSTEGUI, J. & SAHEKI, T. 2002. Expression of three mitochondrial solute carriers, citrin, aralar1 and ornithine transporter, in relation to urea cycle in mice. *Biochim Biophys Acta,* 1574, 283-92.

BERRY, M. N., GREGORY, R. B., GRIVELL, A. R., PHILLIPS, J. W. & SCHON, A. 1994. The capacity of reducing-equivalent shuttles limits glycolysis during ethanol oxidation. *Eur J Biochem,* 225, 557-64.

BERRY, M. N., PHILLIPS, J. W., GREGORY, R. B., GRIVELL, A. R. & WALLACE, P. G. 1992. Operation and energy dependence of the reducing-equivalent shuttles during lactate metabolism by isolated hepatocytes. *Biochim Biophys Acta,* 1136, 223-30.

BOLEN, S., FELDMAN, L., VASSY, J., WILSON, L., YEH, H.-C., MARINOPOULOS, S., WILEY, C., SELVIN, E., WILSON, R. & BASS, E. B. 2007. Systematic review: comparative effectiveness and safety of oral medications for type 2 diabetes mellitus. *Annals of internal medicine,* 147, 386-399.

BREMER, J. & DAVIS, E. J. 1975. Studies on the active transfer of reducing equivalents into mitochondria via the malate-aspartate shuttle. *Biochim Biophys Acta,* 376, 387-97.

BRIDGES, H. R., JONES, A. J., POLLAK, M. N. & HIRST, J. 2014. Effects of metformin and other biguanides on oxidative phosphorylation in mitochondria. *Biochem J,* 462, 475-87.

BROWN, L. J., KOZA, R. A., EVERETT, C., REITMAN, M. L., MARSHALL, L., FAHIEN, L. A., KOZAK, L. P. & MACDONALD, M. J. 2002. Normal thyroid thermogenesis but reduced viability and adiposity in mice lacking the mitochondrial glycerol phosphate dehydrogenase. *J Biol Chem,* 277, 32892-8.

BRUNMAIR, B., LEST, A., STANIEK, K., GRAS, F., SCHARF, N., RODEN, M., NOHL, H., WALDHAUSL, W. & FURNSINN, C. 2004. Fenofibrate impairs rat mitochondrial function by inhibition of respiratory complex I. *J Pharmacol Exp Ther,* 311, 109-14.

CALZA, G., NYBERG, E., MAKINEN, M., SOLIYMANI, R., CASCONE, A., LINDHOLM, D., BARBORINI, E., BAUMANN, M., LALOWSKI, M. & ERIKSSON, O. 2018. Lactate-Induced Glucose Output Is Unchanged by Metformin at a Therapeutic Concentration - A Mass Spectrometry Imaging Study of the Perfused Rat Liver. *Front Pharmacol,* 9, 141.

CAMERON, A. R., LOGIE, L., PATEL, K., ERHARDT, S., BACON, S., MIDDLETON, P., HARTHILL, J., FORTEATH, C., COATS, J. T., KERR, C., CURRY, H., STEWART, D., SAKAMOTO, K., REPISCAK, P., PATERSON, M. J., HASSINEN, I., MCDOUGALL, G. & RENA, G. 2018. Metformin selectively targets redox control of complex I energy transduction. *Redox Biol,* 14, 187-197.

CAO, J., MENG, S., CHANG, E., BECKWITH-FICKAS, K., XIONG, L., COLE, R. N., RADOVICK, S., WONDISFORD, F. E. & HE, L. 2014. Low concentrations of metformin suppress glucose production in hepatocytes through AMP-activated protein kinase (AMPK). *J Biol Chem,* 289, 20435-46.

CHANDA, D., PARK, J. H. & CHOI, H. S. 2008. Molecular basis of endocrine regulation by orphan nuclear receptor Small Heterodimer Partner. *Endocr J,* 55, 253-68.

CHAO, L. H. & AVRUCH, J. 2019. Cryo-EM insight into the structure of MTOR complex 1 and its interactions with Rheb and substrates. *F1000Res,* 8.

CHEN, K., QIAN, W., JIANG, Z., CHENG, L., LI, J., SUN, L., ZHOU, C., GAO, L., LEI, M., YAN, B., CAO, J., DUAN, W. & MA, Q. 2017. Metformin suppresses cancer initiation and progression in genetic mouse models of pancreatic cancer. *Mol Cancer,* 16, 131.

CHEN, S., ZHOU, J., XI, M., JIA, Y., WONG, Y., ZHAO, J., DING, L., ZHANG, J. & WEN, A. 2013. Pharmacogenetic variation and metformin response. *Curr Drug Metab,* 14, 1070-82.

CHOWDHURY, S. K., GEMIN, A. & SINGH, G. 2005. High activity of mitochondrial glycerophosphate dehydrogenase and glycerophosphate-dependent ROS production in prostate cancer cell lines. *Biochem Biophys Res Commun,* 333, 1139-45.

CLAUS, T. H., EL-MAGHRABI, M. R., REGEN, D. M., STEWART, H. B., MCGRANE, M., KOUNTZ, P. D., NYFELER, F., PILKIS, J. & PILKIS, S. J. 1984. The role of fructose 2,6-bisphosphate in the regulation of carbohydrate metabolism. *Curr Top Cell Regul,* 23, 57-86.

CLAUS, T. H., SCHLUMPF, J. R., EL-MAGHRABI, M. R. & PILKIS, S. J. 1982. Regulation of the phosphorylation and activity of 6-phosphofructo 1-kinase in isolated hepatocytes by alpha-glycerolphosphate and fructose 2,6-bisphosphate. *J Biol Chem,* 257, 7541-8.

COMTE, B., VIDAL, H., LAVILLE, M. & RIOU, J. P. 1990. Influence of thyroid hormones on gluconeogenesis from glycerol in rat hepatocytes: a dose-response study. *Metabolism,* 39, 259-63.

COOK, D. E., BLAIR, J. B. & LARDY, H. A. 1973. Mode of action of hypoglycemic agents. V. Studies with phenethylbiguanide in isolated perfused rat liver. *J Biol Chem,* 248, 5272-7.

COOL, B., ZINKER, B., CHIOU, W., KIFLE, L., CAO, N., PERHAM, M., DICKINSON, R., ADLER, A., GAGNE, G., IYENGAR, R., ZHAO, G., MARSH, K., KYM, P., JUNG, P., CAMP, H. S. & FREVERT, E. 2006. Identification and characterization of a small molecule AMPK activator that treats key components of type 2 diabetes and the metabolic syndrome. *Cell Metab,* 3, 403-16.

CORTON, J. M., GILLESPIE, J. G., HAWLEY, S. A. & HARDIE, D. G. 1995. 5-aminoimidazole-4-carboxamide ribonucleoside. A specific method for activating AMP-activated protein kinase in intact cells? *Eur J Biochem,* 229, 558-65.

COSTANTE, G., CRUPI, D., CATALFAMO, R. & TRIMARCHI, F. 1990. Stimulation of liver mitochondrial alpha-glycerophosphate dehydrogenase activity by L-thyroxine in thyroidectomized rats: comparison with the suppression of pituitary TSH secretion. *J Endocrinol Invest,* 13, 61-4.

CROOK, M. 2006. *Clinical chemistry & metabolic medicine*, Hodder Arnold London.

D'ALESSIO, D. 2011. The role of dysregulated glucagon secretion in type 2 diabetes. *Diabetes Obes Metab,* 13 Suppl 1, 126-32.

DANG, Q., BROWN, B. S., LIU, Y., RYDZEWSKI, R. M., ROBINSON, E. D., VAN POELJE, P. D., REDDY, M. R. & ERION, M. D. 2009. Fructose-1,6-bisphosphatase inhibitors. 1. Purine phosphonic acids as novel AMP mimics. *J Med Chem,* 52, 2880-98.

DAS, J. 2006. The role of mitochondrial respiration in physiological and evolutionary adaptation. *Bioessays,* 28, 890-901.

DAVIS, E. J., BREMER, J. & AKERMAN, K. E. 1980. Thermodynamic aspects of translocation of reducing equivalents by mitochondria. *J Biol Chem,* 255, 2277-83.

DAWSON, A. P. & THORNE, C. J. 1969. Preparation and some properties of L-3-glycerophosphate dehydrogenase from pig brain mitochondria. *Biochem J,* 111, 27-34.

DAY, P., SHARFF, A., PARRA, L., CLEASBY, A., WILLIAMS, M., HORER, S., NAR, H., REDEMANN, N., TICKLE, I. & YON, J. 2007. Structure of a CBS-domain pair from the regulatory gamma1 subunit of human AMPK in complex with AMP and ZMP. *Acta Crystallogr D Biol Crystallogr,* 63, 587-96.

DELLA-MORTE, D., PALMIROTTA, R., REHNI, A. K., PASTORE, D., CAPUANI, B., PACIFICI, F., DE MARCHIS, M. L., DAVE, K. R., BELLIA, A. & FOGLIAME, G. 2014. Pharmacogenomics and pharmacogenetics of thiazolidinediones: role in diabetes and cardiovascular risk factors. *Pharmacogenomics,* 15, 2063-2082.

DETAILLE, D., GUIGAS, B., CHAUVIN, C., BATANDIER, C., FONTAINE, E., WIERNSPERGER, N. & LEVERVE, X. 2005. Metformin prevents high-glucose-induced endothelial cell death through a mitochondrial permeability transition-dependent process. *Diabetes,* 54, 2179-87.

DUCOMMUN, S., FORD, R. J., BULTOT, L., DEAK, M., BERTRAND, L., KEMP, B. E., STEINBERG, G. R. & SAKAMOTO, K. 2014. Enhanced activation of cellular AMPK by dual-small molecule treatment: AICAR and A769662. *Am J Physiol Endocrinol Metab,* 306, E688-96.

DUNNING, B. E. & GERICH, J. E. 2007. The role of alpha-cell dysregulation in fasting and postprandial hyperglycemia in type 2 diabetes and therapeutic implications. *Endocr Rev,* 28, 253-83.

DYKENS, J. A., JAMIESON, J., MARROQUIN, L., NADANACIVA, S., BILLIS, P. A. & WILL, Y. 2008. Biguanide-induced mitochondrial dysfunction yields increased lactate production and cytotoxicity of aerobically-poised HepG2 cells and human hepatocytes in vitro. *Toxicol Appl Pharmacol,* 233, 203-10.

EATON, S. 2002. Control of mitochondrial beta-oxidation flux. *Prog Lipid Res,* 41, 197-239.

EGGLESTON, L. V. & KREBS, H. A. 1969. Strain differences in the activities of rat liver enzymes. *Biochem J,* 114, 877-9.

EL-MIR, M. Y., DETAILLE, D., G, R. V., DELGADO-ESTEBAN, M., GUIGAS, B., ATTIA, S., FONTAINE, E., ALMEIDA, A. & LEVERVE, X. 2008. Neuroprotective role of antidiabetic drug metformin against apoptotic cell death in primary cortical neurons. *J Mol Neurosci,* 34, 77-87.

EL-MIR, M. Y., NOGUEIRA, V., FONTAINE, E., AVERET, N., RIGOULET, M. & LEVERVE, X. 2000. Dimethylbiguanide inhibits cell respiration via an indirect effect targeted on the respiratory chain complex I. *J Biol Chem,* 275, 223-8.

EVANS, P. F., KING, L. J., PARKE, D. V., MARGETTS, G. & JONES, W. E. 1983. The mechanism of action of phenformin in starved rats. *Biochem Pharmacol,* 32, 3459-63.

FENG, T., SUN, X., HOWARD, L. E., VIDAL, A. C., GAINES, A. R., MOREIRA, D. M., CASTRO-SANTAMARIA, R., ANDRIOLE, G. L. & FREEDLAND, S. J. 2015. Metformin use and risk of prostate cancer: results from the REDUCE study. *Cancer Prev Res (Phila),* 8, 1055-60.

FERRANNINI, E. & DEFRONZO, R. A. 2015. Impact of glucose-lowering drugs on cardiovascular disease in type 2 diabetes. *European heart journal,* 36, 2288-2296.

FERRE, P., SATABIN, P., DECAUX, J. F., ESCRIVA, F. & GIRARD, J. 1983. Development and regulation of ketogenesis in hepatocytes isolated from newborn rats. *Biochem J,* 214, 937-42.

FERRE, P., SATABIN, P., EL MANOUBI, L., CALLIKAN, S. & GIRARD, J. 1981. Relationship between ketogenesis and gluconeogenesis in isolated hepatocytes from newborn rats. *Biochem J,* 200, 429-33.

FINAN, B., CAPOZZI, M. E. & CAMPBELL, J. E. 2019. Repositioning Glucagon Action in the Physiology and Pharmacology of Diabetes. *Diabetes*.

FLYNN, T. G. & MCKAY, D. 1972. Partial purification and characterization of triokinase from ox and human liver. *Biochem J,* 128, 135P.

FOGARTY, S., HAWLEY, S. A., GREEN, K. A., SANER, N., MUSTARD, K. J. & HARDIE, D. G. 2010. Calmodulin-dependent protein kinase kinase-beta activates AMPK without forming a stable complex: synergistic effects of Ca2+ and AMP. *Biochem J,* 426, 109-18.

FORD, R. J., FULLERTON, M. D., PINKOSKY, S. L., DAY, E. A., SCOTT, J. W., OAKHILL, J. S., BUJAK, A. L., SMITH, B. K., CRANE, J. D. & BLÜMER, R. M. 2015a. Metformin and salicylate synergistically activate liver AMPK, inhibit lipogenesis and improve insulin sensitivity. *Biochemical Journal,* 468, 125-132.

FORD, R. J., FULLERTON, M. D., PINKOSKY, S. L., DAY, E. A., SCOTT, J. W., OAKHILL, J. S., BUJAK, A. L., SMITH, B. K., CRANE, J. D., BLUMER, R. M., MARCINKO, K., KEMP, B. E., GERSTEIN, H. C. & STEINBERG, G. R. 2015b. Metformin and salicylate synergistically activate liver AMPK, inhibit lipogenesis and improve insulin sensitivity. *Biochem J,* 468, 125-32.

FORETZ, M., GUIGAS, B., BERTRAND, L., POLLAK, M. & VIOLLET, B. 2014. Metformin: from mechanisms of action to therapies. *Cell Metab,* 20, 953-66.

FORETZ, M., HÉBRARD, S., LECLERC, J., ZARRINPASHNEH, E., SOTY, M., MITHIEUX, G., SAKAMOTO, K., ANDREELLI, F. & VIOLLET, B. 2010. Metformin inhibits hepatic gluconeogenesis in mice independently of the LKB1/AMPK pathway via a decrease in hepatic energy state. *The Journal of clinical investigation,* 120, 2355-2369.

FREEMAN, H. C., HUGILL, A., DEAR, N. T., ASHCROFT, F. M. & COX, R. D. 2006. Deletion of nicotinamide nucleotide transhydrogenase: a new quantitive trait locus accounting for glucose intolerance in C57BL/6J mice. *Diabetes,* 55, 2153-6.

FROGUEL, P. 2000. [Genetics of type II diabetes]. *Arch Mal Coeur Vaiss,* 93 Spec No 4, 7-12.

FULGENCIO, J. P., KOHL, C., GIRARD, J. & PEGORIER, J. P. 2001. Effect of metformin on fatty acid and glucose metabolism in freshly isolated hepatocytes and on specific gene expression in cultured hepatocytes. *Biochem Pharmacol,* 62, 439-46.

FULLERTON, M. D., GALIC, S., MARCINKO, K., SIKKEMA, S., PULINILKUNNIL, T., CHEN, Z. P., O'NEILL, H. M., FORD, R. J., PALANIVEL, R., O'BRIEN, M., HARDIE, D. G., MACAULAY, S. L., SCHERTZER, J. D., DYCK, J. R., VAN DENDEREN, B. J., KEMP, B. E. & STEINBERG, G. R. 2013. Single phosphorylation sites in Acc1 and Acc2 regulate lipid homeostasis and the insulin-sensitizing effects of metformin. *Nat Med,* 19, 1649-54.

GALKIN, A., MEYER, B., WITTIG, I., KARAS, M., SCHAGGER, H., VINOGRADOV, A. & BRANDT, U. 2008. Identification of the mitochondrial ND3 subunit as a structural component involved in the active/deactive enzyme transition of respiratory complex I. *J Biol Chem,* 283, 20907-13.

GARDNER, D. G., SHOBACK, D. & GREENSPAN, F. S. 2007. *Greenspan's basic & clinical endocrinology*, McGraw-Hill Medical.

GARRIB, A. & MCMURRAY, W. C. 1986. Purification and characterization of glycerol-3-phosphate dehydrogenase (flavin-linked) from rat liver mitochondria. *J Biol Chem,* 261, 8042-8.

GELLERICH, F. N., GIZATULLINA, Z., TRUMBECKAITE, S., NGUYEN, H. P., PALLAS, T., ARANDARCIKAITE, O., VIELHABER, S., SEPPET, E. & STRIGGOW, F. 2010. The regulation of OXPHOS by extramitochondrial calcium. *Biochim Biophys Acta,* 1797, 1018-27.

GLINTBORG, D., ALTINOK, M. L., MUMM, H., HERMANN, A. P., RAVN, P. & ANDERSEN, M. 2014. Body composition is improved during 12 months' treatment with metformin alone or combined with oral contraceptives compared with treatment with oral contraceptives in polycystic ovary syndrome. *J Clin Endocrinol Metab,* 99, 2584-91.

GONG, L., GOSWAMI, S., GIACOMINI, K. M., ALTMAN, R. B. & KLEIN, T. E. 2012. Metformin pathways: pharmacokinetics and pharmacodynamics. *Pharmacogenet Genomics,* 22, 820-7.

GONZÁLEZ-MANCHÓN, C., AYUSO, M. S. & PARRILLA, R. 1989. Control of hepatic gluconeogenesis: role of fatty acid oxidation. *Archives of biochemistry and biophysics,* 271, 1-9.

GOUAREF, I., DETAILLE, D., WIERNSPERGER, N., KHAN, N. A., LEVERVE, X. & KOCEIR, E. A. 2017. The desert gerbil Psammomys obesus as a model for metformin-sensitive nutritional type 2 diabetes to protect hepatocellular metabolic damage: Impact of mitochondrial redox state. *PLoS One,* 12, e0172053.

GOWANS, G. J., HAWLEY, S. A., ROSS, F. A. & HARDIE, D. G. 2013. AMP is a true physiological regulator of AMP-activated protein kinase by both allosteric activation and enhancing net phosphorylation. *Cell Metab,* 18, 556-66.

GRAHAM, G. G., PUNT, J., ARORA, M., DAY, R. O., DOOGUE, M. P., DUONG, J. K., FURLONG, T. J., GREENFIELD, J. R., GREENUP, L. C., KIRKPATRICK, C. M., RAY, J. E., TIMMINS, P. & WILLIAMS, K. M. 2011. Clinical pharmacokinetics of metformin. *Clin Pharmacokinet,* 50, 81-98.

GRAHAME HARDIE, D. 2014. AMP-activated protein kinase: a key regulator of energy balance with many roles in human disease. *J Intern Med,* 276, 543-59.

GRAHAME HARDIE, D. 2016. Regulation of AMP-activated protein kinase by natural and synthetic activators. *Acta Pharm Sin B,* 6, 1-19.

GRIGORYAN, O., ABSATAROVA, J., ANDREEVA, E., MELNICHENKO, G. & DEDOV, I. 2014. Effect of metformin on the level of anti-Mullerian hormone in therapy of polycystic ovary syndrome in obese women. *Minerva Ginecol,* 66, 85-9.

GROUP, U. K. P. D. S. 1998. Intensive blood-glucose control with sulphonylureas or insulin compared with conventional treatment and risk of complications in patients with type 2 diabetes (UKPDS 33). *The lancet,* 352, 837-853.

GUAY, C., JOLY, E., PEPIN, E., BARBEAU, A., HENTSCH, L., PINEDA, M., MADIRAJU, S. R., BRUNENGRABER, H. & PRENTKI, M. 2013. A role for cytosolic isocitrate dehydrogenase as a negative regulator of glucose signaling for insulin secretion in pancreatic ss-cells. *PLoS One,* 8, e77097.

GUIGAS, B., BERTRAND, L., TALEUX, N., FORETZ, M., WIERNSPERGER, N., VERTOMMEN, D., ANDREELLI, F., VIOLLET, B. & HUE, L. 2006. 5-Aminoimidazole-4-carboxamide-1-beta-D-ribofuranoside and metformin inhibit hepatic glucose phosphorylation by an AMP-activated protein kinase-independent effect on glucokinase translocation. *Diabetes,* 55, 865-74.

HAMATANI, Y., INOUE, M., KIMURA, K., SHIOTA, M., OHTA, M. & SUGANO, T. 1991. Effects of calmodulin antagonists on hydrogen-translocating shuttles in perfused rat liver. *Am J Physiol,* 261, E325-31.

HANSON, R. W. & RESHEF, L. 1997. Regulation of phosphoenolpyruvate carboxykinase (GTP) gene expression. *Annu Rev Biochem,* 66, 581-611.

HARDIE, D. G. 2006. Neither LKB1 nor AMPK are the direct targets of metformin. *Gastroenterology,* 131, 973; author reply 974-5.

HARDIE, D. G. 2014. AMP-activated protein kinase: maintaining energy homeostasis at the cellular and whole-body levels. *Annu Rev Nutr,* 34, 31-55.

HARDIE, D. G. 2015. AMPK: positive and negative regulation, and its role in whole-body energy homeostasis. *Curr Opin Cell Biol,* 33, 1-7.

HARDIE, D. G., SCHAFFER, B. E. & BRUNET, A. 2016. AMPK: An Energy-Sensing Pathway with Multiple Inputs and Outputs. *Trends Cell Biol,* 26, 190-201.

HARNDAHL, L., SCHMOLL, D., HERLING, A. W. & AGIUS, L. 2006. The role of glucose 6-phosphate in mediating the effects of glucokinase overexpression on hepatic glucose metabolism. *FEBS J,* 273, 336-46.

HARRIS, R. A., CORNELL, N. W., STRAIGHT, C. & VEECH, R. L. 1982. Mechanism responsible for aminooxyacetate and glycolate stimulation of ethanol oxidation by isolated hepatocytes. *Arch Biochem Biophys,* 213, 414-25.

HASENOUR, C. M., RIDLEY, D. E., HUGHEY, C. C., JAMES, F. D., DONAHUE, E. P., SHEARER, J., VIOLLET, B., FORETZ, M. & WASSERMAN, D. H. 2014. 5-Aminoimidazole-4-carboxamide-1-beta-D-ribofuranoside (AICAR) effect on glucose production, but not energy metabolism, is independent of hepatic AMPK in vivo. *J Biol Chem,* 289, 5950-9.

HAWLEY, S. A., FULLERTON, M. D., ROSS, F. A., SCHERTZER, J. D., CHEVTZOFF, C., WALKER, K. J., PEGGIE, M. W., ZIBROVA, D., GREEN, K. A. & MUSTARD, K. J. 2012. The ancient drug salicylate directly activates AMP-activated protein kinase. *Science,* 336, 918-922.

HAWLEY, S. A., PAN, D. A., MUSTARD, K. J., ROSS, L., BAIN, J., EDELMAN, A. M., FRENGUELLI, B. G. & HARDIE, D. G. 2005. Calmodulin-dependent protein kinase kinase-beta is an alternative upstream kinase for AMP-activated protein kinase. *Cell Metab,* 2, 9-19.

HAWLEY, S. A., ROSS, F. A., CHEVTZOFF, C., GREEN, K. A., EVANS, A., FOGARTY, S., TOWLER, M. C., BROWN, L. J., OGUNBAYO, O. A., EVANS, A. M. & HARDIE, D. G. 2010. Use of cells expressing gamma subunit variants to identify diverse mechanisms of AMPK activation. *Cell Metab,* 11, 554-65.

HAYWARD, B., MOLERO, J. C., WINDMILL, K., SANIGORSKI, A., WEIR, J., MCRAE, N. L., ASTON-MOURNEY, K., OSBORNE, B., LIAO, B., WALDER, K. R., MEIKLE, P. J., KONSTANTOPOULOS, N. & SCHMITZ-PEIFFER, C. 2016. Pathways of Acetyl-CoA Metabolism Involved in the Reversal of Palmitate-Induced Glucose Production by Metformin and Salicylate. *Exp Clin Endocrinol Diabetes*.

HE, L., CHANG, E., PENG, J., AN, H., MCMILLIN, S. M., RADOVICK, S., STRATAKIS, C. A. & WONDISFORD, F. E. 2016a. Activation of the cAMP-PKA pathway Antagonizes Metformin Suppression of Hepatic Glucose Production. *J Biol Chem,* 291, 10562-70.

HE, L., CHANG, E., PENG, J., AN, H., MCMILLIN, S. M., RADOVICK, S., STRATAKIS, C. A. & WONDISFORD, F. E. 2016b. Activation of the cAMP-PKA pathway antagonizes metformin suppression of hepatic glucose production. *Journal of Biological Chemistry,* 291, 10562-10570.

HE, L., SABET, A., DJEDJOS, S., MILLER, R., SUN, X., HUSSAIN, M. A., RADOVICK, S. & WONDISFORD, F. E. 2009. Metformin and insulin suppress hepatic gluconeogenesis through phosphorylation of CREB binding protein. *Cell,* 137, 635-46.

HE, L. & WONDISFORD, F. E. 2015. Metformin action: concentrations matter. *Cell metabolism,* 21, 159-162.

HEINZ, S., FREYBERGER, A., LAWRENZ, B., SCHLADT, L., SCHMUCK, G. & ELLINGER-ZIEGELBAUER, H. 2017. Mechanistic Investigations of the Mitochondrial Complex I Inhibitor Rotenone in the Context of Pharmacological and Safety Evaluation. *Sci Rep,* 7, 45465.

HEISHI, M., ICHIHARA, J., TERAMOTO, R., ITAKURA, Y., HAYASHI, K., ISHIKAWA, H., GOMI, H., SAKAI, J., KANAOKA, M., TAIJI, M. & KIMURA, T. 2006. Global gene

expression analysis in liver of obese diabetic db/db mice treated with metformin. *Diabetologia,* 49, 1647-55.

HEMMERLE, H., BURGER, H. J., BELOW, P., SCHUBERT, G., RIPPEL, R., SCHINDLER, P. W., PAULUS, E. & HERLING, A. W. 1997. Chlorogenic acid and synthetic chlorogenic acid derivatives: novel inhibitors of hepatic glucose-6-phosphate translocase. *J Med Chem,* 40, 137-45.

HERS, H. G. & HUE, L. 1983. Gluconeogenesis and related aspects of glycolysis. *Annu Rev Biochem,* 52, 617-53.

HINKE, S. A., MARTENS, G. A., CAI, Y., FINSI, J., HEIMBERG, H., PIPELEERS, D. & VAN DE CASTEELE, M. 2007. Methyl succinate antagonises biguanide-induced AMPK-activation and death of pancreatic beta-cells through restoration of mitochondrial electron transfer. *Br J Pharmacol,* 150, 1031-43.

HIRST, J. 2013. Mitochondrial complex I. *Annu Rev Biochem,* 82, 551-75.

HOLMAN, R. R., PAUL, S. K., BETHEL, M. A., MATTHEWS, D. R. & NEIL, H. A. 2008. 10-year follow-up of intensive glucose control in type 2 diabetes. *N Engl J Med,* 359, 1577-89.

HONG, J., ZHANG, Y., LAI, S., LV, A., SU, Q., DONG, Y., ZHOU, Z., TANG, W., ZHAO, J., CUI, L., ZOU, D., WANG, D., LI, H., LIU, C., WU, G., SHEN, J., ZHU, D., WANG, W., SHEN, W. & NING, G. 2013. Effects of metformin versus glipizide on cardiovascular outcomes in patients with type 2 diabetes and coronary artery disease. *Diabetes Care,* 36, 1304-11.

HUE, L. 1981. The role of futile cycles in the regulation of carbohydrate metabolism in the liver. *Adv Enzymol Relat Areas Mol Biol,* 52, 247-331.

HUE, L. 1982. Role of fructose 2,6-bisphosphate in the stimulation of glycolysis by anoxia in isolated hepatocytes. *Biochem J,* 206, 359-65.

HUNDAL, R. S., KRSSAK, M., DUFOUR, S., LAURENT, D., LEBON, V., CHANDRAMOULI, V., INZUCCHI, S. E., SCHUMANN, W. C., PETERSEN, K. F., LANDAU, B. R. & SHULMAN, G. I. 2000. Mechanism by which metformin reduces glucose production in type 2 diabetes. *Diabetes,* 49, 2063-9.

HUNT, S. M., OSNOS, M. & RIVLIN, R. S. 1970. Thyroid hormone regulation of mitochondrial alpha-glycerophosphate dehydrogenase in liver and hepatoma. *Cancer Res,* 30, 1764-8.

HUNTER, R. W., HUGHEY, C. C., LANTIER, L., SUNDELIN, E. I., PEGGIE, M., ZEQIRAJ, E., SICHERI, F., JESSEN, N., WASSERMAN, D. H. & SAKAMOTO, K. 2018. Metformin reduces liver glucose production by inhibition of fructose-1-6-bisphosphatase. *Nat Med,* 24, 1395-1406.

IIJIMA, M., JALIL, A., BEGUM, L., YASUDA, T., YAMAGUCHI, N., XIAN LI, M., KAWADA, N., ENDOU, H., KOBAYASHI, K. & SAHEKI, T. 2001. Pathogenesis of adult-onset type II citrullinemia caused by deficiency of citrin, a mitochondrial solute carrier protein: tissue and subcellular localization of citrin. *Adv Enzyme Regul,* 41, 325-42.

INZUCCHI, S. E., BERGENSTAL, R. M., BUSE, J. B., DIAMANT, M., FERRANNINI, E., NAUCK, M., PETERS, A. L., TSAPAS, A., WENDER, R. & MATTHEWS, D. R. 2015. Management of hyperglycaemia in type 2 diabetes, 2015: a patient-centred approach. Update to a position statement of the American Diabetes Association and the European Association for the Study of Diabetes. *Diabetologia,* 58, 429-442.

INZUCCHI, S. E., LIPSKA, K. J., MAYO, H., BAILEY, C. J. & MCGUIRE, D. K. 2014. Metformin in patients with type 2 diabetes and kidney disease: a systematic review. *JAMA,* 312, 2668-75.

IOSSA, S., MOLLICA, M. P., LIONETTI, L., BARLETTA, A. & LIVERINI, G. 1995. Hepatic mitochondrial respiration and transport of reducing equivalents in rats fed an energy dense diet. *Int J Obes Relat Metab Disord,* 19, 539-43.

JACQUEL, A., LUCIANO, F., ROBERT, G. & AUBERGER, P. 2018. Implication and Regulation of AMPK during Physiological and Pathological Myeloid Differentiation. *Int J Mol Sci,* 19.

JENKINS, C. M., YANG, J., SIMS, H. F. & GROSS, R. W. 2011. Reversible high affinity inhibition of phosphofructokinase-1 by acyl-CoA: a mechanism integrating glycolytic flux with lipid metabolism. *J Biol Chem,* 286, 11937-50.

JIANG, G. & ZHANG, B. B. 2003. Glucagon and regulation of glucose metabolism. *Am J Physiol Endocrinol Metab,* 284, E671-8.

JORGENSEN, C. H., GISLASON, G. H., ANDERSSON, C., AHLEHOFF, O., CHARLOT, M., SCHRAMM, T. K., VAAG, A., ABILDSTROM, S. Z., TORP-PEDERSEN, C. & HANSEN, P. R. 2010. Effects of oral glucose-lowering drugs on long term outcomes in patients with diabetes mellitus following myocardial infarction not treated with emergent percutaneous coronary intervention--a retrospective nationwide cohort study. *Cardiovasc Diabetol,* 9, 54.

JORGENSEN, S. B., VIOLLET, B., ANDREELLI, F., FROSIG, C., BIRK, J. B., SCHJERLING, P., VAULONT, S., RICHTER, E. A. & WOJTASZEWSKI, J. F. 2004. Knockout of the alpha2 but not alpha1 5'-AMP-activated protein kinase isoform abolishes 5-aminoimidazole-4-carboxamide-1-beta-4-ribofuranosidebut not contraction-induced glucose uptake in skeletal muscle. *J Biol Chem,* 279, 1070-9.

KAHN, R. & FONSECA, V. 2008. Translating the A1C Assay. *Diabetes Care,* 31, 1704-7.

KAWAGUCHI, T., OSATOMI, K., YAMASHITA, H., KABASHIMA, T. & UYEDA, K. 2002. Mechanism for fatty acid "sparing" effect on glucose-induced transcription: regulation of carbohydrate-responsive element-binding protein by AMP-activated protein kinase. *J Biol Chem,* 277, 3829-35.

KHAILOVA, L. S., ROKITSKAYA, T. I., KOTOVA, E. A. & ANTONENKO, Y. N. 2017. Effect of Cyanide on Mitochondrial Membrane Depolarization Induced by Uncouplers. *Biochemistry (Mosc),* 82, 1140-1146.

KIM, Y. D., LI, T., AHN, S. W., KIM, D. K., LEE, J. M., HWANG, S. L., KIM, Y. H., LEE, C. H., LEE, I. K., CHIANG, J. Y. & CHOI, H. S. 2012. Orphan nuclear receptor small heterodimer partner negatively regulates growth hormone-mediated induction of hepatic gluconeogenesis through inhibition of signal transducer and activator of transcription 5 (STAT5) transactivation. *J Biol Chem,* 287, 37098-108.

KIM, Y. D., PARK, K. G., LEE, Y. S., PARK, Y. Y., KIM, D. K., NEDUMARAN, B., JANG, W. G., CHO, W. J., HA, J., LEE, I. K., LEE, C. H. & CHOI, H. S. 2008. Metformin inhibits hepatic gluconeogenesis through AMP-activated protein kinase-dependent regulation of the orphan nuclear receptor SHP. *Diabetes,* 57, 306-14.

KJOBSTED, R., TREEBAK, J. T., FENTZ, J., LANTIER, L., VIOLLET, B., BIRK, J. B., SCHJERLING, P., BJORNHOLM, M., ZIERATH, J. R. & WOJTASZEWSKI, J. F. 2015.

Prior AICAR stimulation increases insulin sensitivity in mouse skeletal muscle in an AMPK-dependent manner. *Diabetes,* 64, 2042-55.

KNEER, N. & LARDY, H. 2000. Thyroid hormone and dehydroepiandrosterone permit gluconeogenic hormone responses in hepatocytes. *Arch Biochem Biophys,* 375, 145-53.

KOBAYASHI, K., SINASAC, D. S., IIJIMA, M., BORIGHT, A. P., BEGUM, L., LEE, J. R., YASUDA, T., IKEDA, S., HIRANO, R., TERAZONO, H., CRACKOWER, M. A., KONDO, I., TSUI, L. C., SCHERER, S. W. & SAHEKI, T. 1999. The gene mutated in adult-onset type II citrullinaemia encodes a putative mitochondrial carrier protein. *Nat Genet,* 22, 159-63.

KOJIC DAMJANOV, S., DERIC, M. & EREMIC KOJIC, N. 2014. Glycated hemoglobin A1c as a modern biochemical marker of glucose regulation. *Med Pregl,* 67, 339-44.

KOWALL, B., STANG, A., RATHMANN, W. & KOSTEV, K. 2015. No reduced risk of overall, colorectal, lung, breast, and prostate cancer with metformin therapy in diabetic patients: database analyses from Germany and the UK. *Pharmacoepidemiol Drug Saf,* 24, 865-74.

KRAEV, A. 2014. Parallel universes of Black Six biology. *Biol Direct,* 9, 18.

KRISTENSEN, D. E., ALBERS, P. H., PRATS, C., BABA, O., BIRK, J. B. & WOJTASZEWSKI, J. F. 2015. Human muscle fibre type-specific regulation of AMPK and downstream targets by exercise. *J Physiol,* 593, 2053-69.

KRUPANIDHI, S., SEDIMBI, S. K., VAISHNAV, G., MADHUKAR, S. S. & SANJEEVI, C. B. 2009. Diabetes--role of epigenetics, genetics, and physiological factors. *Zhong Nan Da Xue Xue Bao Yi Xue Ban,* 34, 837-45.

KUNTE, H., SCHMIDT, S., ELIASZIW, M., DEL ZOPPO, G. J., SIMARD, J. M., MASUHR, F., WEIH, M. & DIRNAGL, U. 2007. Sulfonylureas improve outcome in patients with type 2 diabetes and acute ischemic stroke. *Stroke,* 38, 2526-2530.

KURUMBAIL, R. G. & CALABRESE, M. F. 2016. Structure and Regulation of AMPK. *EXS,* 107, 3-22.

LANOUE, K. F., BRYLA, J. & BASSETT, D. J. 1974. Energy-driven aspartate efflux from heart and liver mitochondria. *J Biol Chem,* 249, 7514-21.

LEE, J. M., SEO, W. Y., SONG, K. H., CHANDA, D., KIM, Y. D., KIM, D. K., LEE, M. W., RYU, D., KIM, Y. H., NOH, J. R., LEE, C. H., CHIANG, J. Y., KOO, S. H. & CHOI, H. S. 2010. AMPK-dependent repression of hepatic gluconeogenesis via disruption of CREB.CRTC2 complex by orphan nuclear receptor small heterodimer partner. *J Biol Chem,* 285, 32182-91.

LEE, Y. S., CHANDA, D., SIM, J., PARK, Y. Y. & CHOI, H. S. 2007. Structure and function of the atypical orphan nuclear receptor small heterodimer partner. *Int Rev Cytol,* 261, 117-58.

LIN, S. C. & HARDIE, D. G. 2018. AMPK: Sensing Glucose as well as Cellular Energy Status. *Cell Metab,* 27, 299-313.

LIU, J. F., MA, Y., WANG, Y., DU, Z. Y., SHEN, J. K. & PENG, H. L. 2011. Reduction of lipid accumulation in HepG2 cells by luteolin is associated with activation of AMPK and mitigation of oxidative stress. *Phytother Res,* 25, 588-96.

LOCHHEAD, P. A., SALT, I. P., WALKER, K. S., HARDIE, D. G. & SUTHERLAND, C. 2000. 5-aminoimidazole-4-carboxamide riboside mimics the effects of insulin on the expression of the 2 key gluconeogenic genes PEPCK and glucose-6-phosphatase. *Diabetes,* 49, 896-903.

LOU, P. H., HANSEN, B. S., OLSEN, P. H., TULLIN, S., MURPHY, M. P. & BRAND, M. D. 2007. Mitochondrial uncouplers with an extraordinary dynamic range. *Biochem J,* 407, 129-40.

MA, L., ROBINSON, L. N. & TOWLE, H. C. 2006. ChREBP*Mlx is the principal mediator of glucose-induced gene expression in the liver. *J Biol Chem,* 281, 28721-30.

MADIRAJU, A. K., ERION, D. M., RAHIMI, Y., ZHANG, X. M., BRADDOCK, D. T., ALBRIGHT, R. A., PRIGARO, B. J., WOOD, J. L., BHANOT, S., MACDONALD, M. J., JURCZAK, M. J., CAMPOREZ, J. P., LEE, H. Y., CLINE, G. W., SAMUEL, V. T., KIBBEY, R. G. & SHULMAN, G. I. 2014. Metformin suppresses gluconeogenesis by inhibiting mitochondrial glycerophosphate dehydrogenase. *Nature,* 510, 542-6.

MADIRAJU, A. K., QIU, Y., PERRY, R. J., RAHIMI, Y., ZHANG, X. M., ZHANG, D., CAMPOREZ, J. G., CLINE, G. W., BUTRICO, G. M., KEMP, B. E., CASALS, G., STEINBERG, G. R., VATNER, D. F., PETERSEN, K. F. & SHULMAN, G. I. 2018.

Metformin inhibits gluconeogenesis via a redox-dependent mechanism in vivo. *Nat Med,* 24, 1384-1394.

MALDONADO, E. N., DEHART, D. N., PATNAIK, J., KLATT, S. C., GOOZ, M. B. & LEMASTERS, J. J. 2016. ATP/ADP Turnover and Import of Glycolytic ATP into Mitochondria in Cancer Cells Is Independent of the Adenine Nucleotide Translocator. *J Biol Chem,* 291, 19642-50.

MALIN, S. K., NIGHTINGALE, J., CHOI, S. E., CHIPKIN, S. R. & BRAUN, B. 2013. Metformin modifies the exercise training effects on risk factors for cardiovascular disease in impaired glucose tolerant adults. *Obesity (Silver Spring),* 21, 93-100.

MARUTHUR, N. M., TSENG, E., HUTFLESS, S., WILSON, L. M., SUAREZ-CUERVO, C., BERGER, Z., CHU, Y., IYOHA, E., SEGAL, J. B. & BOLEN, S. 2016. Diabetes Medications as Monotherapy or Metformin-Based Combination Therapy for Type 2 Diabetes: A Systematic Review and Meta-analysis. *Ann Intern Med,* 164, 740-51.

MCCUNE, S. A., FOE, L. G., KEMP, R. G. & JURIN, R. R. 1989. Aurintricarboxylic acid is a potent inhibitor of phosphofructokinase. *Biochem J,* 259, 925-7.

MCGARRY, J. D. & FOSTER, D. W. 1980. Regulation of hepatic fatty acid oxidation and ketone body production. *Annual review of biochemistry,* 49, 395-420.

MCKENNA, M. C., WAAGEPETERSEN, H. S., SCHOUSBOE, A. & SONNEWALD, U. 2006. Neuronal and astrocytic shuttle mechanisms for cytosolic-mitochondrial transfer of reducing equivalents: current evidence and pharmacological tools. *Biochem Pharmacol,* 71, 399-407.

MENG, S., CAO, J., HE, Q., XIONG, L., CHANG, E., RADOVICK, S., WONDISFORD, F. E. & HE, L. 2015. Metformin activates AMP-activated protein kinase by promoting formation of the alphabetagamma heterotrimeric complex. *J Biol Chem,* 290, 3793-802.

MERRILL, G. F., KURTH, E. J., HARDIE, D. G. & WINDER, W. W. 1997. AICA riboside increases AMP-activated protein kinase, fatty acid oxidation, and glucose uptake in rat muscle. *Am J Physiol,* 273, E1107-12.

MILLER, R. A., CHU, Q., XIE, J., FORETZ, M., VIOLLET, B. & BIRNBAUM, M. J. 2013. Biguanides suppress hepatic glucagon signalling by decreasing production of cyclic AMP. *Nature,* 494, 256-260.

MINARIK, P., TOMASKOVA, N., KOLLAROVA, M. & ANTALIK, M. 2002. Malate dehydrogenases--structure and function. *Gen Physiol Biophys,* 21, 257-65.

MITSUHASHI, A., KIYOKAWA, T., SATO, Y. & SHOZU, M. 2014. Effects of metformin on endometrial cancer cell growth in vivo: a preoperative prospective trial. *Cancer,* 120, 2986-95.

MONTAGUE, W. & TAYLOR, K. W. 1969. Islet-cell metabolism during insulin release. Effects of glucose, citrate, octanoate, tolbutamide, glucagon and theophylline. *Biochem J,* 115, 257-62.

MRACEK, T., DRAHOTA, Z. & HOUSTEK, J. 2013. The function and the role of the mitochondrial glycerol-3-phosphate dehydrogenase in mammalian tissues. *Biochim Biophys Acta,* 1827, 401-10.

MULLER, J., LIPS, K. S., METZNER, L., NEUBERT, R. H., KOEPSELL, H. & BRANDSCH, M. 2005. Drug specificity and intestinal membrane localization of human organic cation transporters (OCT). *Biochem Pharmacol,* 70, 1851-60.

MUNDAY, M. R. & HEMINGWAY, C. J. 1999. The regulation of acetyl-CoA carboxylase--a potential target for the action of hypolipidemic agents. *Adv Enzyme Regul,* 39, 205-34.

MUSI, N., HAYASHI, T., FUJII, N., HIRSHMAN, M. F., WITTERS, L. A. & GOODYEAR, L. J. 2001. AMP-activated protein kinase activity and glucose uptake in rat skeletal muscle. *Am J Physiol Endocrinol Metab,* 280, E677-84.

NADERPOOR, N., SHORAKAE, S., DE COURTEN, B., MISSO, M. L., MORAN, L. J. & TEEDE, H. J. 2015. Metformin and lifestyle modification in polycystic ovary syndrome: systematic review and meta-analysis. *Hum Reprod Update,* 21, 560-74.

NATALI, A. & FERRANNINI, E. 2006. Effects of metformin and thiazolidinediones on suppression of hepatic glucose production and stimulation of glucose uptake in type 2 diabetes: a systematic review. *Diabetologia,* 49, 434-41.

NAUCK, M. A. 2014. Update on developments with SGLT2 inhibitors in the management of type 2 diabetes. *Drug Des Devel Ther,* 8, 1335-80.

NIRAULA, S., DOWLING, R. J., ENNIS, M., CHANG, M. C., DONE, S. J., HOOD, N., ESCALLON, J., LEONG, W. L., MCCREADY, D. R., REEDIJK, M., STAMBOLIC, V. & GOODWIN, P. J. 2012. Metformin in early breast cancer: a prospective window of opportunity neoadjuvant study. *Breast Cancer Res Treat,* 135, 821-30.

NOVOTNA, M., PODZIMEK, S., BROUKAL, Z., LENCOVA, E. & DUSKOVA, J. 2015. Periodontal diseases and dental caries in children with type 1 diabetes mellitus. *Mediators of inflammation,* 2015.

O'BRIEN, A. J., VILLANI, L. A., BROADFIELD, L. A., HOUDE, V. P., GALIC, S., BLANDINO, G., KEMP, B. E., TSAKIRIDIS, T., MUTI, P. & STEINBERG, G. R. 2015. Salicylate activates AMPK and synergizes with metformin to reduce the survival of prostate and lung cancer cells ex vivo through inhibition of de novo lipogenesis. *Biochem J,* 469, 177-87.

OAKHILL, J. S., SCOTT, J. W. & KEMP, B. E. 2012. AMPK functions as an adenylate charge-regulated protein kinase. *Trends Endocrinol Metab,* 23, 125-32.

OH, K. J., HAN, H. S., KIM, M. J. & KOO, S. H. 2013. Transcriptional regulators of hepatic gluconeogenesis. *Arch Pharm Res,* 36, 189-200.

OHNISHI, T. 1998. Iron-sulfur clusters/semiquinones in complex I. *Biochim Biophys Acta,* 1364, 186-206.

OLOKOBA, A. B., OBATERU, O. A. & OLOKOBA, L. B. 2012. Type 2 diabetes mellitus: a review of current trends. *Oman medical journal,* 27, 269.

ORR, A. L., ASHOK, D., SARANTOS, M. R., NG, R., SHI, T., GERENCSER, A. A., HUGHES, R. E. & BRAND, M. D. 2014. Novel inhibitors of mitochondrial sn-glycerol 3-phosphate dehydrogenase. *PLoS One,* 9, e89938.

OUYANG, J., PARAKHIA, R. A. & OCHS, R. S. 2011. Metformin activates AMP kinase through inhibition of AMP deaminase. *J Biol Chem,* 286, 1-11.

OWEN, M. R., DORAN, E. & HALESTRAP, A. P. 2000. Evidence that metformin exerts its anti-diabetic effects through inhibition of complex 1 of the mitochondrial respiratory chain. *Biochemical Journal,* 348, 607-614.

OWEN, M. R. & HALESTRAP, A. P. 1993. The mechanisms by which mild respiratory chain inhibitors inhibit hepatic gluconeogenesis. *Biochim Biophys Acta,* 1142, 11-22.

PAYNE, V. A., ARDEN, C., WU, C., LANGE, A. J. & AGIUS, L. 2005. Dual role of phosphofructokinase-2/fructose bisphosphatase-2 in regulating the compartmentation and expression of glucokinase in hepatocytes. *Diabetes,* 54, 1949-57.

PECINOVA, A., DRAHOTA, Z., KOVALCIKOVA, J., KOVAROVA, N., PECINA, P., ALAN, L., ZIMA, M., HOUSTEK, J. & MRACEK, T. 2017. Pleiotropic Effects of Biguanides on Mitochondrial Reactive Oxygen Species Production. *Oxid Med Cell Longev,* 2017, 7038603.

PEGORIER, J. P., DUEE, P. H., CLOUET, P., KOHL, C., HERBIN, C. & GIRARD, J. 1989. Octanoate metabolism in isolated hepatocytes and mitochondria from fetal, newborn and adult rabbit. Evidence for a high capacity for octanoate esterification in term fetal liver. *Eur J Biochem,* 184, 681-6.

PELANTOVA, H., BUGANOVA, M., HOLUBOVA, M., SEDIVA, B., ZEMENOVA, J., SYKORA, D., KAVALKOVA, P., HALUZIK, M., ZELEZNA, B., MALETINSKA, L., KUNES, J. & KUZMA, M. 2016. Urinary metabolomic profiling in mice with diet-induced obesity and type 2 diabetes mellitus after treatment with metformin, vildagliptin and their combination. *Mol Cell Endocrinol,* 431, 88-100.

PERNICOVA, I. & KORBONITS, M. 2014. Metformin--mode of action and clinical implications for diabetes and cancer. *Nat Rev Endocrinol,* 10, 143-56.

PRESTON, M. A., RIIS, A. H., EHRENSTEIN, V., BREAU, R. H., BATISTA, J. L., OLUMI, A. F., MUCCI, L. A., ADAMI, H. O. & SORENSEN, H. T. 2014. Metformin use and prostate cancer risk. *Eur Urol,* 66, 1012-20.

PRYOR, H. J., SMYTH, J. E., QUINLAN, P. T. & HALESTRAP, A. P. 1987. Evidence that the flux control coefficient of the respiratory chain is high during gluconeogenesis from lactate in hepatocytes from starved rats. Implications for the hormonal control of gluconeogenesis and action of hypoglycaemic agents. *Biochem J,* 247, 449-57.

QI, H., NIELSEN, P. M., SCHROEDER, M., BERTELSEN, L. B., PALM, F. & LAUSTSEN, C. 2018. Acute renal metabolic effect of metformin assessed with hyperpolarised MRI in rats. *Diabetologia,* 61, 445-454.

QIU, B. Y., TURNER, N., LI, Y. Y., GU, M., HUANG, M. W., WU, F., PANG, T., NAN, F. J., YE, J. M., LI, J. Y. & LI, J. 2010. High-throughput assay for modulators of mitochondrial membrane potential identifies a novel compound with beneficial effects on db/db mice. *Diabetes,* 59, 256-65.

QUINLAN, P. T. & HALESTRAP, A. P. 1986. The mechanism of the hormonal activation of respiration in isolated hepatocytes and its importance in the regulation of gluconeogenesis. *Biochem J,* 236, 789-800.

REHEMAN, A., TASNEEM, S., NI, H. & HAYWARD, C. P. 2010. Mice with deleted multimerin 1 and alpha-synuclein genes have impaired platelet adhesion and impaired thrombus formation that is corrected by multimerin 1. *Thromb Res,* 125, e177-83.

RENA, G., HARDIE, D. G. & PEARSON, E. R. 2017. The mechanisms of action of metformin. *Diabetologia,* 60, 1577-1585.

RENA, G., PEARSON, E. R. & SAKAMOTO, K. 2013. Molecular mechanism of action of metformin: old or new insights? *Diabetologia,* 56, 1898-906.

RIDER, M. H., BERTRAND, L., VERTOMMEN, D., MICHELS, P. A., ROUSSEAU, G. G. & LOUIS, H. U. E. 2004. 6-phosphofructo-2-kinase/fructose-2, 6-bisphosphatase: head-to-head with a bifunctional enzyme that controls glycolysis. *Biochemical Journal,* 381, 561-579.

ROBERTS, P. G. & HIRST, J. 2012. The deactive form of respiratory complex I from mammalian mitochondria is a Na+/H+ antiporter. *J Biol Chem,* 287, 34743-51.

ROGNSTAD, R. & CLARK, D. G. 1974. Effects of aminooxyacetate on the metabolism of isolated liver cells. *Arch Biochem Biophys,* 161, 638-46.

RONCHI, J. A., FIGUEIRA, T. R., RAVAGNANI, F. G., OLIVEIRA, H. C., VERCESI, A. E. & CASTILHO, R. F. 2013. A spontaneous mutation in the nicotinamide nucleotide transhydrogenase gene of C57BL/6J mice results in mitochondrial redox abnormalities. *Free Radic Biol Med,* 63, 446-56.

ROSS, F. A., JENSEN, T. E. & HARDIE, D. G. 2016. Differential regulation by AMP and ADP of AMPK complexes containing different gamma subunit isoforms. *Biochem J,* 473, 189-99.

RYDSTROM, J. 2006. Mitochondrial NADPH, transhydrogenase and disease. *Biochim Biophys Acta,* 1757, 721-6.

SABINA, R. L., PATTERSON, D. & HOLMES, E. W. 1985. 5-Amino-4-imidazolecarboxamide riboside (Z-riboside) metabolism in eukaryotic cells. *J Biol Chem,* 260, 6107-14.

SAHEKI, T., IIJIMA, M., LI, M. X., KOBAYASHI, K., HORIUCHI, M., USHIKAI, M., OKUMURA, F., MENG, X. J., INOUE, I., TAJIMA, A., MORIYAMA, M., ETO, K., KADOWAKI, T., SINASAC, D. S., TSUI, L. C., TSUJI, M., OKANO, A. & KOBAYASHI, T. 2007. Citrin/mitochondrial glycerol-3-phosphate dehydrogenase double knock-out mice recapitulate features of human citrin deficiency. *J Biol Chem,* 282, 25041-52.

SAJAN, M. P., IVEY, R. A., 3RD & FARESE, R. V. 2013. Metformin action in human hepatocytes: coactivation of atypical protein kinase C alters 5'-AMP-activated protein kinase effects on lipogenic and gluconeogenic enzyme expression. *Diabetologia,* 56, 2507-16.

SANAKA, M., YAMAMOTO, T. & KUYAMA, Y. 2008. Retention, fixation, and loss of the [13C] label: a review for the understanding of gastric emptying breath tests. *Dig Dis Sci,* 53, 1747-56.

SANDERS, M. J., ALI, Z. S., HEGARTY, B. D., HEATH, R., SNOWDEN, M. A. & CARLING, D. 2007a. Defining the mechanism of activation of AMP-activated protein kinase by the small molecule A-769662, a member of the thienopyridone family. *Journal of biological chemistry,* 282, 32539-32548.

SANDERS, M. J., GRONDIN, P. O., HEGARTY, B. D., SNOWDEN, M. A. & CARLING, D. 2007b. Investigating the mechanism for AMP activation of the AMP-activated protein kinase cascade. *Biochem J,* 403, 139-48.

SCHAFER, G. 1976. On the mechanism of action of hypoglycemia-producing biguanides. A reevaluation and a molecular theory. *Biochem Pharmacol,* 25, 2005-14.

SCHOLZ, T. D., TENEYCK, C. J. & SCHUTTE, B. C. 2000. Thyroid hormone regulation of the NADH shuttles in liver and cardiac mitochondria. *J Mol Cell Cardiol,* 32, 1-10.

SCHONFELD, P. & WOJTCZAK, L. 2016. Short- and medium-chain fatty acids in energy metabolism: the cellular perspective. *J Lipid Res,* 57, 943-54.

SEGLEN, P. O. 1976. Preparation of isolated rat liver cells. *Methods Cell Biol,* 13, 29-83.

SELIZER, H. S. 1980. Efficacy and safety of oral hypoglycemic agents. *Annual review of medicine,* 31, 261-272.

SELLINGER, O. Z. & LEE, K. 1964. THE INDUCTION OF MITOCHONDRIAL ALPHA-GLYCEROPHOSPHATE DEHYDROGENASE BY THYROID HORMONE: EVIDENCE FOR ENZYME SYNTHESIS. *Biochim Biophys Acta,* 91, 183-6.

SERVIDDIO, G., BELLANTI, F. & VENDEMIALE, G. 2013. Free radical biology for medicine: learning from nonalcoholic fatty liver disease. *Free Radic Biol Med,* 65, 952-68.

SHAW, R. J., LAMIA, K. A., VASQUEZ, D., KOO, S. H., BARDEESY, N., DEPINHO, R. A., MONTMINY, M. & CANTLEY, L. C. 2005. The kinase LKB1 mediates glucose homeostasis in liver and therapeutic effects of metformin. *Science,* 310, 1642-6.

SIBILLE, B., KERIEL, C., FONTAINE, E., CATELLONI, F., RIGOULET, M. & LEVERVE, X. M. 1995. Octanoate affects 2,4-dinitrophenol uncoupling in intact isolated rat hepatocytes. *Eur J Biochem,* 231, 498-502.

SIBILLE, B., RONOT, X., FILIPPI, C., NOGUEIRA, V., KERIEL, C. & LEVERVE, X. 1998. 2,4 Dinitrophenol-uncoupling effect on delta psi in living hepatocytes depends on reducing-equivalent supply. *Cytometry,* 32, 102-8.

SKOV, V., CANGEMI, C., GRAM, J., CHRISTENSEN, M. M., GRODUM, E., SORENSEN, D., ARGRAVES, W. S., HENRIKSEN, J. E. & RASMUSSEN, L. M. 2014. Metformin, but not rosiglitazone, attenuates the increasing plasma levels of a new cardiovascular marker, fibulin-1, in patients with type 2 diabetes. *Diabetes Care,* 37, 760-6.

SMITH, B. K., FORD, R. J., DESJARDINS, E. M., GREEN, A. E., HUGHES, M. C., HOUDE, V. P., DAY, E. A., MARCINKO, K., CRANE, J. D., MOTTILLO, E. P., PERRY, C. G., KEMP, B. E., TARNOPOLSKY, M. A. & STEINBERG, G. R. 2016. Salsalate (Salicylate)

Uncouples Mitochondria, Improves Glucose Homeostasis, and Reduces Liver Lipids Independent of AMPK-beta1. *Diabetes,* 65, 3352-3361.

SONG, X., CAI, W. & LI, L. 2016. Axin PPI Networks: New Interacting Proteins and New Targets? *Curr Top Med Chem,* 16, 3678-3690.

SPECHT, C. G. & SCHOEPFER, R. 2001. Deletion of the alpha-synuclein locus in a subpopulation of C57BL/6J inbred mice. *BMC Neurosci,* 2, 11.

STAPPENBECK, R., HODSON, A. W., SKILLEN, A. W., AGIUS, L. & ALBERTI, K. G. 1990. Optimized methods to measure acetoacetate, 3-hydroxybutyrate, glycerol, alanine, pyruvate, lactate and glucose in human blood using a centrifugal analyser with a fluorimetric attachment. *J Automat Chem,* 12, 213-20.

STEINBERG, G. R. & CARLING, D. 2019. AMP-activated protein kinase: the current landscape for drug development. *Nat Rev Drug Discov*.

SULLIVAN, J. E., BROCKLEHURST, K. J., MARLEY, A. E., CAREY, F., CARLING, D. & BERI, R. K. 1994. Inhibition of lipolysis and lipogenesis in isolated rat adipocytes with AICAR, a cell-permeable activator of AMP-activated protein kinase. *FEBS Lett,* 353, 33-6.

TALEUX, N., GUIGAS, B., DUBOUCHAUD, H., MORENO, M., WEITZEL, J. M., GOGLIA, F., FAVIER, R. & LEVERVE, X. M. 2009. High expression of thyroid hormone receptors and mitochondrial glycerol-3-phosphate dehydrogenase in the liver is linked to enhanced fatty acid oxidation in Lou/C, a rat strain resistant to obesity. *J Biol Chem,* 284, 4308-16.

THORSBY, P., UNDLIEN, D. E., BERG, J. P., THORSBY, E. & BIRKELAND, K. I. 1998. [Diabetes mellitus--a complex interaction between heredity and environment]. *Tidsskr Nor Laegeforen,* 118, 2519-24.

THULÉ, P. M. & UMPIERREZ, G. 2014. Sulfonylureas: a new look at old therapy. *Current diabetes reports,* 14, 473.

TIMMERMANS, A. D., BALTEAU, M., GELINAS, R., RENGUET, E., GINION, A., DE MEESTER, C., SAKAMOTO, K., BALLIGAND, J. L., BONTEMPS, F., VANOVERSCHELDE, J. L., HORMAN, S., BEAULOYE, C. & BERTRAND, L. 2014. A-

769662 potentiates the effect of other AMP-activated protein kinase activators on cardiac glucose uptake. *Am J Physiol Heart Circ Physiol,* 306, H1619-30.

TOYE, A. A., LIPPIAT, J. D., PROKS, P., SHIMOMURA, K., BENTLEY, L., HUGILL, A., MIJAT, V., GOLDSWORTHY, M., MOIR, L., HAYNES, A., QUARTERMAN, J., FREEMAN, H. C., ASHCROFT, F. M. & COX, R. D. 2005. A genetic and physiological study of impaired glucose homeostasis control in C57BL/6J mice. *Diabetologia,* 48, 675-86.

TRAN, L., ZIELINSKI, A., ROACH, A. H., JENDE, J. A., HOUSEHOLDER, A. M., COLE, E. E., ATWAY, S. A., AMORNYARD, M., ACCURSI, M. L., SHIEH, S. W. & THOMPSON, E. E. 2015. Pharmacologic treatment of type 2 diabetes: oral medications. *Ann Pharmacother,* 49, 540-56.

TUCKER, G. T., CASEY, C., PHILLIPS, P. J., CONNOR, H., WARD, J. D. & WOODS, H. F. 1981. Metformin kinetics in healthy subjects and in patients with diabetes mellitus. *Br J Clin Pharmacol,* 12, 235-46.

VAN DIJK, T. H., VAN DER SLUIJS, F. H., WIEGMAN, C. H., BALLER, J. F., GUSTAFSON, L. A., BURGER, H. J., HERLING, A. W., KUIPERS, F., MEIJER, A. J. & REIJNGOUD, D. J. 2001. Acute inhibition of hepatic glucose-6-phosphatase does not affect gluconeogenesis but directs gluconeogenic flux toward glycogen in fasted rats. A pharmacological study with the chlorogenic acid derivative S4048. *J Biol Chem,* 276, 25727-35.

VAN SCHAFTINGEN, E. & HERS, H. G. 1981. Inhibition of fructose-1,6-bisphosphatase by fructose 2,6-biphosphate. *Proc Natl Acad Sci U S A,* 78, 2861-3.

VASILAKOU, D., KARAGIANNIS, T., ATHANASIADOU, E., MAINOU, M., LIAKOS, A., BEKIARI, E., SARIGIANNI, M., MATTHEWS, D. R. & TSAPAS, A. 2013. Sodium–glucose cotransporter 2 inhibitors for type 2 diabetes: a systematic review and meta-analysis. *Annals of internal medicine,* 159, 262-274.

VINCENT, M. F., BONTEMPS, F. & VAN DEN BERGHE, G. 1992. Inhibition of glycolysis by 5-amino-4-imidazolecarboxamide riboside in isolated rat hepatocytes. *Biochem J,* 281 (Pt 1), 267-72.

VINCENT, M. F., MARANGOS, P. J., GRUBER, H. E. & VAN DEN BERGHE, G. 1991. Inhibition by AICA riboside of gluconeogenesis in isolated rat hepatocytes. *Diabetes,* 40, 1259-66.

VINCENT, M. F., VAN DEN BERGHE, G. & HERS, H. G. 1989. D-xylulose-induced depletion of ATP and Pi in isolated rat hepatocytes. *Faseb j,* 3, 1855-61.

VINOGRADOV, A. D. & GRIVENNIKOVA, V. G. 2016. Oxidation of NADH and ROS production by respiratory complex I. *Biochim Biophys Acta,* 1857, 863-71.

VIOLLET, B. & FORETZ, M. 2013. Revisiting the mechanisms of metformin action in the liver. *Ann Endocrinol (Paris),* 74, 123-9.

VIOLLET, B., GUIGAS, B., GARCIA, N. S., LECLERC, J., FORETZ, M. & ANDREELLI, F. 2012. Cellular and molecular mechanisms of metformin: an overview. *Clinical science,* 122, 253-270.

VON MORZE, C., OHLIGER, M. A., MARCO-RIUS, I., WILSON, D. M., FLAVELL, R. R., PEARCE, D., VIGNERON, D. B., KURHANEWICZ, J. & WANG, Z. J. 2018. Direct assessment of renal mitochondrial redox state using hyperpolarized (13) C-acetoacetate. *Magn Reson Med,* 79, 1862-1869.

VYTLA, V. S. & OCHS, R. S. 2013. Metformin increases mitochondrial energy formation in L6 muscle cell cultures. *J Biol Chem,* 288, 20369-77.

WANG, C., ZHANG, J., ZHANG, M., CHEN, H. & YING, W. 2015. Aralar plays a significant role in maintaining the survival and mitochondrial membrane potential of BV2 microglia. *Int J Physiol Pathophysiol Pharmacol,* 7, 107-14.

WEI, M., LIU, Y., BI, Y. & ZHANG, Z. J. 2019. Metformin and pancreatic cancer survival: Real effect or immortal time bias? *Int J Cancer*.

WILCOCK, C. & BAILEY, C. J. 1994. Accumulation of metformin by tissues of the normal and diabetic mouse. *Xenobiotica,* 24, 49-57.

WILLIAMSON, D. H., LUND, P. & KREBS, H. A. 1967. The redox state of free nicotinamide-adenine dinucleotide in the cytoplasm and mitochondria of rat liver. *Biochem J,* 103, 514-27.

WINDER, W. W., WILSON, H. A., HARDIE, D. G., RASMUSSEN, B. B., HUTBER, C. A., CALL, G. B., CLAYTON, R. D., CONLEY, L. M., YOON, S. & ZHOU, B. 1997. Phosphorylation of rat muscle acetyl-CoA carboxylase by AMP-activated protein kinase and protein kinase A. *J Appl Physiol (1985),* 82, 219-25.

WON, J. H., PARK, S., HONG, S., SON, S. & YU, J. W. 2015. Rotenone-induced Impairment of Mitochondrial Electron Transport Chain Confers a Selective Priming Signal for NLRP3 Inflammasome Activation. *J Biol Chem,* 290, 27425-37.

WONG, H. S., DIGHE, P. A., MEZERA, V., MONTERNIER, P. A. & BRAND, M. D. 2017. Production of superoxide and hydrogen peroxide from specific mitochondrial sites under different bioenergetic conditions. *J Biol Chem,* 292, 16804-16809.

WOODS, A., DICKERSON, K., HEATH, R., HONG, S. P., MOMCILOVIC, M., JOHNSTONE, S. R., CARLSON, M. & CARLING, D. 2005. Ca2+/calmodulin-dependent protein kinase kinase-beta acts upstream of AMP-activated protein kinase in mammalian cells. *Cell Metab,* 2, 21-33.

WORLD HEALTH, O. 2006. Definition and diagnosis of diabetes mellitus and intermediate hyperglycaemia: report of a WH.

WU, C., OKAR, D. A., STOECKMAN, A. K., PENG, L. J., HERRERA, A. H., HERRERA, J. E., TOWLE, H. C. & LANGE, A. J. 2004. A potential role for fructose-2,6-bisphosphate in the stimulation of hepatic glucokinase gene expression. *Endocrinology,* 145, 650-8.

XIAO, B., SANDERS, M. J., UNDERWOOD, E., HEATH, R., MAYER, F. V., CARMENA, D., JING, C., WALKER, P. A., ECCLESTON, J. F., HAIRE, L. F., SAIU, P., HOWELL, S. A., AASLAND, R., MARTIN, S. R., CARLING, D. & GAMBLIN, S. J. 2011. Structure of mammalian AMPK and its regulation by ADP. *Nature,* 472, 230-3.

YAMADA, K., HOSOKAWA, M., FUJIMOTO, S., FUJIWARA, H., FUJITA, Y., HARADA, N., YAMADA, C., FUKUSHIMA, M., UEDA, N., KANEKO, T., MATSUYAMA, F., YAMADA, Y., SEINO, Y. & INAGAKI, N. 2008. Effect of corosolic acid on gluconeogenesis in rat liver. *Diabetes Res Clin Pract,* 80, 48-55.

YANG, H. & YANG, L. 2016. Targeting cAMP/PKA pathway for glycemic control and type 2 diabetes therapy. *Journal of molecular endocrinology,* 57, R93-R108.

ZANG, M., ZUCCOLLO, A., HOU, X., NAGATA, D., WALSH, K., HERSCOVITZ, H., BRECHER, P., RUDERMAN, N. B. & COHEN, R. A. 2004. AMP-activated protein kinase is required for the lipid-lowering effect of metformin in insulin-resistant human HepG2 cells. *J Biol Chem,* 279, 47898-905.

ZHANG, C. S., LI, M., MA, T., ZONG, Y., CUI, J., FENG, J. W., WU, Y. Q., LIN, S. Y. & LIN, S. C. 2016. Metformin Activates AMPK through the Lysosomal Pathway. *Cell Metab,* 24, 521-522.

ZHANG, C. S., LI, M., ZONG, Y. & LIN, S. C. 2018. Determining AMPK Activation via the Lysosomal v-ATPase-Ragulator-AXIN/LKB1 Axis. *Methods Mol Biol,* 1732, 393-411.

ZHANG, Y., HAGEDORN, C. H. & WANG, L. 2011. Role of nuclear receptor SHP in metabolism and cancer. *Biochim Biophys Acta,* 1812, 893-908.

ZHANG, Y. L., GUO, H., ZHANG, C. S., LIN, S. Y., YIN, Z., PENG, Y., LUO, H., SHI, Y., LIAN, G., ZHANG, C., LI, M., YE, Z., YE, J., HAN, J., LI, P., WU, J. W. & LIN, S. C. 2013. AMP as a low-energy charge signal autonomously initiates assembly of AXIN-AMPK-LKB1 complex for AMPK activation. *Cell Metab,* 18, 546-55.

ZHOU, G., MYERS, R., LI, Y., CHEN, Y., SHEN, X., FENYK-MELODY, J., WU, M., VENTRE, J., DOEBBER, T. & FUJII, N. 2001. Role of AMP-activated protein kinase in mechanism of metformin action. *The Journal of clinical investigation,* 108, 1167-1174.

ZHOU, M., XIA, L. & WANG, J. 2007. Metformin transport by a newly cloned proton-stimulated organic cation transporter (plasma membrane monoamine transporter) expressed in human intestine. *Drug Metab Dispos,* 35, 1956-62.

ZHOU, P. T., LI, B., LIU, F. R., ZHANG, M. C., WANG, Q., LI, Y. Y., XU, C., LIU, Y. H., YAO, Y. & LI, D. 2017. Metformin is associated with survival benefit in pancreatic cancer patients with diabetes: a systematic review and meta-analysis. *Oncotarget,* 8, 25242-25250.

ZHU, A., ROMERO, R. & PETTY, H. R. 2009. An enzymatic fluorimetric assay for glucose-6-phosphate: application in an in vitro Warburg-like effect. *Analytical biochemistry,* 388, 97-101.

ZICKERMANN, V., WIRTH, C., NASIRI, H., SIEGMUND, K., SCHWALBE, H., HUNTE, C. & BRANDT, U. 2015. Structural biology. Mechanistic insight from the crystal structure of mitochondrial complex I. *Science,* 347, 44-9.

ZOROVA, L. D., POPKOV, V. A., PLOTNIKOV, E. Y., SILACHEV, D. N., PEVZNER, I. B., JANKAUSKAS, S. S., BABENKO, V. A., ZOROV, S. D., BALAKIREVA, A. V., JUHASZOVA, M., SOLLOTT, S. J. & ZOROV, D. B. 2018. Mitochondrial membrane potential. *Anal Biochem,* 552, 50-59.